# Evaluation of the Role of Epstein-Barr virus and Cellular Gene Expression in Paediatric and Adult Transplant Recipients

Auburn, Helen

*Awarding institution:*
King's College London

**Title:** Evaluation of the Role of Epstein-Barr virus and Cellular Gene Expression in Paediatric and Adult Transplant Recipients

**Author:** Helen Auburn

# Evaluation of the Role of Epstein-Barr virus and Cellular Gene Expression in Paediatric and Adult Transplant Recipients

*by*

Helen Auburn

A thesis submitted to King's College London

for the degree of Doctor of Philosophy

Division of Immunology, Infection & Inflammatory Disease

Guy's, King's & St Thomas' School of Medicine

King's College London

University of London

## DECLARATION OF AUTHORSHIP

This thesis is a presentation of my original research work. Wherever information has been derived from other sources every effort has been made to indicate this in the thesis.

Helen Auburn

## CONTRIBUTIONS BY OTHERS

The pre-hybridisation and hybridisation microarray work (RNA integrity analysis, first and second-strand cDNA synthesis (generation of antisense RNA, aRNA), T7 *in-vitro* transcription to produce biotin-labelled aRNA, purification and fragmentation of aRNA, and hybridisation of fragmented aRNA to GeneChips®) was carried out by me and Dr Estibaliz Aldecoa-Otalora Astarloa. Dr Matt Arno and Dr Estibaliz Aldecoa-Otalora Astarloa carried out the pre-processing data analysis (Conversion of raw signal intensities into signal values using MAS 5.0 software). The data analysis, including annotations of gene ontologies, calculation of fold-changes from signal values, regulation of gene expression (Presented in Table 7.2), as well as the bioinformatics analysis using gene ontology in MetaCore software was carried out by myself.

## ACKNOWLEDGEMENTS

I would like to acknowledge all those who made this thesis possible. Firstly, I would like to thank my examiners, Professor Paul J Farrell, and Reverend Dr John Philpott-Howard for providing a thorough examination of the thesis. I would also like to thank my supervisors Dr Melvyn Smith and Dr Mark Zuckerman for providing the opportunity to carry out this study, and to members of my PhD committee, Professor Jo Spencer, Professor Farzin Farzaneh and Dr Nicholas Lea, for their advice and guidance throughout the study. I am grateful to Dr Matthew Arno and Dr Estibaliz Aldecoa-Otalora Astarloa at The Genomics Centre, King's College London for assistance with the microarray analysis, and Dr Estibaliz Aldecoa-Otalora Astarloa for conducting the aRNA labelling, *in vitro* transcription and aRNA hybridisations. I am also grateful to my colleagues in the virology department at King's College Hospital, and to all my friends and family for their immense support and encouragement throughout the study. Finally, I would like to thank the Health Protection Agency, London, who supported this study.

## ABSTRACT

Post-transplant lymphoproliferative disease (PTLD) is a life-threatening complication after solid organ, bone-marrow and haematopoietic stem cell transplantation. While early diagnosis is known to predict encouraging outcomes, no specific markers exist for the early detection of PTLD. Epstein-Barr virus (EBV) infection is considered to be an important risk factor for PTLD. However, the correlations between EBV DNA loads and the onset of PTLD are inconclusive. The aim of this study was to identify potential biomarkers for the early onset of PTLD. To accomplish this, we examined EBV and cellular gene expression patterns in (i) the context of EBV lytic induction in a lymphoblastoid cell line (LCL) model system, (ii) PTLD versus non-PTLD transplant patients. In addition we examined the contributions of lytic virus replication vs. latent infection to the onset of PTLD. We used real-time two-step RT-PCR assays with SYBR green detection to analyse EBV gene expression (76 lytic, 12 latent [$n$ = 88 genes]), following 12-*O*-tetradecanoyl-13-phorbol acetate/sodium butyrate (TPA/NaB) induction of Raji cells. We identified 22 highly induced EBV genes (>90-fold) at 24 hrs post-induction. Using genome-wide Affymetrix microarrays, we identified cellular genes that were highly differentially expressed and regulated during the EBV lytic induction phase, 112 of which were regulated specifically by EBV, and 14 chosen for further study. We developed and validated real-time two-step TaqMan RT-PCR assays for clinical validation. Altogether, we evaluated 17 cellular and 14 EBV candidate genes in whole blood from paediatric solid organ transplant (SOT) recipients and adult umbilical cord transplant (UBCT) recipients, with and without PTLD. We detected a higher number and level of expression of EBV latent and lytic genes in PTLD patients, notably, *BALF5*, *EBNA-LP* and *LMP-1,* and in association with viral loads. Further, we detected latency III and more varied EBV latent gene expression patterns in PTLD. We also detected four cellular genes (*CXCL9, CXCL10, CDC2,* and *CHI3L1*) that were differentially expressed in PTLD vs. non-PTLD patients. To conclude, these findings suggest a basis for the likely microenvironment in which PTLD could develop. Further evaluation of candidate EBV and cellular markers could facilitate a more specific diagnosis of PTLD.

# TABLE OF CONTENTS

## INDEX OF TABLES

## INDEX OF FIGURES

# ABBREVIATIONS

| | |
|---|---|
| ***ACTB*** | Beta actin |
| **AP-1** | Activated protein 1 |
| **ASHM** | Aberrant somatic hypermutation |
| **aRNA** | Antisense ribonucleic acid |
| **bp** | base pairs |
| **BCR** | B cell receptor |
| **BL** | Burkitt's lymphoma |
| **BMT** | Bone marrow transplant |
| **cDNA** | Complementary DNA |
| **Cp** | Bam HIC fragment promoter |
| **CMV** | Cytomegalovirus |
| **CTL** | Cytotoxic T cell response |
| **DMSO** | Dimethyl sulphoxide |
| **DNA** | Deoxyribonucleic acid |
| **E** | Early |
| **E-AD** | Early antigen diffuse |
| **EDTA** | Ethylene diamine tetra-acetic acid |
| **EBNA** | EBV nuclear antigen |
| **EBV** | Epstein-Barr virus |
| **EBVwt** | EBV wild type |
| **FBS** | Foetal bovine serum |
| **GC** | Germinal centre |
| **GC** | Gastric carcinoma |
| **GO** | Gene ontology |
| **gDNA** | Genomic DNA |
| **gp** | Glycoprotein |
| **HL** | Hodgkin's lymphoma |
| **HLA** | Human leukocyte antigen |
| **HSCT** | Haematopoietic stem cell transplant |
| **IFN** | Interferon |
| **IFN-γ** | Interferon-gamma |
| **Ig** | Immunoglobulin |
| **IgG** | Immunoglobulin G |
| **IgV** | Immunoglobulin variable |
| **IL** | Interleukin |
| **IP-10** | Interferon-inducible protein 1P-10 |
| **IE** | Immediate-early |
| **IM** | Infectious mononucleosis |
| **KCH** | King's College Hospital |
| **L** | Late |
| **LCL** | Lymphoblastoid cell line |
| **LMP** | Latent membrane protein |
| **mins** | Minutes |
| **Mig** | Monocyte-induced by interferon-gamma |

| | |
|---|---|
| **MIP-1α** | Macrophage inflammatory protein 1 alpha |
| **ml** | Millilitre |
| **miRNAs** | MicroRNAs |
| **mRNA** | Messenger ribonucleic acid |
| **M-PTLD** | Monomorphic PTLD |
| **NaB** | Sodium butyrate |
| **NF-kB** | Nuclear factor-kappa B |
| **NPC** | Nasopharyngeal carcinoma |
| **OHL** | Oral hairy leukoplakia |
| **ORF** | Open reading frame |
| ***oriLyt*** | Origin of lytic replication |
| ***oriP*** | Origin of plasmid |
| **PBMCs** | Peripheral blood mononuclear cells |
| **PCR** | Polymerase chain reaction |
| **PH** | Plasmacytic hyperplasia |
| **PKC** | Protein kinase C |
| **P-PTLD** | Polymorphic PTLD |
| **PTLD** | Post-transplant lymphoproliferative disease |
| **RANTES** | Regulated upon activation, normal T cell expressed and secreted |
| **RIS** | Reduction in immunosuppression |
| **RNA** | Ribonucleic acid |
| **rpm** | Revolutions per minute |
| **RT** | Reverse transcription |
| **RT-PCR** | Reverse-transcription polymerase chain reaction |
| **SOT** | Solid organ transplant |
| **TARC** | Thymus and activation-regulated chemokine |
| **Th** | T helper |
| TPA | 12-*O*-tetradecanoyl-13-phorbol acetate |
| **UCBT** | Umbilical cord blood transplant |
| **VCA** | Viral capsid antigen |
| **WHO** | World Health Organisation |
| **Wp** | Bam HI W fragment promoter |
| **ZRE** | Z-response elements |

# 1 CHAPTER 1. GENERAL INTRODUCTION

## *1.1 EPSTEIN-BARR VIRUS*

### 1.1.1 Classification of Epstein-Barr virus

Over 100 herpesviruses have been discovered, several of which are human herpesviruses of the herpesviridae family *Alpha-*, *Beta-*, and *Gammaherpesvirinae*, and infect the sensory ganglia, secretory glands and lymphoid or epithelial cells, respectively (Table 1.1) (Edelman, 2005). Epstein-Barr virus (EBV) or *Human herpesvirus 4* (HHV-4) is classified as a member of the genus *Lymphocryptovirus* (LCV), which belongs to the subfamily *Gammaherpesvirinae* within the *Herpesviridae* family (Fields et al., 2007). The gammaherpesvirus family contains two genera, the lymphocryptovirus (LCV) and rhadnovirus (RDV). EBV is the only LCV and HHV-8 the only RDV. A common feature shared amongst many of the viruses in the LCV genus is their lymphotropism; defined as their ability to infect B and T lymphocytes (Fields et al., 2007).

**Table 1-1 Classification of human herpesviruses**

| Herpesvirus subfamily | Herpesvirus |
|---|---|
| ***Alphaherpesviruses*** | Herpes simplex viruses 1 (HSV-1) |
| ***Alphaherpesviruses*** | Herpes simplex viruses 2 (HSV-2) |
| ***Betaherpesviruses*** | Varicalla-zoster virus (VZV) |
| ***Betaherpesviruses*** | Human cytomegalovirus (HCMV) |
| ***Betaherpesviruses*** | Human herpesviruses 6 (HHV-6) |
| ***Betaherpesviruses*** | Human herpesviruses 7 (HHV-7) |
| ***Gammaherpesviruses*** | Human herpes virus 4 (HHV-4)/Epstein-Barr virus (EBV) |
| ***Gammaherpesviruses*** | Human herpesvirus 8 (HHV-8) |

### 1.1.2 Structure of EBV

As for other herpesviruses, the EBV virion is approximately 200 nm in diameter and consists of four common elements, a toroid-shaped protein core containing the linear double-stranded DNA genome, an icosahedral capsid, an amorphous protein tegument and an outer lipid envelope (Figure 1.0) (Fields et al., 2007).

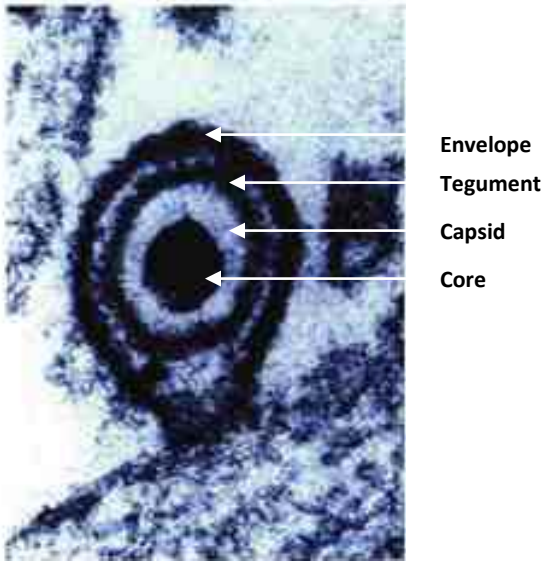


**Figure 1-1 Structure of Herpesviruses**

Electron micrograph of a herpesvirus particle (diameter ~ 120-200 nm). The herpesvirus virion structure consists of a double-stranded DNA genome within an icosahedral capsid surrounded by tegument and an outer lipid envelope with numerous glycoprotein projections (Young and Rickinson, 2004). EBV is approximately 200 nm in diameter. The core contains the 172 kbp linear, double-stranded DNA genome, surrounded by the capsid, a 100-120 nm protein shell with $T$ = 16 icosahedral symmetry made up of 162 capsomers, and the entire core and DNA genome termed nucleocapsid. The tegument surrounds the capsid and consists of 1-20 proteins. The envelope is the outer layer, which is derived from cellular membranes and encloses the tegument and is embedded with approximately 10 membrane glycoproteins.

### 1.1.3 EBV genome and organisation

The EBV genome is a linear, double-stranded DNA, approximately 172 kbp in length, and with a 60% G+C content (Fields et al., 2007). Upon infection, the genome circularises into a double-stranded episome (Figure 1.2). The EBV genome consists of four components common to all herpesviruses, including a large unique (U) region flanked by series of 0.5 Kb terminal direct repeats (Figure 1.3)(Cheung and Kieff, 1982). In addition, two origins of replication *oriLyt* and *oriP* are found within UL (Figure 1.3). EBV was the first herpesvirus to be completely cloned and fully sequenced using its *Bam*HI restriction digest sites (Baer et al., 1984). The *Bam*HI fragments were sequenced and open reading frames (ORFs) designated according to the order of direction (right or leftward) of transcription from the *Bam*HI restriction fragment or their putative functions (Fields et al., 2007). More recently, the EBV wild-type (EBVwt) strain was created by assembling sequences of EBV strains B95.8 and Raji (de Jesus et al., 2003a). According to the National Center for Biotechnology Information (NCBI), the EBV type 1 (EBV-1) genome contains 94 genes of which 94 are protein coding, including several spliced forms (Farrell et al., 1983). In addition, approximately 45 structural RNAs have been identified (de Jesus et al., 2003a; Smith et al., 2000).

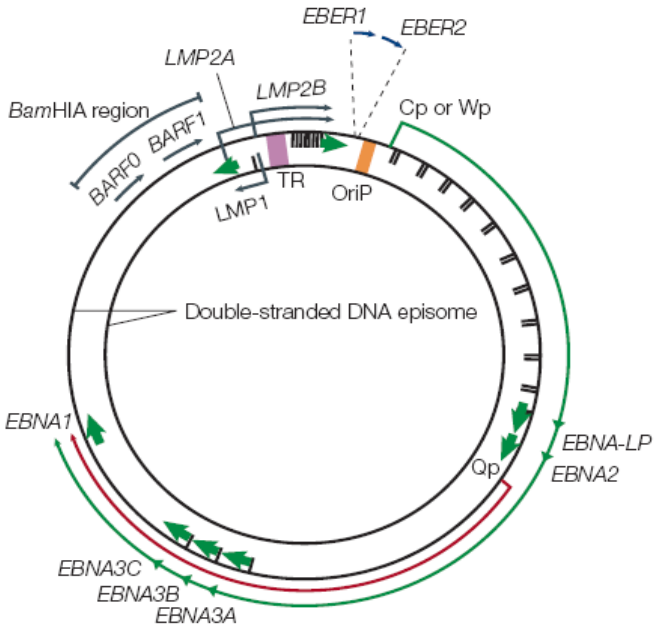


**Figure 1-2 The Epstein-Barr (EBV) genome**

Diagram showing the circularised double-stranded EBV DNA episome and the location and transcription of the EBV latent genes Locations of the three promoters Cp, Wp and Qp within the unique long ($U_L$) region are shown. The outer green arrow shows latent EBV genes transcribed from Cp or Wp whereas the red arrow shows latent genes transcribed from Qp. The origin of replication (*oriP*) is shown in orange. The terminal repeat (TR) joins the sequences together. Adapted from Young et al. 2004.

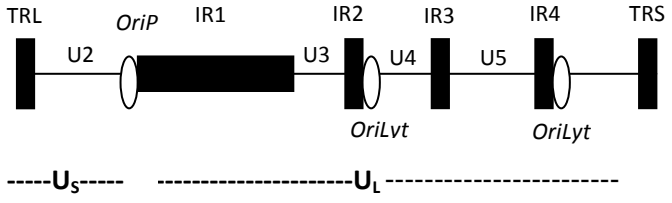


**Figure 1-3 Schematic of the linear Epstein-Barr virus (EBV) genome**

The schematic diagram shows the linear double-stranded EBV DNA episome and location and transcription of the latent EBV genes. The EBV genome is split into two regions of unique sequences ($U_L$ and $U_S$), the 134kbp unique long sequence domain ($U_L$), containing most of the viral coding capacity and 6kbp unique short sequence domain ($U_S$) and split by the presence of 3kbp internal direct repeats (IR1), and flanked by 538-bp direct terminal repeat regions (TRL and TRS). The plasmid origin (*oriP*) is contained within $U_S$ and two origins of lytic replication (*oriLyt*) are contained within $U_L$ of the EBV genome. The $U_L$ region is split further into four shorter domains (U2, U3, U4 and U5) by the presence of three short direct repeat elements (IR2, IR3 and IR4) that transcribe EBV latent proteins. Adapted from Young et al. 2004.

### 1.1.4 EBV types 1 and 2

EBV is classified into two subtypes: EBV-1 and EBV-2 (also known as type A and B), based on sequence variations in genes encoding the EBV nuclear antigens (EBNA-2, EBNA-3A, EBNA-3B and EBNA-C and EBNA-LP) (Arrand et al., 1989; Fields et al., 2007). In general, sequence variations are greater in EBNA-2 compared to the other EBNAs, with a 53% amino acid sequence identity between EBV-1 and EBV-2 (Dambaugh et al., 1984; McCann et al., 2001; Rowe et al., 1989; Sample et al., 1990). EBV-1 is more efficient at transforming B cells *in vitro* than EBV-2 and EBNA-2 variation is attributable to the differences in transformation efficiency (Cohen et al., 1989; Rickinson et al., 1987).

## *1.2 BIOLOGY OF EBV INFECTION*

### 1.2.1 Primary infection of EBV

Early events of primary EBV infection include entry of EBV into the oropharyngeal epithelium, although whether B lymphocytes or epithelial cells are infected first is uncertain (Shannon-Lowe et al., 2006). EBV preferentially infects resting (naive) B cells, although epithelial cells and resting memory B cells are also infected (Li et al., 1992; Sixbey et al., 1984). Additionally, under certain circumstances T cells, natural killer cells, smooth muscle cells and monocytes can also be infected (Hutt-Fletcher, 2007). In general, EBV undergoes brief lytic replication in epithelial cells of the oropharynx (Li et al., 1992). Subsequently, EBV remains latent in memory B lymphocytes (Babcock et al., 1998).

### 1.2.2 EBV entry of B lymphocytes

EBV entry of B lymphocytes involves direct attachment to the B lymphocyte followed by internalisation through fusion between the viral envelope and B cell membrane. EBV uses the viral envelope glycoprotein gp350/220 to bind the complement receptor type 2 (CR2) also known as CD21 on the B lymphocyte surface (Figure 1.3). CR2 is the primary receptor for EBV. Eight additional glycoproteins are implicated in EBV entry, although gp350/220 is the most commonly used due to its high abundance on the surface of the virus particle (Hutt-Fletcher, 2007). Once in the endosomal compartment, fusion requires interactions between the core fusion complex gH/gL/gB of gp42, gp85 and gp25 (Spear and Longnecker, 2003) and human leukocyte antigen (HLA) class II co-receptor. This interaction transforms the core fusion complex from a metastable to active state and requires binding of EBV envelope glycoprotein gp42 to gHgL

forming the complex gHgLgp42. During fusion the EBV membrane fuses with the endosomal lipid envelope on the B lymphocyte and the virus becomes de-enveloped (Hutt-Fletcher, 2007).

### 1.2.3 EBV entry of epithelial cells

Attachment of EBV to epithelial cells is less clear, since CR2 is not usually expressed in epithelial cells and the other ligands and receptors involved are unknown. However, when an epithelial cell expresses CR2, EBV can enter through interactions between CR2 and gp350, as it does for B lymphocytes (Borza and Hutt-Fletcher, 2002; Li et al., 1992). Interactions with other cell surface proteins are thought to mediate EBV attachment to CR2-negative epithelial cells, including gHgL and the putative receptor gHgLR (Borza and Hutt-Fletcher, 2002; Molesworth et al., 2000). The mechanism of fusion of EBV and epithelial cells is unclear and does not require gp42. Interestingly, gp42 can inhibit entry into epithelial cells (Hutt-Fletcher, 2007). Cell transfer of EBV to epithelial cells through the formation of B-cell-epithelial conjugates is an alternative route of entry. In this mechanism, EBV is not internalised but attaches to B lymphocytes through gp350/CD21 complexes from where they transfer efficiently to CD21-negative epithelial cells, enhancing infectivity by up to 10,000-fold (Shannon-Lowe et al., 2006).

### 1.2.4 EBV cell tropism

Cell tropism is shown in Figure 1.4. (Borza and Hutt-Fletcher, 2002). EBV cell tropism is dependent on gp42 and the cell type from which EBV is produced (Borza and Hutt-Fletcher, 2002; Farrell, 2002). Normally, gp42 forms part of the fusion complex gH/gL/gp42. However,

virus produced in B cells is relatively depleted of gp42 (gH/gL), due to sequestering by HLA Class II. As a result, gH/gL targets the HLA Class II co-receptor on other B cells less effectively than on HLA class II-negative epithelial cells. Conversely, in virus produced from epithelial cells, gp42 (gH/gL/gp42) are relatively more abundant and more efficient at targeting the HLA Class II co-receptors on B cells.

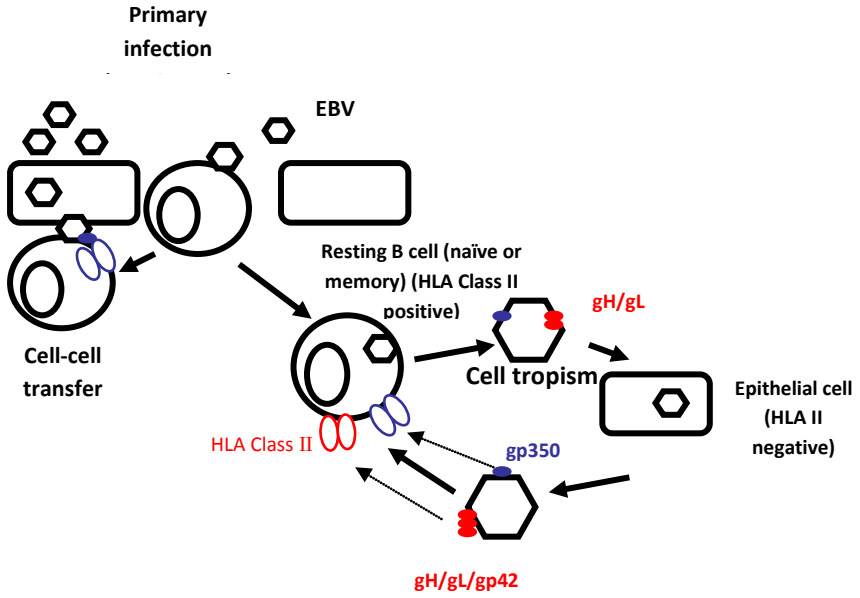


**Figure 1-4 Putative models of EBV entry, infection and cell tropism**

EBV infects resting B cells through interaction of gp350/220 with CD21 on the B cells and gHgLgp42 fusion complex with HLA Class II co-receptor on B cells. EBV produced from B cells is depleted of gp42 (gHgL), increasing efficiency of infection of HLA Class II negative epithelial cells, but not B cells. EBV produced from epithelial cells infects B cells with increased efficiency through interaction of gHgLgp42 with HLA Class II co-receptor on B cells. EBV mediates B cell-epithelial cell transfer through interaction of gp350/220 with CD21 on B cells, but no internalisation and formation of B cell-epithelial conjugates at cell synapse allowing transfer of EBV to epithelial cells. Adapted from Farrell et al. 2002

### 1.2.5 Post-fusion events

Fusion of EBV from the endosomal compartment of the B lymphocyte enables the release of virus into the cytoplasm. EBV exists as a de-enveloped virion in the cytoplasm and the tegumented capsid must transfer to the nucleus, where the genome is replicated, packaged and released as new viral particles (Fields et al., 2007). However, the exact mechanisms for post-fusion events in EBV are poorly understood. What is known from other herpesviruses, is that transfer from the cell membrane occurs in a reversal of the budding process required to produce the enveloped virus in the first place (Hutt-Fletcher, 2007).

### 1.2.6 Assembly and egress

The exact mechanism for EBV packaging and release is poorly understood and likely mechanisms are largely postulated from studies in other herpesviruses. During the DNA packaging process, the replicated genome is cleaved from branched concatemers into unit-length genomes that are packaged into pre-formed capsids (Tsurumi et al., 2005).

## *1.3 EBV LATENT INFECTION*

### 1.3.1 Overview of latent EBV infection

Like all herpesviruses, EBV can establish both latent and lytic replication during its life cycle. EBV can exist as a latent infection *in vivo* in both epithelial cells as well as B lymphocytes, however, B lymphocytes are the principle reservoir of latent EBV and the source of new EBV progeny upon EBV reactivation and infection of other EBV-naive B cells (Fields et al., 2007).

Following initial infection of resting primary B lymphocytes, the linear EBV genome circularises and persists as a closed circular DNA molecule or episome within the nucleus. Approximately 10-100 episomes are maintained within the latently infected B lymphocyte. These episomes are self-replicating and are dependent on cellular DNA replication, where replication occurs only once per cycle. During latent infection of B lymphocytes only a restricted number of genes are expressed with no viral production. The latency genes are involved in functions such as stimulating cell proliferation, inhibition of apoptosis, blocking viral lytic replication, and ensuring accurate and equal partitioning of episomal viral genomes to daughter cells (Miller and El-Guindy, 2002). During latency, the EBV lytic genes are most likely repressed through host-driven methylation of viral DNA (Hammerschmidt and Sugden, 1988). Moreover, during latent EBV infection, only a few EBV genes are expressed and there is no production of infectious virus (Fields et al., 2007).

### 1.3.2 EBV latent gene expression

EBV expresses a small subset of latent genes including six EBV nuclear antigens (EBNA's) 1, 2, 3A, 3B, 3C and LP and three latent membrane proteins (LMP's) 1, 2A and 2B. Several of these have transforming and oncogenic properties including EBNA-2, EBNA-3A, EBNA-3C and LMP-1 (Hickabottom et al., 2002; Kempkes et al., 1995; Parker et al., 1996; Wang et al., 1985). In addition, other small non-coding RNAs are actively expressed during B cell transformation *in vitro* (Young and Rickinson, 2004), including the highly abundant non-polyadenylated and non-coding EBV-encoded RNAs, EBER-1 and EBER-2 (EBER's), a set of highly spliced non-coding *Bam*HI A rightward transcripts (BART's), also known as complementary strand transcripts

(CSTs), one small nucleolar RNA (snoRNA) (Feederle et al., 2011), as well as 44 mature microRNAs (miRNAs) derived from 25 precursor-miRNAs, the functions of which may control viral latency (Pfeffer et al., 2004; Riley et al., 2012). The functions of the latent genes and RNA transcripts are summarised in Table 1.2.

**Table 1-2 EBV latent genes and their proposed functions**

| Latent gene | Proposed function |
|---|---|
| ***A73 / RPMS1 splice*** | Part of BARTs family, Unknown function; EBNA-2 homologue; negatively regulates activity of EBNA-2 and NotchIC |
| ***BARF0*** | Part of BARTs family, Unknown function Interaction with Notch, putative maintenance of latency |
| ***microRNAs*** | Putative role in RNA silencing; proposed to target three viral transcripts (BALF5, LMP-1 and LMP-2) for degradation; control of viral latency |
| ***EBER's*** | Small non-coding RNAs, Unknown function, putative interaction of IFN responses; role in tumorigenicity of BL cells, association with cellular proteins, lupus antigen (LA), EBER-associated ribosomal protein (EAP, L22 (rpL22)), double-stranded (ds) RNA-dependent protein kinase (PKR) and retinoic acid inducible-gene I (RIG-I) |
| ***EBNA-1*** | Essential for B-cell transformation, replication and maintenance of EBV episome, DNA binding phosphoprotein, activates promoter Qp, |
| ***EBNA-2*** | Essential for transformation, oncoprotein, transcriptional activator of EBV and cellular genes, Notch homologue, Activates promoter, Cp, up-regulates LMP-1; Promotes G0-G1 transition in co-operation with EBNA-LP |
| ***EBNA-3A*** | Essential for B-cell transformation, oncoprotein Transcriptional regulator |
| ***EBNA-3B*** | Transcriptional regulator, not essential for B-cell transformation; growing evidence for a role in B-cell transformation |
| ***EBNA-3C*** | Nuclear protein, essential for B-cell transformation |
| ***EBNA-LP*** | Nuclear phosphoprotein, highly spliced *BWRF1* ORF, 12 exons, enhances EBNA-2 transactivation; participates in B-cell transformation and B-cell growth; binds p53 and pRb |
| ***LMP-1*** | Essential for B-cell transformation, mimics CD40; key oncogene; up-regulates anti-apoptotic proteins bcl-2 and A20 and viral IL-10; recruits chemokines |
| ***LMP-2A / 2B*** | LMP-2A, interference with protein kinase signalling, gene terminal protein, essential for B-cell transformation; Inhibits signalling through BCR and promotes survival during B-cell development; LMP-2B, negative regulator of LMP-2A; unknown function |

### 1.3.3 EBV latency gene expression programmes

EBV exhibits four latency gene expression programmes known as latency types 0, I, II and III, each of which is based largely on the expression of the *EBNAs* and *LMPs* and associated with the

differentiation state of host B cells (Table 1.3) (Babcock et al., 2000; Rowe et al., 1992; Rowe et al., 1987; Thorley-Lawson and Gross, 2004). The latency III programme (growth programme) is characterised by expression of the full set of latent genes, including the *EBNAs*, *LMP-1* and *LMP-2*. *In vivo*, latency III is expressed in naive B cells during primary EBV infection and associated with B-cell proliferation and immortalisation (Farrell, 1995; Joseph et al., 2000). Latency III is also expressed in most B cell lymphomas in immunosuppressed patients. *In vitro*, latency III is expressed in EBV-transformed LCLs and represents an *in vitro* model of PTLD (Niedobitek et al., 1997a; Rowe et al., 1998; Young and Rickinson, 2004). The latency II programme (Default programme) is characterised by the expression of *EBNA-1, LMP1, LMP-2A* and *2B* genes and is expressed in nasopharyngeal carcinoma (NPC), gastric cancer, Hodgkin's disease (HD) and some T and B cell lymphomas (Fahraeus et al., 1988). Latency I is characterised by the restricted expression of the *EBNA-1* gene only, and is observed in proliferating memory B cells in healthy individuals (Chen et al., 1995). Latency I is found predominantly in Burkitt's lymphoma (BL) and derived LCLs (Tierney et al., 2000). A fourth programme, latency 0 is observed *in vivo* in quiescent memory B cells and expresses none of the latent genes, enabling EBV to persist within the peripheral memory B cell pool undetected by the $CD8^+$ T cell response (Babcock et al., 1998). Moreover, latency I, II and III are expressed in different EBV-associated cancers, which originate from the different stages of infected B cells (Table 1.3) (Thorley-Lawson and Gross, 2004).

**Table 1-3 EBV latency programmes used for EBV persistence and disease *in vivo***

| Latency programme | EBV genes expressed | Infected B cell type | Function | Expression in disease |
|---|---|---|---|---|
| **Latency III (Growth programme)** | *EBNA-1, 2, 3a, 3b, 3c, LP, LMP-1, LMP-2A* and *LMP2B, EBER's, BART's* | Naive | Activate B cell | Infectious mononucleosis, PTLD |
| **Latency II (Default programme)** | *EBNA-1, LMP-1* and *LMP-2A, EBER's, BART's, miRNAs* | Germinal centre | Differentiate activated B cell into memory | Hodgkin lymphoma, Nasopharyngeal carcinoma |
| **Latency I** | *EBNA-1, EBER's, BART's, miRNAs* | Dividing peripheral memory | Allow virus in latency program cell to divide | Burkitt's lymphoma, Primary effusion lymphoma |
| **Latency 0** | None | Peripheral memory | Allow life time persistence | Memory B lymphocytes in peripheral blood of healthy EBV seropositive carriers |

(Table Adapted from Thorley-Lawson et al., 2004)

### 1.3.4 Regulation of EBV latency

Following infection of B cells, the linear, uncoated EBV genome is transferred to the nucleus, where it re-circularises, leading to transcription of all the latent genes (Young and Rickinson, 2004). The EBV transcription patterns are regulated largely through differential EBV promoter usage (Wp, Cp and Qp) (Figure 1.2). The BamHI W (Wp) and BamHI C (Cp) upstream promoters are involved in driving the expression of all the EBNA genes during latency III and they function in a mutually exclusive fashion (Woisetschlaeger et al., 1989). The Qp promoter leads to the selective expression of EBNA-1 during latency I, whereas latency II is initiated by transcription from Qp and LMP promoters (Rowe et al., 1992; Schaefer et al., 1991; Zetterberg et al., 1999) (Rowe et al., 1992; Woisetschlaeger et al., 1989; Woisetschlaeger et al., 1990). Infection of B cells with EBV, initially leads to exclusive use of Wp and initial expression of EBNA-2 and EBNA-LP, followed by an EBNA-2 autoregulated switch from Wp to Cp, leading

to the ordered expression of EBNA-1, EBNA-2, EBNA-3A, EBNA-3B and EBNA-3C (latency III) from a long 120kb Wp/Cp transcript (Schlager et al., 1996; Woisetschlaeger et al., 1991; Woisetschlaeger et al., 1990).

*EBNA-2* and *EBNA-LP* are the first EBV genes expressed early after B-cell infection (8-12 hrs) (Allday et al., 1989; Fields et al., 2007; Rooney et al., 1989a), transcribed from a bicistronic unit under exclusive transcription from Wp, located upstream of Cp (Schlager et al., 1996; Thorley-Lawson and Gross, 2004; Woisetschlaeger et al., 1989; Woisetschlaeger et al., 1990). EBNA-2 functions as the principle transcriptional activator of the Cp promoter of viral genes (Wang et al., 1987; Wang et al., 1991), whereas EBNA-LP enhances EBNA-2 activation (Peng et al., 2005). By 36 hrs, EBNA-2 autoregulates the switch from Wp to Cp, giving rise to a long 120 kb Wp/Cp transcript from which all the EBNA genes (1, 2, 3A, 3B and 3C) are differentially spliced (Schlager et al., 1996; Woisetschlaeger et al., 1991; Woisetschlaeger et al., 1990). At the same time, EBNA-LP co-activates EBNA-2 transcription of LMP-1 and LMP-2A/B from EBNA-2 responsive promoters, and EBNA-1 from promoter Qp, leading to the default programme (latency II) which is essential for differentiation of latently infected B cells into memory B cells (Fahraeus et al., 1990; Sample et al., 1986). Transcription from the promoter, Qp (Figure 1.2), leads to exclusive expression of EBNA-1 (latency I) and EBV persistence (Schaefer et al., 1995; Young and Rickinson, 2004). By 48 hrs after infection the full repertoire of EBV latent genes is expressed.

### 1.3.5 EBV latent DNA replication

EBV persists in host B lymphocytes as a covalently closed circular DNA episome (EBNA-1/*oriP*) (Young and Rickinson, 2004). These episomes are self-replicating and dependent on cellular DNA replication proteins and EBNA-1 for latent DNA replication. EBNA-1 has two key functions during latent EBV DNA replication, including genome maintenance and retention and partition at division (Yates et al., 1984; Yates et al., 1985). Replication of the EBV episome is mediated by the cellular DNA replication machinery, occurring once per cell division cycle (Adams, 1987) and partitioning to daughter cells during mitotic division (Kirchmaier and Sugden, 1995), and is initiated within the origin of DNA replication, *oriP*, located in the short unique domain ($U_S$) of the viral genome (Figure 1.0). The *oriP* consists of two sequence elements with high-affinity EBNA-1 binding sites, FR, the family of repeat element (30 bp repeats)(FR) and the dyad symmetry element (DS), each separated by approximately 960 base pairs, both required for replication (Reisman et al., 1985). EBNA-1 is essential for latent DNA replication that directly binds and activates *oriP* (Yates et al., 1985). EBNA-1 mediates genome replication from within *oriP* by first interacting with EBNA-1 binding sites within the DS element of *oriP*. Therefore, the main purpose for EBNA-1 may be to stabilise the replicated DNA during partition at division. To complete replication of the episome, EBNA-1 interacts with the FR element within *oriP* and tethers the viral genome to the host chromosome through interactions with cellular chromosome-associated protein, ensuring that EBV episomes are evenly partitioned upon cell division. Latent EBV DNA replication occurs once per cell cycle during S phase, where DNA is amplified as circular plasmid molecules (Tsurumi and Kudoh, 2005).

### 1.3.6 EBV persistence *in vivo*

Following primary infection, EBV establishes a life-long latent infection in circulating resting memory B lymphocytes, where it persists as an episome, typically at a frequency of 1 to 50 copies per million B lymphocytes (Babcock et al., 1998; Miyashita et al., 1997). The exact mechanism as to how EBV establishes persistence in the memory B cell pool is uncertain. According to the proposed model of EBV persistence *in vivo*, EBV exploits the normal B-cell differentiation pathway, and uses its transforming properties to specifically provide activation signals to newly infected naive B lymphocytes which differentiate at the germinal centre (GC) into resting memory B lymphocytes where they persist (Thorley-Lawson, 2001). During primary infection, EBV particles produced either in tonsils or that enter tonsillar tissue infect resting (naive) B cells. The transforming properties of the latent proteins drive the naive B cells to become proliferating lymphoblasts, which migrate towards follicular areas where they form follicles known as the GC. Within the GC, EBV expresses the more restricted pattern of gene expression (latency II), that provide survival signals to prevent apoptosis and enable the GC B lymphocytes to differentiate into long-lived resting memory B cells. These memory B cells exit the GC and escape immune recognition by switching to the latency I programme, and then latency 0, where no genes are expressed. EBV is able to persist in memory B cells since they are long-lived and remain undetected by the immune response (Babcock et al., 1998; Joseph et al., 2000). Periodic reactivation of EBV, possibly from memory B cell activation within lymphoid tissues results in differentiation into plasma cells followed by viral replication and infection of naive B lymphocytes (Thorley-Lawson, 2001). Occasional reactivation of memory B cells results in latency III expression (Young and Rickinson, 2004). Therefore it is apparent from this model

that the role of the latent proteins is in establishing persistent infection and EBV uses different latency programmes (Table 1.4) to establish persistence *in vivo.*

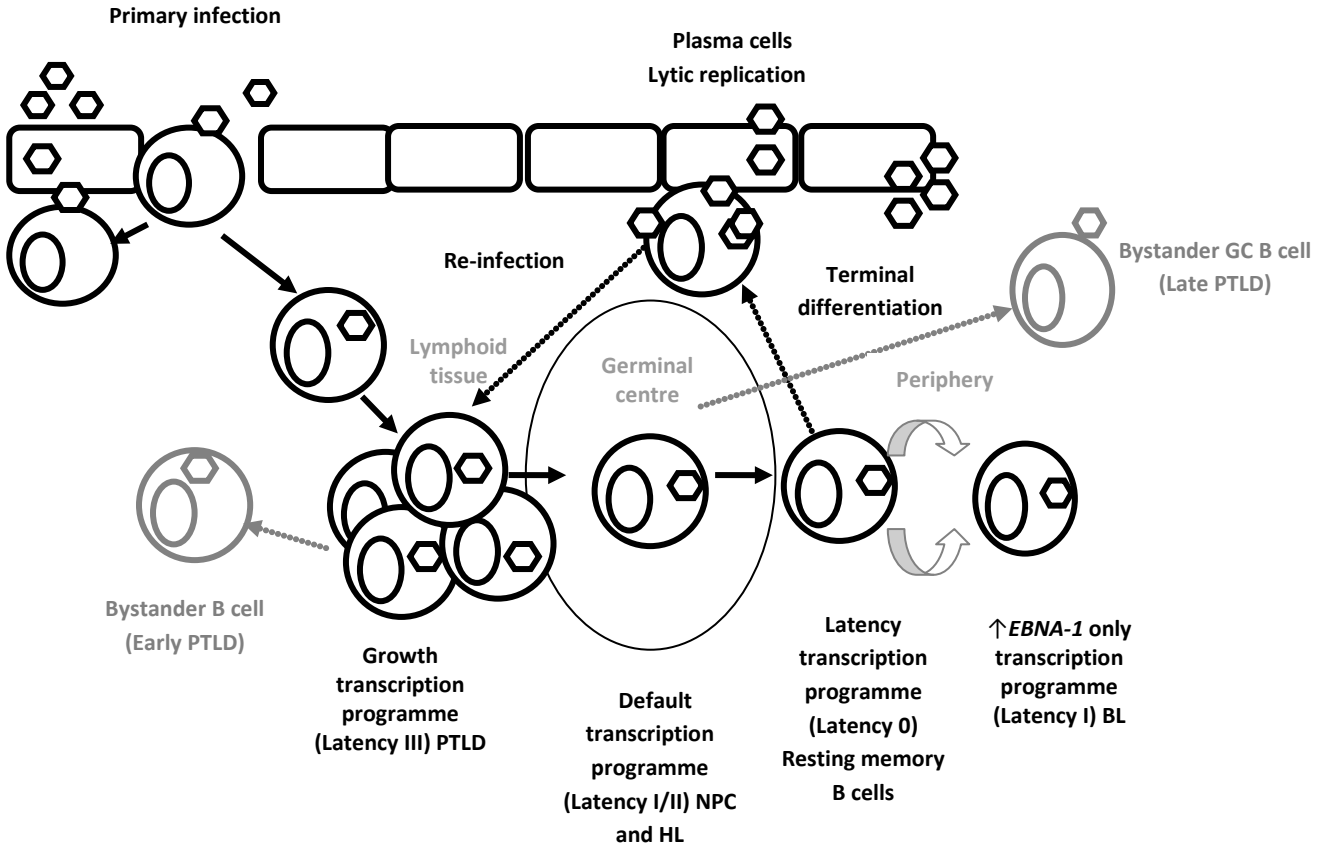


**Figure 1-5 Schematic drawing of proposed models of EBV persistence and reactivation *in vivo***

EBV infects naive resting B cells that are activated into lymphoblasts expressing latency III. In the presence of a cytotoxic T cell response these lymphoblasts proliferate and differentiate through the germinal centre where latency I and II is expressed, into memory B cells. After exiting the germinal centre memory B cells enter the peripheral blood where they persist for life. In memory B cells, all latent genes are down-regulated in latency 0. These memory B cells circulate in the periphery and occasionally reactivate in the tonsillar region, where they receive signals to undergo terminal differentiation into plasma cells, releasing newly infected virus that re-infects naive B cells and also lymphoblasts. In the absence of an immune response lymphoblasts can proliferate uncontrolled into PTLD. Rarely infection of bystander cells can also proliferate into PTLD. Adapted from (Thorley-Lawson and Allday, 2008).

## *1.4 EBV LYTIC REPLICATION*

### 1.4.1 Overview of EBV lytic replication

To complete the EBV life cycle, the EBV genome reactivates to enter the lytic cycle in the nucleus where it is transcribed into mRNA by host RNA polymerase II and progeny virus produced in three temporally regulated phases: (i) transcription of the viral genome, (ii) replication of the viral genome and (iii) assembly and egress of new progeny virus (Fields et al., 2007). During these phases of lytic replication, three classes of genes are expressed including: immediate-early (IE), early (E) and late (L) genes, according to their appearance following activation of the lytic cascade (Takada and Ono, 1989). Over 70 EBV lytic genes are expressed during the lytic cycle, including two immediate-early genes, approximately 30 early genes and 40 late genes (Fields et al., 2007).

### 1.4.2 Immediate-Early genes

EBV lytic replication is initiated by the expression of two IE genes *BZLF1* and *BRLF1*, that encode the transcription factors BZLF1 (also known as Z, Zta, ZEBRA or EB1) (Chevallier-Greco et al., 1986b; Countryman and Miller, 1985) and BRLF1 (also called Rta or R)(Hardwick et al., 1988), respectively. BZLF1 and BRLF1 are essential in activating the cascade of lytic-cycle gene expression (Chevallier-Greco et al., 1986b; Countryman and Miller, 1985; Ragoczy and Miller, 1999; Rooney et al., 1989b; Takada et al., 1986; Zalani et al., 1996). However, BZLF1 is the key lytic transactivator and the first gene expressed in the lytic cycle (Amon et al.,

2004a). Rta is autoactivated by itself and Zta (Liu and Speck, 2003). Together, both co-operate to promote lytic cycle activation by regulating several early gene promoters (Feederle et al., 2000b; Flemington and Speck, 1990; Hardwick et al., 1988; Kenney et al., 1989; Quinlivan et al., 1993), leading to the activation of all early and late lytic genes and subsequently viral DNA replication and virion production (Inman et al., 2001). The IE genes are also expressed in the absence of host protein synthesis (Biggin et al., 1987; Flemington et al., 1991; Takada and Ono, 1989).

### 1.4.3 Zta/ZEBRA

Zta belongs to the basic-leucine zipper (bZIP) family of transcription factors (Chang et al., 1990; Chen et al., 2009; Wang et al., 2005) that shares partial amino acid homology to the cellular activating protein 1 (AP-1) family of transcription factors, including c-Fos, Fra-1, c-Jun and Jun-B (Chen et al., 2009; Countryman et al., 2009; Farrell et al., 1989). Zta functions as a sequence-specific DNA binding transcription factor (Farrell et al., 1989) activates lytic-cycle gene expression through the direct binding of AP-1 and AP1-1-like motifs known as Z response elements (ZREs) within several EBV early and cellular gene promoters (Chang et al., 1990; Farrell et al., 1989; Lieberman et al., 1990). Moreover, Zta can activate itself through interactions with ZREs within its own promoter, Zp (Flemington and Speck, 1990). Zta functions as a sequence-specific DNA binding phosphoprotein *in vivo* and requires phosphorylation within its carboxyl region for enhanced DNA binding and activation (Chen et al., 2009). Phosphorylation at serine residue 186 (Ser186) within the Zta carboxyl region results in lytic cycle activation following initial activation of the BRLF1 promoter, Rp (Adamson and Kenney,

1998; Francis et al., 1999; Francis et al., 1997) whereas phosphorylation by casein kinase II leads to activation of late lytic gene expression (El-Guindy and Miller, 2004). Zta and Rta also interact with ZREs within *oriLyt* domains to initiate replication of EBV DNA during the lytic cycle (Fixman et al., 1992). Phosphorylation at S173 within the Zta carboxyl region leads to enhanced Zta binding and viral replication (Chen et al., 2009; Kolman et al., 1993). The EBV genome is extensively methylated in latently infected cells (Ernberg et al., 1989; Minarovits et al., 1991). Methylation may suppress lytic gene expression, whilst preventing latent gene expression and maintaining EBV persistence *in vivo* by immune evasion (Paulson and Speck, 1999; Robertson and Ambinder, 1997). Zta has a high affinity for methlyated DNA and activates lytic EBV gene expression from the methylated EBV genome (Bhende et al., 2005), through sequence-specific binding to highly methylated cytosine-phosphatidyl-guanosine (CpG) motifs within ZREs (Bhende et al., 2005; Chen et al., 2009) located in promoter regions of several early lytic genes (Kalla et al., 2010), and preferentially activates methylated DNA of the BRLF1 promoter, Rp (Bhende et al., 2004). Zta can regulate the expression of cellular genes including c-Fos, Fra-1, Jun and Jun-B through binding to the AP-1 site (Chen et al., 2009), as well as regulation of p53 and c-myc through interactions with another domain (Zhang et al., 1994) and the secretion of numerous cytokines namely IL-10, IL-8, TNFα and IFN-γ through interactions with ZREs within these genes (Chen et al., 2009).

### 1.4.4 Reactivation of latency *in vitro*

EBV can transform primary resting B lymphocytes *in vitro* and induce them indefinitely into proliferating B lymphocytes known as lymphoblastoid cell lines (LCLs). EBV is harboured in

LCLs as an extrachromosomal EBV episome. LCLs are normally characterised by the constitutive expression of all nine latency genes and mRNA transcripts, known as latency III, as well as several B-cell activation markers (Young and Rickinson, 2004). Examples of available LCLs include Raji, B95.8, Akata, Daudi and P3HR-1, which are characterised by mutations in the EBV genome and expression of the different latency programmes (Fields et al., 2007). Latently infected EBV can be induced into viral replication through various stimuli. A number of agents can reactivate the EBV lytic cycle *in vitro* by activating BZLF1 expression (Fields et al., 2007). These include phorbol esters such as 12-*O*-tetradecanoyl phorbol-13-acetate (TPA), which activate the protein kinase C (PKC) pathway (Davies et al., 1991). TPA is often used in synergy with sodium butyrate (NaB), a histone deacetylase inhibitor (Luka et al., 1979). Other inducing agents include the demethylating agent azacytidine, halogenated pyrimidines such as 5-iododeoxyuridines; nitrosamines, calcium ionophores, superinfection with P3HR1 and more physiologically relevant stimuli including, cytokine transforming growth factor-β (TGF-β)(di Renzo et al., 1994) and cross-linking of B-cell surface receptor (BCRs) with anti-immunoglobulin (anti-IgG) antibodies of Akata cells (Fields et al., 2007; Shimizu and Takada, 1993b; Takada, 1984).

### 1.4.5 Phorbol ester induction of ZEBRA

Phosphorylation is a common mechanism for regulating the function of proteins (Bhende et al., 2005) and Zta requires phosphorylation within its carboxyl-terminal domain to enhance its DNA binding affinity for lytic cycle activation (Chen et al., 2009). Phorbol esters, such as TPA are among the most reproducible and widely used lytic cycle inducers (Davies et al., 1991) and the

PKC pathway has been linked to phosphorylation of Zta at serine 186 (ser186) within the C-terminal domain, and is essential for lytic cycle activation by TPA (Baumann et al., 1998b).

### 1.4.6 EBV early genes

Approximately 30 EBV early genes are transcribed following expression of the IE transactivator BZLF1. The early genes are not transcribed prior to replication of the EBV genome as demonstrated in the presence of inhibitors of protein synthesis (Fields et al., 2007; Yuan et al., 2006). The majority of these genes encode proteins that act as enzymes in EBV DNA replication. However, as summarised in Table 1.4, these genes also have roles in transcription regulation, RNA transport and stability, viral protein kinase activity, apoptosis, inhibition, and immune evasion (Fields et al., 2007).

**Table 1-4 EBV early genes and their proposed functions**

| Gene | Proposed function |
|---|---|
| *BALF1* | Bcl-2 homologue, suppressor of anti-apoptosis protein BHRF1, potential role in tumorigenicity and metastasis |
| *BALF2* | Single-strand DNA binding protein (mDBp), part of replication fork/machinery |
| *BALF3* | Terminase large subunit/ATPase |
| *BALF5* | Viral DNA polymerase |
| *BaRF1* | Ribonucleotide reductase |
| *BARF1* | Binds hCSF-1, probable immunomodulation, oncogene, |
| *BBLF2* | Part of helicase-primase complex |
| *BBLF3* | Part of helicase-primase complex |
| *BBLF4* | Helicase, part of helicase-primase complex |
| *BcRF1* | Unknown function; probable TATT binding function |
| *BDLF4* | Protein (gp115) |
| *BFLF1* | Cytosolic zinc-binding protein, cysteine rich;Egress of capsids from nucleus; putative role in DNA packaging |
| *BFLF2* | Putative tegument; Nuclear localization of capsids & DNA, nuclear membrane phosphoprotein, part of intracellular virions, egress protein, complex with BFRF1 |
| *BFRF1* | Nuclear membrane protein p38, transmembrane with large cytoplasm domain, complex with BFLF2 key protein for EBV |

| | |
|---|---|
| | maturation |
| *BFRF2* | Unknown function; not included in virions |
| *BGLF4* | Serine/threonine protein kinase (PK), Phosphorylation of BMRF1, EBNA-LP, translation elongation factor 1 and motifs recognised by cdc2 kinase, production of infectious virus, |
| *BGLF5* | Alkaline exonuclease & Host-shutoff immune evasion |
| *BHRF1* | Bcl-2 homologue (Anti-apoptotic activity) |
| *BILF1* | G-protein coupled receptor gp64; Immunoregulatory function; Immune evasion by targeting MHC 1 for degradation; potential cell transformation |
| *BKRF3* | Uracil-DNA glycosylase |
| *BLLF2* | Unknown function |
| *BLLF3* | dUTP pyrophosphatase, dUTPase |
| *BSMLF1 (SM)* | RNA binding protein, regulates mRNA stability of viral DNA polymerase RNAs, processing and export of mRNA transcripts from nucleus to cytoplasm, enhances STAT1 expression |
| *BMRF1* | Viral DNA polymerase-processivity factor, early antigen protein (EA-D, polymerase accessory protein); transactivator of *oriLyt* and cellular gastrin promoter, replication protein |
| *BNLF2a* | Potential membrane protein; immune evasion; TAP inhibitor |
| *BNLF2b* | Putative gp141 |
| *BORF2* | Viral dUTPase gene, deoxynucleotide metabolism |
| *BRRF1* | Enhancement of lytic cycle induction, transcription factor |
| *BSLF1* | Primase, subumit of the helicase-primase complex, part of the replication machinery |
| *BXLF1* | Viral thymidine kinase, deoxynucleotide metabolism, phosphorylation of acyclovir |
| *BXRF1* | Nucleoprotein |
| *LF1* | Protein LF1, contains a dUTPase like domain |
| *LF2* | Protein LF2, contains a dUTPase like domain |
| *LF3* | Proline-rich protein LF3, unknown function, tandem repeats, region containing *ori*Lyt |

### 1.4.7 EBV lytic DNA replication

EBV lytic DNA replication is initiated from the origin of lytic replication (*oriLyt*) and highly dependent on several EBV-encoded proteins (Hammerschmidt and Sugden, 1988). The EBV genome is amplified 100-1000 fold during the viral productive cycle (Tsurumi et al., 2005). This process probably occurs through a rolling circle mechanism involving the formation of long head-to-tail concatemers that are cleaved into unit-length DNA genomes and packaged into viral capsids (Daikoku et al., 2005; Zimmermann and Hammerschmidt, 1995). Lytic EBV replication requires seven EBV proteins including the immediate-early transactivator Zta as well as six early

proteins (BALF5, BMRF1, BALF2, BBLF4, BSLF1 and BBLF2/3), that function as the DNA polymerase, DNA polymerase processivity factor, the single-stranded DNA binding protein and helicase, primase and primase-associated proteins, respectively (Fixman et al., 1995). Zta is indispensable for initiating lytic replication by directly binding and activating ZREs within promoters of *oriLyt* (Schepers et al., 1996). Moreover, through binding to *oriLyt*, Zta is also thought to mediate and stabilise interactions between the six EBV early replication proteins to form a replication initiation complex at *oriLyt* (Gao et al., 1998; Tsurumi et al., 2005), from which viral replication can proceed. All replication proteins, with the exception of Zta are thought to participate at replication forks to synthesize leading and lagging strands of the concatameric EBV genome (Tsurumi, 2001).

### 1.4.8 EBV late genes

Approximately 40 EBV late genes are transcribed following EBV replication. Expression of these genes is prevented by inhibitors of DNA synthesis (Yuan et al., 2006). The late genes encode predominantly structural proteins, including six capsid proteins, numerous tegument proteins and ten envelope glycoproteins, of which gp350/220 is the most abundant (Johannsen et al., 2004). The EBV late proteins function largely in assembly, egress and fusion, of which five glycoproteins (gb, gH, gL, gM and gN) are essential, although structural proteins required for viral DNA packaging are poorly characterised. The EBV late genes and their functions are summarised in Table 1.5.

**Table 1-5 EBV late structural proteins and their proposed functions**

| Gene | Structural protein type | Proposed function |
|---|---|---|
| *BALF4* | Envelope glycoprotein gB/gp110 | Fusion |
| *BBLF1* | Myristylated tegument protein anchored in envelope | Alkaline exonuclease; homologue of herpesvirus UL11 |
| *BBRF1* | Portal capsid protein | |
| *BBRF2* | Tegument protein | Unknown function |
| *BBRF3* | Envelope glycoprotein gM | Putative role in post-fusion events, part of gM/gN complex |
| *BcLF1* | Major capsid protein | Capsid assembly |
| *BCRF1* | Viral interleukin-10 (vIL-10) homologue | Protects virus from host response |
| *BdRF1* | Scaffold protein | Capsid assembly |
| *BDLF1* | Triplex 2 | Capsid assembly |
| *BDLF2* | Putative tegument | Unknown function |
| *BDLF3* | Putative envelope glycoprotein gp150 | Entry, virus lacking gp150 is more infectious for epithelial cells |
| *BDLF3.5* | Putative tegument | Unknown function |
| *BDRF1* | Putative ATPase subunit of terminase | putative DNA-packaging protein |
| *BFRF1A* | | Unknown function |
| *BFRF3* | Small capsid protein | Capsid assembly |
| *BGLF1* | Glycoprotein gp115 | DNA packaging |
| *BGLF2* | Tegument protein MyrPBP | |
| *BGLF3.5* | Putative tegument protein; Splice | Unknown function |
| *BGLF3* | Putative tegument protein, UL14 homologue | Unknown function |
| *BGRF1* | DNA-packaging protein, | putative ATPase subunit of terminase |
| *BILF2* | Membrane glycoprotein gp78/55 | Strucutral component |
| *BKRF2* | Glycoprotein L precursor gL/p25 | Fusion, attachment to epithelial cell co-receptor, part of gHgLgp42 |
| *BKRF4* | Putative tegument phosphoprotein | Unknown function |
| *BLLF1a* | Envelope glycoprotein gp350 | Attachment to complement receptor 2 (CR2, CD21) |
| *BLLF1b* | Envelope glycoprotein gp220, obtained through in-frame splicing from BLLF1 Membrane glycoprotein gp78/55 | Attachment to complement receptor 2 (CR2, CD21) |
| *BLRF1* | Membrane glycoprotein gN | Putative role in post-fusion events, part of gM/gN complex |
| *BLRF2* | Tegument protein p23 | Unknown function |
| *BMRF2* | Multiple transmembrane glycoprotein | Unknown function, binds integrins, important for infection of epithelial cells; |
| *BNRF1* | Major tegument protein (MTP) | Viral surface protein involved in B lymphocyte binding |
| *BOLF1* | Large tegument protein-binding protein | Binding protein |
| *BORF1* | Triplex 1 | Capsid assembly |
| *BPLF1* | Large tegument protein | Debiquinating enzyme |
| *BRRF2* | Putative tegument protein | Unknown function |
| *BSRF1* | Palmitylated tegument protein (PalmP) | |
| *BTRF1* | Putative tegument | Capsid maturation |
| *BVLF1* | Putative tegument protein | Unknown function |
| *BVRF1* | Putative DNA packaging tegument protein; capsid-associated tegument protein | Seals DNA inside capsid; |
| *BVRF2* | Maturational protease | Capsid assembly |
| *BWRF1* | Putative tegument | Unknown function |
| *BXLF2* | Envelope glycoprotein gH/gp85 | Fusion, attachment to epithelial cell co- |

| | | |
|---|---|---|
| | | receptor, part of gHgLgp42 complex, chaperone for gH |
| *BZLF2* | Envelope glycoprotein gp42; | Interaction with HLA Class II co-receptor on B cells, part of gHgLgp42 complex |
| *BVLF1* | Putative tegument protein | Unknown function |

### 1.4.9 Viral homologues

In addition, four EBV lytic genes encode cellular homologues to assist EBV replication and production of infectious virus and prevent apoptosis of the infected host cell (Fields et al., 2007). These include viral interleukin-10 homologue (vIL-10; BCRF1), which functions to protect EBV from the host response, two bcl-2 homologues (BHRF1 and BALF1), which function in anti-apoptosis and a colony stimulating factor 1 (CSF-1) homologue (BARF1) that inhibits the IFN alpha response, by mimicking the IFN alpha receptor (Middeldorp et al., 2003).

## *1.5 EPIDEMIOLOGY OF EBV INFECTION*

The prevalence of EBV-1 and -2 varies depending on geographical location. Over 90% of the adult population are infected with EBV worldwide (Henle et al., 1969). EBV-1 is the most predominant subtype, particularly amongst healthy South East Asian and Caucasian individuals in the Western world where 80-90% are infected and the rest are infected by EBV-2. In contrast, EBV-2 is most predominant in equatorial Africa, except for New Guinea where both types are prevalent (Fields et al., 2007). In immunocompromised patients such as transplant recipients and HIV patients, multiple EBV-1 and -2 subtypes have been demonstrated and the pathogenesis of infection for both EBV subtypes is thought to be the same (Gratama and Ernberg, 1995; Rowe et al., 1998; Yao et al., 1998; Yao et al., 1991).

## *1.6 PATHOGENESIS OF EBV*

Up to 90% of the world's adult population become infected by EBV during their life-time (Henle et al., 1979). Primary EBV infections are usually acquired following contact with infected saliva after which the individual remains a life-long carrier. The epidemiology of EBV is different in underdeveloped compared to developed countries. In underdeveloped countries, most individuals acquire their primary EBV infection during early childhood with up to 90% of infants infected by the age of two and are either asymptomatic or have non-specific symptoms. In developed countries where overall hygiene standards are superior, two peaks of EBV infection are seen: (i) in pre-school infants and children (1-6 y) and (ii) in adolescents or young adults (15-25 y) (Crawford et al., 2006).

### 1.6.1 Infectious mononucleosis

Primary EBV infection usually occurs sub-clinically during childhood. However, EBV infection during late adolescence or adulthood manifests itself as infectious mononucleosis in 20-75% of cases (Crawford, 2001; Crawford et al., 2006; McAulay et al., 2007). Infectious mononucleosis is an acute benign self-limiting lymphoproliferative disorder (or immunopathological disease) accompanied by fever, pharyngeal inflammation and cervical lymphadenopathy (Hadinoto et al., 2008; Papesch and Watkins, 2001) and is characterised by a vigorous expansion of activated EBV-specific $CD8^+$ T cells (CTLs) circulating during the acute phase (Crawford, 2001; Crawford et al., 2006).

### 1.6.2 The immune response to EBV infection

$CD8^+$ T cells are the main effectors of the cell-mediated immune response and responsible for keeping EBV infection under control, whereas $CD4^+$ T cells are responsible for orchestrating virus-specific immune responses and essential for priming as well as maintenance of $CD8^+$ T cells (Robertson, 2005). $CD4^+$ T cells are classically divided into T helper (Th) cell subsets, Th1 and Th2 that elicit Th1 and Th2 responses, respectively (Gamadia et al., 2004). Polarisation of $CD4^+$ T cells determines whether a humoral (Th2) or cell mediated response (Th1) is elicited (Robertson, 2005). For instance, Th1 cells secrete effector cytokines, mainly interferon-gamma (IFN-γ), resulting in the expansion of $CD8^+$ T cells, effectors of a cell-mediated immune response that control EBV infection through cytolytic mechanisms (Maloy et al., 2000; Rentenaar et al., 2000). By contrast, Th2 cells are crucial for priming and maintenance of $CD8^+$ T cells through secretion of interleukin (IL)-4, IL-5 and IL-6 (Constant and Bottomly, 1997). Infectious mononucleosis is associated with a vigorous expansion of activated EBV-specific CTLs, consisting primarily of $CD8^+$ T cells directed against epitopes of EBV lytic antigens and to a lesser extent (2.5%), against latent epitopes (Callan et al., 1996). Moreover, the symptoms of infectious mononucleosis are attributable to cytokines, namely IFN-γ and IL-2 secreted by a Th1 response (Corsi et al., 2004). Although activated during acute and persistent infection, the frequency of $CD4^+$ T cells is much lower than $CD8^+$ T cells. Moreover, $CD4^+$ T cells target different latent epitopes than $CD8^+$ T cells (Williams et al., 2004). CTLs also contain significant numbers (around 10%) of natural killer (NK) cells that release inflammatory cytokines during innate immunity and are largely responsible for the clinical symptoms associated with primary infection and the activated Th1 immune response (Robertson, 2005). More recently, regulatory T

cells ($T_{reg}$) have been shown to contribute to the establishment of persistent EBV infection (Wingate et al., 2009).

### 1.6.3 EBV-associated diseases

Following a primary EBV infection in immunocompetent individuals, EBV remains as a life-long latent infection of the B cell compartment. However, EBV has the potential to transform B cells and epithelial cells leading to the development of several human cancers including Burkitt's lymphoma (BL), Hodgkin's disease (HL), nasopharyngeal carcinoma (NPC), gastric carcinoma (GC), and AIDS-associated lymphomas (AIDS-L) in immunosuppressed individuals (Gulley et al., 1996; Kennedy et al., 2003; Liebowitz, 1994; MacMahon et al., 1991; Raab-Traub, 2002; Weiss et al., 1989). In addition, post-transplant lymphoproliferative disease (PTLD) is a serious complication following allograft transplantation in immunosuppressed individuals and EBV infection is implicated in PTLD pathogenesis (Hopwood and Crawford, 2000; Rooney et al., 1995).

## *1.7 POST-TRANSPLANT LYMPHOPROLIFERATIVE DISEASE*

### 1.7.1 Overview of PTLD

PTLD is a B cell lymphoma that is frequently associated with an impaired T cell response in haematopoietic stem cell transplant (HSCT) and solid organ transplant (SOT) recipients who receive immunosuppressive drugs to prevent graft versus host disease (GvHD), as well as in

patients with acquired immunodeficiency (AIDS) caused by HIV infection (AIDS-related lymphoma) (Bhatia et al., 1996; Hopwood and Crawford, 2000). In HSCT, PTLD arises from the high dose radiation or myeloablative conditioning regimens used to either cause T-cell depletion or prevent graft rejection (Penn et al., 1969). In immunocompetent individuals, CTLs modulate the proliferation of EBV latently-infected B lymphocytes. However, in transplant recipients receiving immunosuppressants to prevent allograft rejection, this T cell response is impaired leading to uncontrolled proliferation of B lymphocytes, hyperplasia or frank PTLD (Cohen, 2000).

### 1.7.2 Classification of PTLD

PTLD represents a wide spectrum of EBV lymphoproliferative states including both hyperplastic and neoplastic entities and is now included in the World Health Organisation (WHO) classification of neoplastic diseases (Harris et al., 1997). According to these guidelines, PTLD is classified into four subtypes (Table 1.6) based on clinical and histological features: (i) early lesions, which include reactive plasmacytic hyperplasias (PH) and infectious mononucleosis-like illness PTLD (IM-like PTLD); (ii) polymorphic PTLD (P-PTLD) (including polymorphic lymphoma or polymorphic B-cell hyperplasia, which can also be a monoclonal lesion); (iii) monomorphic PTLD (M-PTLD) 'Lymphomatous' PTLD, also called immunoblastic lymphoma or myeloma, that include B-cell neoplasms and T-cell/NK cell neoplasms; and (iv) Hodgkin lymphoma (HL) and HL-like PTLD, which are very infrequent. Each type of PTLD is thought to represent the different stages of disease progression. Nearly all early PTLDs are polyclonal and associated with an EBV infection, whereas M-PTLD and P-PTLD are usually monoclonal, EBV-

negative and associated with genetic alterations (Table 1.6) (Harris et al., 1997; Knowles et al., 1995). Early PTLD occurs within the first two years after transplant, frequently in paediatric patients and are usually EBV-associated and polyclonal proliferations. Early PTLDs can be aggressive and fatal but usually regress in response to reduction in immunosuppression (RIS) (Harris et al., 1997). P-PTLD and M-PTLD may also arise soon after transplant, although M-PTLD tends to occur late. Compared to P-PTLD, M-PTLD is frequently associated with genetic alterations of proto-oncogenes and tumor suppressor genes, is highly aggressive and generally does not respond well to RIS (Dotti et al., 2002; Harris et al., 1997; Robertson, 2005).

**Table 1-6 World Health Organisation Classification of PTLD**

| Categories of PTLD | EBV status & latency phenotype | Clonal status IgVH or TCR rearrangements | Oncogene/tumour suppressor gene changes | Time from graft to PTLD | Incidence | Prognosis |
|---|---|---|---|---|---|---|
| **Early lesions** Plasmacytic hyperplasia (PH), infectious mononucleosis-like lesion (IM) | Always EBV positive (primary EBV infection) Latency III | Polyclonal | None | Within 3 months | 5% | Aggressive, responds well to RIS |
| **Polymorphic *PTLD*** (Intermediate stage)Polymorphic B cell hyperplasia and polymorphic B cell lymphoma | Always EBVpositive Latency II and III | Polyclonal or monoclonal | None | Variable | 15-20% | Variable response to RIS |
| **Monomorphic B cell *lymphomas:*** Diffuse large B cell lymphoma (DLBCL), Burkitt's lymphoma or Burkitt's-like lymphoma (BL) and myeloma or plasmacytoma-like lesions<br>**Monomorphic *T-cell lymphomas***: peripheral T cell lymphoma, hepatosplenic | Frequently EBVpositive<br>Rarely EBVpositive | Monoclonal | Cytogenetic abnormalities and mutations in *p53*, *Ras*, or *c-myc*. | 3 months to 2 year (median 1.3 year) | >60%<br><5% | Refractory to RIS (Aggressive malignancy with poor prognosis) |
| **Other types** (rare) Classic Hodgkin lymphoma-like PTLD | Frequently EBV positive | Monoclonal | None | 3.5 – 7 year | <5% | ? |

EBV, Epstein-Barr Virus; PTLD, post-transplant lymphoproliferative disorder; ;RIS, reduction in immunosuppression; IgVH, immunoglobulin V heavy chain; TCR, T-cell receptor; Adapted from Harris et al. 1997 and Trappe et al. 2006

### 1.7.3 EBV and PTLD

Up to 90% of PTLD cases are EBV positive and express the latency III programme, although more restricted (heterogeneous) latency patterns have been found at the single cell level (Brink et al., 1997; Paya et al., 1999; Siemer et al., 2008; Young et al., 1989). However, cases (23-42%) of EBV-negative PTLDs have also been demonstrated (Leblond et al., 1998; Nelson et al., 2000). PTLDs are rare and usually fatal when diagnosed late. Nearly all cases of PTLD are of B cell origin (Allen et al., 2001). In addition, most are of recipient origin in SOT recipients, usually from reactivated EBV and of donor origin in HSCT recipients (Baumforth et al., 1999). However, in paediatric SOT recipients, in particular liver transplant recipients, PTLDs are usually associated with primary EBV infection acquired from the donor organ (Capello et al., 2009). PTLD usually develops within the first six months post transplant (Curtis et al., 1999). Although the reason for PTLD is unclear, it is likely that any factor that reduces T-cell immunity and increases B cell proliferation could precipitate the condition (Siemer et al., 2008).

### 1.7.4 Origin of PTLD

One theory for the origin of PTLD is based on the hypothetical model of latent EBV persistence (Figure 1.5)(Thorley-Lawson and Gross, 2004). Thorley-Lawson *et al.* propose that EBV would normally use the growth programme to differentiate into resting memory B cells and any B cells unable to exit the cell cycle would be targeted by EBV-specific CTLs. Based on the model of EBV persistence, EBV lymphomas such as PTLD would arise when so-called ‘by stander B cells’ (naive B cells in HD and BL) are infected by EBV and unable to exit the germinal centre as resting memory B cells (Robertson, 2005; Thorley-Lawson and Gross, 2004). EBV normally infects and activates naive or primary resting B cells to become

proliferating lymphoblasts that differentiate into memory cells and exit the cell cycle, without progression to PTLD. This is irrespective of the immune status since PTLD tumours that arise are not derived from naive B cells. Therefore, Thorley-Lawson *et al.* suggest that PTLD may arise when B cell types, other than naïve B cells, known as bystander cells are infected by EBV by chance and driven into the growth programme. An alternative theory is that B cells derived from the germinal centre (GC) or memory B cells could express the growth programme and, unable to exit the cell cycles proliferate into PTLD in the absence of an effective T-cell response. Moreover, EBV-seronegative recipients are at increased risk for PTLD since EBV DNA loads are elevated during primary EBV infection increasing the likelihood of EBV infection of bystander B cells (Robertson, 2005; Thorley-Lawson and Gross, 2004). Therefore, PTLD can arise in a rare event when EBV transforms bystander B cells into proliferating lymphocytes in the presence of an impaired T-cell immune response that cannot eliminate these rare B cells (Siemer et al., 2008). Recently, it has been confirmed that PTLD, in particular late PTLD, is derived from B cells that have experienced the GC reaction, whose development is the result of accumulating genetic alterations of proto-oncogenes and several tumour-suppressor genes, namely *c-MYC*, *BCL-6* and *p53* (Cesarman et al., 1998; Vakiani et al., 2008). The genetic alterations of proto-oncogenes involve aberrant somatic hypermutation (ASHM), targeting immunoglobulin variable genes (IgV) (Capello et al., 2003; Cerri et al., 2004; Timms et al., 2003). Moreover, ASHM is demonstrated almost exclusively in M-PTLD. Notably, about 50% of PTLDs express a functional surface B cell receptor (BCR) as a result of ASHM (Brauninger et al., 2003; Timms et al., 2003). EBV is thought to rescue these abnormal BCR-deficient B cells from apoptosis, by substituting two of its latent apoptotic proteins LMP1 and LMP2A for the BCR, enabling progression to PTLD (Bechtel et al., 2005).

### 1.7.5 Incidence and risk factors for PTLD

The cumulative incidence of PTLD is much lower in HSCT recipients (0.5-1%) compared with SOT recipients (1-20%) and highest within the first six months post-transplant for both groups (Curtis et al., 1999). Risk factors for SOT include EBV serostatus pre-transplant, primary EBV infection, transplant type, intensity of immunosuppression, CMV co-infection, length of post-transplant follow-up and transplant age independent of EBV serostatus (Beveridge et al., 1984; Cox et al., 1995; Walker, 1995; Walker et al., 1995). Internationally, the incidence of PTLD varies widely according to the transplant type with highest rates reported for lung and small bowel (10-20%), followed by heart or heart-lung (heart 2-10%, lung 4-8%), and liver (2-8%) and lowest for kidney transplant recipients (2%) (Jain et al., 2002; Leblond and Choquet, 2004; Opelz and Dohler, 2004). The incidence also varies according to the different immunosuppressive regimens used (Penn, 1991). In addition, length of time post-transplant is another risk factor; the cumulative risk of PTLD shows a gradual increase in the first two (10%), five (30%) and over five years (60%) post-transplant (Dotti et al., 2002). However, EBV seronegativity pre-transplant is considered to be the most important risk factor for PTLD, since patients acquire a primary EBV infection immediately after transplant. Paediatric patients, of which 90% are seronegative at transplant, are at particular risk, where PTLD accounts for 52% of cases (Ho et al., 1988; Holmes and Sokol, 2002). The incidence of PTLD is highest in some paediatric series compared with adults (2-3% versus 10%) (Jain et al., 2002; Leblond and Choquet, 2004). The incidence is also greatest in the first 3 months post-transplant (Katz et al., 2007). Moreover, primary EBV infection, not reactivation, is considered a greater risk factor (Allen et al., 2005; Benden et al., 2005; Ho et al., 1988; Scheenstra et al., 2004). Cytomegalovirus (CMV) seronegativity pre-transplant is also associated with an increased risk for PTLD (Manez et al., 1994). Major risk factors for allo-SCT recipients include T-cell depletion, age (≥50 years), specific anti-

lymphocyte therapy for Graft versus host disease (GvHD) and human leukocyte antigen (HLA) mismatch (related and unrelated) (Baumforth et al., 1999; Curtis et al., 1999; Zutter et al., 1988). The incidence increases up to 22-24% when two or more risk factors are involved (Curtis et al., 1999; Rooney et al., 1998). In patients with no risk factors a cumulative incidence of 0.2% versus 8.1% for patients with three or more risk factors has been reported (Landgren et al., 2009). In allo-SCT recipients, the recipient's age, EBV-seronegative status and underlying disease are not major risk factors for PTLD, as they are for SOT recipient's (Landgren et al., 2009).

### 1.7.6 Clinical features of PTLD

The clinical features of PTLD are often non-specific and include fever, sweats, generalised malaise, enlarged tonsils, and cervical lymphadenopathy or sepsis-like syndrome with rapidly progressing lymphoma (Shroff and Rees, 2004). In recipients who have acquired a primary EBV infection, the symptoms are more distinct and closely resemble infectious mononucleosis. PTLD may affect any organ including the central nervous system (CNS), bone marrow, intestine, kidneys, liver, spleen and lungs. Often diffuse disease is diagnosed only at autopsy in patients thought to have sepsis or GvHD (McWilliams et al., 2006). Therefore symptoms of PTLD appear diverse and often occur simultaneously, making an accurate diagnosis difficult. For this reason, histological investigations are required to differentiate IM from PH and other neoplasm's (Shroff and Rees, 2004). PTLD can be successfully treated with reduction of immunosuppression to reconstitute the immune system. Other treatment options include antiviral therapy, use of anti-B-cell monoclonal antibody such as Rituximab®, interferon-alpha (IFN-α), radiation therapy, chemotherapy and more recently, cytotoxic T cell therapy is being investigated as both prophylactic and therapeutic measures (Loren et al., 2003).

## *1.8 DIAGNOSIS OF PTLD*

The heterogeneous and extranodal presentation of PTLD can make its diagnosis extremely difficult. During the early signs and symptoms of PTLD, imaging techniques are used to localise the tumour. In addition, B cell clonality tests, serology and, more recently, polymerase chain reaction (PCR) for early diagnosis further aid PTLD diagnosis (Cohen, 2000; Gulley and Tang, 2008).

### 1.8.1 Histology

Histopathological analysis of tissue biopsy for morphological features remains the principle method for determining a definitive diagnosis of PTLD and moreover, for distinguishing the different subtypes of PTLD. For histopathological analysis, light microscopy is used to examine infiltrates of lymphocytes for morphological changes. Moreover, immunohistochemistry (IHC) and *in-situ* hybridisation (ISH) are essential for detecting EBV infections, usually by EBV latent antigen expression in the tumour biopsy (Gulley and Tang, 2008). IHC usually involves flow cytometry, western blot and enzyme-linked immunosorbent assays (ELISA) for detection of antibodies against LMP-1 or EBNA-2 antigens, whereas ISH is a highly sensitive technique that typically stains for EBV-encoded RNAs (EBERs) to confirm EBV-associated PTLD (Gulley and Tang, 2008; Lones et al., 1997).

### 1.8.2 Immunophenotyping and molecular analysis

B cell clonality tests are useful but not essential for classification of polyclonal or monoclonal PTLD and are based on determination of cell surface heavy and light chain Ig expression. In addition, abnormal cells may be positive for B-cell markers (CD19, CD20, CD21 and CD22). Although highly specific for PTLD diagnosis, the techniques involved are not available in all

transplant centres (Preiksaitis and Keay, 2001). Following the interpretation of histopathological, immunophenotyping and molecular analysis, patients are classified into one of four PTLD subtypes according to WHO criteria (Table 1.6) (Harris, 1997).

### 1.8.3 Serology

Serology is performed by measuring IgG antibodies to the EBV viral capsid antigen (VCA), early antigen (EA) and the EBV nuclear antigen (EBNA). In immunocompetent individuals, primary EBV infection results in seroconversion and the detection of VCA IgM, IgG and early antigen (EA-D) antibodies which defines acute EBV infection. While IgM only lasts a few months, IgG remains for life. Antibodies to EBNA develop late in infection during convalescence and also persist for life. The absence of all antibodies defines no EBV infection and is seen in EBV-seronegative individuals. Serology has limited use in PTLD diagnosis for a number of reasons including the lack of detectable antibodies. For instance, EBNA-1 IgG is not detected during acute infection in persistently immunosuppressed patients (Cen et al., 1993; Preiksaitis and Keay, 2001). Further, in EBV-seropositive patients, declining EBNA-1 IgG correlates with elevated EBV DNA loads and PTLD development (Preiksaitis et al., 1992; Preiksaitis and Keay, 2001; Riddler et al., 1994). It is however the standard approach for diagnosis of a primary EBV infection in previously EBV-naive individuals, although it is useful for predicting the risk of developing PTLD, which is greatest in EBV-seronegative recipients.

### 1.8.4 Early diagnosis of PTLD

Early diagnosis of PTLD is crucial for a successful outcome by enabling prompt therapeutic interventions (Gulley and Tang, 2008). While PTLD is traditionally diagnosed by histology,

several newer approaches have been employed for the early diagnosis of PTLD including: (i) Detection of IgM-related protein in serum and urine of patients with PTLD using monoclonal antibody tests (Badley et al., 1996); (ii) Detection of CD19+ B cells in the peripheral blood of PTLD versus non-PTLD patients; and (iii) more encouragingly, the use of polymerase chain reaction (PCR) for the serial monitoring of EBV DNA loads in clinical samples of patients at high risk of PTLD (Preiksaitis and Keay, 2001).

#### 1.8.4.1 Polymerase chain reaction for viral load monitoring

EBV DNA is considered to reflect EBV-induced B-cell proliferation and EBV DNA levels in PBMCs, plasma or whole blood has been proposed as a means of identifying SOT or HSCT recipients at risk of PTLD (Baldanti et al., 2000; Thorley-Lawson and Gross, 2004). PCR is a highly sensitive method for quantifying viral loads and differentiating healthy low-level viral load carriers from high-viral load carriers at risk of disease (Gulley and Tang, 2008). A number of methods have been developed to quantify EBV DNA levels in peripheral blood, including semi-quantitative PCR (Green et al., 1998; Gustafsson et al., 2000; Lucas et al., 1998; Riddler et al., 1994; Rowe et al., 1997; Rowe et al., 2001; Savoie et al., 1994), end-point dilution (Kenagy et al., 1995; Riddler et al., 1994), quantitative competitive PCR (Bai et al., 1997; Baldanti et al., 2000; Rowe et al., 1997; Stevens et al., 2001; Stevens et al., 1999; Yang et al., 2000), and more recently, real-time quantitative PCR (Jabs et al., 2001; Kimura et al., 1999; Niesters et al., 2000; Wagner et al., 2001). Real-time PCR assays enable rapid virus detection in a closed system, with high sensitivity and low contamination due to removal of post-amplification detection procedures (Gulley and Tang, 2008).

EBV DNA viral load monitoring is widely used in transplant centres not only for routine monitoring, but for early diagnosis and pre-emptive therapy before overt EBV-associated

PTLD develops (Holmes et al., 2002). A number of studies have demonstrated a correlation between high viral loads in the peripheral blood that precede the development of PTLD (Baldanti et al., 2000; Gartner et al., 2002; Hoshino et al., 2001; Kenagy et al., 1995; Lucas et al., 1998; Riddler et al., 1994; Savoie et al., 1994; Wagner et al., 2002; Wagner et al., 2001). However, others have previously shown that increased viral loads alone do not always precede PTLD (Hopwood et al., 2002; Lucas et al., 1998; Savoie et al., 1994), particularly in SOT recipients (Dolcetti, 2007). In general, PTLD in the paediatric cohort is associated with very high viral loads in the peripheral blood that often precede onset of clinical symptoms (Green et al., 1998; Kenagy et al., 1995; Lucas et al., 1998; Scheenstra et al., 2004). These viral loads decline when PTLD regresses in response to therapy (Lee et al., 2005). Furthermore, recent findings from serial viral load monitoring have identified two groups of patients with viral loads that do not correlate with the onset of PTLD: (i) those with chronic high viral loads (Gotoh et al., 2010; Green and Webber, 2007; Qu et al., 2000; Rowe et al., 1997) and (ii) those with persistently low viral loads (Green et al., 2000). In the latter study, persistently low viral loads within the first six months post-transplant were suggested as predictive markers for PTLD in paediatric intestinal transplant recipients since none of the recipients developed PTLD (Green et al., 2000). Therefore, although high viral loads are sensitive for the early diagnosis of PTLD they are not always specific (Green and Webber, 2002). Moreover, viral loads should not be used exclusively for early diagnosis of PTLD (Scheenstra et al., 2004). This together with the lack of standardisation in the assays and extraction methods used has made comparisons between viral loads amongst transplant centres difficult, particularly when determining a predictive cut-off level (Dolcetti, 2007). Therefore alternative markers are required.

### 1.8.4.2 Alternative early predictive markers of PTLD

Although useful in the pre-emptive management of PTLD, the use of EBV viral load alone in the early diagnosis of PTLD is insufficient and additional monitoring tests are required to improve their specificity and positive predictive value in PTLD in paediatric and adult SOT and HSCT recipients (Gartner and Preiksaitis, 2010). Several approaches have been investigated including measuring T-cell responses associated with elevated EBV viral loads (Clave et al., 2004; Meij et al., 2003; Sebelin-Wulf et al., 2007; Smets et al., 2002). One of these studies showed an association between impaired recovery of $CD8^+$ T cells and viral load and risk for EBV reactivation and PTLD (Meij et al., 2003). Other markers for PTLD that could aid PTLD diagnosis include measuring EBV gene expression, marked hypergammagobulinaemia, serological measurement of responses to EBV EA, measurement of T cell responses such as host cytokines IL-10 and IL-6, as well as host gene polymorphisms (Lee et al., 2006; Randhawa et al., 1995; Tosato et al., 1993), and serum IgE. Further, elevated EBV DNA loads in the presence of reduced immune responses were for the first time, shown to be more reliable predictors for PTLD, especially within high-risk EBV seronegative patients (Smets et al., 2002). Given that there is no absolute correlation between EBV viral load and PTLD development at the moment, measuring EBV gene expression in association with high EBV viral loads has been suggested as a potential approach (Rowe et al., 1998). The role of EBV in the pathogenesis of PTLD is unclear. Latent EBV infection is predominant in PTLD, in particular EBV latency III patterns are frequently associated with PTLD biopsy tissue and known to drive B-cell proliferation (Brink et al., 1997; Thorley-Lawson and Gross, 2004; Young et al., 1989). However, relatively little is known about the role of EBV lytic genes in PTLD development (Rowe et al., 1998). The demonstration of EBV lytic gene expression in tumour biopsies, suggests a role for EBV lytic replication and PTLD development (Montone et al., 1996; Niedobitek et al., 1997b; Oudejans et al., 1995;

Rea et al., 1994b). Therefore, analysis of host cellular gene expression together with EBV latent/lytic gene expression in relation to elevated EBV viral loads would provide additional information to help identify sensitive yet specific novel predictive markers of PTLD and possibly a predictive cut-off level.

#### 1.8.4.3 Early diagnosis of PTLD at King's College Hospital

In particular, the identification of early PTLD markers would benefit two transplantation cohorts at King's College Hospital (KCH): the paediatric solid organ transplant (SOT) recipients and adult umbilical cord blood transplant (UCBT) recipients. KCH is a leading institute for transplantation in the UK and one of the largest transplant centres in Europe, undertaking 160 transplants each year. Around 60 paediatric liver transplants and 20 adult UCBT are performed a year, for the treatment of acute liver failure and haematological malignancies such as leukaemia, respectively. As a result, the incidence of PTLD is increasing and early diagnosis is highly desirable to improve patient survival and prevent graft loss in these cohorts. Therefore, the availability of diagnostic tests to accurately identify transplant recipients at high risk for PTLD is lacking and alternative markers are required.

## *1.9 AIMS OF STUDY*

The aims of this study were to identify novel EBV and cellular gene markers that could be used to develop improved diagnostic assays for the early detection of PTLD. In order to identify these markers, the following three experimental approaches were undertaken:

(i) To identify highly induced EBV genes by analysing the expression of 88 EBV genes during the latent-lytic switch in the Raji cell line (an *in vitro* model system) using real-time RT-PCR with SYBR green based detection (Chapter 3)

(ii) To identify highly differentially regulated and expressed cellular genes in response to the EBV lytic induction phase in Raji cells, using Affymetrix human genome U133 Plus 2.0 GeneChip® arrays (Chapter 4)

(iii) To develop and validate real-time TaqMan PCR assays for the detection of EBV and cellular gene expression in whole blood samples from PTLD and non-PTLD transplant recipients, and to determine associations between gene expression levels and viral load (Chapter 5)

# 2 CHAPTER 2. MATERIALS AND METHODS

## 2.1 Suppliers and Manufacturer's

American Tissue Culture Collection, LGC standards, Teddington, Middlesex, UK

Sigma-Aldrich Company Ltd, Dorset, England, UK

Invitrogen Ltd, Paisley, UK

Hettich Zentrifugen, Buckinghamshire, UK

QIAGEN Fleming Way, Crawley, UK

Ambion Huntingdon, Cambridgeshire, UK

LabTech International Ltd Acorn House, The Broyle, Ringmer, East Sussex, UK

VWR International Merck House, Poole, Dorset, UK

Applied Biosystems Warrington, UK

Amersham Biosciences, UK Ltd

Metabion International AG, Lena-christ-str, Martinsried, Germany

Advanced Biotechnologies Ltd Abgene House, Bleinhem Road, Epsom, Surrey, UK

Bio-Rad Laboratories Ltd Bio-Rad, Hemel Hempstead, Hertfordshire, UK

Agilent Technologies UK Ltd Berkshire, UK

Affymetrix UK Ltd High Wycombe, UK

STAR LAB Ltd Milton Keynes, UK

Sarstedt Ltd 68 Boston Road, Beaumont Leys Leicestershire

SANYO Biomedical Europe

## 2.2 Materials (Equipment/Reagents/Plastic ware)

### 2.2.1 Equipment and instrumentation

Agilent® 2100 Bioanalyser (Agilent)

$CO_2$ incubator (SANYO MCO-17AIC)

GeneAmp® PCR system 9700 (Applied Biosystems)

GeneChip® scanner 3000 7G (Agilent)

Hettich Rotina 420R centrifuge (Hettich Zentrifugen, Cat. No. 4701)

Hettich haematocrit 210 centrifuge (Hettich Zentrifugen, Cat. No. 2104)

HG U133 Plus 2.0 GeneChip® (Affymetrix)

Magnetic stand-96 (Ambion P/N AM10027)

NanoDrop ND-8000™ Spectrophotometer (LabTech)

Perkin Elmer thermal cycler, PTC-225 (Applied Biosystems)

Rotorgene 6000™ (Qiagen)

Vortex mixer (STAR LAB)

### 2.2.2 Cell culture reagents

2-mercaptoethanol (Sigma-Aldrich Cat.No. M-7522)

Buffer RLT lysis buffer (Qiagen Cat. No. 79216)

Dimethyl sulphoxide (DMSO) (Sigma-Aldrich Cat. No. D2650)

Ethanol (Sigma-Aldrich Cat. No. 200-578-6)

Foetal Bovine Serum (FBS) (Sigma-Aldrich Cat. No. F2442-100ML)

Hanks' balanced salt solution (HBSS) (Sigma-Aldrich Cat. No. H9269)

L-glutamine (Sigma-Aldrich Cat. No. G7513)

Penicillin-Streptomycin solution (PSS) (LGC Promochem Cat. No. 30-2300)

Phorbol 12-myristate 13-acetate (PMA/TPA) (Sigma-Aldrich Cat. No. 79350-1MG)

Phorbol 12-myristate 13-acetate 1 mg/ml (Sigma-Aldrich Cat. No. 79346-1MG)

Phosphate buffered salt solution pH 7.2 (Invitrogen Cat. No. 20012-027)

Raji cell line (LGC Promochem Cat. No. ATCC-CCL-86™)

Ramos cell line (LGC Promochem Cat. No. ATCC-1596™)

RPMI-1640 medium 1X 500 ml (Invitrogen Cat. No. SKU#21875-091)

Sodium butyrate (SB) ≥99.0% (Sigma-Aldrich Cat. No. 19364-250MG)

Synth-a-Freeze® Cryopreservation Medium (Invitrogen GIBCO Cat. No. R-005-50)

Trypan Blue 0.4% solution (Sigma-Aldrich Cat. No. T8154)

### 2.2.3 PCR and molecular reagents

1 Kbp DNA ladder (Invitrogen Cat. No. 15615-016)

RNase-free DNase Set (DNASE70-SET) (Qiagen Cat. No. 79254)

EBV B95.8 quantitated viral DNA control (Autogen Bioclear Cat. No. 08-926-000)

Ethidium bromide, 10 mg/ml (Invitrogen Cat. No. 15585-011)

High Capacity cDNA Reverse Transcription kit (Applied Biosytems Cat. No. 4368814)

iQ SYBR Green Supermix (Bio-Rad Cat. No. 170-8884)

QIAshredder™ (Qiagen Cat. No. 79564)

Molecular grade water (Sigma-Aldrich Cat.No. 95284-100ML)

RETROSCRIPT® kit (AMBION Cat. No. AM1710)

RNeasy® Mini kit (Qiagen Cat. No. 74104)

Sterile RT-PCR grade RNase free water (Ambion Cat No. AM9935)

TaqMan® Gene Expression Assays (Applied Biosystems)

TaqMan® Gene Expression Master Mix (Applied Biosystems Cat.No. 4369016)

Tris-ethylamine diamine (TE) buffer solution pH 8.0(Sigma-Aldrich Cat.No. 93283)

Tris-borate Ethylamine (TBE) buffer 10X concentrate (Sigma-Aldrich Cat.No. T4415-1L)

Whole blood RNA extraction kit (Qiagen Cat.No. 52304)

UltraPure™Agarose (Invitrogen Cat.No. 16500-500)

QIAamp® RNA Blood Mini Kit (Qiagen Cat. No. 52304)

Message Amp$^{TM}$ Premier RNA amplification kit (Ambion, Cat.No. AM1792)

Gel loading: Orange G (Sigma-Aldrich Cat.No.) mixed with 5 ml of 100% glycerol

### 2.2.4 Plasticware

Conical tubes 15 ml; Conical tubes 50 ml (Ambion Cat.No.AM12500 ; Cat.No. AM12501)

Freezing-container Nalgene® Mr.Frosty (Sigma-Aldrich Cat.No. C1562)

Hemocytometer (VWR International Cat.No.720-0585)

Nuclease-free filter tips (STAR LAB UK Ltd Cat.Nos.S1121-3810 (0.1-10µl); S1120-1810 (1-20µl); S1120-8810 (1-200µl); S1122-1830 (101-1000µl)

Nunc® cryo tube vials (Sigma-Aldrich Cat.No. V7384-ICS)

RNase free microfuge tubes (Ambion Cat.No. AM12400)

Rotor-gene PCR tubes 0.1 ml (Qiagen Cat.No. 981103)

Sarstedt polypropylene microcentrifuge tubes 1.5 ml (Sigma-Aldrich Cat.No.72692)

Serological pipette sterile 10 ml, Ind. Wrapped 200 (STAR LAB Cat.No. E4860-1011)

Sterile graduated Pasteur pipettes 3 ml (VWR International Cat.No. 612-1747)

Tissue culture flasks T75 $cm^3$ (VWR Cat.No. 202-0200)

## *2.3 EBV GENE EXPRESSION ANALYSIS*

### 2.3.1 Cell culture

#### 2.3.1.1 Cell lines

Raji is an EBV-positive human B-cell line derived from Burkitt's lymphoma cells following infection of peripheral blood mononuclear cells (PBMCs), and is defective for DNA replication and late antigen expression (Pulvertaft, 1964). Ramos is an EBV-negative Burkitt's lymphoma cell line that is frequently used as a negative control. Cell lines were obtained from the American Tissue Culture Collection (ATCC). Raji (ATCC; CCL-86) and Ramos (ATCC; CCL-1596) cell lines were cultured in RPMI 1640 (Sigma-Aldrich) supplemented with L-glutamine 2 mM, 10% heat-inactivated foetal calf serum (Sigma-Aldrich) and 100 International Units (IU) penicillin/ml and maintained in a 5% $CO_2$ incubator at 37ºC. Cell lines were maintained in 75 $cm^3$ tissue culture flasks (VWR International) at a density of 3.5 x $10^5$ cells/ml. Cells were split every 2-3 days at dilutions of 1/3. Cell viability was assessed using trypan blue (Sigma-Aldrich) exclusion as described in section 2.3.1.2.

#### 2.3.1.2 Cell counts using Trypan Blue exclusion

Cell counts were performed using the trypan blue exclusion method described in ''Cell Culture Manual'' (Sigma-Aldrich). Briefly, cell suspensions were prepared by mixing 200 µl of cell culture, 300 µl of Hank's buffered salt solution (HBSS) and 500 µl of 0.4% trypan blue w/v (Sigma-Aldrich) and allowed to stand for 15 minutes before transfer to both chambers of the hemocytometer (VWR). The average number of cells in all five counting chambers was counted and multiplied by a dilution factor of five to determine (i) the number

of cells counted per ml of cell culture and (ii) the total number of cells in a 10 ml tissue culture volume.

#### 2.3.1.3 Cryopreservation of cells

Cell stocks for Raji and Ramos cells were cryopreserved for later use. Cells were first counted using trypan blue exclusion (see section 2.3.1.2) and reseeded to a density of 3 x $10^5$ cells per ml of cell culture. Cells were centrifuged at 500 x *g* for 5 min and re-suspended in 1 ml freezing media (10% dimethyl sulphoxide (DMSO) and 90% v/v foetal calf serum (FCS); (Sigma-Aldrich) prior to transfer into pre-cooled 2 ml cryovial tubes. Cryovials were transferred immediately to -80ºC for overnight storage and transferred to liquid nitrogen for long-term storage.

#### 2.3.1.4 Lytic cycle induction

For lytic cycle induction, Raji and Ramos cells were reseeded on day 1 at densities of 5x$10^5$ cells per ml and induced 24 hrs later at a density of 1x$10^6$ cells per ml with 12-*O*-tetradecanoyl-13-phorbol acetate (TPA) (Sigma-Aldrich) and sodium butyrate (NaB) (Sigma-Aldrich) at final concentrations of 30 ng/ml and 2mM, respectively. Duplicate cell culture flasks were set up for induced Raji and Ramos cultures, harvested at 0, 2, 6, 24 and 48 hrs post-induction. Duplicate flasks were also set-up for uninduced Raji and Ramos cells at the same time-points.

#### 2.3.1.5 Cell harvesting

Cells were harvested at 0, 2, 6, 24 and 48 hrs. Briefly, 10 ml of cell culture was transferred using sterile 10 ml pipettes (StarLab) from each tissue culture flask into sterile RNase-free 15 ml centrifuge tubes (Ambion). Cell cultures were centrifuged at 500 x *g* for 5 min and cell

pellets re-suspended in 600 µl of RLT buffer (Qiagen) with 10% v/v 2-mercaptoethanol (Sigma-Aldrich) and the cell lysate vortexed for a minimum of 15 s or until the cell pellet was no longer visible. Cell lysates were transferred immediately to -80ºC for up to 1 month until RNA extraction.

## 2.4 Molecular Methods

### 2.4.1 Total RNA Extraction

Total RNA was prepared from induced and uninduced Raji and Ramos cells at the various time-points: 0, 2, 6, 24 and 48 hrs and extracted using the RNeasy® Mini Kit (Qiagen), according to manufacturer's instructions. Briefly, frozen cell lysates were thawed during 5 minute incubation in a 37°C water bath prior to cell homogenisation and RNA extraction. Cells lysates were transferred to QiaShredder columns (Qiagen) and centrifuged at 22,130 x *g* for 2 min. Total RNA was extracted from the homogenised lysates using the RNeasy® Mini extraction kit (Qiagen), according to the manufacturer's instructions. Briefly, equal volumes (600 µl) of 70% ethanol (Sigma-Aldrich) were added to the homogenised lysates and mixed well by pipetting. Six hundred microlitres of the lysate was transferred to QIAamp mini spin columns and centrifuged at 11,290 x *g* for 1 min and the supernatant discarded. The remaining 600 µl was transferred to the same QIAamp mini spin column, re-centrifuged as before and the supernatant discarded. Six hundred microlitres of RW1 wash buffer was applied to the spin column and the spin column centrifuged at 11,290 x *g* for 1 min and the collected supernatant discarded. Contaminating genomic DNA was eliminated by an on-column DNase digestion after the first RW1 wash and prior to the first RPE elution step using the RNase-free DNase Set (Qiagen). Briefly, 70 µl of DNase I buffer (Qiagen) was mixed with 10 µl of DNase I stock (Qiagen) and 80 µl of the DNase mixture applied to the QIAamp

mini spin column for on-column DNAse digestion during a 15 min incubation at room temperature. Residual DNase I was then eliminated from the column following a second RW1 wash step by centrifugation at 11,290 x *g* for 1 min and the supernatant discarded. An additional centrifugation step at 22,130 x *g* was performed prior to the first elution step to remove all residual RW1 wash buffer. Next 60 µl of RPE elution buffer was applied to the spin column and centrifuged for 11,290 x *g* and total RNA eluted into new RNase free collection tubes and aliquots transferred immediately to -80ºC for storage prior to reverse-transcription.

### 2.4.2 Quantification of total RNA

The concentration (ng/µl) and purity of total RNA was determined at an absorbance of 260/280 nm using a NanoDrop ND-8000™ spectrophotometer (LabTech International).

### 2.4.3 Reverse Transcription

Two micrograms of total RNA was reverse-transcribed into cDNA using the RETROscript® Kit (Ambion) according to the manufacturer's instructions. Briefly, prior to reverse transcription, 12 µl reactions were set-up consisting of 2 µg total RNA and 2 µl of random decamers (50 µM) and the mixture heat-denatured at 75 ºC for 3 minutes in a water bath. The reaction mix was transferred immediately to ice for 5 min, centrifuged briefly and returned to ice. Following heat denaturation of RNA, 8 µl reaction mixes were set-up on ice consisting of 10X RT buffer, dNTP mix (2.5 mM each dNTP), 10 U/µl RNase inhibitor (RNase I) and 100 U/µl of Moloney-murine leukaemia virus reverse transcriptase (MMLV-RT) and applied to the previous 12 µl reaction mix. Reverse transcription was carried out in 20 µl reactions in a water bath at 42ºC for 1 hr and reverse transcriptase inactivated with a final incubation at

92ºC for 10 min. All cDNAs were diluted 1/10 with sterile nuclease free water (Qiagen) and cDNA aliquots transferred immediately for storage at -20ºC until real-time PCR analysis.

### 2.4.4 Quality controls for total RNA

The presence of residual genomic DNA in the total RNA extract was evaluated by performing a minus RT-reaction (minus M-MLV RT) as described in section 2.4.3 with the RT-enzyme substituted by sterile RNase-free water (Ambion), followed by PCR amplification using the programme described in section 2.4.7. All 'minus RT' controls were carried out with 2 µg total RNA.

### 2.4.5 Primer sequences for real-time PCR gene expression analysis

Eighty-nine EBV genes of known open reading frames (ORFs), were investigated for gene expression analysis and cDNAs derived from these genes amplified by real-time PCR. Of the 89 genes, seven were splice variants (*BBLF2/BBLF3*, *BGRF1/BDRF1*, *EBNA3B/3C* and *BWRF1*. PCR primer sequences for 78 of 89 transcripts including the single copy housekeeping gene, Beta-actin (*ACTB*) were obtained from the literature (Pan et al., 2005). Three of the 89 published primer sets *LMP-2A* (previously *LMP-2*); *BKRF2* (previously gp25) and (*BSMLF1*) (previously *BSLF1* and *BMLF1*) were redesigned using the Invitrogen Oligo Perfect™ Designer software (Invitrogen, UK) for newly available GenBank sequences of the EBV-1 genome (Accession number NC_007605) found at the National Center for Biotechnology Information (NCBI) (http://www.ncbi.nih.gov). PCR primers were subsequently designed using the Invitrogen design software for a further seven genes (*A73/RPMS1, BDLF3.5, BFRF1A, BGLF3.5, LF1, LF2* and *LF3*) and an additional primer set for *BARF0* was published (Kienzle et al., 1998) to encompass the entire EBV-1 genome (Accession number NC_007665). Criteria for primer design consisted of: Tm of 58-60 °C,

18-30 bp length, and 20-80% GC content. Primer sequences for all 89 EBV genes and *ACTB* are shown in Table 2.1. The product length (bp) ranges from 57-289 bp. All primer sequences were obtained from Metabion International. Of note, *BERF1* (also known as *EBNA-3A*) was subsequently excluded from gene expression analysis. In addition, primer pairs for the fifteen overlapping genes were excluded from further analysis.

### 2.4.6 Real-time PCR for validation of primer specificity

All 89 primer pairs were validated for EBV amplification by PCR as described below using control DNA from the EBV strain B95-8 (Advanced Biotechnologies, Cat. No. 08-702-000), cDNA from induced Raji cells and gDNA from induced EBV-negative Ramos cells. PCR was carried out using the following PCR reaction and PCR programme described below. Real-time PCR analysis was performed using a Rotor-Gene 6000™ real-time instrument (Qiagen). Amplification of cDNA (1/10 dilution) and genomic DNA (gDNA) template was performed in triplicate using the iQ™ SYBR Green I Supermix (BioRad) with 1 µl of each cDNA template amplified in each 25 µl reaction volume:

For a single reaction:

| | |
|---|---|
| iQ™ SYBR Green I 2X Supermix (BioRad) | 12.5 µl |
| Primer detection mix (10 pmols F/R) | 2 µl |
| Sterile nuclease-free water | 9.5 µl |
| cDNA template | 1 µl |
| Total reaction volume | 25 µl |

Real-time PCR was performed using the following programme:

95ºC for 10 min (hold)

50 cycles of:

95ºC for 10 sec (denaturation)

57ºC for 20 sec (annealing)

72ºC for 20 sec (extension)

Final extension:

72ºC for 1 min (hold)

Melt-curve analysis:

Ramp from 72ºC to 99ºC

Rising by 1ºC pre-melt to 5ºC

Fluorescence data was acquired during the extension step for 5 sec, when SYBR green I dye is released from the amplified double-stranded DNA and fluoresces. Melt-curve analysis was also used to verify primer specificity by the detection of single peaks. Real-time PCR with SYBR Green I detection is just as specific and sensitive as detection with probes. However, SYBR Green hybridises to all double-stranded DNA, resulting in the potential detection of non-specific amplicons (Qiagen, UK).

### 2.4.7 Agarose gel analysis of EBV specific PCR products

All 89 PCR products were analysed by 2% agarose gel electrophoresis. Agarose gels were prepared by melting 2g agarose powder (Invitrogen) in 100 ml of 1 X Tris-Borate-EDTA (TBE) buffer (Sigma-Aldrich) for 2 min at maximum power in a microwave. The melted agarose was cooled for 2 minutes before the addition of 5 µl of 10 mg/ml ethidium bromide (EtBr) (Sigma-Aldrich) and then swirled gently to distribute the EtBr before being poured into casting plates and allowed to set for 20 minutes before samples were loaded. Briefly, 10 µl of PCR products were mixed with 3 µl orange G gel loading dye and loaded onto agarose

gels. Twenty microlitres of 1 Kbp DNA ladder (Invitrogen) was loaded into the first well of each gel to enable comparative estimates of PCR product size. PCR products were separated by electrophoresis at 100 V for approximately 1 hr until the loading dye reached the end of the gel. PCR products were then visualised under ultra-violet (UV) illumination.

### 2.4.8 Validation of real-time PCR

Real-time PCR was performed on cDNA diluted at 1/2, 1/5, 1/10 and 1/20 dilutions in nuclease free water to assess the sensitivity of detection of the cDNA using PCR programme described in section 2.4.6. PCR amplification was tested on all cDNAs using primer sets (Shown in Table 2.1) for the immediate-early gene *BZLF1*, and the reference control *ACTB.*

#### 2.4.8.1 PCR controls

PCR controls included 1 µl of cDNA from EBV-negative Ramos cells (negative control), 1 µl of control DNA from the EBV strain B95-8 (Advanced Biotech Cat.No. 08-702-000), and 1 µl of sterile nuclease free water as a non-template background control.

### 2.4.9 Analysis of real-time PCR data

#### 2.4.9.1 Threshold cycle

The threshold cycle (Ct) is the cycle number at which the fluorescence generated within a reaction crosses the threshold line, usually set sufficiently above background fluorescence (Applied Biosystems). The Ct is a relative measure of the concentration of target in the PCR reaction; high Ct indicates low concentration of template, whereas low Ct indicates high concentration of target molecules in the sample (Bustin and Nolan, 2004).

#### 2.4.9.2 Comparative quantitation (ΔΔCt)

Relative expression was quantified using the 'Comparative Quantitation' method or $2^{-\Delta\Delta Ct}$ method (Schmittgen and Livak, 2008), similar to the previously published ΔΔCt method (Livak and Schmittgen, 2001) supplied on the Rotorgene software (version 5.0). ΔΔCt enables the dynamic amplification efficiency of each run to be determined by taking into account the take-off point, similar to the Ct (ΔΔCt) (Applied Biosystems). The Rotorgene software automatically calculates the take-off point for each amplified target. Relative expression was quantified as follows:

##### 2.4.9.2.1 Calculation of relative expression levels to *ACTB*

To calculate the ΔCt value or normalised value (i.e., relative expression to *ACTB*), the means of triplicate Ct values for *ACTB* were subtracted from the means of triplicate Ct values for each target using the formula: $\Delta Ct = Ct_{TARGET} - Ct_{ACTB}$.

##### 2.4.9.2.2 Calculation of fold-change

To calculate the ΔΔCt value (or fold-change), the ΔCt value for induced sample was divided by the ΔCt for uninduced sample using GraphPad Prism 5.0 software (Graphpad Prism, La Jolla, CA).

### 2.4.10 Statistical analysis

Data analysis including statistics and graphs were performed in GraphPad Prism. The statistical significance of fold-change was calculated using the student's pair wise t test. A *P*-value of less than 0.05 was considered statistically significant.

**Table 2-1 Primer sequences used for real-time PCR analysis of EBV gene expression**

| Target gene | Sequence | Amplicon size (bp) | Reference |
|---|---|---|---|
| *A73/RPMS1* | 5’-AGACACTCGATATCGAAGGCCAG-3’<br>5’-TCACCTTTGGCTGGTACAGC-3’ | 154 | In-house |
| *BALF1* | 5’-CTGTGCTACACAGTGGTGTT-3’<br>5’-GCAAACCAGAGTCTGCGATA-3’ | 116 | Pan et al. 2005 |
| *BALF2* | 5’-AAACTACGCTGTGGAGCA-3’<br>5’-AACTGCAGGTAGTAGG-3’ | 81 | Pan et al. 2005 |
| *BALF3* | 5'-CATCCTCCTTCCCCGTTT-3'<br>5'-GGCCTCTCTCGAGTTCTC-3' | 94 | Pan et al. 2005 |
| *BALF4* (gp110) | 5'-GGGCCTGTTGATGGTGTT-3'<br>5'-CGCGTACCAGCCATTGTA-3' | 106 | Pan et al. 2005 |
| *BALF5* | 5’-CAGCAGGCCTACTTCTA-3’<br>5’-AGGGTGATCTTGTGGTAGTC-3’ | 182 | Pan et al. 2005 |
| *BaRF1* | 5’-CGCTGCCTCCCTGTTATACA-3’<br>5'-TCCACGAGCCTCGATGAA-3' | 121 | Pan et al. 2005 |
| *BARF1* | 5'-GCTGTCACCGCTTTCTTG-3'<br>5'-GTGGTGCATGCGCCCAAT-3' | 138 | Pan et al. 2005 |
| *BARF0* | 5’-CCATATCAGGGAAGTCAGGA-3’<br>5’-CTGTTTACCCAGACCCTGAG-3’ | 250 | (Kienzle et al., 1998) |
| *BBLF1* | 5'-TGCCGACGACGAGTCAAC-3'<br>5'-TCGAGCCCCTCGTTGGTT-3' | 146 | Pan et al. 2005 |
| *BBLF2* | 5'-TCGACTACCGAACTCAAC-3'<br>5'-CGGTCTCGGGTTCTAAAT-3' | 125 | Pan et al. 2005 |
| *BBLF3* | 5'-GAGACCCGAGGCAGACAA-3'<br>5'-ACACGTGGCTTCCAGAGA-3’ | 173 | Pan et al. 2005 |
| *BBLF4* | 5’-AGAGCACCAGCGTTAG-3’<br>5’-ATAGACGGTTGGGCAGTA-3’ | 132 | Pan et al. 2005 |
| *BBRF1* | 5'-GATCTGCCAGCTCCTGAA-3'<br>5'-CAGGTTGTTGGAGGCATC-3' | 220 | Pan et al. 2005 |
| *BBRF2* | 5’-GCCCTGCTCTCGATGATTGA-3’<br>5’-TCCTCCAGGTCGTGGTACTT-3’ | 173 | Pan et al. 2005 |
| *BBRF3* | 5’-CCTCATCCTGCCCATCTTCT-3’<br>5'-CTTGGCGGAGACAAAGAC-3' | 154 | Pan et al. 2005 |
| *BcLF1* | 5'-CAGCGGACATTCATTGTG-3'<br>5’-CCACGTACTCTGCGTACT-3’ | 130 | Pan et al. 2005 |
| *BcRF1* | 5’-GAGATGCCCAGGGATTCACA-3’ | 170 | Pan et al. 2005 |

| | | | |
|---|---|---|---|
| | 5’-CACGGCAGACGTGGCTTATT-3’ | | |
| *BCRF1* | 5'-TCTCCGCAGACCCCATTT-3'<br>5'-TCCCTCCGCCGTTACTCT-3' | 104 | Pan et al. 2005 |
| *BDLF1* | 5’-ATTTGGACGAGAGCATGCCA-3’<br>5’-CAGGAGAATCTTCTGCAGCA-3’ | 112 | Pan et al. 2005 |
| *BDLF2* | 5'-GCCTCCACGCTGTTTCAT-3'<br>5'-CCCCACCGGCATAAAGCT-3' | 121 | Pan et al. 2005 |
| *BDLF3* | 5'-GACTAGCGCCCCTATAAC-3'<br>5'-GGTGGATGCGTTGGAAGT-3' | 110 | Pan et al. 2005 |
| *BDLF3.5* | 5’-TCAGAGACCTCCTGCTCAA-3’<br>5’-CGGATGCTCTGAAAGACAG-3’ | 151 | In-house |
| *BDLF4* | 5'-GCGAGTACCACGTATGTG-3'<br>5'-GGTCCTGTGTGTCTTGTC–3’ | 150 | Pan et al. 2005 |
| *BDRF1* | 5’-TTCGTGCACACCAAGGACAAGA-3’<br>5’-GCGTAGATGAGCCTCTCAAA-3’ | 93 | Pan et al. 2005 |
| *BdRF1* | 5’-CCCTCTACCGCAAGGACATA-3’<br>5’-GACGTATCTGGGCACTTCGT-3’ | 197 | Pan et al. 2005 |
| *BERF1* | 5’-ACGGCACAGGCTTGGAAT-3’<br>5’-TCGTTTGCCCGCTCTCAT-3’ | 246 | Pan et al. 2005 |
| *BFLF1* | 5'- TACGAGTCCCTCTCTCCA-3'<br>5'-GCCTGTGATGAGGCTAGA -3' | 162 | Pan et al. 2005 |
| *BFLF2* | 5’-CTTTCCCAACCCAGCCTTCT-3’<br>5’-CAAGCAGGTCTCTGGGATGT-3’ | 150 | Pan et al. 2005 |
| *BFRF1* | 5’-CGGACGACGATGCAGTTTCT-3’<br>5'-GACTTGACCAGACCGAGA-3' | 111 | Pan et al. 2005 |
| *BFRF1A* | 5’-GTTTCTCGCCTATGATCCAC-3’<br>5’-AAATAAGACCTCACGCTGGA-3’ | 156 | In-house |
| *BFRF2* | 5’-CTTGTCCCTTTCAGTGGTCA-3’<br>5’-CAGGCAGCTATTCTATCGGA-3’ | 126 | Pan et al. 2005 |
| *BFRF3* | 5'-GGTGCTCATGCACACCTT-3'<br>5'-CCGGAGGCTGCTAATAGA-3' | 154 | Pan et al. 2005 |
| *BGLF1* | 5'-TCGAGAACCCCAGCAACA-3'<br>5'-AATGGCCCGACGGGTCTT-3' | 140 | Pan et al. 2005 |
| *BGLF2* | 5'-GCGGTGCCTGTGGAGATT-3'<br>5'-GTCCCAGTGGGATGATCT-3' | 142 | Pan et al. 2005 |
| *BGLF3* | 5'-AATTGCGCTGGCCTGGAA-3'<br>5'-CACGCACGTCCAAGTACA-3' | 290 | Pan et al. 2005 |
| *BGLF3.5* | 5’-CCGCTCTAGCTGCTTGTAGT-3’<br>5’-AAGAGCCTCGGTAGAAAAGAG-3’ | 224 | In-house |
| *BGLF4* | 5'-GATCCGACCCGCTCTACTTT-3'<br>5'-GGTCAGGCCCATGTCTAAGT-3' | 101 | Pan et al. 2005 |

| | | | |
|---|---|---|---|
| *BGLF5* | 5’-TCCACGGCACAACTACTTCT-3’<br>5’-AGAAGGCCGTCACAATGTTC-3’ | 128 | Pan et al. 2005 |
| *BGRF1* | 5'-ACCCTCTGGTGGGCACAA-3'<br>5'-AGGGCTCGCACCGAACAT-3' | 131 | Pan et al. 2005 |
| *BHRF1* | 5’-CTGCAGGACATTGTGTTGTAA-3’<br>5’-TCAGTCCAGCAAGAAACAAA-3’ | 189 | Pan et al. 2005 |
| *BILF1* | 5'-GCTCTGGGTGCTGGGAAA-3'<br>5'-CGCCATACCCAAGTGAGT-3' | 118 | Pan et al. 2005 |
| *BILF2* | 5’-CCTGCAGCGTTCCTAGCA-3’<br>5’-ACGGCCAAGGGCAGTTGT-3’ | 88 | Pan et al. 2005 |
| *BKRF2* | 5’-TGCTGTTGGTGTATTTCTGG-3’<br>5’-GTTGCTCCCATTCTTAGGTG-3’ | 212 | In-house |
| *BKRF3* | 5’-TTGGCTGGGCGTGGTTTACT-3’<br>5'-AGAGGTCAGAACCAGATG-3' | 140 | Pan et al. 2005 |
| *BKRF4* | 5'-GGACGTGAGTGACACTGA–3<br>5'-GCTCTCGCTGTAGTCAGA-3' | 157 | Pan et al. 2005 |
| *BLLF1a* (gp350) | 5’-CCATACGAAGGCTGTCTAC-3’<br>5’-GCTTACTTGTTGCTCCTCTC-3’ | 163 | Pan et al. 2005 |
| *BLLF1b* (gp220) | 5’-CCTTAGGAGGAACAAGTCC-3’<br>5’-GGCTGGTGTCACCTGTGTTA-3’ | 212 | Pan et al. 2005 |
| *BLLF2* | 5’-ACAGATTACGGCGGTGATTC-3’<br>5’-TAACCGGTGGGCTCGTAAAAGT-3’ | 118 | Pan et al. 2005 |
| *BLLF3* | 5’-CACCACAGGCCGACAATCTT-3’<br>5’-AAGGAGGTGAGGTGGTGCTT-3’ | 188 | Pan et al. 2005 |
| *BLRF1* | 5'-CGCTTCCAGTCCCACAAA-3'<br>5'-CTAATCCGTCAGCAGCGT-3' | 218 | Pan et al. 2005 |
| *BLRF2* | 5’-CTCGCCTGGAGTCTGAGAAT-3’<br>5’-CCGTGGCCTGCGTAATCATT-3’ | 150 | Pan et al. 2005 |
| *BMRF1* | 5’-GGATCTCTACGTCACCACGT-3’<br>5'-GCCAGACCTGTAAAACCT-3' | 235 | Pan et al. 2005 |
| *BMRF2* | 5’-TCTGGCTTTGGGCTCTGGAA-3’<br>5'-ATGGAGGGTCTCCTTCAG-3' | 133 | Pan et al. 2005 |
| *BNLF2a* | 5'-ATGGTACACGTCCTGGAG-3'<br>5'-TTAGATGAGGAGCAGGCA-3' | 182 | Pan et al. 2005 |
| *BNLF2b* | 5’-GCGACTGATCCGCAGAAA-3’<br>5'-TTATCCACACCATCCCAA–3’ | 154 | Pan et al. 2005 |
| *BNRF1* | 5’-AGTGACCATCACTATGCC-3’<br>5’-GTGCTCTGCAAACATCTC-3’ | 58 | Pan et al. 2005 |
| *BOLF1* | 5’-GAGAATGGCCGCGAGTTT-3’<br>5’-TGGACCTAAATCCGGAACA-3’ | 188 | Pan et al. 2005 |
| *BORF1* | 5'-TACACGCCAGCTCCTTCAAC-3'<br>5'-CGGCCGTGATTCATTAGG-3' | 133 | Pan et al. 2005 |

| | | | |
|---|---|---|---|
| *BORF2* | 5'-TGACCCAGGCCCTCTATA-3'<br>5'-TCTCCGGCAGCTTCGTTT-3' | 134 | Pan et al. 2005 |
| *BPLF1* | 5'-GCTAATAAGG.AGTAGGGACCGA-3'<br>5'-AGTTCGGAAGTGAGCAGTTG-3' | 117 | Pan et al. 2005 |
| *BRLF1* | 5'-AAACTCCTATCCTCGTGTCC-3'<br>5'-CGGGAGACTTTCGAGTTCAT-3' | 140 | Pan et al. 2005 |
| *BRRF1* | 5'-GCTGTTCCTGGCAAGAGTCT-3'<br>5'-GGCGATGTCACGCTGTTCAT-3' | 145 | Pan et al. 2005 |
| *BRRF2* | 5'-TTGCTCCGGGCTATCGTG-3'<br>5'-AGGACACGGGCGTCGTAT-3' | 233 | Pan et al. 2005 |
| *BSLF1* | 5'-TTCTCTCGTGGAACTGCAGCTT-3'<br>5'-TCTAGGTAGGTGGATAGAC-3' | 159 | Pan et al. 2005 |
| *BSMLF1* | 5'-CAACCAACAAGGACACATGG-3'<br>5'-CTCGCGTGTTAGGAAGGAAG-3' | 238 | In-house |
| *BSRF1* | 5'-TGCGGGCTCTGGCTCTTT-3'<br>5'-GCCCATCGTCTGCTCATT-3' | 162 | Pan et al. 2005 |
| *BTRF1* | 5'-CGCACCATCCGGGATATT-3'<br>5'-CTGTCGCCCGATGTCGTG-3' | 168 | Pan et al. 2005 |
| *BVLF1* | 5'-CAGTATTCATCCGGCACCTT-3'<br>5'-TTTTGCACCTATCCCTGACC-3' | 128 | Pan et al. 2005 |
| *BVRF1* | 5'-CATGTCGGCTAATGCCAT-3'<br>5'-CACTTCTGTCATCAGC-3' | 101 | Pan et al. 2005 |
| *BVRF2* | 5'-CCAGCTCCCTCTGAAGAA-3'<br>5'-TCGAGGCTGCGCTAAAGA-3' | 115 | Pan et al. 2005 |
| *BXLF1* | 5'-GCCGTGACATCTAATACT-3'<br>5'-AGTAGGCTTTTGGTGTG-3' | 108 | Pan et al. 2005 |
| *BXLF2* (gp85) | 5'-CGTCTATGCTTAACCGCTAC-3'<br>5'-ATTCAGGCCGCTAATGACTC-3' | 152 | Pan et al. 2005 |
| *BXRF1* | 5'-CCAACCCGCAAAGCGTTA-3'<br>5'-CTCAGGGATCGCTGGTTT-3' | 160 | Pan et al. 2005 |
| *BWRF1* | 5'-TCTGTCCTTCAGAGGAACCA-3'<br>5'-CCTCACTTTACAGACAGTGCAC-3' | 120 | Pan et al. 2005 |
| *BZLF1* | 5'-AGCCTGCTCCTGAGAATGCT-3'<br>5'-CCACTGCTGCTGCTGTTTGA-3' | 150 | Pan et al. 2005 |
| *BZLF2* (gp42) | 5'-GCCATCGCACTTGTTATT-3'<br>5'-ACCGGCCAGACCTCTACATT-3' | 125 | Pan et al. 2005 |
| *EBER1* | 5'-AGGACCTACGCTGCCCTAGA-3'<br>5'-AAAACATGCGGACCACCAGC-3' | 168 | Pan et al. 2005 |
| *EBNA-1* | 5'-GACAAAGCCCGCTCCTACCT-3'<br>5'-AGCCCCTTCCACCATAGGTG-3' | 99 | Pan et al. 2005 |
| *EBNA-2* | 5'-AAGGGCAAGTCCAGGGACAA-3'<br>5'-CATTGGATGGGCCAGGAGTT-3' | 154 | Pan et al. 2005 |

| | | | |
|---|---|---|---|
| *EBNA-3A* | 5’-GCCCTGGATGACAACATGGA-3’<br>5’-CAGGTGGGCATCTTCTGCTT-3’ | 138 | Pan et al. 2005 |
| *EBNA-3B* | 5’-CCCTTGCGGATGCAGCCAAT-3’<br>5’-GGCTGATATGGAATG.TGCCC-3’ | 124 | Pan et al. 2005 |
| *EBNA-3C* | 5’-CACCCAGTGAAGCGCACAAA-3’<br>5’-GCTCCACGGTCACTGATGAT-3’ | 112 | Pan et al. 2005 |
| *EBNA-LP* | 5’-CCTCGGACAGCTCCTAAGAA-3’<br>5’-ACCGCTTACCACCTCCTCTT-3’ | 115 | Pan et al. 2005 |
| *LF1* | 5’-TCTAGGATAGCCGCACCTAC-3’<br>5’-GAACTCTGCCCTTCAGTGTC-3’ | 178 | In-house |
| *LF2* | 5’-AGAGGTAGGGGTTCTTGACC-3’<br>5’-CTACTTTACGGTCGCGTTTT-3’ | 189 | In-house |
| *LF3* | 5’-CAGAATAACAGGGGAAGCAA-3’<br>5’-GGGCATTGGTGTAACAATAAA-3’ | 157 | In-house |
| *LMP-1* | 5’-CTCCTCTTGGCGCTACTGTT-3’<br>5’-GGCTCCAAGTGGACAGAGAA-3’ | 153 | Pan et al. 2005 |
| *LMP-2A* | 5’-CTCTCACTTCTACTCTTGGCAG-3’<br>5’-AGTCAAACGGCGCCATCTCCTT-3’ | 255 | In-house |

bp, base pairs

## *2.5 AFFYMETRIX HUMAN GENOME MICROARRAY ANALYSIS*

### 2.5.1 Microarray procedures

#### 2.5.1.1 Total RNA extraction and integrity analysis

Total RNA was extracted from duplicate flasks of induced and uninduced Raji and Ramos cells, harvested at 24 hr time-points using the RNeasy® Mini Kit (Qiagen) according to manufacturer's instructions as described in section 2.4.1. The concentration of total RNA extract was measured on the NanoDrop ND-8000™ Spectrophotometer (LabTech International) as described in section 2.4.2 and the quality of total RNA was assessed further using an RNA 6000 Nano assay chip with the Agilent RNA LabChip Kit and run on an Agilent® 2100 Bioanalyser (Agilent), according to manufacturer's instructions. Total RNA from the duplicate culture flasks representing induced and uninduced cells was pooled, standardised to 100 ng/µl total RNA and heat-denatured by incubation at 70°C for 2 min prior to first-strand cDNA synthesis.

#### 2.5.1.2 Reverse transcription to synthesise first-strand cDNA

Antisense RNA (aRNA) was generated from total RNA in two steps: a first-strand cDNA synthesis followed by second-strand cDNA synthesis to generate double-stranded cDNA template that was subjected to T7 *in-vitro* transcription (IVT) to produce biotin-labelled antisense RNA (aRNA). First-strand cDNA was synthesised from 100 ng of total RNA with the Message Amp$^{TM}$ Premier RNA amplification Kit (Ambion) according to manufacturer's instructions. Briefly, oligo-dTs were used to

generate first-strand cDNA by addition of 5 µl of standardised total RNA (500 ng) to the following first-strand reaction mix:

First-strand reaction mix for a single reaction:

| | |
|---|---|
| First-strand buffer mix | 4 µl |
| First strand enzyme mix | 1 µl |
| Total volume | 5 µl |

The first-strand reaction mix was set-up on ice and all reagents added in the order listed above. The reaction was mixed well by vortexing and centrifuged briefly. Next 5 µl of the reaction mix was transferred to PCR tubes to which 5 µl of total RNA was added, giving a total reaction volume of 10 µl. The reaction mix was mixed once more by vortexing, centrifuged briefly and returned to ice. The reaction tubes were transferred to a Perkin Elmer thermal cycler (Applied Biosystems) and first-strand synthesis carried out at 42°C for 2 hrs with a final hold at 4°C. Following incubation, reaction tubes were centrifuged briefly and placed immediately on ice prior to second-strand cDNA synthesis.

**2.5.1.3 Second-strand cDNA synthesis**

First-strand cDNA was used directly in a second reaction to generate double-stranded DNA (dsDNA) template for IVT. The second-strand reaction mix was set-up on ice in the following reaction:

Second-strand reaction mix for a single reaction:

| | |
|---|---|
| Nuclease-free water | 13 µl |
| Second-strand buffer mix | 5 µl |
| Second strand enzyme mix | 2 µl |
| Total reaction volume | 20 µl |

The second-strand master mix was mixed thoroughly by gentle vortexing, centrifuged briefly and placed on ice. Next, 20 µl of the reaction mix was transferred to PCR tubes containing 10 µl of the first-strand cDNA samples. The reaction mix (30 µl) was mixed well by vortexing, centrifuged briefly and returned to ice. Second-strand cDNA synthesis was carried out in a pre-cooled Perkin Elmer thermal cycler for 1 hr at 16°C followed by 10 min at 65°C. After this incubation step, the reaction tubes were centrifuged briefly and transferred immediately to –20°C for overnight storage prior to IVT the following day.

#### 2.5.1.4 *In vitro* transcription to synthesise biotin-labelled aRNA

The following day, double-stranded cDNA template was subjected to IVT to generate biotin-labelled aRNA using Message Amp$^{TM}$ Premier RNA Amplification Kit (Ambion) according to the manufacturer's instructions. All reaction mixtures for the IVT were set-up at room temperature (RT). The T7 IVT master mix was set-up in the following reaction:

T7 IVT master mix for a single reaction:

| | |
|---|---|
| Nuclease-free water | 4 µl |
| T7 Biotin IVT mix | 20 µl |
| T7 enzyme mix | 6 µl |
| Total reaction volume | 30 µl |

The IVT master mix reagents were added in the order listed above. The reaction was mixed thoroughly by gently vortexing and centrifuged briefly. Next, 30 µl of the T7 master mix was transferred to PCR tubes containing the double-stranded cDNA template synthesised the previous evening (30 µl). The entire reaction was mixed thoroughly by gently vortexing, centrifuged briefly and immediately transferred to a

thermal cycler. The IVT reaction was carried out overnight for 16 hrs at 40°C. After incubation, the reaction was placed on ice prior to the aRNA purification step.

#### 2.5.1.5 Purification of biotin-labelled aRNA

For the first step of the aRNA purification, 40 µl of nuclease-free water (heated to 50-60°C for a minimum of 10 min) was added to each biotin-labelled aRNA resulting in a total reaction volume of 100 µl. The reaction mix was mixed thoroughly by vortexing, centrifuged briefly and transferred to a new nuclease-free 1.5 ml sarstedt tube. Next, 60 µl of aRNA binding buffer was added to each aRNA sample and the entire sample transferred to the wells of a U-bottom plate. Immediately after transfer, 120 µl of 100% ethanol was added to each aRNA sample, the reaction mixed by pipetting up and down three times, and the entire plate shaken for 3 min at 5,000 x *g*. Purification of aRNA involved two washing steps. For the first wash step, the 96-well plate was placed on a magnet for 5 min. After 5 min, the supernatant was discarded and the beads re-suspended in 100 µl of wash buffer, and shaken for 1 min at 6,000 x *g* and returned to the magnet for 5 min. The supernatant was discarded and the wash step repeated (shake for 1 min, magnet for 5 min). After the second wash, the supernatant was discarded and the plate removed from the magnet. A final shake was performed for 1 min at full speed to remove all traces of ethanol. The final step in the purification involved an elution step. In this step, 50 µl of aRNA elution buffer (pre-heated to 50-60°C) was added to the 96-well plate and the reaction mixed by gently pipetting up and down 2-3 times and shaken vigorously for 3 min at full speed. The plate was transferred to a magnetic stand for 5 min and the supernatant (approximately 50 µl) transferred to a second 96-well plate for fragmentation of aRNA.

### 2.5.1.6 Fragmentation of biotin-labelled aRNA

Prior to fragmentation, the quality of aRNA was assessed with the Agilent bioanalyser as described in section 2.5.1.1. The aRNA fragmentation reaction mix was set-up in the following reaction:

30 µl reaction volume (15.51 µg in 31 µl*)

| Sample (µg/µl) for 15.5 µg | Sample volume (µl) | Volum $H_20$ (µl) | 5X array fragmentation buffer |
|---|---|---|---|
| 1.54 | 10.05 | 14.75 | 6.2 µl |
| 2.16 | 7.16 | 17.64 | 6.2 µl |
| 1.05 | 14.66 | 10.14 | 6.2 µl |
| 2.10 | 7.38 | 17.42 | 6.2 µl |
| 0.99 | 15.57 | 9.23 | 6.2 µl |

*1 µl was used in the bioanalyser

The aRNA was fragmented by incubating the fragmentation reaction at 94ºC for 35 min. After the incubation, the reaction mix was immediately placed on ice ready to hybridise to the array. The fragmented aRNA was next analysed on the Agilent bioanalyser. Briefly, 1 µl of fragmented aRNA was heat-denatured at 70ºC for 2 min and run on the bioanalyser (Figure 4.2).

### 2.5.1.7 Hybridisation of fragmented aRNA

The fragmented aRNA was used immediately in the following hybridisation reaction:

Hybridisation master mix for a single reaction:

| | |
|---|---|
| Fragmented biotinylated aRNA | 25 µl |
| Control oligo B2 (3 nM) | 4.2 µl |
| 20X hybridisation controls | 12.5 µl |
| 2X hybridisation mix | 125 µl |
| DMSO | 25 µl |
| $H_20$ | 58.3 µl |
| Total reaction volume | 250 µl |

Twenty-five microlitres of hybridisation mix was added to 25 µl of the fragmented aRNA and immediately transferred to -80ºC until hybridisation to the arrays. Fragmented aRNA from duplicate replicates of induced and uninduced Raji and Ramos cells were hybridised to a total of eight Affymetrix (HG-U133 Plus 2.0 GeneChips® and signal intensity measured.

### 2.5.2 Microarray Data Analysis

#### 2.5.2.1 Affymetrix data acquisition

Following aRNA hybridisation, each HG U133 Plus 2.0 GeneChip® was scanned by laser using the GeneChip® scanner 3000 7G and the fluorescence signal recorded. Raw signal intensity data (CEL.file) captured from the scanner was analysed using the microarray suite 5.0 (MAS 5.0) algorithm (Affymetrix Suite v5.0) built into the Affymetrix GeneChip® operating software (GCOS). Using MAS 5.0, several processing steps were undertaken to transform the raw data (in the form of probe set intensities) into expression levels in an absolute analysis, followed by several filtering steps to identify highly differentially expressed genes in a pair-wise comparison of induced and uninduced conditions.

Affymetrix arrays consist of thousands of probe sets (Figure 2.1). The HG U133 Plus 2.0 GeneChip® contains 54,675 probe sets (Figure 2.1) that interrogate 38,500 genes (Irizarry et al., 2003; Lipshutz et al., 1999). Each probe set consists of 11-20 short (25-mer) oligonucleotide pairs that span different sections of the gene, with some genes being detected by multiple probe sets. Each probe pair consists of a perfect-match (PM) oligonucleotide and its mismatch (MM). The MM probe is identical to

the PM probe except for a single substitution (13th base) of the 25-mer oligo and serves to measure non-specific hybridisation (Irizarry et al., 2003). In order to measure the expression levels of a particular mRNA transcript, the signal intensity for each probe set (11-20) is summarised and the mean signal intensity calculated for the gene. The use of pairs of PM and MM probe sets provides accurate and reproducible gene expression measurements when Affymetrix arrays are used.


**Figure 2-1 Affymetrix probe-set**

Example of 11-20 short (25-mer) perfect match (PM) and mismatch probe (MM) set used to interrogate gene transcripts in the Affymetrix HG U133 Plus 2.0 GeneChip®. Each probe set typically contains 11-20 pairs of perfect match (PM) and mismatch (MM) probe pairs. The mismatch has a mutation at the 13th base and serves to detect non-specific hybridisation. Signal intensities of the summarised probe pairs are generated to provide a single gene expression level for each probe set and hence for the gene transcript. Each gene can be interrogated by multiple probe sets. Taken from the MAS 5.0 algorithm

### 2.5.2.2 Affymetrix calibration for absolute analysis of single arrays

Data pre-processing is required to transform raw signal intensities for each probe-set (Figure 2.0) into single gene expression measurements or signal value (i.e. the absolute data) through removal of non-specific hybridization signals and control for sample variation. Typically, three pre-processing steps are required: (i) Background correction (ii) Normalisation and (iii) Expression summary, although not necessarily in that order (Harrison et al., 2007). The processed data is saved as a CHP.file for comparative analysis of baseline and experimental arrays.

#### 2.5.2.2.1 Background correction

Background correction or perfect match (PM) correction refers to the adjustment of PM signal intensities to account for non-specific hybridisation signals. Negative values are excluded when the MM intensity exceeds the PM signal (MM ≥ PM = exclude negative values). MAS 5.0 assigns each probe set a detection call of present (P), marginal (M) or absent (A) that indicates how reliably each transcript is detected (Liu et al., 2002). MAS 5.0 uses probe pair (PM-MM) intensities to produce detection *P*-values for the detection calls (Pepper et al., 2007).

#### 2.5.2.2.2 Normalisation

Normalisation of each array is necessary before the array can be compared alongside other arrays by correcting for differences in overall mRNA levels and technical variations such as differences in processing of arrays (Bolstad et al., 2003). Normalisation of each HG-U133 Plus 2.0 array was performed by global scaling so that the average signal of each array equalled arbitrary target signal intensities (TGT) of 100 to enable signal comparisons between each array. Global scaling was performed by scaling the signal intensities for all probe sets and taking the average signal as the trimmed mean (i.e., mean of the middle 96% of the ranked data, ignoring the top 2% and bottom 2% of values) so that each array was scaled to the same mean intensity.

#### 2.5.2.2.3 Expression summary

Expression summary is required to transform signal intensity from each probe set into a measure of relative mRNA abundance (Harrison et al., 2007), reflected in the signal value. The real signal value is determined by calculating the mean signal intensity for each probe pair by taking the log of the PM after subtraction of the MM probe value: Real Signal = log (PM-MM). Signal values refer to the absolute data (.CHP file) and were used to perform comparative analyses between experimental and baseline GeneChips® arrays (Hubbell et al., 2002; Irizarry et al., 2003).

### 2.5.2.3 Pair-wise comparison analysis

Following data pre-processing, comparison analysis was performed between induced and uninduced arrays to estimate differential gene expression changes between the two conditions. Comparison analysis requires several filtering steps to identify lists of highly differentially regulated and expressed probe sets. The purpose of filtering is to bias towards selecting probe sets that are most significantly and highly expressed by excluding those probe sets that are not reliably expressed or low expressed and thus uninformative (Hackstadt and Hess, 2009). Therefore, the MAS 5.0 algorithm was required to filter data by: (i) detection call and (ii) change call and (iii) signal change. A subsequent analysis step was performed to bias for the top 250 most highly differentially expressed probe sets. The tiered filtering approach is illustrated in Figure 2.2 and described below.

#### 2.5.2.3.1 Filtering on all probe sets called absent

Filter 1 removed all probe sets called absent during pre-processing, leaving only probe sets that were present in at least one array. By filtering on absent calls, all probe sets with low signal intensity and not highly expressed were removed.

#### 2.5.2.3.2 Filtering on probe sets not changing

Filter 2 removed all probe sets showing no change (NC) between induced and uninduced arrays. Change call refers to the direction of gene expression. Five possibilities for the change include: increase (I), marginal increase (MI), no change (NC), decrease (D) and marginal decrease (MD). By filtering out all probe sets called NC, only probe sets that were definitely changed (i.e., I or D) between the induced and uninduced array were selected.

#### 2.5.2.3.3 Filtering on probe sets changing by less than two-fold

Filter 3 removed all probe sets whose expression did not change by 2-fold. The signal log ratio (SLR) refers to the magnitude in gene expression and represents the ratio between two samples for each probe sets, expressed as the $\log_2$ ratio, where a SLR of 1.0 indicates a 2-fold change. Hence, a SLR of +1.0 indicates a 2-fold increase and a SLR of -1.0 indicates a 2-fold decrease. By removing all probe sets with a SLR $\geq$1.0 (2-fold increase) and $\leq$1.0 (2-fold decrease), only probe sets that changed by at least 2-fold between the induced and uninduced arrays remained.

#### 2.5.2.3.4 Ranking to bias selection of highly differentially expressed probe sets

In summary, we have filtered on the basis of probe sets being absent in samples, probe sets not changing between both samples and also probe sets changing by less than a 2-fold cut-off (Figure 2.2). The remaining list also contains probe sets that have low signal values for both samples, but an apparently high SLR. We felt that these probe sets should be removed from further analysis because it was likely that the observed SLR was due to experimental noise. Therefore, to bias for probe sets with a higher overall signal, by removing probe sets that displayed high SLR but low signal values (low overall signal), the following formula was applied to the data: Sum signals ($Signal_{(induced)}$ + $Signal_{(uninduced)}$) x magnitude of SLR. For example, two probe sets (Probe set A and B) have the same SLR (6) but different signal values; Probe set A has a signal of 1.0 (induced) and 0.01 (uninduced), whereas Probe set B has a signal of 100 (induced) and 1.0 (uninduced). By applying the formula for Probe set A: Sum ($1.0_{(induced)}$ +$0.01_{(uninduced)}$) x6, the resulting signal is 6.06, known as 'sum signals x SLR', whereas for Probe set B: Sum ($100_{(induced)}$ +$1.0_{(uninduced)}$) x6, the resulting signal is 606, representing a 100-fold difference in signal value between Probe set A and Probe set B. Therefore, by using this formula, genes with the same SLR can be distinguished. This formula (unpublished) was performed by Dr Matt Arno at the Genomics Centre, KCL in lieu of statistical analysis using ANOVA, since only duplicate, not triplicate arrays were analysed. The result of this selection is a set of highly differentially expressed probe sets (Figure 2.1). In order to focus on a small group of highly differentially expressed genes, the top 250 most commonly modulated probe sets were selected from the ranked 'sum signals x SLR'values of an overlap between two duplicate induced arrays (Figure 2.2).

#### 2.5.2.3.5 Calculating fold change from signal log ratio

The fold change for each probe set was determined by taking the average SLR for each probe set from experiment 1 and 2 (induced versus uninduced SLR), and then calculating the fold-change where a SLR of +1.0 and -1.0 equals a 2-fold increase or decrease. Probe sets (Table 4.1) were identified using the Affymetrix NetAffyx™ Analysis Centre found at www.netaffyx.com.

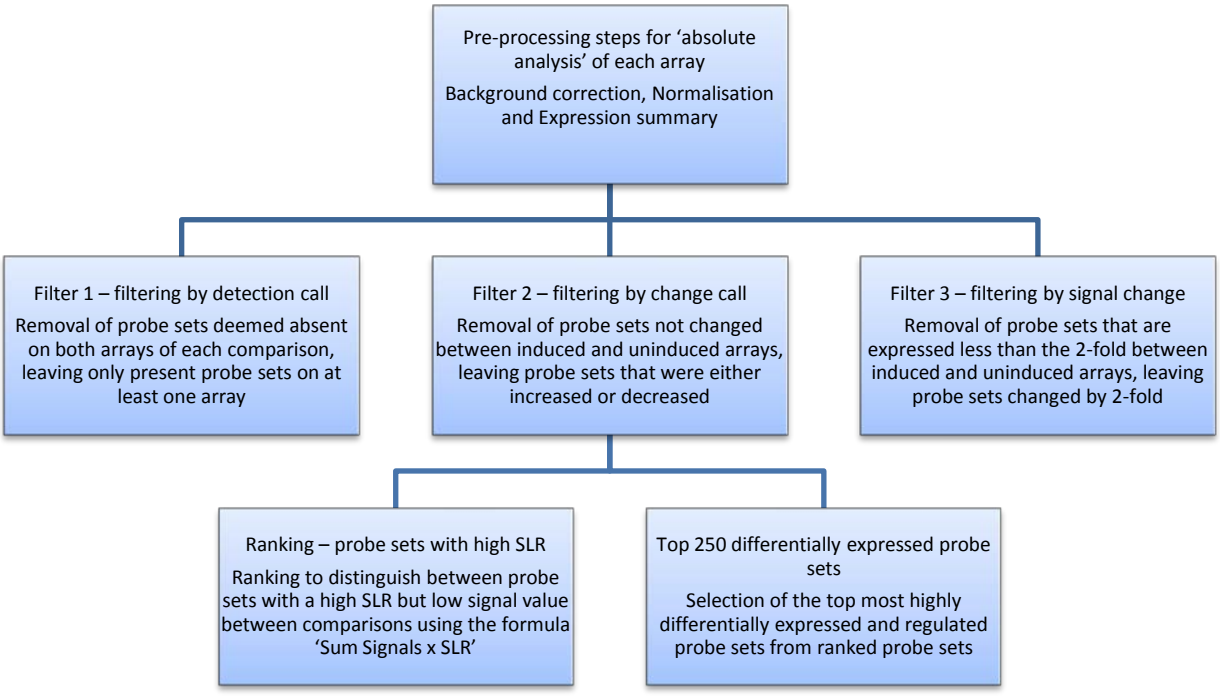


**Figure 2-2 Filtering steps to identify highly differentially expressed probe sets**

Pre-processing steps including (i) Background correction; (ii) Normalisation and (iii) Expression summary were performed for absolute analysis on each single induced and uninduced array. Three filters were performed during comparison analysis of duplicate induced and uninduced arrays. Filter 1 removes all absent probe sets on both arrays, leaving only present probe-sets, filter 2 removes all probe-sets not changing between the comparison, leaving only increased or decreased probe sets and filter 3 removes all probe sets changing less than 2-fold, leaving probe sets changing by 2-fold or more. Two final analysis steps were performed to distinguish between genes with a high SLR but low signal value and select the top 250 most differentially expressed and regulated probe sets

### 2.5.3 Molecular Methods

#### 2.5.3.1 Validation of Affymetrix data by real-time PCR

After the array analyses, 22 candidate genes (Table 4.) were selected for further validation according to the following criteria: (i) not regulated in response to lytic cycle inducers (TPA/NaB); (ii) known regulation in EBV-associated PTLD and/or EBV infection; (iii) highly regulated with a biological function of interest, and (iv) highly represented within Gene Ontology. However, in this study, 17 of 22 genes were investigated, since cDNA template was limiting. Real-time PCR (described in section 2.4.6) was run in triplicate on cDNA (diluted 1/100) derived from the same total RNA extracted from duplicate induced and uninduced Raji cells and hybridized onto HG-U133 Plus 2.0 GeneChip® arrays. Briefly, 4 µl of cDNA was mixed with 2X TaqMan® Gene Expression Master Mix (Applied Biosystems) and 20X TaqMan® Gene Expression Assays (final 2X concentration) made up to a final volume of 20 µl with sterile nuclease-free water (Ambion). Each reaction mixture was set up as follows:

PCR mix for a single reaction:

| | |
|---|---|
| Applied Biosystems TaqMan® Gene Expression Master Mix | 10 µl |
| Applied Biosystems TaqMan® Gene Expression Assays (20X) | 1 µl |
| cDNA template (1-100 ng) | 4 µl |
| Ambion Nuclease-free water | 5 µl |
| Total reaction volume | 20 µl |

Microarray validation was performed in triplicate for each of the 22 cellular candidate genes using the same real-time PCR programme described in section 2.4.6, omitting melt curve analysis:

95ºC for 10 min (hold)
50 cycles of:
95ºC for 10 sec (denaturation)
57ºC for 20 sec (annealing/extension)

TaqMan® gene expression assays for 17 host cellular candidate genes are listed in Table 2.2. All candidate genes were normalised to the endogenous control *ACTB* (Hs99999903_m1) listed in Table 2.2 and relative expression levels, fold change and significance of fold change calculated as described in sections 2.4.9.

**Table 2-2 TaqMan gene expression assays for real-time PCR**

| Gene Expression Assay ID | Gene name |
|---|---|
| Hs99999903_m1* | *ACTB* |
| Hs00229474_m1 | *ANP32E* |
| Hs00234142_m1 | *CCL3* |
| Hs00174575_m1 | *CCL5* |
| Hs99999075_m1 | *CCL22* |
| Hs00174349_m1 | *CD52* |
| Hs00364293_m1 | *CDC2* |
| Hs01072230_g1 | *CHI3L1* |
| Hs00171042_m1 | *CXCL10* |
| Hs00171065_m1 | *CXCL9* |
| Hs00610314_m1 | *HDGF1* |
| Hs00192713_m1 | *ISG15* |
| Hs00924169_m1 | *LRMP* |
| Hs00174349_m1 | *MAD2L1* |
| Hs00696862_m1 | *PCNA* |
| Hs00243115_m1 | *RASA1* |
| Hs00243182_m1 | *RGS13* |
| Hs00609691_m1 | *TIMP1* |

Reference control*

#### 2.5.3.2 TaqMan gene expression assays

Primers specific for the cellular genes were selected from an assortment of optimised TaqMan® gene expression assays provided by Applied Biosystems (Listed in Table 2.2). Selection criteria for the TaqMan® gene expression assays included (i) where possible, assays must span an exon-exon junction to avoid detection from contaminating chromosomal DNA (ending with suffix_m1) (ii) identification of the most mRNAs including those spotted on the HG-U133 Plus 2.0 array, and (iii) inventoried.

### 2.5.4 Bioinformatics Analysis

#### 2.5.4.1 Functional network and pathway analysis using Metacore

MetaCore (GeneGo bioinformatics software, Inc., St. Joseph, MI) is an integrated software suite, based on a manually curated database of human protein-protein interactions, protein-DNA interactions, and transcriptional factors, metabolic and signaling pathways for identification of Gene Ontology processes (Nikolsky et al., 2005). Affymetrix data sets (6,517 and 5,437 probe sets) (from the pair wise comparison) were uploaded as their Affymetrix probe set IDs, SLR and *P*-values for SLR into GeneGo MetaCore™ (GeneGo bioinformatics software, Inc) for identification of three biological processes: (i) biological process (ii) and canonical pathway analysis (iii) disease biomarkers and then ranked according to their *P*-value. Probe sets that were up- and down-regulated 1.5 fold with a significance of $P<0.05$ were first uploaded into MetaCore™ and an enrichment workflow analysis performed that provides the ten most highly represented gene networks shown as significant enrichment analysis histograms. For network and pathway analysis, the data sets were uploaded into MetaCore and biological networks constructed.

## *2.6 GENE EXPRESSION ANALYSIS IN WHOLE BLOOD*

### 2.6.1 Study design

A case-control study was undertaken in the Virology department at King's College Hospital, to identify viral and cellular genes that could be used as diagnostic marker(s) for early detection of PTLD. Ethical approval was not applicable for the study.

### 2.6.2 Study groups

Twenty-one paediatric transplant recipients who underwent solid organ transplant (SOT) between 2000 – 2009 and two adult umbilical cord blood transplant (UCBT) recipients who underwent transplantation for haematological malignancies between 2008 between and 2010 were investigated. From these, seven cases of PTLD were diagnosed during the period of 2008 – 2010. The demographic and clinical details of all available patients and unmatched controls are shown in Tables 2.3 and 2.4. Therefore the study groups consisted of:

**(i) Paediatric transplant recipients** who developed PTLD following liver and small bowel transplant (Table 2.3). These patients were transplanted primarily for the treatment of acute liver failure (ALF), and small intestinal bowel transplantation for acute intestinal failure. Altogether, five cases of PTLD were available for investigation during the period of 2009 – 2010. Two of the five patients were orthotopic liver transplant (OLT) recipients and the remainder were small bowel transplant recipients. Transplant dates were

known for 4/5 patients. The median age of patients at transplant was 72 months (Range: 1-192 months). Three cases were female and two were male.

**(ii) Adult transplant recipients** one of which developed PTLD and a second who remained at high risk (non-PTLD). Both patients were diagnosed as having haematological malignancies, primarily acute myeloid leukaemia (AML) and subsequently underwent UCBT. Two of 13 UCBT recipients were available for investigation during the period of 2009 – 2010 (Table 2.4). Multiple samples were available for each patient. The median age of the patients at transplant was 29.5 years (Range 28 – 31 years). Both cases were female.

**(iii) 'Unmatched' paediatric controls –** The control group consisted of 16 paediatric SOT recipients who were not diagnosed with PTLD (denoted: non-PTLD) (Table 2.3). Controls were selected based on viral loads since matching by age and sex was limited by the small population to draw from in our laboratory. Transplant dates were not known for 14/16 controls. All controls were evaluated for analysis of EBV gene expression patterns. However, for the cellular gene expression analysis, 5 closely matched controls, based on sampling times post-transplant (≤12 months), were selected as controls for the cellular gene expression analysis. Controls were matched 1:1 with PTLD cases. The median age of these five controls at transplantation was 12 months (range 0.4 –144 months).

**Table 2.3 Clinical details from paediatric PTLD cases and controls**

| Variables | Cases (*n* = 5) | Controls (*n* = 5) |
|---|---|---|
| Sex (F:M) | 2:3 | 1:4 |
| EBV serostatus pre-transplant Positive Negative | VCA IgG negative (*n* = 4)/VCA IgG indeterminate (*n* = 1) | VCA IgG negative (*n* = 3)/VCA IgG indeterminate (*n* = 1)/EBV-seronegative (*n* = 1) |
| Age at transplant (months) (median, ranges) | (median 72, range 1 – 192 months) | (median 12, range 0.4 – 144 months) |

PTLD, post-transplant lymphoproliferative disorder; VCA, viral capsid antigen; IgG, immunoglobulin; -, not diagnosed; F, female; M, male

**Table 2.4 Clinical details of the single adult PTLD case and control**

| Variables | Cases (*n* = 1) | Controls (*n* = 1) |
|---|---|---|
| Sex (F:M) | female | female |
| EBV pre-transplant serostatus | VCA IgG positive | VCA IgG positive |
| Age at transplant (months) (median, ranges) | (median 0, 336 months) | (median 0, 360 months) |

PTLD, post-transplant lymphoproliferative disorder; VCA, viral capsid antigen; IgG, immunoglobulin; -, not diagnosed; F, female

### 2.6.3 Virological laboratory data

All patients were monitored routinely for EBV DNA loads by real-time quantitative PCR amplification during the first year following transplant using an in-house EBV assay based on the method described previously by Jabs *et al.*, 2001 (Wagner et al., 2001). Viral loads ≤10 genome copies/ml and ≥10 copies/ml were considered negative and positive, respectively. Serology was performed to determine pre-transplant EBV status using an ELISA (DiaSorin). EBV recipient status was available for all patients however the donor status was not. Of the 20 paediatric patients investigated, at the time of transplant, 8 patients were EBV-seropositive, 3 VCA-IgG indeterminate and nine EBV-seronegative, whereas post-transplant, five developed PTLD, 16 remained PTLD negative (non-PTLD), one remained EBV seronegative

with no EBV viraemia (≤10 copies/ml) and four had primary EBV infection based on development of an EBV viraemia, including 2 PTLD and 2 non-PTLD patients. All adult patients were EBV-seropositive pre-transplant, whereas post-transplant only one patient developed PTLD. PTLD was diagnosed by histological analysis and EBV confirmed in biopsy tissue by EBER *in-situ* hybridisation.

### 2.6.4 Whole blood samples

Overall, 299 fresh whole blood samples were collected prospectively from paediatric and adult transplant recipients during a six month period between October 2009 and April 2010 and subjected to isolation of the non-red blood cell (non-RBC) fraction, followed by total RNA extraction. Clinical samples consisted of consecutive samples of EDTA-treated whole blood collected weekly or fortnightly for each patient. However, of the 299 samples, preference was given to samples with ≥30 ng/µl total RNA and of varying viral loads to ensure sufficient total RNA for real-time PCR analysis. In this study, 33 samples of different viral loads (ranging from ≤10 copies/ml to 197,629 copies/ml) from 20 patients were subject to gene expression analysis, including 15 samples from 5 paediatric PTLD patients and 18 from 16 non-PTLD patients (Figure 2.3). An additional 12 samples (ranging from ≤10 copies/ml to 477,642 copies/ml) were analysed from two adult patients, including 6 samples each from a PTLD and non-PTLD patient (Figure 2.3).

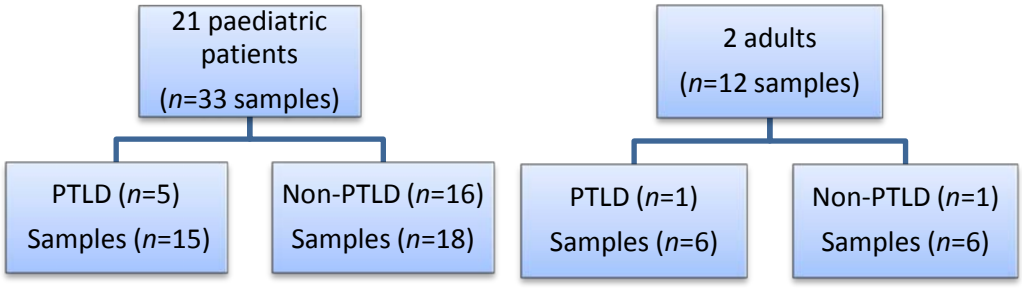


**Figure 2-3 Schematic diagram showing the patient study cohort**

2.6.4.1 **Isolation of the non-RBC fraction**

The non-RBC fraction was isolated within 24 hrs of collection using the QIAamp RNA Blood Mini Kit (Qiagen). Briefly, whole blood samples were transferred from collection tubes into 15 ml RNase-free centrifuge tubes (Ambion) using sterile 3 ml pipettes (VWR International). Where possible, 1.5 ml of whole blood was used. Next, five volumes of erythrocyte lysis (EL) buffer was added to whole blood samples: 7.5 EL buffer: 1.5 ml whole blood or 2.5 ml EL buffer: 0.5 ml whole blood. The whole blood: EL lysate was mixed briefly by gentle vortexing and incubated on ice for 15 minutes, with two additional vortexes during incubation. Whole blood:EL samples were centrifuged at 400 x *g* for 10 min in a 4ºC centrifuge, the supernatant discarded and the cell pellets re-suspended by pipetting in 1 volume of EL buffer (3 ml EL buffer: 1.5 ml whole blood and 1 ml EL buffer: 0.5 ml whole blood) prior to 5 min incubation on ice. The re-suspension was centrifuged at 400 x *g* for 10 min followed by complete removal of supernatant and the cell pellets re-suspended in 600 µl of RLT buffer containing 10 µl/ml 2-mercaptoethanol (Sigma-Aldrich) and the sample vortexed for 15 s to mix or longer until no visible pellet remained. Cell lysates were transferred immediately to -80ºC for long-term storage prior to RNA extraction.

### 2.6.5 Molecular Methods

#### 2.6.5.1 Total RNA extraction from white blood cell lysates

Total RNA was isolated from homogenized lysates using the QIAamp® RNA Blood Mini Kit (Qiagen) according to manufacturer's instructions. Briefly, prior to RNA extraction, white blood cell lysates were thawed by incubating for 5 min at 37ºC in a water-bath. Lysates were homogenized by transferring the lysates to shredder spin columns and centrifuging at 22,130 x *g* for 2 min. Next, the homogenized lysate was mixed with 600 µl of 70% ethanol by pipetting up and down 5-6 times. Next, 600 µl of the ethanol: lysate mixture was transferred to a mini spin column and centrifuged for 1 min at 11,290 x *g*. The supernatant was discarded and the remaining ethanol:lysate was transferred to the same spin column with new collection tube and re-centrifuged for 1 min at 11,290 x *g*. For the first wash step, the supernatant was discarded, a new collection tube added and 350 µl of RW1 wash buffer added to each spin column, and centrifuged for 1 min at 11,290 x *g*. On-column DNase digestion was performed using the RNase-free DNase Set kit (Qiagen) as described in section 2.4.1. For the second wash step, 350 µl of RW1 wash buffer was added to each spin column and centrifuged at 11,290 x *g* for 1 min. The supernatant was discarded and a new spin column added. Next, 500 µl of RPE wash buffer was added to each spin column, centrifuged for 1 min at 11,290 x *g*, the supernatant discarded and a new collection tube provided. A final wash step was performed with 500 µl of RPE, this time centrifuged at 22,130 x *g* for 3 min. Next, new collection tubes were provided and each spin column centrifuged at full speed for 1 min to remove residual wash buffer. For the elution step, 30 µl of RNase-free water was added to the centre of each spin column and incubated for 1 min at room temperature. Total RNA was eluted by

centrifuging at 11,290 x *g* for 1 min. An additional 30 µl of RNase-free water was added to the spin column, incubated for 1 min at room-temperature and centrifuged for 1 min at 11,290 x *g*, leaving a total elution volume of 60 µl total RNA. The concentration and quality of total RNA extract was determined immediately on the NanoDrop™ ND-8000 instrument (LabTech International) as described previously in section 2.4.2. Subsequently, total RNA was transferred immediately for long-term storage at -80°C, prior to RT.

### 2.6.5.2 Reverse-transcription

Reverse transcription of total RNA derived from whole blood samples was performed from 300 ng of total RNA (standardised to 30 ng/µl) using the High-Capacity Reverse-Transcription kit (Applied Biosystems), according to manufacturer's instructions. Briefly, reverse-transcription was carried out on 10 µl of total RNA with random primers, reverse-transcription buffer (RT buffer), dNTPs and 125 U Multiscribe™ reverse transcriptase. Each RT was carried out on ice in a final volume of 20 µl and set-up in 0.2 ml PCR tubes (Qiagen) in the following order:

RT mix for a single reaction:

| | |
|---|---|
| RT buffer | 4 µl |
| dNTPs | 2 µl |
| RNAse inhibitor | 1 µl |
| Reverse-transcriptase | 1 µl |
| Sterile RNAse-free water | 2 µl |
| Total RNA template | 10 µl |
| Total reaction volume | 20 µl |

The reverse-transcription master mix (minus total RNA) was set-up on ice in the order listed above, mixed by gently pipetting 2-3 times and centrifuged briefly. Next, 10 µl of total RNA was added to the reaction mix, and the reaction mix mixed 2-3 times by pipetting, centrifuged briefly and placed in a pre-programmed thermal cycler (Applied Biosystems). Reverse-transcription was carried out at 37ºC for 2 hrs and an indefinite hold at 4ºC. All cDNAs were diluted 1/3 in sterile PCR grade water and transferred immediately to -20ºC prior to real-time PCR.

#### 2.6.5.3 Primers and probes used for PCR gene expression analysis

TaqMan MGB probe sequences were designed for 17 EBV gene targets using the Invitrogen design software 'software oligo3 primer output' (Invitrogen, UK). All probes were synthesized by Applied Biosystems and were 5'-labeled with FAM. All primers were synthesised previously by Metabion as described in section 2.4.5 and shown in Table 2.1. All 17 primer and corresponding probe sequences used for EBV gene expression profiling are listed in Table 2.3. For detection of host cellular gene targets, 17 TaqMan® gene expression assays shown in Table 2.2 were selected from a Collection of Applied Biosystem gene expression assays (www.appliedbiosystems.com) as described previously in section 2.5.3.2.

#### 2.6.5.4 Real-time TaqMan PCR for gene expression profiling

Gene expression profiles were analysed using the same real-time PCR programme as described in section 2.5.3.1. Briefly, real-time PCR was performed on cDNAs (diluted 1/3) using the Applied Biosystems Gene Expression Master Mix (Applied Biosystems). PCR was conducted in a total volume of 20 µl consisting of 2X Gene

Expression Master Mix, 20X TaqMan® gene expression assays and/or EBV detection mix and sterile nuclease-free water. For detection of EBV gene targets, primer/probe detection mixes were prepared, containing 10 pmol of each forward/reverse primer and 5 pmol of each TaqMan probe in a total volume of 100 µl and 1 µl used per reaction. The PCR master-mix was set-up on ice as follows:

| PCR mix for a single reaction: | |
|---|---|
| 2X Gene Expression Master mix | 10 µl |
| TaqMan® Gene expression assay (20X)/EBV detection mix | 1 µl |
| Sterile DNAse/RNase-free water | 5 µl |
| cDNA template (100 ng) | 4 µl |
| Total reaction volume | 20 µl |

The PCR reaction mix was mixed gently by inverting 2-3 times and then centrifuged briefly. 16 µl of master mix was added to 0.1 ml PCR tubes (Qiagen) with 4 µl diluted cDNA added to each reaction mix. All PCR reactions were performed in triplicate for each target in 0.2 ml tubes as described in section 2.5.3.1. Relative quantification was determined using the comparative quantitation method described in section 2.4.9.

### 2.6.6 Statistical analysis

All graphs and statistical analyses were performed using GraphPad Prism v5.0 software (GraphPad Prism, La Jolla, California, USA). The Mann-Whitney U-test was used to compare the relative expression levels between PTLD and non-PTLD groups. *P*-values $<0.05$ were considered statistically significant.

**Table 2-3 Primer and probe sequences for clinical validation by using real-time PCR**

| Gene name | Primer sequence (5’ – 3’) | TaqMan probe sequence (5’ – 3’) |
|---|---|---|
| *EBNA1* | 5’-GACAAAGCCCGCTCCTACCT-3’<br>5’-AGCCCCTTCCACCATAGGTG-3’ | 6FAM-CTG TGT GCA GCT TTG ACG AT-MGBNFQ |
| *EBNA2* | 5’-AAGGGCAAGTCCAGGGACAA-3’<br>5’-CATTGGATGGGCCAGGAGTT-3’ | 6FAM-CTT GGA GAC CAG AGC CAA AC-MGBNFQ |
| *EBNA3A* | 5’-GCCCTGGATGACAACATGGA-3’<br>5’-CAGGTGGGCATCTTCTGCTT-3’ | 6FAM-ATC TAC CTC GGT TGT GCA GG-MGBNFQ |
| *EBNA3B* | 5’-CCCTTGCGGATGCAGCCAAT-3’<br>5’-GGCTGATATGGAATG.TGCCC-3’ | 6FAM-TTA ATC ATC CAG TGG GAC CC-MGBNFQ |
| *EBNA3C* | 5’-CACCCAGTGAAGCGCACAAA-3’<br>5’-GCTCCACGGTCACTGATGAT-3’ | 6FAM-TAA GGC AGA AGC ACA AAG CA-MGBNFQ |
| *EBNALP* | 5’-CCTCGGACAGCTCCTAAGAA-3’<br>5’-ACCGCTTACCACCTCCTCTT-3’ | 6FAM-ACC CAG ACG AGT CCG TAG AA-MGBNFQ |
| *LMP1* | 5’-CTCCTCTTGGCGCTACTGTT-3’<br>5’-GGCTCCAAGTGGACAGAGAA-3’ | 6FAM-TGA GTG ACT GGA CTG GAG GA-MGBNFQ |
| *LMP2* | 5’-CTCTCACTTCTACTCTTGGCAG-3’<br>5’-AGTCAAACGGCGCCATCTCCTT-3’ | 6FAM-TTC TGG TGA TGC TTG TGC TC-MGBNFQ |
| *BALF5* | 5’-CAGCAGGCCTACTTCTA-3’<br>5’-AGGGTGATCTTGTGGTAGTC-3’ | 6FAM-CAG GCC TAC TTC TAC GCC AG-MGBNFQ |
| *BDLF4* | 5'-GCGAGTACCACGTATGTG-3'<br>5'-GGTCCTGTGTGTCTTGTC–3’ | 6FAM-TTT CCT TTG TGT TCC CTT GC-MGBNFQ |
| *BGLF4* | 5'-GATCCGACCCGCTCTACTTT-3'<br>5'-GGTCAGGCCCATGTCTAAGT-3' | 6FAM-TGT CGC AGA TGT GGA ACC T-MGBNFQ |
| *BMRF1* | 5’-GGATCTCTACGTCACCACGT-3’<br>5'-GCCAGACCTGTAAAACCT-3' | 6FAM-CTC TGA GTG TGG GGC CAT AC-MGBNFQ |
| *BPLF1* | 5’-GCTAATAAGG.AGTAGGGACCGA-3’<br>5’-AGTTCGGAAGTGAGCAGTTG-3’ | 6FAM-TCT TAA AGG ACT GGT CGG GA-MGBNFQ |
| *BRRF1* | 5’-GCTGTTCCTGGCAAGAGTCT-3’<br>5’-GGCGATGTCACGCTGTTCAT-3’ | 6FAM-CCA TCG TCC CCA AGA TCT TA-MGBNFQ |
| *BVRF1* | 5’-CATGTCGGCTAATGCCAT-3’<br>5’-CACTTCTGTCATCAGC-3’ | 6FAM-AAC CTG AAC TTT ACC AAC TC-MGBNFQ |
| *BXLF1* | 5’-GCCGTGACATCTAATACT-3’<br>5’-AGTAGGCTTTTGGTGTG-3’ | 6FAM-ATC CTG CCC CTT TAC CCT AC-MGBNFQ |
| *BZLF1* | 5’-AGCCTGCTCCTGAGAATGCT-3’<br>5’-CCACTGCTGCTGCTGTTTGA-3’ | 6FAM-CTC AGC TGT TCC CAG TCT CC-MGBNFQ |

# 3 CHAPTER 3. REAL-TIME RT-PCR ANALYSIS OF EBV GENE EXPRESSION DURING THE EBV LYTIC INDUCTION PHASE IN RAJI CELLS

## 3.1 INTRODUCTION

In the immunocompetent host, expansion of EBV-transformed B lymphocytes is kept in check by a functional host CTL response. In immunosuppressed transplant patients there is uncontrolled expansion of EBV-latently infected B lymphocytes leading to PTLD, often as a result of EBV reactivation. EBV can transform B cells *in vitro* into LCLs (Young and Rickinson, 2004) that express latency III, which has also been noted in EBV-positive B cells in PTLD tumour biopsies (Brink et al., 1997). While the EBV latent genes, in particular *LMP-1* and *EBNA-2*, are known to be expressed in PTLD and have pathogenic roles, the role of the EBV lytic genes and therefore viral replication is less clear (Fields et al., 2007; Rowe et al., 1998). The latent-lytic switch has significant implications for pathogenesis. While latency is the most predominant phase found in PTLD, the virus must replicate lytically to enable transmission between cells and individuals (Countryman et al., 2009). EBV replication has been detected in PTLD biopsies and non-malignant oral hairy leukoplakia (OHL) (Montone et al., 1996; Walling et al., 2003). Further, several lytic genes have emerged as having transforming properties, including *BARF1* and *BILF1*, suggesting a role in the development of EBV-associated diseases such as PTLD (Lyngaa et al., 2010; Sheng et al., 2003). Since specific predictive markers for PTLD are lacking, we wanted to identify highly regulated EBV latent and lytic genes that could serve as potential markers for the early detection of this disease. A suitable experimental model for measuring EBV gene expression during the latent-lytic switch is the EBV-transformed Burkitt's lymphoma nonproducer Raji cell line, a Burkitt's lymphoma cell line (Pulvertaft, 1965). Raji cells are defective for EBV DNA lytic replication and as a consequence, late lytic gene expression is not detected (Chevallier-Greco et al.,

1986a; Decaussin et al., 1995; Laux et al., 1988). EBV-negative Ramos cells served as controls. The latent-lytic switch can be induced in Raji cells following treatment with TPA (Zur Hausen et al., 1978) a protein kinase agonist which activates the PKC pathway (Gradoville et al., 2002), in synergy with NaB, which functions as a histone deacetylase inhibitor (Luka et al., 1979). Moreover, Raji cells exhibit a latency III pattern of EBV gene expression. This is significant since latency III patterns have been associated with PTLD, making this a suitable model system for investigating EBV gene expression upon lytic induction in the context of PTLD (Brink et al., 1997).

### 3.1.1 Objectives of Chapter 3

EBV gene expression profiles were analysed in induced and uninduced Raji cells at 0, 2, 6, 24 and 48 hr time-points by real-time PCR with SYBR Green I chemistry.

The aims of the experiments described in this chapter were three-fold:

(i) To validate the real-time PCR assays for evaluation of EBV gene expression profiling in whole blood samples from PTLD and non-PTLD patients.

(ii) To examine the changes in relative expression of all 88 EBV genes during the latent-lytic switch.

(iii) To identify any highly induced EBV latent or lytic genes in order to evaluate their potential as predictive markers of PTLD.

## 3.2 RESULTS

### 3.2.1 Analytical validation of primer specificity using EBV B95-8 genomic DNA

Prior to the expression analysis, a commercially purchased stock of genomic DNA (gDNA) extracted from B95-8 cells was used to confirm the specificity of the EBV primer sets. EBV B95-8 gDNA was used as template in real-time PCR assays, where each primer set was evaluated for single peaks by melting curve analysis. To confirm the amplification of single products, PCR products from each PCR reaction were analysed on 2% agarose gels. Melt curve analysis and visualisation of PCR products demonstrated single products of the expected size for all primer sets (Panels A-E, Figure 3.1), with the exception of *BOLF1*, which showed non-specific amplicons (Lane 2, Panel D, Figure 3.1). Following validation of primer specificity, three deletions (*LF1*, *LF2* and *LF3*) from the B95-8 EBV genome were confirmed by the absence of specific amplicons of the expected size (Panel E, Figure 3.1) (Parker et al., 1990). The absence of these PCR products gives further confidence for the specificity of our PCR assays.

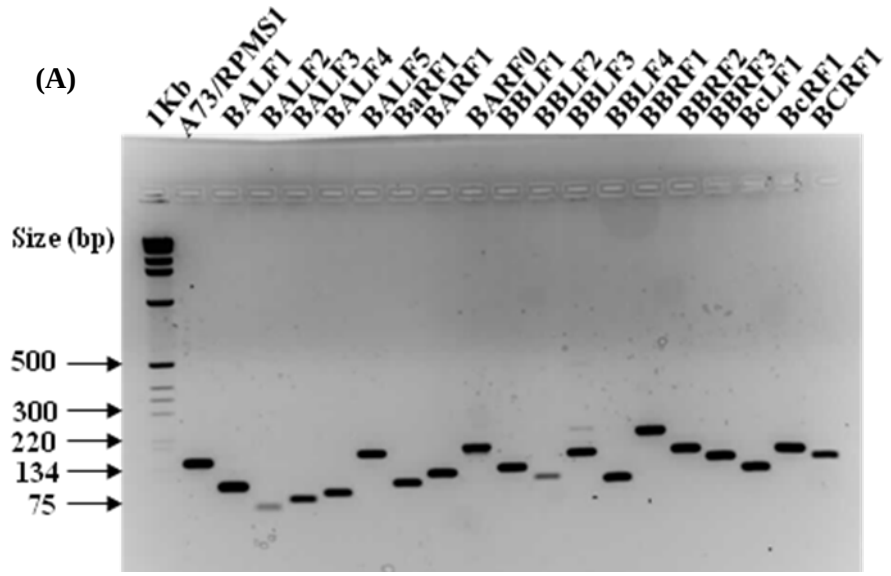
(A)
1Kb
A73/RPMS1
BALF1
BALF2
BALF3
BALF4
BALF5
BaRF1
BARF1
BARF0
BBLF1
BBLF2
BBLF3
BBLF4
BBRF1
BBRF2
BBRF3
BcLF1
BcRF1
BCRF1
Size (bp)
500
300
220
134
75

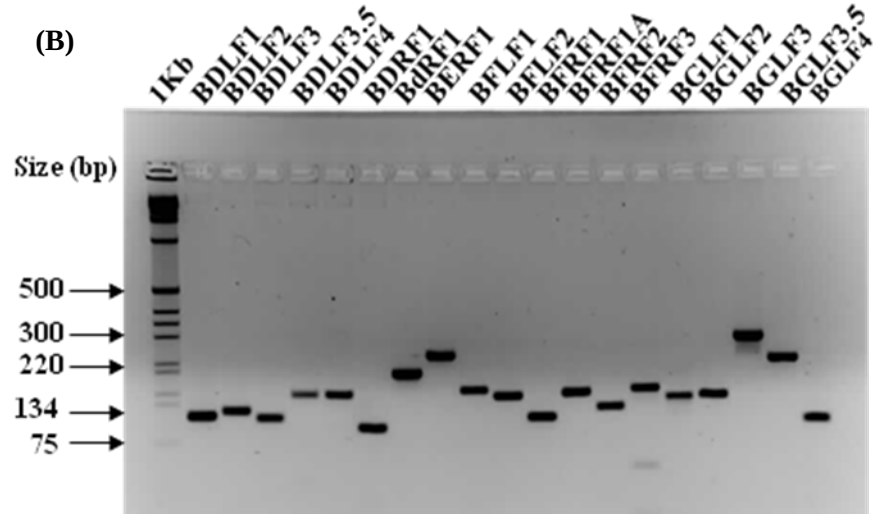
(B)
1Kb
BDLF1
BDLF2
BDLF3
BDLF3.5
BDLF4
BDRF1
BdRF1
BERF1
BFLF1
BFLF2
BFRF1
BFRF1A
BFRF2
BFRF3
BGLF1
BGLF2
BGLF3
BGLF3.5
BGLF4
Size (bp)
500
300
220
134
75

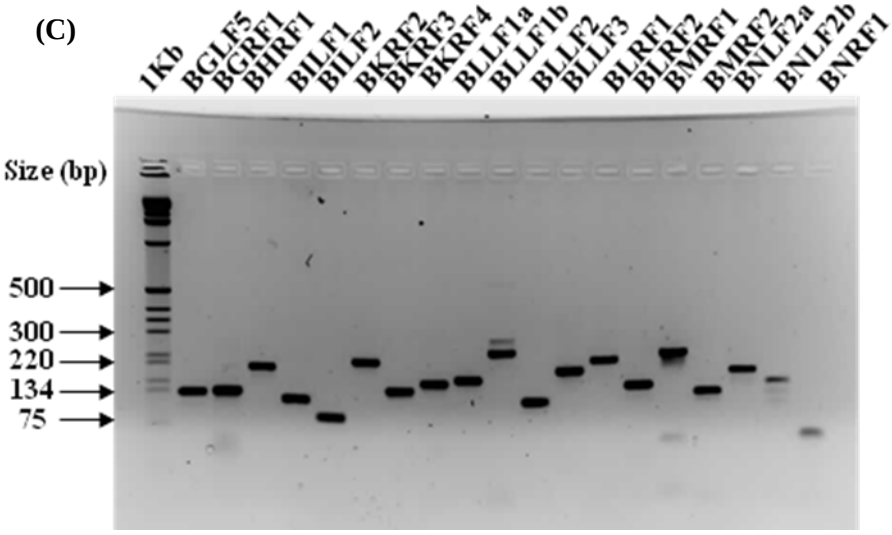
(C)
1Kb
BGLF5
BGRF1
BHRF1
BILF1
BILF2
BKRF2
BKRF3
BKRF4
BLLF1a
BLLF1b
BLLF2
BLLF3
BLRF1
BLRF2
BMRF1
BMRF2
BNLF2a
BNLF2b
BNRF1
Size (bp)
500
300
220
134
75

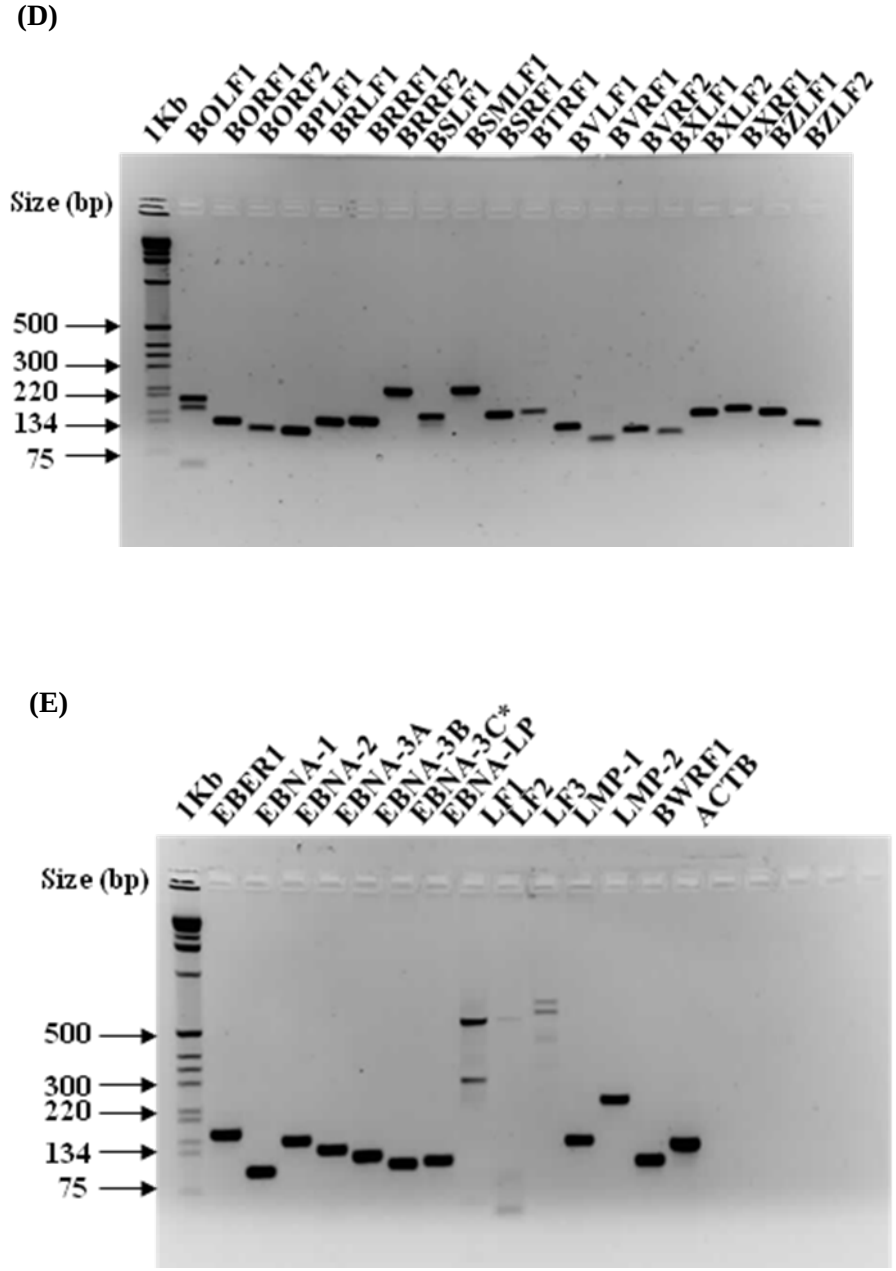


**Figure 3-1 Specificity of EBV primers using EBV B95-8 gDNA**

Agarose gel electrophoresis of 89 PCR products amplified using control DNA from EBV strain B95-8 (AbGene) as template. PCR amplification was performed using B95.8 control gDNA (Abgene). Real-time PCR was performed on gDNA using the BioRad iQ Sybr Green supermix with primers specific for the 89 EBV genes shown. Ten microlitres of double-stranded DNA PCR product was analysed by 2% agarose gel electrophoresis. The DNA was stained with Ethidium bromide prior to electrophoresis. (**A-E**) PCR products for the various EBV genes (bp); Lane 1, 1 Kbp molecular weight marker (M) (Invitrogen) and Lane 90, endogenous control *ACTB*. Asterisk indicates deletions from the B95.8 EBV genome.

### 3.2.2 Quality control of extracted total RNA for real-time PCR

Total RNA was extracted from induced Raji and Ramos cells, treated with DNase and reverse-transcribed into cDNA for gene expression analysis by real-time PCR. To confirm the absence of residual gDNA in the total RNA extract, a no reverse transcriptase (RTase) control was carried out and analysed by real-time PCR alongside other samples. Elimination of 'detectable' gDNA was demonstrated by the absence of an amplification curve following real-time PCR (details not shown). Additionally, no EBV gene expression could be detected in the no-RTase controls.

### 3.2.3 Analytical validation of primer specificity in cDNA from Raji cells

To confirm the ability of all 89 EBV primer sets to amplify EBV gene expression products, total RNA was extracted from TPA/NaB induced Raji cells at 24 hrs following lytic induction. It has been shown previously that most EBV gene products are expressed within 24 hrs following TPA/NaB induction (Pan et al., 2005). Total RNA was converted into cDNA and subjected to real-time PCR with all 89 EBV primer sets. Of the 89 primer sets, 85 gave single peaks in melting curve analysis as well as single PCR products of the expected size when analysed on 2% agarose gels (Panels A-E, Figure 3.2). Three genes (*BALF1*, *BZLF2* and *BARF1*) are deleted from the Raji EBV genome (Hatfull et al., 1988), along with two truncations (*BALF2*, and *EBNA-3C*) (Hatfull et al., 1988). PCR products were not detected for all four deletions confirming the two deletions in the Raji EBV genome (Panels A-E, Figure 3.2). However, *BALF2* showed low-level amplification in cDNA from induced Raji cells (Lane 3, Panel A, Figure 3.2). As expected, PCR products were detected for all five genes following amplification with genomic DNA from wild type B95-8 cells (Panels A-E, Figure 3.1). However, a weakly intense band was detected for *BALF2* (Lane 3, Panel A, Figure 3.1).

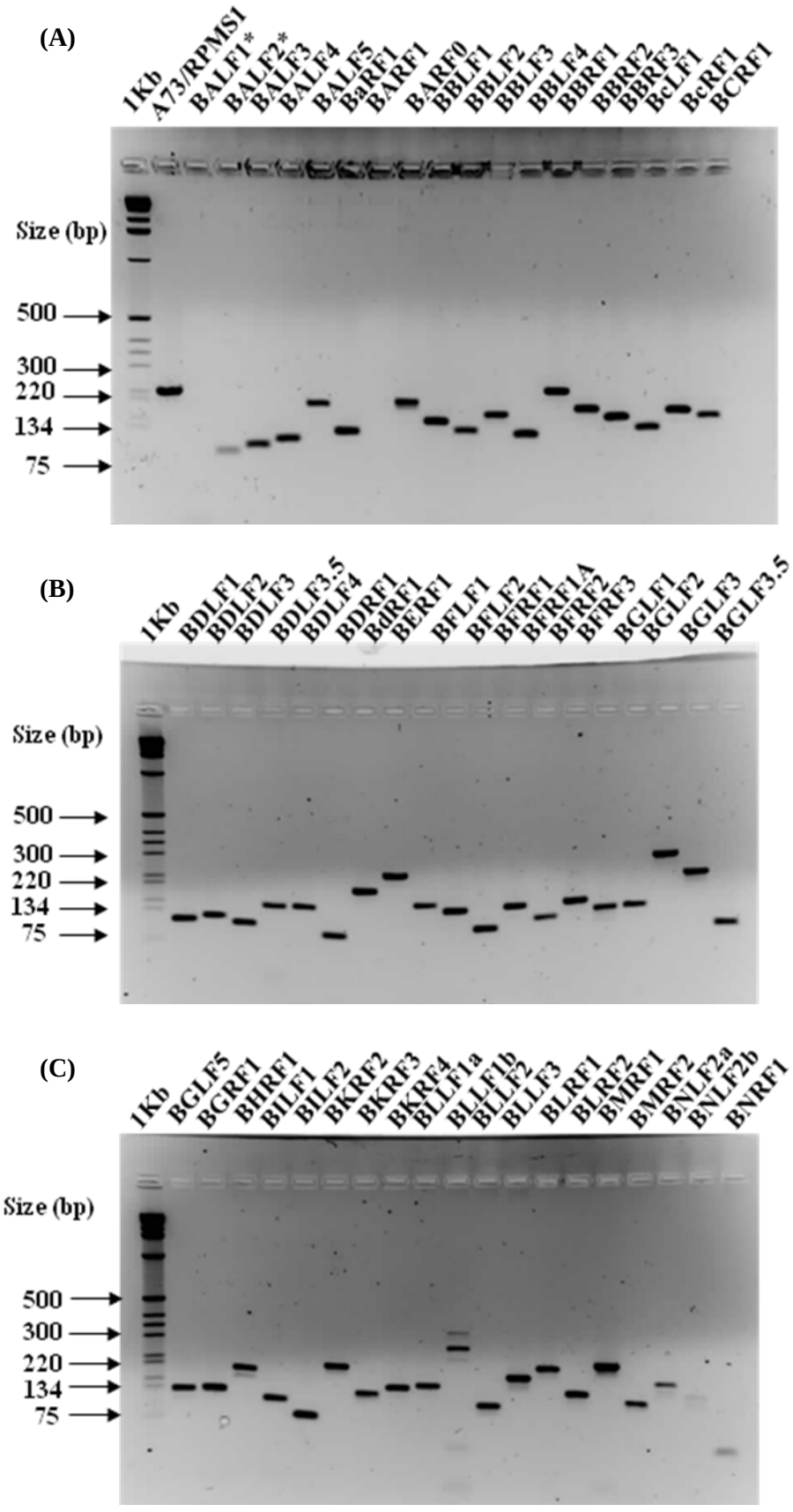
(A)
1Kb
A73/RPMS1
BALF1*
BALF2*
BALF3
BALF4
BALF5
BaRF1
BARF1
BARF0
BBLF1
BBLF2
BBLF3
BBLF4
BBRF1
BBRF2
BBRF3
BcLF1
BcRF1
BCRF1
Size (bp)
500
300
220
134
75
(B)
1Kb
BDLF1
BDLF2
BDLF3
BDLF3.5
BDLF4
BDRF1
BdRF1
BERF1
BFLF1
BFLF2
BFRF1
BFRF1A
BFRF2
BFRF3
BGLF1
BGLF2
BGLF3
BGLF3.5
Size (bp)
500
300
220
134
75
(C)
1Kb
BGLF5
BGRF1
BHRF1
BILF1
BILF2
BKRF2
BKRF3
BKRF4
BLLF1a
BLLF1b
BLLF2
BLLF3
BLRF1
BLRF2
BMRF1
BMRF2
BNLF2a
BNLF2b
BNRF1
Size (bp)
500
300
220
134
75

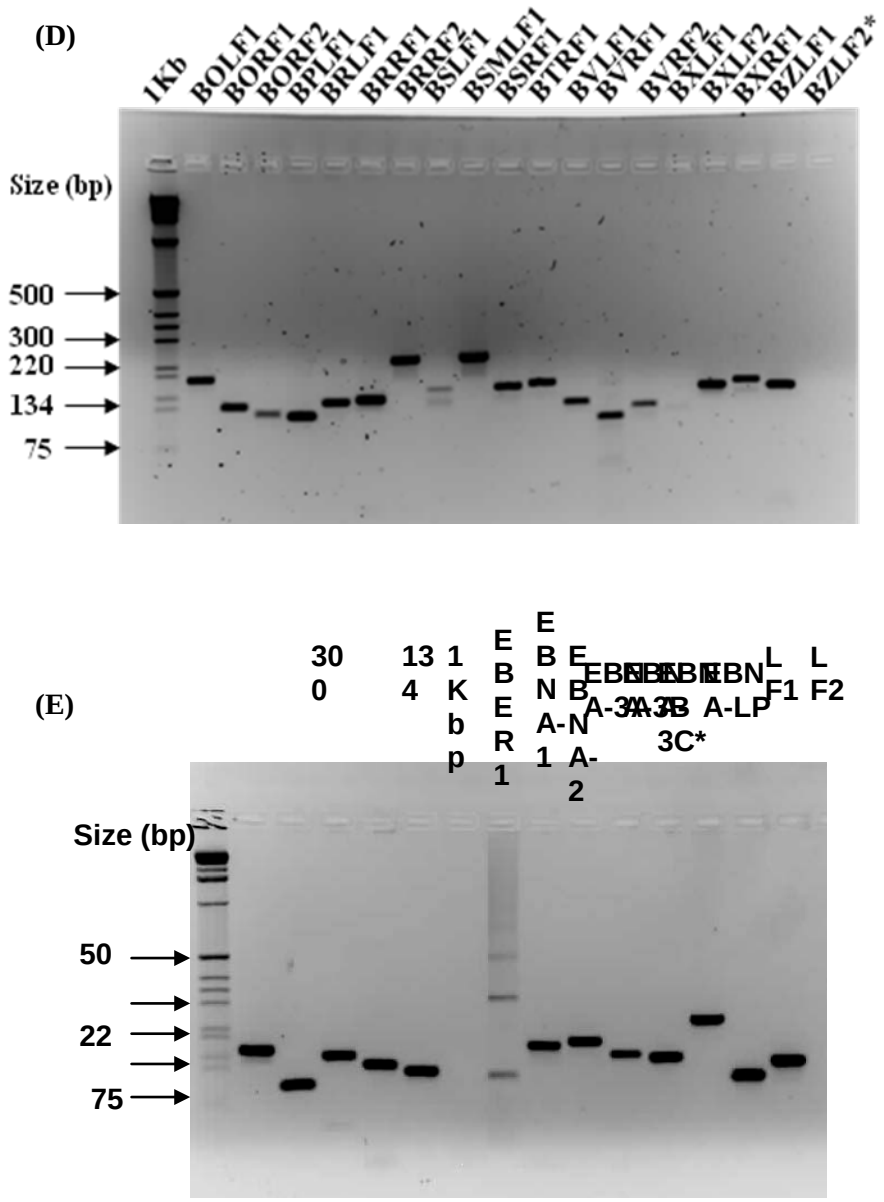


**Figure 3-2 Specificity of EBV primers using Raji cDNA**

Agarose gel electrophoresis of 89 PCR products amplified from Raji cDNA. Real-time PCR was performed using cDNA derived from total RNA from Raji cells stimulated with TPA/NaB and harvested at 24 hr time-points. Real-time PCR was performed on gDNA using the BioRad iQ Sybr Green supermix with primers specific for the 89 EBV genes shown. Ten microlitres of double-stranded DNA PCR product was analysed by 2% agarose gel electrophoresis. The DNA was stained with Ethidium bromide prior to electrophoresis. (**A**-**E**) PCR products for the various EBV genes (bp); Lane 1, 1 Kbp molecular weight marker (M) (Invitrogen) and Lane 90 show the endogenous control *ACTB*. Asterisk indicates deletions from the Raji EBV genome.

### 3.2.4 Analytical validation of primer specificity using EBV-negative Ramos

To confirm that amplification of single products from EBV B95.8 virus and Raji cells was not due to host cellular gDNA and gene expression, respectively, gDNA from the EBV negative Ramos cell line was tested by real-time PCR. The PCR products from B95-8 and Raji cells (Panels A-E, Figure 3.1 and 3.2) were compared to those amplified from Ramos (Panels A-E, Figure 3.3). No specific single peaks were detected by melt-curve analysis on gDNA from Ramos cells. The lack of specific products was confirmed further by the absence of PCR products of the expected size following PCR amplification of gDNA from Ramos cells. In all of our subsequent PCR assays, multiple peaks by melt-curve analysis were used to determine non-specific amplification.

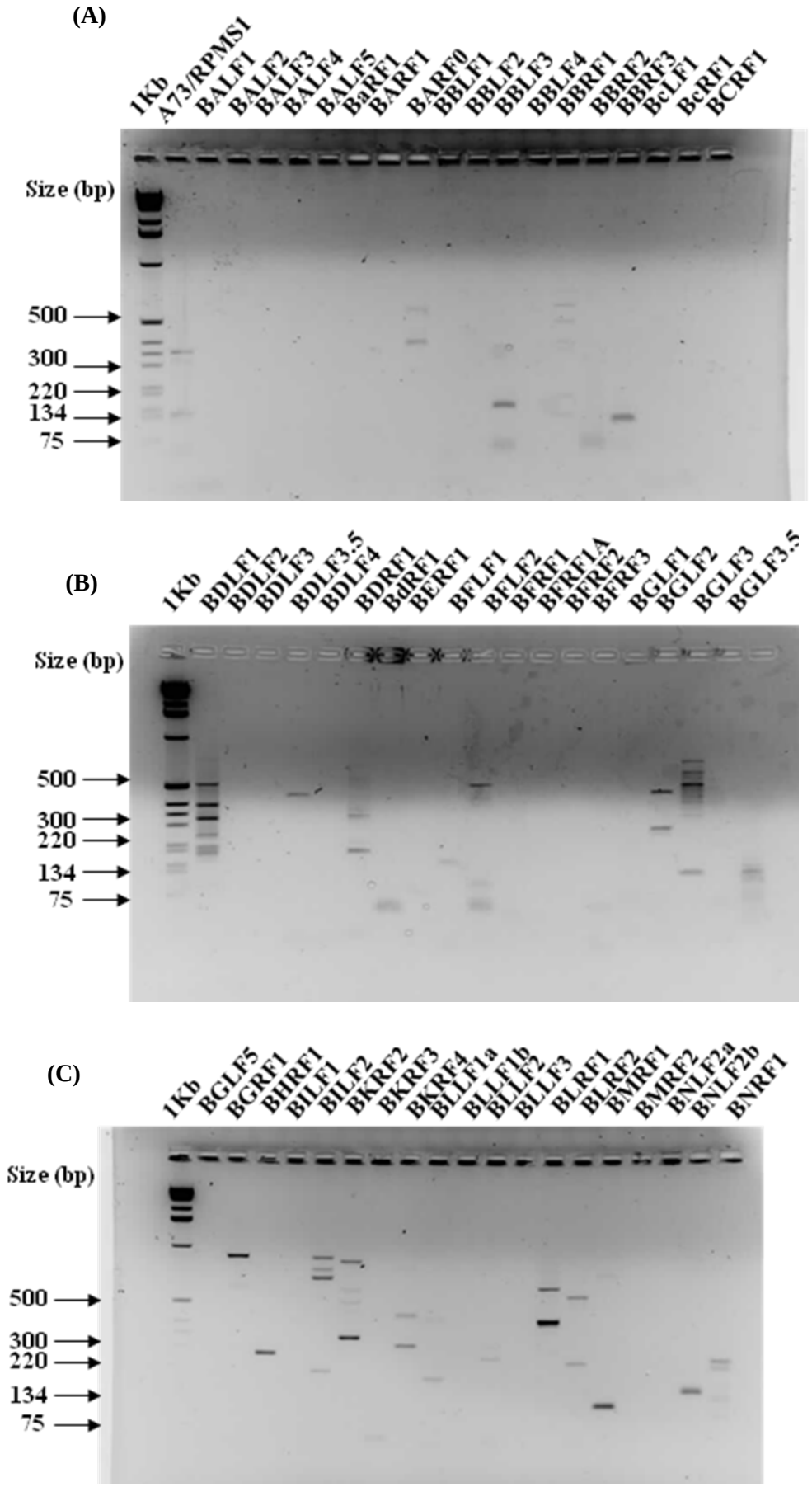
(A)
1Kb
A73/RPMS1
BALF1
BALF2
BALF3
BALF4
BALF5
BaRF1
BARF1
BARF0
BBLF1
BBLF2
BBLF3
BBLF4
BBRF1
BBRF2
BBRF3
BcLF1
BcRF1
BCRF1
Size (bp)
500
300
220
134
75
(B)
1Kb
BDLF1
BDLF2
BDLF3
BDLF3.5
BDLF4
BDRF1
BdRF1
BERF1
BFLF1
BFLF2
BFRF1
BFRF1A
BFRF2
BFRF3
BGLF1
BGLF2
BGLF3
BGLF3.5
Size (bp)
500
300
220
134
75
(C)
1Kb
BGLF5
BGRF1
BHRF1
BILF1
BILF2
BKRF2
BKRF3
BKRF4
BLLF1a
BLLF1b
BLLF2
BLLF3
BLRF1
BLRF2
BMRF1
BMRF2
BNLF2a
BNLF2b
BNRF1
Size (bp)
500
300
220
134
75

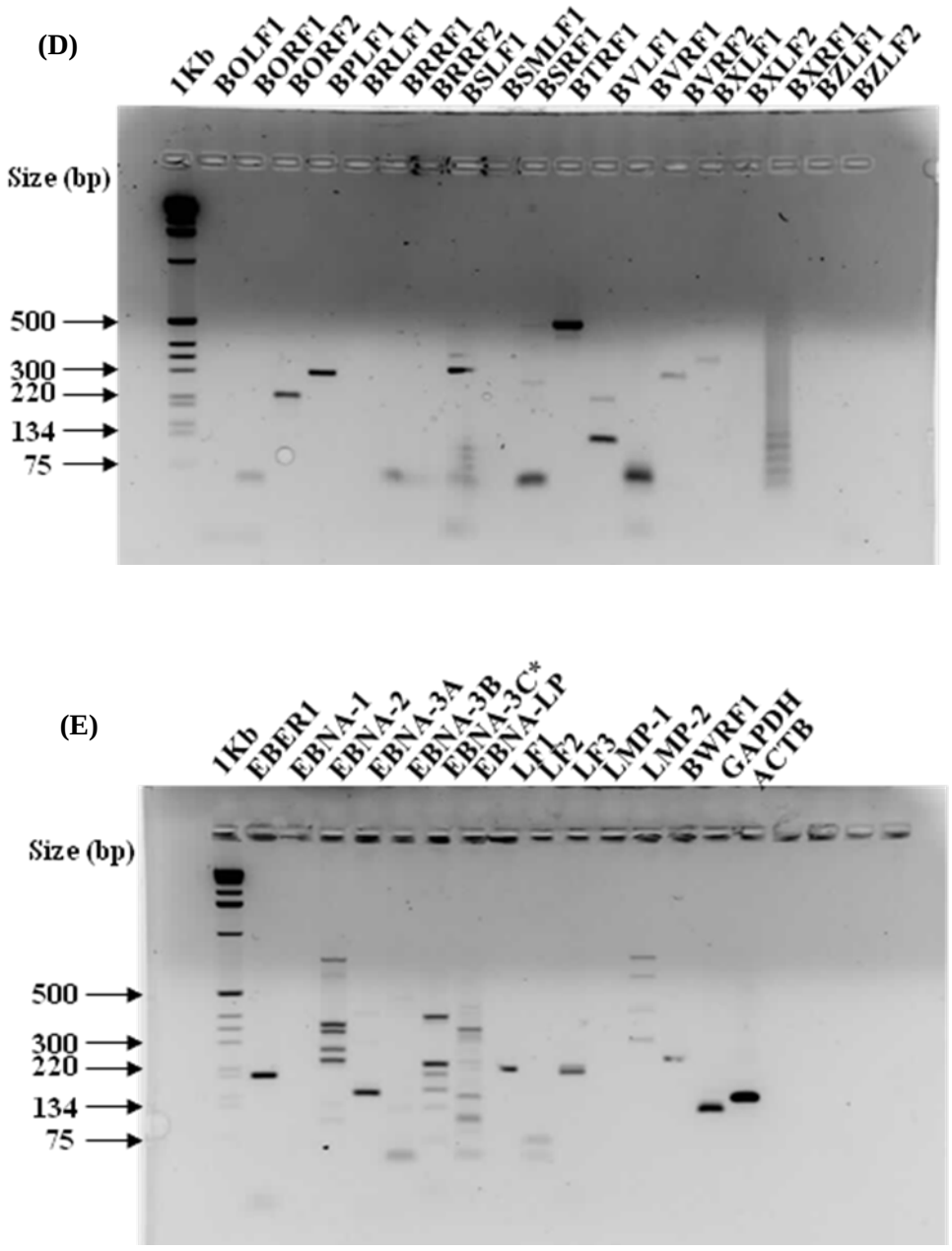


**Figure 3-3 Specificity of EBV primers using gDNA from EBV-negative Ramos cells**

Agarose gel electrophoresis of 89 PCR products amplified from Ramos gDNA. Real-time PCR was performed using cDNA derived from total RNA from Ramos cells stimulated with TPA/NaB and harvested at 24 hr time-points. Real-time PCR was performed using gDNA isolated from 2 x $10^6$ Ramos cells using the Qiagen DNeasy extraction kit. Real-time PCR was performed on gDNA using the BioRad iQ Sybr Green supermix with primers specific for the 89 EBV genes shown. Ten microlitres of double-stranded DNA PCR product was analysed by 2% agarose gel electrophoresis. The DNA was stained with Ethidium bromide prior to electrophoresis. (**A**-**E**) PCR products for the various EBV genes (bp); Lane 1, 1 Kbp molecular weight marker (M) (Invitrogen) and Lane 90, endogenous control *ACTB*.

### 3.2.5 Validation of real-time PCR assay sensitivity

To demonstrate that sufficient cDNA would be available for the entire EBV gene expression analysis, a small-scale sensitivity study was carried out. Dilutions (1/2-1/20) of cDNA were tested using primers specific to *BZLF1* and *ACTB* and the Ct values for the differing amounts of templates compared. Both targets were detectable in all the dilutions (Panels A and B, Figures 3.4). From these experiments, 1/10 dilutions of cDNA were used in real-time PCR.

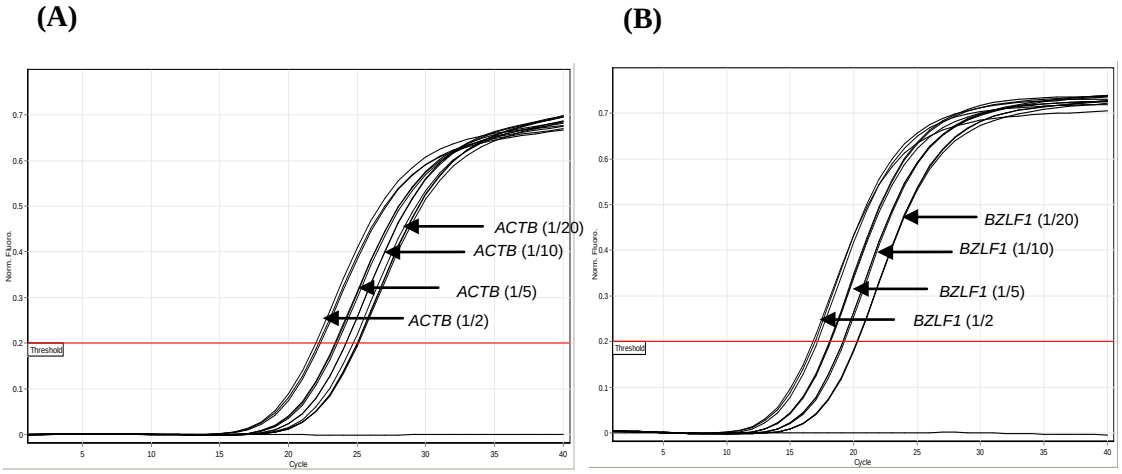


**Figure 3-4 Sensitivity of detection of *ACTB* and *BZLF1* from induced Raji cells**

Raji cells were stimulated with 30 ng/ml TPA and 3mM NaB and harvested at 24 hr time-points. Total RNA was isolated from the harvested cells using the Qiagen RNeasy Mini Extraction Kit and 2 µg total RNA reverse-transcribed into cDNA using the RetroScript kit. Serial dilutions (1/2 – 1/20) of cDNA template was prepared and amplified by real-time PCR for *ACTB* (**A**) and *BZLF1* (**B**) by amplification with primers specific for *ACTB* AND *BZLF1*. Arrows indicate the serial dilutions for the cDNA amplified by *ACTB* and *BZLF1*. All values are the mean of triplicates.

### 3.2.6 Analysis of fold-changes in EBV gene expression at 0-48 hrs

To examine the expression of 88 of the 89 EBV genes (*BERF1* omitted) during the latent-lytic switch, gene expression was measured following TPA/NaB induction of Raji cells compared with uninduced Raji cells. Relative expression levels of all 88 EBV genes (11 latent, 2 immediate-early (IE), 33 early and 42 late genes) (Table 3.2) were analysed in a single biological replicate tested in triplicate at 0, 2, 6, 24 and 48 hr time-points after lytic induction. For the early time-points (0, 2 and 6 hrs), induction levels were below 2-fold (Table 7.1). Relative expression levels were calculated using the delta Ct method as described previously. Because of the relatively small changes in expression levels in the early time-points, subsequent analyses were carried out only on samples from the 24 and 48 hr inductions.

#### 3.2.6.1 Fold-changes of the immediate-early genes at 24-48 hrs

Evidence of EBV lytic induction was demonstrated at 24 hrs after TPA/NaB induction by the expression of the IE gene *BZLF1* with a 19-fold and 156-fold induction above uninduced levels at 24 and 48 hrs, respectively (Figure 3.5; Table 3.1). In contrast, the IE gene *BRLF1* was induced from 3-fold at 24 hrs up to 60-fold at 48 hrs (Figure 3.5). The mean of the variation was low for both *BZLF1* and *BRLF1* (Table 3.1). Hence error bars were not visible (Figure 3.5).

**Table 3-1 Summary of fold-changes of the immediate-early genes**

| Gene (*n*=2) | Mean fold-change at 24 hrs (±SD) | Mean fold-change at 48 hrs (±SD) |
|---|---|---|
| *BRLF1* | 3.69 (±0.01) | 60.33(±1.16) |
| ***BZLF1*** | 19.38 (±1.07) | 156.00(±10.39) |

SD, standard deviation; EBV immediate-early gene selected for further analysis (bold)

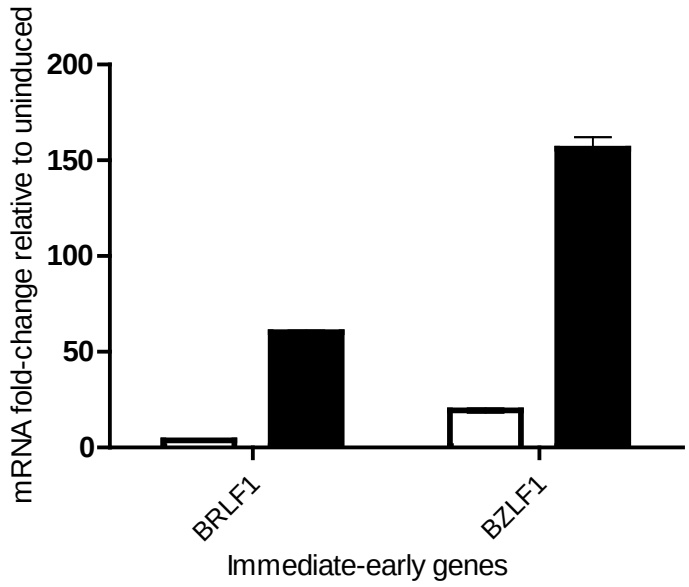


**Figure 3-5 Fold-changes in expression of the EBV immediate-early genes at 24-48 hrs following TPA/NaB induction of Raji cells**

Fold-changes in expression of two immediate-early EBV genes in induced versus uninduced Raji cells. Raji cells were stimulated with TPA/NaB to induce the EBV lytic phase and cells harvested at 24 and 48 hr time-points. Uninduced Raji cells served as the control. After 24 hrs of induction, total RNA was extracted from three biological replicates of induced and uninduced Raji cells using the Qiagen RNeasy mini extraction kit. cDNA was generated from 2 µg total RNA using the Ambion RETROscript™ kit. Real-time PCR was performed on cDNA from three technical replicates using the BioRad iQ SYBR Green supermix with primers specific for the EBV genes shown. ΔCt values were calculated for each gene using the *ACTB* gene as reference according to the comparative quantitation method (ΔΔCt) (Livak and Schmittgen, 2001), provided on the Rotorgene™ software (Qiagen, UK). Relative expression values were converted to fold-change values for each of the replicates ($\Delta Ct_{\text{Induced/Uninduced}}$) using Prism (GraphPad Prism, USA). Data represents the mean fold-change relative to uninduced ±SD of one experiment performed in triplicate.

### 3.2.6.2 Fold-changes of the EBV early genes at 24-48 hrs

Fold-induction levels were determined for all of the 33 EBV early genes and are summarised in Table 3.2. With the exception of the two deletions discussed previously (*BALF1* and *BARF1*), expression was detected in all genes (31/33 [93.94%]) (Panel A, Figure 3.6). This includes the truncation in *BALF2*; induced at 10-fold and 7-fold at 24 hrs and 48 hrs, respectively (Panel A, Figure 3.6).

At the 24 hr time-point, 16/33 (48.48%) early genes were induced above 10-fold (Table 3.5), including 13/33 (39.39%) early genes (*BALF2*, *BALF3*, *BALF5*, *BBLF2*,

*BBLF3, BBLF4, BDLF4, BFLF2, BFRF1, BFRF2, BILF1, BMRF1, BSLF1, BORF2* and *BXRF1*) that were induced between 10-100-fold (Panels A-D, Figure 3.6; Table 3.2) and 3/33 (9.09%) early genes (*BcRF1, BGLF4, BXLF1*) that were induced over 100-fold at 104-, 114- and 153-fold, respectively (Panels B and D, Figure 3.6, Table 3.2). Noticeably, 8/33 (24.24%) genes (*BALF2, BALF3, BALF5, BBLF2, BBLF3, BBLF4, BcRF1* and *BGLF4*) were induced higher at 24 versus 48 hrs (Panels A-C, Figure 3.6; Table 3.2).

At the 48 hr time-point, 25/33 (75.76%) early genes were induced above 10-fold (Table 3.4), including 16/33 (48.48%) genes (*BALF3*, *BaRF1*, *BBLF2*, *BcRF1*, *BGLF4*, *BGLF5*, *BHRF1*, *BILF1*, *BKRF3*, *BLLF3*, *BRRF1*, *BSLF1*, *BSMLF1*, *BXRF1*, *LF1*, *LF2* and *LF3*) that were induced between 10-100-fold and 8/33 (24.24%) genes (*BDLF4, BFLF2, BFRF1*, *BFRF2*, *BILF1*, *BMRF1, BORF2* and *BXLF1*) that were induced over 100-fold (Panels B-D, Figure 3.6 Table 3.2). Notably, two genes *BFRF2* and *BMRF1* were induced over 1000-fold from 24 to 48 hrs (Panels B and C, Figure 3.6; Table 3.2).

**Table 3-2 Summary of fold-changes in expression of the EBV early genes**

| Gene (*n*=33) | Mean fold-change at 24 hrs (±SD) | Mean fold-change at 48 hrs (±SD) |
|---|---|---|
| *BALF1** | - | - |
| *BALF2* | 10.64 (±3.43) | 7.47 (±1.45) |
| *BALF3* | 26.47 (±11.43) | 15.69 (±0.00) |
| ***BALF5*** | 14.15 (±1.20) | 6.23 (±0.34) |
| *BaRF1* | 3.42 (±2.23) | 59.88 (±1.87) |
| *BARF1** | - | - |
| *BBLF2* | 87.60 (±1.49) | 21.77 (±1.16) |
| *BBLF3* | 34.10 (±5.56) | 7.80 (±0.00) |
| *BBLF4* | 54.99 (±33.12) | 9.80 (±2.39) |
| ***BcRF1*** | 104.44 (±91.38) | 63.67 (±2.01) |
| ***BDLF4*** | 12.30 (±11.04) | 141.33 (±7.35) |
| *BFLF1* | 5.37 (±1.30) | 38.67 (±3.06) |
| *BFLF2* | 11.59 (±0.72) | 114.93 (±99.64) |
| ***BFRF1*** | 19.11 (±1.14) | 597.33 (±18.48) |
| ***BFRF2*** | 29.66 (±1.56) | 1406.67 (±1219.59) |
| *BGLF5* | 3.22 (±0.10) | 39.00 (±2.00) |
| ***BGLF4*** | 114.17 (±7.11) | 38.58 (±1.20) |
| *BHRF1* | 0.45 (±0.11) | 11.77 (±1.37) |
| *BILF1* | 12.13 (±1.34) | 106.28 (±5.56) |
| *BKRF3* | 5.12 (±0.29) | 90.33 (±4.51) |
| *BLLF2* | 9.49 (±1.12) | 102 (±11.53) |
| *BLLF3* | 2.61 (±0.55) | 35.33 (±30.75) |
| ***BMRF1*** | 90.17 (±10.51) | 1323.67 (±343.52) |
| *BNLF2a* | 2.15 (±0.21) | 5.50 (±0.17) |
| *BNLF2b* | 2.10 (±0.12) | 3.67 (±0.40) |
| *BORF2* | 20.25 (±1.23) | 166.00 (±5.20) |
| ***BRRF1*** | 7.19 (±1.00) | 73.33 (±5.86) |
| *BSLF1* | 7.08 (±0.40) | 28.33 (±24.95) |
| *BSMLF1* | 8.30 (±0.00) | 20.33 (±1.16) |
| ***BXLF1*** | 153.00 (±9.88) | 624.00 (±34.00) |
| *LF1* | 7.04 (±1.88) | 11.67 (±1.16) |
| *LF2* | 3.62 (±0.20) | 11.33 (±0.58) |
| *LF3* | 5.53 (±0.00) | 59.00 (±6.00) |

-, not detectable; SD, standard deviation; * deletion; EBV early genes selected for further analysis (bold)

**(A)**

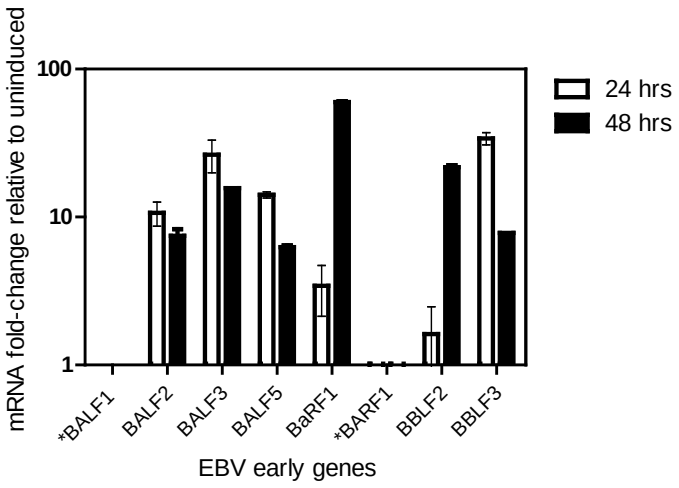
mRNA fold-change relative to uninduced
100
10
1
24 hrs
48 hrs
*BALF1
BALF2
BALF3
BALF5
BaRF1
*BARF1
BBLF2
BBLF3
EBV early genes

**(B)**

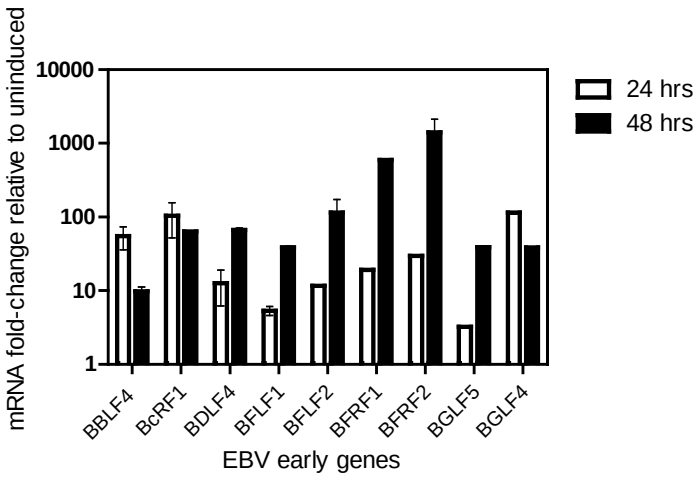
mRNA fold-change relative to uninduced
10000
1000
100
10
1
24 hrs
48 hrs
BBLF4
BcRF1
BDLF4
BFLF1
BFLF2
BFRF1
BFRF2
BGLF5
BGLF4
EBV early genes

**(C)**

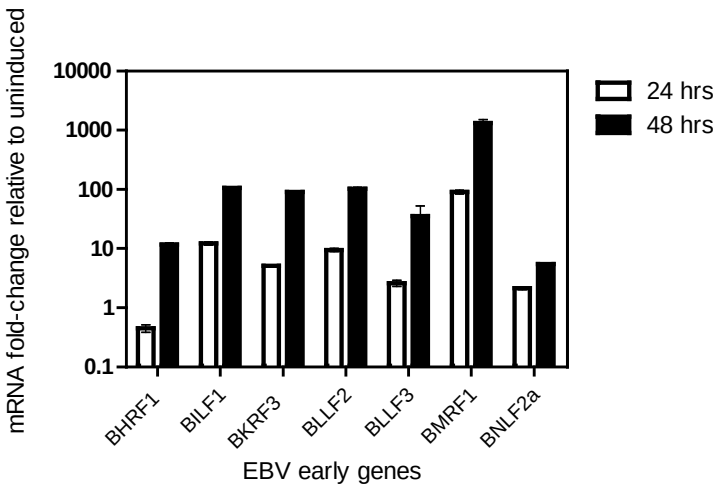
mRNA fold-change relative to uninduced
10000
1000
100
10
1
0.1
24 hrs
48 hrs
BHRF1
BILF1
BKRF3
BLLF2
BLLF3
BMRF1
BNLF2a
EBV early genes

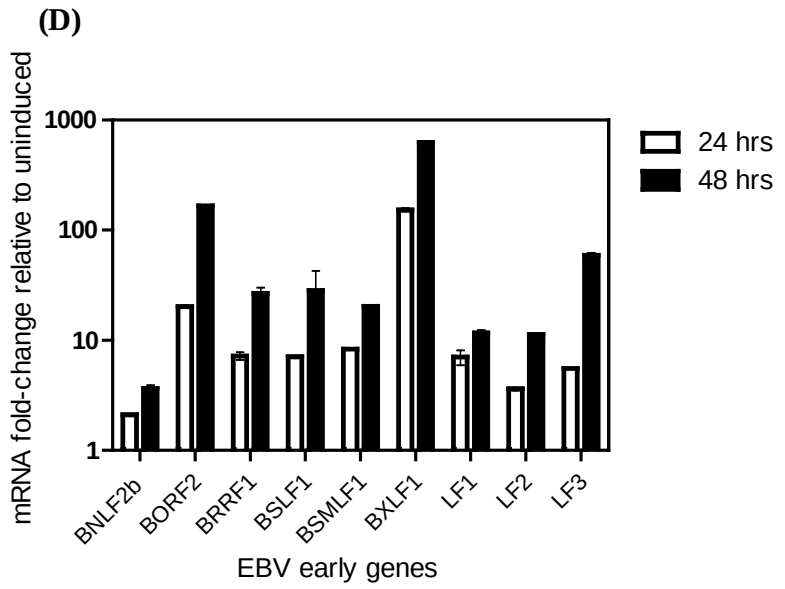


**Figure 3-6 Fold-changes in expression of the EBV early genes at 24-48 hrs following TPA/NaB induction of Raji cells**

Fold-changes in expression of 33 EBV early genes in induced versus uninduced Raji cells **(A-D)**. Raji cells were stimulated with TPA/NaB to induce the EBV lytic phase and cells harvested at 24 and 48 hr time-points. Uninduced Raji cells served as the control. After 24 hrs of induction, total RNA was extracted from three biological replicates of induced and uninduced Raji cells using the Qiagen RNeasy mini extraction kit. cDNA was generated from 2 µg total RNA using the Ambion RETROscript™ kit. Real-time PCR was performed on cDNA from three technical replicates using the BioRad iQ SYBR Green supermix with primers specific for the EBV genes shown. ΔCt values were calculated for each gene using the *ACTB* gene as reference according to the comparative quantitation method (ΔΔCt) (Livak and Schmittgen, 2001), provided on the Rotorgene™ software (Qiagen, UK). Relative expression values were converted to fold change values for each of the replicates ($\Delta Ct_{\text{Induced/Uninduced}}$) using Prism (GraphPad Prism, USA). Asterisks indicate deletions from the Raji EBV genome. Data represents the mean fold-change relative to uninduced ±SD of one experiment performed in triplicate.

### 3.2.6.3 Fold-changes of the EBV late genes at 24-48 hrs

Fold-induction levels were also determined for 42 EBV late genes (Table 3.3), with the exception of deletion *BZLF2* (Panel D, Figure 3.7). Unexpectedly, At the 24 hr time-point, 20/42 (47.62%) genes were induced above 10-fold (Table 3.5), including 18/42 (42.86%) genes (*BBLF1, BBRF2, BcLF1, BDLF2, BDRF1, BdRF1, BFRF1A, BFRF3, BGLF1, BILF2, BKRF4, BOLF1, BPLF1, BTRF1, BVLF1, BVRF2, BWRF1* and *BXLF2*) induced between 10-100-fold (Panels A-D, Figure 3.7) and 2/42 (4.76%) genes (*BMRF2* and *BXLF2)* that were induced over 100-fold at 117- and 103-fold,

respectively (Panels C and D, Figure 3.7). However, despite measuring 11- and 53-fold-induction level at 24 hrs and 48 hrs, respectively for *BWRF1*, this gene is not known to be expressed (Jenson et al., 1987).

At the 48 hr time-point, 33/42 (78.57%) genes were induced above 10-fold (Table 3.5), including 19/42 (45.24%) genes that were induced between 10-100 fold and 13/42 (30.95%) genes (*BDLF3*, *BDRF1*, *BdRF1*, *BFRF1A*, *BFRF3*, *BILF2*, *BKRF4*, *BMRF2*, *BOLF1*, *BORF1*, *BPLF1*, *BVRF1* and *BXLF2*) that were induced over 100-fold, of which three genes (*BdRF1*, *BOLF1* and *BXLF2*) were induced over >1000-fold (Panels B, C and D, Figure 3.7; Table 3.3). Moreover, of the 13 genes induced over 100-fold, only two genes (*BMRF2* and *BXLF2*) were induced highly from >100-fold (117- and 103-fold) at 24 hrs to >800-fold (826- and 1365-fold) at 48 hrs (Panels C and D, Figure 3.7; Table 3.3). In contrast, the other 10 genes were induced from <100-fold at 24 hrs to >100-fold at 48 hr (Table 3.3). Overall, in comparison to the early genes, most late gene expression was increased at 48 hrs following TPA/NaB induction in Raji cells (Table 3.5).

**Table 3-3 Summary of fold-changes in expression of the EBV late genes**

| Gene (*n*=42) | Mean fold-induction at 24 hrs (±SD) | Mean fold-induction at 48 hrs (±SD) |
|---|---|---|
| *BALF4* | 2.38 (±0.20) | 7.01 (±0.23) |
| *BBLF1* | 3.5 (±0.56) | 20.79 (±1.75) |
| *BBRF1* | 6.70 (±5.81) | 1.68 (±1.07) |
| *BBRF2* | 34.74 (±2.05) | 62.50 (±4.44) |
| *BBRF3* | 4.35 (±1.45) | 1.49 (±0.84) |
| *BcLF1* | 32.37 (±5.12) | 41.81 (±4.65) |
| *BCRF1* | 6.92 (±0.62) | 76.61 (±8.34) |
| *BDLF1* | 3.48 (±0.22) | 28.99 (±0.77) |
| *BDLF2* | 23.42 (±0.72) | 45.44 (±39.54) |
| *BDLF3.5* | 2.85 (±0.57) | 91.06 (±2.76) |
| ***BDLF3*** | 3.50 (±0.56) | 313.15 (±19.88) |
| ***BDRF1*** | 17.25 (±0.21) | 900.60 (±393.44) |
| ***BdRF1*** | 27.33 (±2.29) | 1693.23 (±155.22) |
| ***BFRF1A*** | 21.99 (±1.18) | 736.67 (±390.29) |
| ***BFRF3*** | 13.31 (±11.71) | 158.33 (±30.07) |
| *BGLF1* | 10.41 (±1.19) | 38.84 (±2.92) |
| *BGLF2* | 1.49 (±1.31) | 25.33(±1.16) |
| *BGLF3.5* | 1.06 (±0.17) | 8.58 (±0.72) |
| *BGLF3* | 4.15 (±0.51) | 6.30 (±0.70) |
| *BGRF1* | 0.35 (±0.22) | 4.03 (±0.31) |
| ***BILF2*** | 23.76 (±3.12) | 254.33 (±16.17) |
| *BKRF2* | 0.56 (±0.11) | 12.00 (±1.00) |
| ***BKRF4*** | 12.50 (±1.01) | 251.33 (±41.04) |
| *BLLF1a* | 2.63 (±0.29) | 5.67 (±4.93) |
| *BLLF1b* | 2.85 (±0.40) | 13.33 (±0.58) |
| *BLRF1* | 2.70 (±0.52) | 24.67 (±2.08) |
| *BLRF2* | 3.18 (±0.52) | 29.33 (±2.08) |
| ***BMRF2*** | 117.01 (±16.58) | 826.33 (±71.91) |
| *BNRF1* | 4.37 (±0.99) | 59.00 (±51.16) |
| ***BOLF1*** | 58.0 (±3.46) | 1331.33 (±15555.01) |
| ***BORF1*** | 1.45 (±0.24) | 245.33 (±30.60) |
| ***BPLF1*** | 32.73 (±2.70) | 569.80 (±99.98) |
| *BRRF2* | 3.48 (±0.41) | 17.67 (±1.53) |
| *BSRF1* | 5.16 (±1.27) | 70.33 (±5.69) |
| *BTRF1* | 12.03 (±1.31) | 28.33 (±2.08) |
| *BVLF1* | 8.94 (±4.16) | 70 (±4.00) |
| ***BVRF1*** | 27.55 (±3.54) | 219.67 (±17.24) |
| *BVRF2* | 21.40 (±2.76) | 53.33 (±8.51) |
| *BWRF1* | 11.16 (±1.01) | 53.00 (±9.54) |
| ***BXLF2*** | 103.19 (±5.62) | 1365.67 (±657.03) |
| *BXRF1* | 43.81 (±3.62) | 70.68 (±14.98) |
| *BZLF2** | - | - |

-, not detectable; SD, standard deviation; * deletion; EBV late genes selected for further analysis (bold)

**(A)**

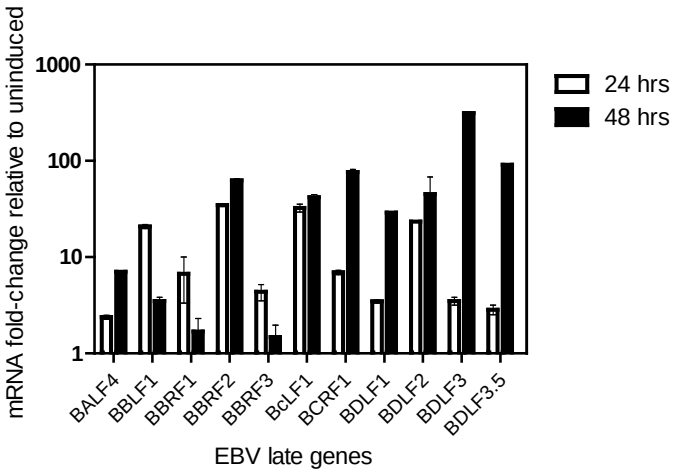
mRNA fold-change relative to uninduced
1000
100
10
1
24 hrs
48 hrs
BALF4
BBLF1
BBRF1
BBRF2
BBRF3
BcLF1
BCRF1
BDLF1
BDLF2
BDLF3
BDLF3.5
EBV late genes

**(B)**

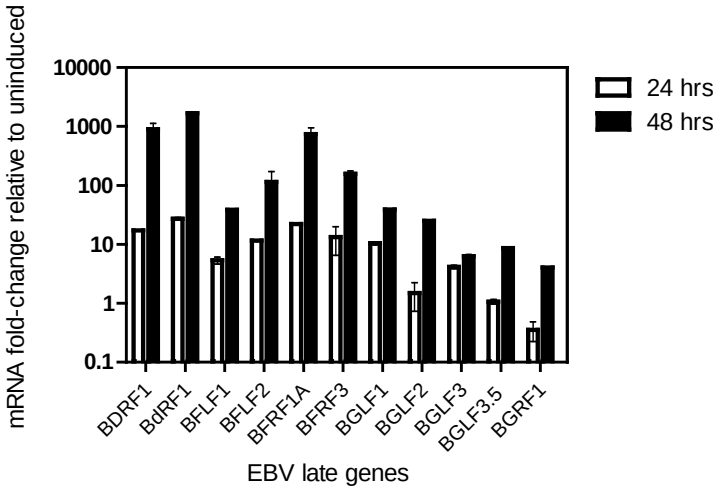
mRNA fold-change relative to uninduced
10000
1000
100
10
1
0.1
24 hrs
48 hrs
BDRF1
BdRF1
BFLF1
BFLF2
BFRF1A
BFRF3
BGLF1
BGLF2
BGLF3
BGLF3.5
BGRF1
EBV late genes

**(C)**

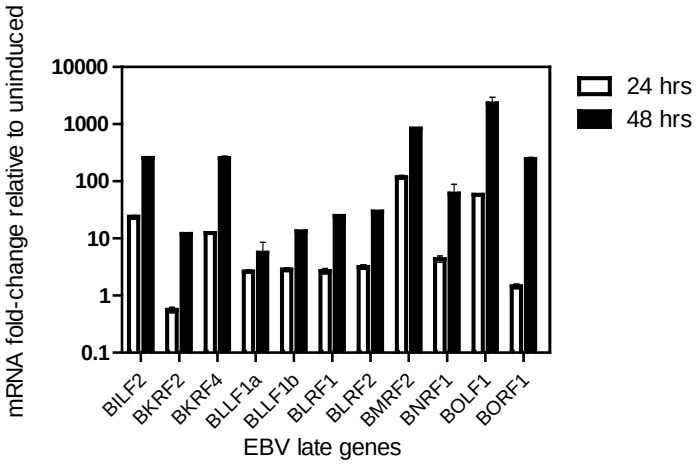
mRNA fold-change relative to uninduced
10000
1000
100
10
1
0.1
24 hrs
48 hrs
BILF2
BKRF2
BKRF4
BLLF1a
BLLF1b
BLRF1
BLRF2
BMRF2
BNRF1
BOLF1
BORF1
EBV late genes

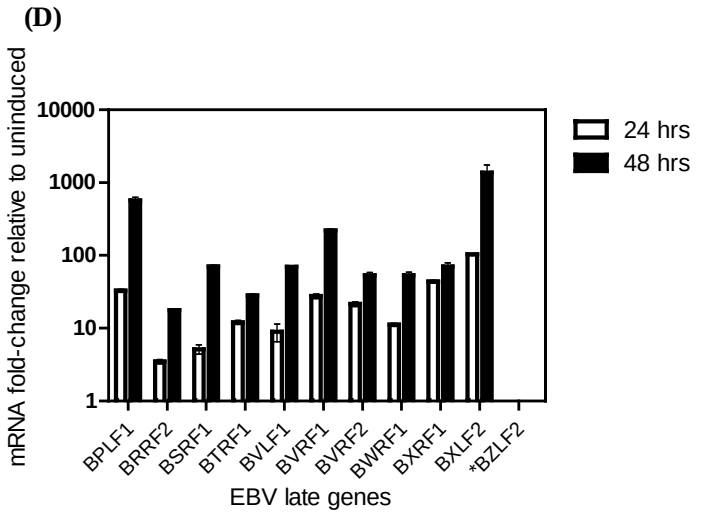


**Figure 3-7 Fold-changes in expression of the EBV late genes at 24-48 hrs following TPA/NaB induction of Raji cells**

Fold-changes in expression of 42 EBV late genes in induced versus uninduced Raji cells (**A-D**). Raji cells were stimulated with TPA/NaB to induce the EBV lytic phase and cells harvested at 24 and 48 hr time-points. Uninduced Raji cells served as the control. After 24 hours of induction, total RNA was extracted from three biological replicates of induced and uninduced Raji cells using the Qiagen RNeasy mini extraction kit. cDNA was generated from 2 µg total RNA using the Ambion RETROscript™ kit. Real-time PCR was performed on cDNA from three technical replicates using the BioRad iQ SYBR Green supermix with primers specific for the EBV genes shown. ΔCt values were calculated for each EBV gene using the *ACTB* gene as reference according to the comparative quantitation method (ΔΔCt) (Livak and Schmittgen, 2001), provided on the RotorGene™ software (Qiagen, UK). ΔCt values were converted to fold-change values for each of the replicates ($\Delta Ct_{\text{Induced/Uninduced}}$) using Prism (GraphPad Prism, USA). Asterisks indicate deletions from the Raji EBV genome. Data represents the mean fold-change relative to uninduced ±SD of one experiment performed in triplicate.

### 3.2.6.4 Fold-changes of the EBV latent genes at 24-48 hrs

Fold-changes were also analysed for 11 latent genes, with the exception of the deletion *EBNA-3C* (Figure 3.8). At the 24 hr time-point, the fold-change for the latent genes was below 2-fold, with the exception of *A73/RPMS1* and *BARF0* which were induced to 2- and 11-fold, respectively (Table 3.4). At the 48 hr time-point, five genes were induced below 2-fold and the remaining induced below 10-fold, with the exception of *EBNA-3A* which was induced over 15-fold (Table 3.4).

**Table 3-4 Summary of fold-changes in the expression of the EBV latent genes**

| Gene (*n*=11) | Fold-change at 24 hrs (±SD) | Fold-change at 48 hrs (±SD) |
|---|---|---|
| *A73/RPMS1* | 2.17 (±0.04) | 5.63(±0.10) |
| *BARF0* | 11.00 (±1.29) | 2.69(±0.16) |
| *EBER1* | 1.43 (±0.11) | 3.73(±0.07) |
| ***EBNA-1*** | 0.67 (±0.03) | 2.87(±0.74) |
| ***EBNA-2*** | 0.18 (±0.01) | 0.28(±0.02) |
| ***EBNA-3A*** | 0.72 (±0.06) | 15.33(±0.67) |
| ***EBNA-3B*** | 1.77 (±0.27) | 0.42(±0.25) |
| ***EBNA-3C**** | - | - |
| ***EBNA-LP*** | 0.26 (±0.01) | 0.18(±0.03) |
| ***LMP1*** | 1.65 (±0.13) | 0.71(±0.06) |
| ***LMP2A*** | 1.25(±0.08) | 1.68(±0.14) |

SD, standard deviation; * deletion; EBV latent genes selected for further analysis (bold)

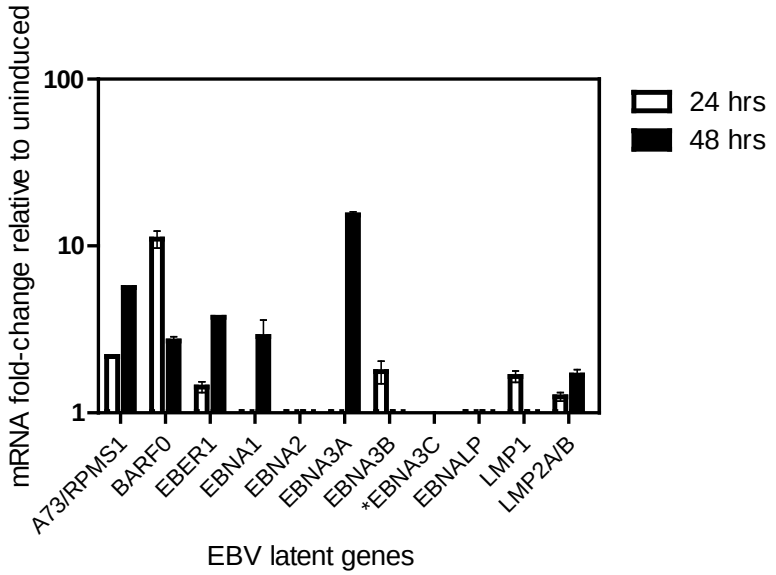


**Figure 3-8 Fold-changes in expression of the EBV latent genes at 24-48 hrs following TPA/NaB induction of Raji cells**

Fold-change in expression of 11 EBV latent genes in induced versus uninduced Raji cells. Raji cells were stimulated with TPA/NaB to induce EBV lytic activation and cells harvested at 24 and 48 hr time-points. Uninduced Raji cells served as the control. After 24 hours of induction, total RNA was extracted from three biological replicates of induced and uninduced Raji cells using the Qiagen RNeasy mini extraction kit. cDNA was generated from 2 µg total RNA using the Ambion RETROscript™ kit. Real-time PCR was performed on cDNA from three technical replicates using the BioRad iQ SYBR Green supermix with primers specific for the EBV genes shown. ΔCt values were calculated for each EBV gene using the *ACTB* gene as reference according to the comparative quantitation method (ΔΔCt) (Livak and Schmittgen, 2001), provided on the RotorGene™ software (Qiagen, UK). ΔCt values were converted to fold change values for each of the replicates ($\Delta Ct_{\text{Induced/Uninduced}}$) using Prism (GraphPad Prism, USA). Asterisks indicate deletions from the Raji EBV genome. Data represents the mean fold change relative to uninduced ±SD of one experiment performed in triplicate.

**Table 3-5 Summary of fold-changes in expression of the EBV early and late genes at 24 and 48 hr time-points following lytic induction in Raji cells**

| | **Early genes** (*n*=33) | | | **Late genes** (*n*=42) | | |
|---|---|---|---|---|---|---|
| | ≤10-fold | ≥10–100-fold | ≥100-fold | ≤10-fold | ≥10–100-fold | ≥100-fold |
| 24 hrs | 17/33 (51.52%) | 13/33 (39.39%) | 3/33 (9.09%) | 22/42 (52.38%) | 18/42 (42.86%) | 2/42 (4.76%) |
| 48 hrs | 9/33 (27.27%) | 16/33 (48.48%) | 8/33 (24.24%) | 10/42 (23.81%) | 19/42 (45.24%) | 13/42 (30.95%) |

## 3.3 DISCUSSION

In this study real-time PCR assays were developed and used to quantify relative expression levels of 88 EBV genes, following induction of the EBV latent-lytic switch in Raji LCLs. In the first instance, the EBV-encoded microRNAs were not examined since we were restricted by the number of targets we could investigate. Future work will involve the analysis of these transcripts. Confidence in the specificity of our assay was determined in three ways. First, all 89 primer sets were validated for EBV analytical specificity with our real-time PCR assays. *BERF1* (also known as EBNA-3A) was excluded from further investigation following analytical validation, resulting in 88/89 genes being analysed, of which fifteen were overlapping in the EBV genome. Seventy-eight of the 89 primer sets were published previously, and primer specificity was validated on amplicons derived from B95-8 genomic DNA template by melt-curve analysis and agarose gel electrophoresis (Pan et al., 2005). In this study, commercially available gDNA derived from the EBV-positive B95.8 cell line was used as PCR template to amplify 89 EBV gene specific primer sets, since the Raji EBV genome contains two deletions (Hatfull et al., 1988). Analysis of the 89 amplicons using Melt-curve analysis and agarose gel electrophoresis yielded both single peaks and bands of the expected sizes.

Second, the 89 primer sets were also assessed for specificity to DNA and RNA present in the cells. The Raji cell line has been used extensively to examine EBV gene expression (Biggin et al., 1987; Gargouri et al., 2011a; Gargouri et al., 2011b; Guo et al., 2010a; Ohashi et al., 2007; Rek et al., 2010). In this study, we validated the detection of EBV specific mRNA, using total RNA extracted from TPA/NaB induced Raji cells. Our results confirmed single products by melt-curve analysis and visualisation of amplification products analysed by agarose gel electrophoresis for 85 of the 89 primers tested. We showed that all primer sets

were specific for the EBV gene targets. Further, we also we detected an amplicon of the expected size for *BWRF1*, which is not known to be expressed (Jenson et al., 1987). Further work is required to determine whether this transcript is translated into a functional protein. Lastly, our EBV primer sets were tested against total RNA extracted from TPA/NaB-induced EBV-negative Ramos cells. Ramos is an EBV-negative Burkitt's lymphoma cell line that is frequently used as an EBV-negative control, particularly for Raji LCLs where an EBV-negative counterpart is not available. This validated the specificity of our assay, since only non-specific amplification was detected by melt-curve analysis and agarose gel electrophoresis of the 89 amplicons. These non-specific products are likely to reflect genomic DNA since SYBR Green I binds non-specifically to all double stranded DNA (Qiagen, UK). Further, no amplification traces were detected during the PCR runs when Ramos cDNA was used as a control and amplified with EBV-specific primers. The sensitivity of our assay was assessed by a titration of cDNA template derived from induced Raji cells, and a 1/10 dilution yielded Ct values of 24 and 16, for *BZLF1* and *ACTB* genes, respectively providing sensitive detection and enough cDNA material for the analysis of all 89 gene targets tested in triplicate.

**Validation of primer specificity for overlapping EBV transcripts**

Many EBV lytic mRNAs are overlapping in the EBV genome (Baer et al., 1984; de Jesus et al., 2003b), sharing 3'-polyadenylation sites. As a result, primers in overlapping sequence regions may amplify more than one transcript, and not all transcripts can be detected uniquely. For instance, primers for shorter mRNAs that are completely contained within another mRNA will certainly amplify one or more mRNA transcripts. Of the 89 amplicons, 15 fell into regions that overlap with multiple transcripts (BFLF2/BFLF1, BFRF1/BFRF2, BORF1/BORF2, BSMLF1/BSLF1, BLRF1/BLRF2, BLLF1/BLLF2, BKRF2/BKRF3,

BBRF1/BBRF2, BXRF1/BVRF1, BVRF2/BdRF1, BaRF1/BMRF1/BMRF2, BBLF1/BGLF5/BGLF4, BGRF1/BGLF2/BGLF1/BDLF4, BDLF3/BDLF2/BDLF1 and BNLF2a/BNLF2b/BNLF1/LMP1), including seven late lytic transcripts (underscored). The mRNAs of BFLF2, BORF2, BMRF1, BMRF2, BSMLF1, BLRF2, BLLF2, BKRF4, BBRF2, BBLF1, BGLF5, BGRF1, BGLF2, BGLF1, BDLF3, BDLF2, BVRF1, BdRF1 and BNLF2a/BNLF2b/LMP-1 are completely contained within the longer transcripts, as illustrated in the EBV transcription map (http://www1.imperial.ac.uk/departmentofmedicine/divisions/infectiousdiseases/viro/epsteinbarr/ebvmap/). For these genes, our measures of transcription will therefore be a combination of the overlapping mRNAs. Thus, the fold-induction levels (Tables 3.2-3.3) may be over-estimated.

A potentially more accurate measurement should be found for the nine (BFLF2, BFRF1, BORF1, BSLF1, BLRF1, BLLF1, BKRF2, BBRF1, BXRF1, BVRF2, BaRF1, BGLF4, BDLF4, BDLF1 and LMP-1) partially overlapping longer transcripts, the exact measurements of these genes can be resolved by subtraction from the longer mRNAs. But, a number of variables could result in measurements that are not accurate, including differences in expression of the transcripts and variations in RT efficiency. Varying levels of a genes transcription can also arise depending on the proximity from the 3'-poly A sites when priming with oligo-dTs. This should not be a factor since we used random primers. In some cases, overlaps of early and late transcripts exist and the early/late distinction is obscured. Therefore, given that our RT-PCR is measuring more than one transcript, the overlapping genes were excluded from further investigation.

**Confirmation of deletions in the Raji EBV genome**

Two major deletions are found within the BamHI A region of the Raji EBV genome, resulting in three deletions (*BALF1*, *BARF1*, *BZLF2*) and two truncations (*BALF2* and *EBNA-3C*) (Hatfull et al., 1988). The first deletion is the 2.9kb sequence, in a region of BamHI A adjacent to the BARF1 oncogene, resulting in a 679-bp deletion of the whole BARF1 sequence (165496 to 166192 bp), encoding a 33-kDa protein capable of transforming rodent fibroblasts (Wei et al., 1994; Wei and Ooka, 1989), and a 256-bp sequence in the BALF2 reading frame (from position 163979 to 164235 bp), encoding a 135-kDa single single-stranded DNA binding protein (mDBP) (Tsurumi et al., 1996). The BALF1 gene, encoding a Bcl-2 homologue, with potential roles in cell survival, tumour formation and metastasis is also deleted in the BamHI A fragment of the Raji EBV genome (Hsu et al., 2012). The second deletion is a 3.5-kbp sequence covering the entire region of the EBNA3C reading frame, resulting in a truncated protein crucial for B-lymphocyte transformation (Tomkinson et al., 1993), and the deletion of the BZLF2 fragment, encoding a type II membrane protein crucial for entry of B cells (Rowe et al., 2011).

While EBNA3C is essential for B-cell immortalisation, BALF2 is essential for lytic DNA replication (Decaussin et al., 1995). Indeed, the deletion of the promoter region leads to the transcription of a truncated protein, with limited or partial function (Baer et al., 1984). As a consequence, the Raji EBV genome is incompetent for transformation, lytic DNA replication and crucially, late lytic gene expression, which is dependent of viral DNA synthesis (Chevallier-Greco et al., 1986a; Decaussin et al., 1995; Laux et al., 1988). Raji can be rescued for replication by providing the BALF2 cDNA in *trans* following super-infection with the EBV strain P3HR-1 (Biggin et al., 1987), and also for transformation, by rescuing the EBNA3C deletion by recombination, which incorporates the wild-type EBNA3C gene

from an overlapping genomic DNA fragment (Robertson et al., 1996). This recombination event renders the resulting virus competent for B-lymphocyte transformation.

We confirmed all five deletions in the induced Raji cDNA. The specificity of our assay was validated further by the detection of these deletions in B95.8 genomic DNA (Figure 3.2 vs. 3.1). Therefore, a major unexpected finding was the detection of late lytic gene expression, as will be discussed here. One of the aims of this study was to identify EBV genes, which were induced after EBV lytic induction, and that could serve as potential markers of PTLD. Overall, at the 24 hr time-point, 9.09% of EBV early genes were induced over 100-fold. By comparison, 4.76% of late genes were also induced above 100-fold. At the 48 hr time-point, 24.24% of the early genes were induced above 100-fold as compared to 30.95% induced above 100-fold. Therefore, while the numbers of highly induced (>100-fold) early genes increased from 9.09% to 24.24% at 24 to 48 hrs, the numbers of 'late genes' also induced over 100-fold from 24 to 48 hrs increased from 4.76% to 30.95%, indicating higher induction of the early genes at an early stage after lytic induction and a 'supposedly' higher induction of the late genes at a later stage after lytic induction (i.e., 48 hrs).

**Detection of immediate-early gene expression**

Evidence for efficient induction of the EBV latent to lytic switch was demonstrated as early as 24 hrs by the expression of the IE gene *BZLF1,* the first gene to be expressed in the lytic cycle (Amon et al., 2004b) with a 19-fold and 156-fold induction at 24 hrs and 48 hrs, respectively. The IE gene *BRLF1* was induced from 3-fold up to 60-fold at 24 and 48 hr time-points, respectively (Figure 3.5). BZLF1 is known to autoregulate its expression (Feederle et al., 2000b). Therefore, the higher levels of BZLF1 expression compared to BRLF1 could be attributable to *BZLF1* autoregulation. EBV replication is regulated by two immediate-early

genes *BZLF1* and *BRLF1* that encode transcriptional activators Zta and Rta of the latent-lytic switch (Chevallier-Greco et al., 1986b; Hardwick et al., 1988; Miller and El-Guindy, 2002; Ragoczy et al., 1998; Ragoczy and Miller, 1999; Speck et al., 1997). Zta binds ZREs in promoters of EBV early genes and cellular genes activating viral DNA replication and packaging and release of infectious virus (Chang et al., 1990; Chen et al., 2009; Farrell et al., 1989). Rta also interacts with numerous cellular proteins and affects the activities of host cells to facilitate lytic replication (Bentz et al., 2010). Together, Zta and Rta are known to promote G0/G1 in Raji cells, indicating their increased expression in this system (Countryman et al., 2009).

**Detection of early lytic gene expression**

The EBV early genes are classically defined as genes expressed following lytic cycle activation, prior to lytic replication, and are expressed in the presence of agents that inhibit viral DNA replication (Robertson, 2005). Of the early genes, three (*BcRF1, BGLF4* and *BXLF1*) were induced to a high level (>100-fold) at 24 hrs. Moreover, two of these genes (*BcRF1* and *BGLF4*) demonstrated peak expression above 100-fold at 24 hrs rather than 48 hrs (Table 3.2). An additional two genes (*BBLF2* and *BMRF1*) were induced over 80-fold at 24 hrs (Table 3.2). Seven genes (*BDLF4, BFLF2, BFRF1, BFRF2, BILF2 BORF2* and *BXLF1*) were induced further (to expression levels above 100-fold) at 48 hrs. Indeed, *BXLF1* induction levels were 153-fold and 634-fold at 24 and 48hrs, respectively. Notably, several genes (*BGLF4, BcRF1, BGLF4, BMRF1, BDLF4, BFLF2* and *BORF2*) are overlapping in the EBV genome, three of which (*BMRF1, BFLF2* and *BORF2*) are fully contained in the overlaps. Therefore, it is highly likely that the fold-induction levels are for these shorter overlapping genes.

**Detection of late lytic cycle gene expression**

Regulation of the late lytic genes is less well understood than for the IE and early genes, but is known to be coupled to viral DNA replication (Gruffat et al., 2012; Robertson, 2005). The late lytic genes are classically defined as genes expressed after the activation of viral DNA replication, and are blocked at the protein level and steady state mRNA levels (Amon et al., 2006b; Serio et al., 1997a). As a consequence, late gene expression is sensitive to the same agents (phosphonoacetic acid, PAA and acyclovir, ACV), that prevent lytic replication (Katz et al., 1989; Rickinson et al., 1978; Summers and Klein, 1976), by targeting the viral DNA polymerase, BALF5 (Lin et al., 1991), suggesting a dependence on this protein and viral lytic DNA replication. In addition, Raji has two major deletions and is defective for viral lytic DNA replication, resulting in the lack of late lytic cycle gene expression (Decaussin et al., 1995; Hatfull et al., 1988). Since we measured the relative expression of 89 genes from the EBV genome, we also measured late gene expression at the 24 and 48 hr time-points, however in the absence of inhibitors of lytic replication. Therefore, an unexpected finding was the detection of late lytic gene expression in the model system. For instance, 14 late genes were induced over 100-fold at 48 hrs (Table 3.3), of which two, *BMRF2* and *BXLF2*, were also induced over 100-fold at 24 hrs, both of which participate in viral entry (Heineman et al., 1988; Kurilla et al., 1995; Tugizov et al., 2003).

The reasons for the detection of late lytic gene products of the expected size was unclear, since we validated for the analytical specificity of the primers and potential contamination with EBV LCLs or wild-type EBV B95.8 gDNA by the following: (i) detection of EBV deletions in the Raji genome and deletions of the B95.8 genome (*LF1*, *LF2* and *LF3*), confirming the absence of B95-8 gDNA contamination; (ii) absence of products of the expected size in Ramos gDNA, (iii) absence of EBV gene expression in a no-RTase control confirming absence of contaminating Raji gDNA and/or Raji LCLs, and (iv) use of Ramos

gDNA and no-template controls during the PCRs, assessing potential gDNA contamination. Therefore, possible explanations for the demonstrated results are likely to be biological rather than technical, two of which are discussed here. Firstly, we did not use inhibitors of lytic DNA replication, such as ACV or PAA in our model system which blocks not only viral lytic DNA replication, but also late lytic gene expression. Therefore, the levels of late lytic gene expression found is very likely to be due to the measurement of 'read-through transcription' from the early lytic genes, including some overlapping mRNAs, into downstream late regions. This would arise from the continual priming of the RNA polymerase through the EBV genome beyond the normal termination signal. As a result, the distinction between early/late lytic cycles is also unclear. Secondly, we measured gene expression in total cellular RNA, not mature cytoplasmic mRNA. Therefore, the likelihood of background cellular mRNA is high, and we could potentially be measuring non-specific amplification of cellular mRNAs. It is not clear what products have been amplified in the results demonstrated, but those detected on agarose gels are likely to represent short specific regions of the cellular RNAs amplified by the primer pairs.

While the regulation of IE and early gene expression is well understood in EBV, the mechanisms regulating late gene expression were poorly understood until recently (Gruffat et al., 2012). Several mechanisms for late gene expression were proposed previously. Serio et al. showed that activation of some late gene promoters (*BcLF1* and *BFRF3*) could be observed on transiently transfected reporter plasmids even if the reporter plasmids did not have the OriLyt sequence *in cis* i.e., in a replication-independent manner (Serio et al., 1998b; Serio et al., 1997b). Similarly, studies performed in Z and R-deleted viruses suggested that viral replication *in cis* was not required for activation of EBV late promoters (Feederle et al., 2000a; Ragoczy and Miller, 1999). By contrast, Amon et al. showed that late lytic gene expression required viral replication *in cis* (Amon et al., 2004a). Notably, *ori lyt* was shown

to be required for the production of virus replication compartments associated with promyelocytic leukaemia protein nuclear bodies (PML-NBs) (Amon et al., 2006a). Taken together, these studies suggested both viral proteins and *trans*-acting factors were involved. Viral proteins have been implicated as regulators of late gene promoters but are poorly understood in other herpesviruses. In the case of HSV-1, several viral proteins (ICP4, ICP8 and ICP27) have been shown to be necessary for the efficient expression of late genes (Gao and Knipe, 1991; Kim et al., 2002; Lester and DeLuca, 2011; Rice and Knipe, 1990; Tang et al., 2003). In murine herpesvirus 68 (MHV-68) and cytomegalovirus (CMV), several viral proteins, namely ORF18, ORF24 and ORF34, respectively have also been shown to be necessary for the expression of late genes. EBV also encodes three homologues (ORF18, ORF24 and ORF34) found in MHV-68 and CMV, including BVLF1.5, BcRF1 and BGLF3 (Arumugaswami et al., 2006; Wong et al., 2007; Wu et al., 2009). Of these proteins, only BcRF1 has a putative function as a homolog to the TATT-binding protein (TBP) (Wyrwicz and Rychlewski, 2007a), and was previously implicated in regulation of late gene expression (Serio et al., 1998a). The role of BcRF1 has recently been characterised during the EBV productive cycle using recombinant assays and to function as a TBP-like protein crucial for EBV late gene expression (Gruffat et al., 2012). Three significant findings were identified in the study: (i) cells only produce virions when transfected with BcRF1; (ii) BcRF1 is critical for the accumulation of late viral transcription but not for viral DNA synthesis and (iii) BcRF1 interacts specifically with TATT sequences present within late gene promoters. Therefore, BcRF1 has been shown to form complexes with TATT motifs within late gene promoters, following DNA replication only, once the viral genome is methylated (Gruffat et al., 2012). These interactions involve viral proteins and are also likely to occur in *trans* with the assistance of other cellular factors (Gruffat et al., 2012). Exactly how BcRF1 forms

complexes with the TATT sequence is under investigation. Taken together, the mechanism proposed supports the findings of the earlier studies (Amon et al., 2004a; Serio et al., 1997b).

Owing to the difficulties discussed previously associated with determining late lytic gene expression, our preliminary analysis focused on EBV early lytic genes with high fold-induction levels at either 24 or 48 hrs. Initially twenty-four genes were identified for further analysis by the criterion of a more than 100-fold induction at either time-point (Tables 3.6 and 3.7). Of these 24 genes, nine were selected for further analysis, since only limited amounts of cDNA material was available for testing (Table 3.6). We focused on these genes since they were highly regulated among the candidate genes and had interesting biological properties. Two genes (*BALF5* and *BRRF1*) were selected based on their biological properties rather than fold-change alone. In addition, three of the 24 candidate genes (*BcRF1, BFRF1* and *BILF1*) were early genes with longer overlaps and were selected for future analysis (Table 3.7). Altogether, nine genes were selected for further analysis (Table 3.6). However, following preliminary evaluation in clinical samples (chapter 5), data was presented for only six of the nine genes, since three genes (*BMRF1, BPLF1,* and *BVRF1*) were realised to be either short overlaps and/or late lytic genes with fold-induction levels that are not likely to be accurate for the explanations described earlier.

**Table 3.6 EBV candidate genes selected for preliminary clinical validation**

| EBV genes | Overlapping genes (Long/Short) | Class | Mean fold-change (24 hrs) | Mean fold-change (48 hrs) |
|---|---|---|---|---|
| *BALF5* | - | E | 14.15 | 6.23 |
| *BDLF4** | Long | E | 12.30 | 141.33 |
| *BGLF4** | Long | E | 114 | 38.58 |
| ***BMRF1**** | Short | E | 90.17 | 1323.67 |
| ***BPLF1*** | - | L | 32.73 | 569.80 |
| *BRRF1* | - | E | 7.19 | 73.33 |
| ***BVRF1**** | Short | L | 27.55 | 219.67 |
| *BXLF1** | Long | E | 153 | 624 |
| *BZLF1* | - | IE | 19 | 156 |

IE, immediate-early genes; E, early genes; L, late genes; *overlapping genes; excluded from analysis (bold)

**Table 3.7 EBV candidate genes selected for future clinical validation**

| EBV genes | Overlapping genes (Long/Short) | Class | Mean fold-change (24 hrs) | Mean fold-change (48 hrs) |
|---|---|---|---|---|
| ***BcRF1**** | Long | E | 104.44 | 63.67 |
| *BDLF3* | - | L | 3.50 | 313.15 |
| *BDRF1* | - | L | 17.25 | 900.60 |
| *BdRF1** | Long | L | 27.33 | 1693.23 |
| *BFRF1A* | - | L | 21.99 | 736.67 |
| ***BFRF1**** | Long | E | 19.11 | 597.33 |
| *BFRF2** | Short | E | 29.66 | 1406.67 |
| *BFRF3* | - | L | 13.31 | 158.33 |
| ***BILF1*** | - | E | 12.13 | 106.28 |
| *BILF2* | - | L | 23.76 | 254.33 |
| *BKRF4* | - | L | 12.50 | 251.33 |
| *BMRF2** | Short | L | 117.01 | 826.33 |
| *BOLF1* | - | L | 58 | 1331.3 |
| *BORF1** | Long | L | 1.45 | 245.33 |
| *BXLF2* | - | L | 103.19 | 1365.67 |

IE, immediate-early genes; E, early genes; L, late genes; *overlapping genes; selected candidate genes highlighted in bold.

## EBV early candidate genes and their biological properties

The majority of early genes function in viral DNA replication (Fields, 2002). Overall, at the 24 hr time-point, 9.09% of the early genes were induced over 100-fold (Table 3.5). Of interest, 7/32 (21.88%) early genes (*BALF2, BALF5, BBLF2, BBLF3, BBLF4, BcRF1,* and *BGLF4*), including *BALF5* that encodes the viral DNA polymerase, demonstrated maximal expression at 24 hrs versus 48 hrs. This implies that EBV lytic replication is occurring at early stages of the lytic cycle since the majority of the early EBV gene products function in viral lytic DNA replication (Tsurumi et al., 2005).

The majority of other early genes (*BaRF1*, *BDLF4*, *BFLF1*, *BFLF2*, *BFRF1*, *BFRF2*, *BGLF5*, *BHRF1*, *BILF1*, *BKRF3*, *BLLF2*, *BLLF3*, *BNLF2a*, *BNLF2b*, *BORF2*, *BRRF1*, *BSLF1*, *BSMLF1, LF1, LF2* and *LF3*) exhibited delayed induction with higher fold-change at 48 hrs versus 24 hrs. Most of these genes were involved in functions other than EBV replication, including some unknown functions (Table 1.4). We also identified six genes (*BFLF2*, *BFRF1*, *BFRF2*, *BILF1*, *BMRF1* and *BXLF1*) that showed increased expression

(>100-fold) over time (24-48 hrs), of which two (*BILF1* and *BXLF1*) are not overlapping. Our findings reveal ten highly induced (>70-fold) early genes (*BcRF1, BDLF4*, *BFLF2*, *BFRF1*, *BFRF2*, *BGLF4*, *BILF1*, *BMRF1 BRRF1* and *BXLF1*) at 24 hrs or 48 hrs that could serve as potential early markers of PTLD (Tables 3.6 and 3.7). However, in the first instance, six genes (*BALF5*, *BDLF4*, *BGLF4*, *BMRF1*, *BRRF1* and *BXLF1*) were selected for further analysis (Table 3.6). We focused on these genes among the highly regulated early candidate genes since they were biologically interesting. However, three genes (*BDLF4*, *BGLF4* and *BMRF1*) are overlapping, of which *BMRF1* is contained within the longer mRNA transcript, and its expression levels may be overestimated.

A brief summary of the proposed functions of all of the EBV early genes is presented in Table 1.4. Further details on the functions of the identified candidate PTLD genes are described here. EBV lytic gene expression has been demonstrated in PTLD alongside latent gene expression (Brink et al., 1997; Rea et al., 1994b). It is presumed that EBV reactivation during immunosuppression can lead to an increase in viral replication that contributes to the development of PTLD (Hopwood et al., 2002). However, the role of the EBV lytic genes and their contribution to PTLD is less clear (Rowe et al., 1998). Examining the gene expression patterns of selected EBV genes may provide an understanding of their involvement in PTLD.

The *BALF5* gene functions as the viral DNA polymerase, essential for EBV lytic DNA replication (Tsurumi, 1991). The *BGLF4* gene encodes the nuclear serine/threonine protein kinase (PK), a virion tegument component that phosphorylates several EBV proteins (Feederle et al., 2009; Johannsen et al., 2004), including BMRF1 (Chen et al., 2000), BZLF1 (Asai et al., 2006; Asai et al., 2009), EBNA-LP (Kato et al., 2003) and EBNA-2 (Yue et al., 2005) as well as numerous cellular proteins including elongation factors (Kawaguchi et al., 2003). *BRRF1,* encodes a transcription factor that enhances lytic cycle induction via the IE protein BRLF1 (Hong et al., 2004; Segouffin-Cariou et al., 2000), whereas *BXLF1* encodes

the viral thymidine kinase (TK) that phosphorylates targets (Littler et al., 1986). Therefore, as mentioned earlier, these genes could contribute to PTLD through an increase in the level of viral replication during an immunosuppressed state.

Additional candidate genes whose functions are unknown include *BDLF4*, which encodes envelope glycoprotein 115 (gp115) (Boeckmann et al., 2003) and *BcRF1,* for which a role as a TATA-binding protein (TBP), important for transcriptional regulation has been proposed (Wyrwicz and Rychlewski, 2007b). Furthermore, the BcRF1 protein has very recently been shown to be essential for activation of late gene expression via interactions with TATT motifs within the promoters of these genes (Gruffat et al., 2012). Interestingly, we detected maximal fold-induction levels of BcRF1 at 24 hrs (104-fold vs. 66-fold), reflecting its early requirements during the viral life cycle. Therefore, it would be interesting to investigate this gene further as a potential biomarker of PTLD. *BDLF4* is up-regulated by the early gene *BSMLF1* (also known as SM) which encodes the RNA export protein BSMLF1, essential for EBV lytic DNA replication. This suggests that BDLF4 is a BSMLF1-dependent protein and a clear marker of EBV replication (Han et al., 2007).

**EBV late genes and their biological properties**

The majority of EBV late genes encode structural components of the EBV virion involved in viral assembly and egress (Fields et al., 2007). Studies have shown that the EBV late genes are demonstrated less frequently in PTLD as compared to the early genes, suggesting that productive infection does not always occur (Rea et al., 1994b). Since the detection of late lytic gene expression was unclear we chose to investigate the early lytic genes only.

**EBV latent gene expression**

*In vitro*, latency III is demonstrated by expression of all latent genes including EBV-encoded RNAs (EBERs) and *Bam*HI A rightward transcripts (BARTs) (Young and Rickinson, 2004). We also detected latent gene expression in Raji LCLs following activation of the lytic cycle, although full latency III was not observed. At the 24 hr time-point, 2/11 (18%) latent RNAs (*A73/RPMS1* and *BARF0*), were induced over 2-fold, both of which were BART RNAs (Kusano and Raab-Traub, 2001; Smith et al., 2000; Zhang et al., 2001). *BARF0* was induced maximally to 11-fold at 24 hrs. Although the exact function of BARF0 *in vivo* is uncertain, its expression has been demonstrated in biopsy tissue of several malignancies, including PTLD, where it is presumed to participate in maintenance of latency, however, not B-cell transformation (van Beek et al., 2003). The remaining nine latent genes were down-regulated, confirming disruption of latency.

At the 48 hr time-point, increased latent gene expression (induced >2-fold) was detected in 5/11 (45.45%) latent genes (*A73/RPMS1, BARF0, EBER-1, EBNA-1* and *EBNA-3A*) (Table 3.4). *EBNA3A* was induced over 13-fold at 48 hrs. EBNA-3A functions as a transcriptional regulator of gene expression during latency (Hertle et al., 2009). In addition, EBNA-3A has been shown to co-operate with EBNA-2 to induce anti-apoptosis, a process likely to contribute to malignancies such as PTLD (Anderton et al., 2008).

Our findings are in keeping with other studies where latent (but not latency III), gene expression was detected during lytic cycle activation (Yuan et al., 2006). In particular, expression of the EBNA3s was detected during lytic cycle activation (Yuan et al., 2006). Other studies have demonstrated increasing latent gene expression including expression of *EBNA1*, *EBNA2* and *LMP1* during lytic cycle reactivation (Rowe et al., 1992). Similarly, Lu and colleagues showed detection of *EBNA2*, *EBNA3A* and *EBNA3C* during lytic replication

(Lu et al., 2006). Further, concomitant increases in latent gene expression with early lytic gene expression have also been detected (Bernasconi et al., 2006). The co-expression of latency III during EBV lytic replication could facilitate EBV replication (Chen et al., 2009; Yuan et al., 2006). Latency III has been implicated with PTLD (Brink et al., 1997). In order to gain a better understanding of the functions of the EBV latent gene products and their contribution to PTLD, all eight EBV latent genes (*EBNA-1, EBNA-2, EBNA3A, EBNA-3B, EBNA-3C, EBNA-LP, LMP-1* and *LMP-2*) were chosen for further analysis.

**Comparison with EBV gene expression in TPA induced B95.8 cells**

In the present study, we used real-time PCR to analyse relative expression levels of 88 EBV genes, including six spliced forms following TPA/NaB induction of Raji cells at 24 and 48 hrs. Seventy-eight of the 88 primer sets were published previously and used to investigate EBV gene expression following TPA induction in B95.8 cells at 24 and 48 hrs (Pan et al., 2005). Consistent with our study, lytic activation was demonstrated following the induction of *BZLF1* and *BRLF1*. Overall, they showed that the majority of EBV genes were induced following TPA induction, with 12 of the 80 (15%) genes and a further 20 genes (25%) induced highly at 24 and 48 hrs, respectively. Notably *BILF2*, *BBLF4*, *BFRF2*, *BSLF1* (now *BSMLF1*), *EBER1* and *EBNA-3A* were induced highly in their study, consistent with ours. In comparison to their study, we detected much stronger fold-induction levels in our model system. However, following manual calculation of the ddCt (fold-change) for the dCt values of the genes in their study, we detected higher levels of induction than described in their study. This made it difficult to compare fold-induction levels for these genes. One possible explanation for the higher levels of fold induction detected in our system could be the synergistic effect of TPA/NaB versus TPA alone in their study, which results in enhanced

lytic induction. Despite the demonstration of latent and lytic gene expression, these findings suggest variations in the levels of EBV gene expression between different systems.

**Limitations of study**

Two major limitations are associated with the study. Firstly, the choice of cell line in which we measured EBV gene expression was not optimal since Raji has two major deletions and is defective for late lytic gene expression (Decaussin et al., 1995). Therefore, expression levels of the entire EBV genome were not assessed. Further, the mechanism of lytic induction using the phorbol ester, TPA is uncertain (Baumann et al., 1998a). Alternative cell lines could provide more suitable models for measuring EBV gene expression, such as the Akata cells line, which is induced to enter the lytic phase by IgG cross-linking, offering a more specific and physiological method for lytic activation (Amon et al., 2004a; Shimizu and Takada, 1993a). Secondly, a control for inhibition of viral lytic DNA replication, such as PAA or ACV was not included in the model system. In summary, in the model system used here, we detected highly induced EBV early and unexpectedly, late genes at 24 and 48 hrs, respectively. The demonstration of late lytic gene expression is likely to be due to 'run through' transcription from either early genes into late regions' or non-specific amplification of background cellular mRNAs, since total RNA was used. Profound expression of the majority of the early genes at the 48 hr time-point was likely to be due to prolonged TPA/NaB treatment (Pan et al., 2005). Notably, induction over 1000-fold was detected for 2/33 (6%) early genes (*BMRF1* and *BXLF1*) and 3/42 (7%) late genes (*BdRF1, BOLF1* and *BXLF2*), of which three (*BMRF1*, *BdRF1* and *BXLF2*) were overlapping and excluded from further analysis. In addition, we detected concomitant latent gene expression in lytic induced Raji cells, which could facilitate viral replication (Chen et al., 2009; Yuan et al., 2006). We

also demonstrated the real-time PCR assays evaluated here to be a sensitive, specific and rapid approach for EBV gene expression analyses in LCLs, and in doing so validated the primer pairs for this purpose. Using these assays, the majority of EBV genes were detectable and we were able to identify highly induced EBV lytic candidate genes. Owing to limited amounts of cDNA material, only 14 genes (six lytic, eight latent) were selected for further analysis. In order to evaluate the contribution of the EBV lytic genes to PTLD, the remaining lytic genes could also be investigated in future studies.

# 4 CHAPTER 4. IDENTIFICATION OF HIGHLY DIFFERENTIALLY EXPRESSED AND REGULATED CELLULAR GENES USING THE AFFYMETRIX HUMAN GENOME U133 PLUS 2.0 GENECHIP®

## 4.1 INTRODUCTION

In the previous chapter, EBV gene expression profiles were analysed in TPA/NaB induced Raji cells using real-time PCR. A number of highly induced EBV candidate genes were identified, indicating successful EBV lytic induction in the model system. As reliable predictive markers of PTLD are lacking, and EBV lytic genes, such as *BZLF1* are known to regulate cellular gene expression, our aim was to identify additional cellular genes regulated by EBV during the lytic induction phase that could serve as potential markers for PTLD (Carter et al., 2002; Chang et al., 2006; Hahn et al., 2005; Morrison and Kenney, 2004; Morrison et al., 2004). Several studies have sucessfully used DNA microarrays to analyse cellular gene regulation in response to EBV lytic replication, EBV infection, EBV-associated PTLD in biopsy tissue, and EBNA-2 induction in *in vitro* systems (Allen et al., 2009; Baran-Marszak et al., 2002; Broderick et al., 2009; Craig et al., 2007; Spender et al., 2002; Spender et al., 2006; Yuan et al., 2006). Therefore, we chose to use this technique to investigate the cellular response to the early phase of the EBV lytic cycle.

DNA Microarray technology is a widely used technique to measure global changes in gene expression levels following the simultaneous expression of thousands of genes in a given sample under a number of different biological conditions. Consequently, widely used applications for microarray gene expression profiling include the identification of genes that could serve as potential diagnostic markers of disease or disease progression, by screening patient samples (Davis and Staudt, 2002). The principle of microarray technology is to generate a signal intensity that reflects the abundance of gene expression in a given sample under a particular condition compared to its control. In order to achieve this, DNA microarrays consist of an array of thousands to tens of thousands of DNA fragments or probes (either synthetic oligonucleotides, cDNAs or PCR amplicons) spotted onto their

surface, each of which represents a gene transcript. Following hybridisation of fluorescently labelled cDNA or aRNA to the immobilised probes, a fluorescent signal is emitted, which is proportional to the amount of cDNA hybridised to the probe and present in the original sample. It is this measurement that determines the differential expression of a gene, by comparing signal intensities with other reference genes from the organism under investigation. DNA microarrays can be either a glass slide or silicon chip, also known as a gene chip although earlier arrays were based on nylon membrane technology.

Affymetrix GeneChip® arrays are the most popular type of high density oligonucleotide arrays available and are used widely by many researchers (Irizarry et al., 2003; Lipshutz et al., 1999). As mentioned previously, the Affymetrix HG U133 Plus 2.0 GeneChip® contains 54,675 probe-sets that interrogate 38,500 genes (Irizarry et al., 2003; Lipshutz et al., 1999). We chose this chip since it covers the whole human genome and allowed us to interrogate all cellular genes as candidate markers. In this study, we used HG U133 Plus 2.0 GeneChips® to analyse host cellular gene expression profiles in cDNA derived from TPA/NaB induced Raji and Ramos cells at 24 hrs post-induction, since the early genes were highly induced at this time-point. Microarray analysis was performed in duplicate and a pair-wise comparison performed on four arrays (induced and uninduced Raji cells). The duplicate experiments represent two biological replicates, one of which demonstrated high lytic gene expression as described in chapter 3. A second pair-wise analysis was performed on four arrays (induced and uninduced EBV-negative Ramos cells) to eliminate any background host gene expression due to the effects of the induction stimulus alone (TPA/NaB). Therefore a total of eight arrays were analysed.

### 4.1.1 Objectives of chapter

The aims of the experiments described in this chapter were three-fold:

(i) To identify cellular genes which are highly differentially expressed and regulated in response to the EBV lytic induction phase following TPA/NaB treatment

(ii) To identify the overall representative Gene Ontology of cellular genes regulated in response to the EBV lytic induction phase

(iii) Using the data generated in (i) and (ii) to identify cellular candidate genes as potential markers of PTLD

## 4.2 RESULTS

### 4.2.1 Validation of RNA integrity

Total RNA was extracted from two independent experiments with induced and uninduced Raji and Ramos cells. The quality of the total RNA was assessed on the Agilent® 2100 Bioanalyser (Figure 4.1). Antisense RNA (aRNA) and fragmented aRNA derived from this total RNA were also analysed using the Agilent® 2100 Bioanalyser to ensure successful fragmentation (Figure 4.2). The RNA integrity for total RNA, aRNA and fragmented aRNA was high as demonstrated by the 2:1 ratio of 28S and 18S ribosomal RNA (rRNA), and broad profiles (fragmented aRNA)(Figure 4.2, panel B). The same process was used to confirm the integrity of total RNA extracted from the induced and uninduced Ramos cells. Total RNA was reverse-transcribed into cDNA as described previously (section 2.4.3) and the fragmented cRNA finally analysed on the DNA arrays.

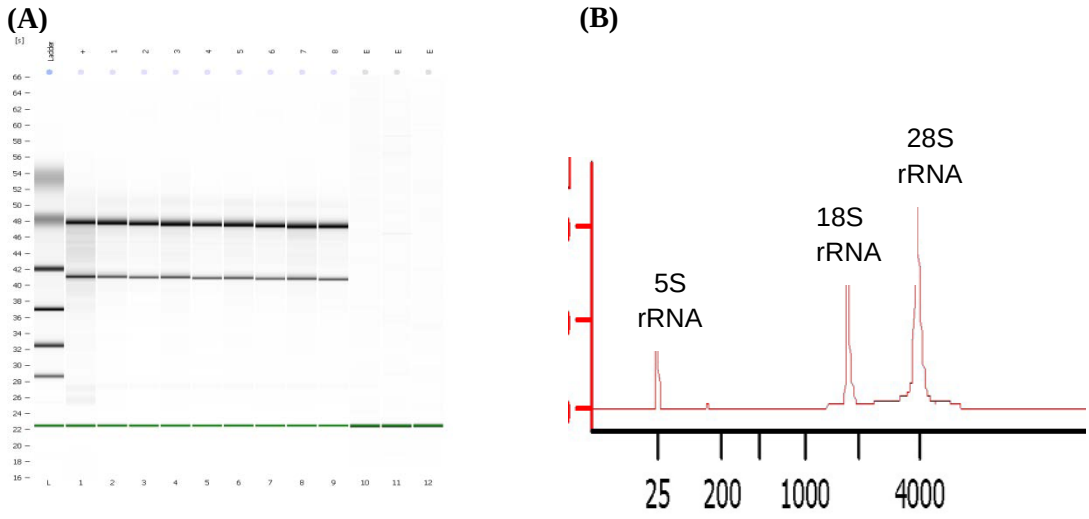


**Figure 4-1 Validation of total RNA integrity**

Gel image and Bioanalyser electropherogram for total RNA derived from the Raji cell line induced for the EBV lytic cycle with TPA/NaB. Total RNA was isolated from duplicate biological replicates of TPA/NaB induced and uninduced Raji cells. Total RNA was analysed on an Agilent® Bioanalyser RNA 6000 Nano chip. (**A**) Panel A shows the gel image. (**B**) Panel B shows traces of intact RNA representing 2:1 ratios for the 28S (right trace) and the 18S (left trace) rRNAs. The far left trace likely represents 5S RNA. The 2:1 ratio represents high-integrity total RNA. The y-axis represents the fluorescence units (FU) and the x-axis the nucleotide (nt) length. Marker = RNA 6000 Ladder (P/N#am7152).

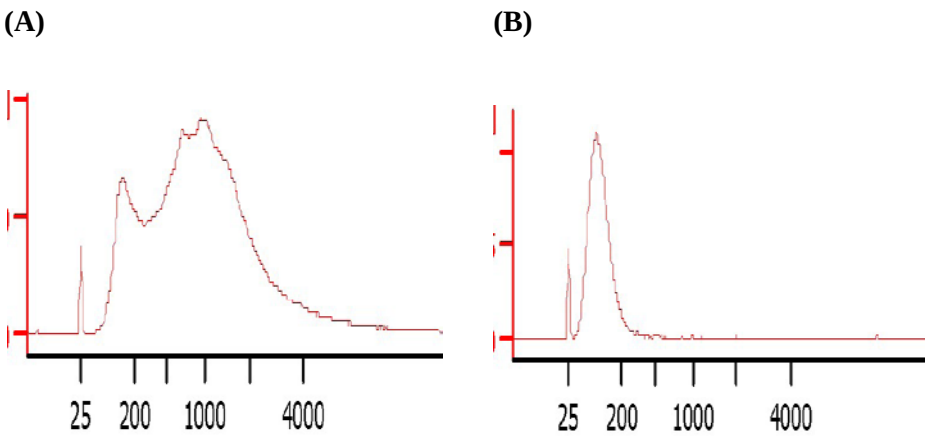


**Figure 4-2 Validation of aRNA fragmentation**

Gel image and Bioanalyser electropherogram for total RNA derived from pooled duplicate biological replicates of TPA/NaB induced Raji cells. Approximately 200 ng total RNA was amplified into aRNA using the MessageAmp™ Premier RNA amplification kit (Ambion) followed by aRNA fragmentation. The quality of fragmented aRNA (**A**) and unfragmented aRNA (**B**) was analysed on an Agilent Bioanalyser RNA 6000 Nano chip. The broad peaks shown in panel A represent successful fragmentation of aRNA. Marker = RNA 6000 Ladder (P/N#am7152)

### 4.2.2 Identification of differentially expressed probe sets regulated over 2-fold

Affymetrix MAS 5.0 analysis was performed on aRNA derived from induced and uninduced Raji cells at 24 hrs post-induction. In order to identify highly differentially expressed and regulated cellular genes, several filtering steps were applied to all probe sets on the arrays (Figure 2.2), as described (section 2.5.2.3). In the third filtering step, a minimum 2-fold cut-off threshold was used leaving 6,517 and 5,437 probe sets in replicates a and b, respectively. From the overlap of the 6,517 and 5,437 probe sets, a total of 3,884 probe sets were identified that were commonly modulated in both biological replicates (Figure 4.3). These probe sets were analysed further to identify the most highly differentially expressed and regulated genes.

### 4.2.3 Identification of the top most highly differentially expressed probe sets

A sub-set of probe sets was selected from the overlap of 3,884 probe sets, by using the method 'sum (signals) x SLR', described previously (section 2.5.2.3.4), to remove genes with high SLR but low signal values that represent overall low signals. The 250 most differentially expressed genes were ranked. Of these probe sets, 191 (76.4%) were commonly modulated in both biological replicates (Table 7.2). The identification of genes regulated specifically by EBV infection was next determined by comparison with the Ramos cell line.

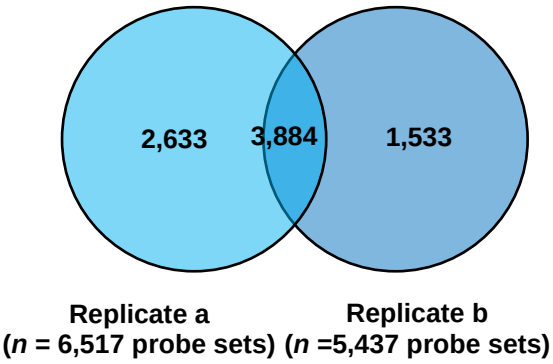


**Figure 4-3 Overlay of differentially expressed probe sets between induced Raji replicates**

Venn diagram showing the overlay between 6,517 and 5,437 probe sets from the two replicates that was differentially expressed (≥2-fold) in the Affymetrix HG U133 Plus 2.0 GeneChip® array. A total of 3,884 probe sets were commonly regulated. Also shown are 2,633 and 1,533 genes regulated only in replicate a and b, respectively.

### 4.2.4 Identification of probe sets regulated specifically by EBV lytic replication

In order to identify which of the 191 highly differentially expressed probe sets (171 genes) were expressed specifically by EBV replication and not in response to lytic cycle reagents, a second overlap of the 191 probe sets with the 199 most highly differentially expressed probe sets from TPA/NaB induced EBV-negative Ramos cells was assessed (Figure 4.4). The overlap identified 58 probe sets (57 genes) commonly modulated in both induced Raji and Ramos cells and 133 probe sets (112 genes) regulated in Raji cells alone (Table 7.2). Next, the fold-changes for each of the 58 probe sets (57 genes) were compared between induced

Raji and Ramos cells to determine the likelihood that these genes were regulated in response to the lytic cycle inducers.

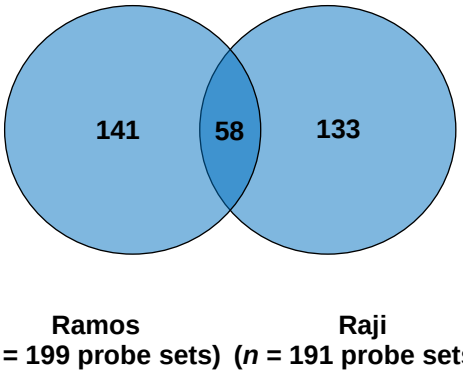


**Figure 4-4 Overlay of top most highly differentially expressed and regulated probe sets between induced Raji and Ramos replicates**

Venn diagram showing the overlay between the top 191 and 199 differentially expressed probe sets (≥2-fold) identified on the Affymetrix HG U133 Plus 2.0 GeneChip® from TPA/NaB induced Raji and Ramos biological replicates, respectively. The top 191 most differentially expressed probe sets (≥2-fold) were identified from the overlay of 3,884 probe sets commonly modulated between 6,157 and 5,437 probe sets from Raji biological replicates a and b and compared to the top 199 differentially expressed probe sets identified from duplicate biological replicates of induced Ramos cells, with 58 probe sets (57 genes) commonly modulated in both TPA/NaB induced Raji and Ramos cells. Also shown are 141 probe sets and 133 probe sets regulated in Ramos and Raji cells, respectively.

### 4.2.5 Identification of 58 host probe sets regulated by lytic cycle inducers

The 58 probe sets (57 genes) commonly modulated in both induced Raji and Ramos cells included 31 up-regulated probe sets (31 genes) and 27 down-regulated probe sets (26 genes) (Table 7.2). The regulation and fold-change for all 58 probe sets (57 genes) was subsequently compared between Raji and Ramos cells. Since Raji cells do not have an EBV-negative counterpart, EBV-negative Ramos cells were used as controls for the effects of the inducing agents. Given the genetic differences between the cell lines, the reliability of the data could be increased by increasing the numbers of replicates used. However, in this genome-wide analysis, only two replicates were analysed for each cell line. The direction of regulation of all genes was similar between Raji and Ramos cells, with all 31 probe sets (31 genes) that

were increased in Raji also increased in Ramos and all 27 probe sets (26 genes) that were decreased in Raji also decreased in Ramos (Table 7.2). Moreover, the fold-change for all 58 probe sets (57 genes) was similar between Raji and Ramos cells. All 58 probe sets were subsequently excluded from the 191 probe sets leaving a sub-set of 133 probe sets (112 genes) which we were confident were not regulated by TPA/NaB.

### 4.2.6 Identification of 133 probe sets regulated specifically by EBV replication

Of the 133 probe sets (112 genes) regulated specifically by EBV lytic infection, 77 (57.89% [64 genes]) were up-regulated and the remaining 56 (42.10% [49 genes]) down-regulated (Table 7.2). The assessment of fold-changes for each probe set, revealed that the most up-regulated gene was *CHI3L1*, a chitinase (18.1-fold up-regulated), and the most down-regulated gene was *RGS13*, a regulator of G-protein signaling 13 (-8.7-fold down-regulated). The median fold-change of the up-and down-regulated genes were 4.95 (range: 2.1 – 18.1) and -3.6 (range: -2.1 – -8.7), respectively. The 133 probe sets were subject to further analysis.

### 4.2.7 Identification of multiple probe sets that map to the same transcript

Affymetrix HG U133 Plus 2.0 GeneChip® arrays contain 11-20 probe sets that span each gene transcript to enhance reproducibility and accuracy of the hybridisation signal intensity (Figure 2.1). In order to decipher the total number of individual differentially regulated genes from within the 133 EBV-specific probe sets, as well as the reproducibility of the Affymetrix data, genes represented by two or more of the probe sets were identified. In total, 112 unique genes were identified. Of the 112 genes, 21 were represented by multiple probe sets, including 14 up- and 7 down-regulated genes (Table 4.1). Moreover, with the exception of SQSTM1, fold-changes were similar for multiple probe sets in 20 (95.24%) of these genes, demonstrating high reproducibility of the Affymetrix data. Three of the genes (*CCL5*,

*ANP32E* and *LRMP*) demonstrating reproducibility across probes were selected as candidate markers. The average fold-change for each of these genes was 9, -3.25 and -3.5-fold, respectively (Table 4.1).

**Table 4-1 Identification of multiple probe sets for cellular genes**

| Probe sets | Gene symbol | Fold-change for each probe set (Average fold-change) |
|---|---|---|
| 209969_s_at; 200887_s_at | *STAT-1* | 10.3-, 6.1-fold (8.2) |
| 201694_s_at; 201693_s_at | *EGR1* | 11.2-, 10.3-fold (10.8) |
| i405_i_at; 1555759_a_at; 204655_at | ***CCL5*** | 8.4-, 9-, 9.6-fold (9) |
| 208581_x_at; 204326_x_at | *MT1X* | 6.8-, 6.5-fold (6.7) |
| 225842_at; 217996_at | *PHLDA1* | 11.8-, 13.1-fold (12.5) |
| 202497_x_at; 202499_s_at | *SLC2A3* | 10-, 8.9-fold (9.5) |
| 204747_at; 229450_at | *IFIT3* | 7-, 6.5-fold (6.8) |
| 213112_s_at; 201471_s_at | *SQSTM1* | 12.4-, 6.5-fold (9.5) |
| 200866_s_at; 200871_s_at | *PSAP* | 4.8-, 4.1-fold (4.5) |
| 35820_at; 212737_at | *GM2A* | 4.9-, 4.2-fold (4.6) |
| 210592_s_at; 203455_s_at | *SAT1* | 4.2-, 3.8-fold (4) |
| 201625_s_at; 201627_s_at; 201626_at | *INSIG1* | 4.2-, 3-, 2.3-fold (3.2) |
| -34210_at; 204661_at | *CD52* | 3-, 2.9-fold (3) |
| 214211_at; 200748_s_at | *FTH1* | 4.7-, 2.25-fold (3.5) |
| 200772_x_at; 211921_x_at | *PTMA* | -2.1-, -2.4-fold (-2.3) |
| 40189_at; 213047_x_at | *SET* | -2.3-, -2.4-fold (-2.4) |
| 211714_x_at; 209026_x_at; 212320_at | *TUBB* | -2.3-, -2.6-, -2.7-fold (-2.5) |
| 214938_x_at; 200680_x_at; 224731_at | *HMGB1* | -2.6-, -5.6-, -3.2-fold (-3.8) |
| 201306_s_at; 201305_x_at | ***ANP32E*** | -3.1-, -3.3-fold (-3.2) |
| 208956_x_at; 209932_s_at | *DU2* | -2.25-, -3.6-fold (-3) |
| 204674_at; 35974_at | ***LRMP*** | -3.4-, -3.6-fold (-3.5) |

Cellular genes with multiple probe sets selected for further analysis (bold)

### 4.2.8 Identification of cellular genes as candidate markers

In order to increase the probability of identifying an effective diagnostic marker, 22 of the 112 EBV-regulated cellular genes were selected for preliminary analysis in clinical samples (Table 4.2). These genes fulfilled the following criteria: (i) not regulated in response to lytic cycle inducers (TPA/NaB); (ii) regulation in EBV-associated PTLD and/or EBV infection that was previously demonstrated in the literature; (iii) highly regulated cellular genes with biological functions of interest, and (iv) cellular genes identified in significantly represented

networks in Gene Ontology analysis. Owing to limited cDNA material derived from the whole blood samples, only 17 of the 22 genes were subject to gene expression profiling (high-lighted in bold in Table 4.2).

#### 4.2.8.1 Regulation of cellular candidate genes

Details of the 22 candidate genes are presented in Table 4.2. Thirteen (59.09%) of these candidates (*CHI3L1, TIMP-1, CXCL9, CCL5, ULBP2, ISG15, ANXA2, RASA1, CCL22, CXCL10, CCL3, CD52* and *VIM*), were up-regulated, including *CHI3L1*, which was the most up-regulated gene (18.1-fold, $P<0.0084$) (Table 7.2). The remaining nine (40.91%) genes (*IGJ, HDGF1, ANP32E, PCNA, LRMP, MAD2L1, CDC2, HMGB1* and *RGS13*) were down-regulated, including *RGS13*, which was the most down-regulated gene (-8.7, $P<0.001$).

#### 4.2.8.2 Identification of cellular candidate genes in PTLD

A literature search revealed eight genes (*CD52, ANP32E, PCNA, MAD2L1, CDC2, LRMP, HMGB1* and *TIMP1*) differential regulation in EBV-monomorphic PTLD (M-PTLD) relative to EBV-negative M-PTLD (Craig et al., 2007). All eight genes were involved in DNA replication (*HMGB1*, *PCNA*), transcription (*ANP32E*), cell cycle regulation (*MAD2L1*, *CDC2*), vesicle fusion and anti-apoptosis (*LRMP*), cell proliferation (*TIMP-1*) and anti-apoptosis (*CD52*). Owing to their involvement in PTLD, all eight genes were selected as candidates for gene expression profiling. Biological annotations for all 22 candidates are presented in Table 4.2. Several of the up-regulated genes (5/13 [38.46%]) are involved in chemotaxis, inflammatory response and signal transduction (*CCL5, CCL22, CXCL10, CCL3,* and *HDGF1*). Conversely, the majority (5/9 [55.56%]) of the down-regulated genes are involved in cell cycle regulation, egulation of transcription, and DNA replication (*MAD2L1, CDC2, ANP32E, HDGF1,* and *HMGB1*).

## Table 4-2 Summary of highly differentially expressed and regulated cellular candidate genes

| Probe set ID | Gene symbol | Gene name | Biological process | Cellular compartment | Fold-change | *P*-value |
|---|---|---|---|---|---|---|
| **209395_at** | ***CHI3L1*** | chitinase 3-like 1 (cartilage glycoprotein-39) | Chitin catabolic process | Extracellular | 18.1 | *P*<0.0084 |
| **201666_at** | ***TIMP-1*** | TIMP metallopeptidase inhibitor 1 | Positive regulation of cell proliferation/Negative regulation of membrane protein | Extracellular region | 14.7 | *P*<0.00002 |
| **203915_at** | ***CXCL9*** | chemokine (C-X-C motif) ligand 9 | Chemotaxis, defense, immune response, signal transduction, cell-cell signalling | Extracellular region/extracellular space | 10.2 | *P* <0.0001 |
| **1405_i_at** | ***CCL5*** | chemokine (C-C motif) ligand 5 | Chronic inflammatory response, chemotaxis, cell adhesion, signal transduction, negative regulation of viral replication, response to NF-kappa B | Extracellular | 9.6 | *P* <0.0003 |
| **238542_at** | *ULBP2* | UL16 binding protein 2 | Immune response, antigen processing, NK cell activation | Extracellular | 8 | *P*<0.0001 |
| **205483_s_at** | ***ISG15*** | ISG15 ubiquitin-like modifier | Cell-cell signalling, response to virus, ISG15-protein conjugation | Extracellular | 6.4 | *P*<0.0001 |
| **201590_x_at** | *ANXA2* | annexin A2 | Fibrinoloysis | Extracellular | 5.9 | *P*<0.0001 |
| **210621_s_at** | ***RAS p21*** | RAS p21 protein activator (GTPase activating protein) 1 | Cell adhesion, anti-apoptosis, signalling cascade | Plasma membrane | 5.4 | *P*<0.0001 |
| **207861_at** | ***CCL22*** | chemokine (C-C motif) ligand 22 | Chemotaxis, inflammatory response, immune response, cell signalling, response to virus | Extracellular | 4.4 | *P*<0.0018 |
| **204533_at** | ***CXCL10*** | chemokine (C-X-C motif) ligand 10 | Chemotaxis, inflammatory response, cell cycle, signal transduction | Extracellular | 4 | *P*<0.0001 |
| **205114_ s_at** | ***CCL3*** | chemokine (C-C motif) ligand 3 | Chemotaxis, inflammatory response, cell cycle, signal transduction | Extracellular | 3.7 | *P*<0.0007 |
| **201426_s_at** | *VIM* | Vimentin | Cell motion | Cytoplasm/plasma membrane | 3.3 | *P*<0.0001 |
| **34210_at** | ***CD52*** | CD52 molecule | Respiratory burst | Plasma membrane | 3 | *P*<0.0035 |

Table 4-2 continued

| Probe set ID | Gene symbol | Gene name | Biological process | Cellular compartment | Fold-change | *P*-value |
|---|---|---|---|---|---|---|
| **212592_at** | *IGJ* | immunoglobulin J polypeptide, linker protein for immunoglobulin alpha and mu polypeptides | | Extracellular | -2.6 | *P*<0.0015 |
| **200896_x_at** | ***HDGF1*** | hepatoma-derived growth factor (high-mobility group protein 1-like | Regulation of transcription, cell proliferation, signal transduction | Extracellular | -4.1 | *P*<0.0001 |
| **221505_at** | ***ANP32E*** | acidic (leucine-rich) nuclear phosphoprotein 32 family, member E | Unknown (likely regulation of transcription) | Nucleus,cytoplasm | -2.4 | *P*<0.0014 |
| **201202_at** | ***PCNA*** | proliferating cell nuclear antigen | DNA replication | Nucleus | -2.9 | *P*<0.0001 |
| **204674_at** | ***LRMP*** | lymphoid-restricted membrane protein | Vesicle fusion | Integral to plasma membrane | -3.4 | *P*<0.0084 |
| **203362_s_at** | ***MAD2L1*** | MAD2 mitotic arrest deficient-like 1 | Cell division (cell cycle) | Chromosome | -5.3 | *P*<0.00113 |
| **203213_at** | ***CDC2*** | cell division cycle 2, G1 to S and G2 to M | Anti-apoptosis, cell cycle | Plasma membrane | -5.4 | *P*<0.0004 |
| **200680_x_at** | *HMGB1* | high-mobility group box 1 | DNA unwinding during replication | Nucleus, chromosome | -5.6 | *P*<0.0001 |
| **210258_at** | ***RGS13*** | regulator of G-protein signaling 13 | G-protein coupled receptor signalling pathway | Plasma membrane | -5.7 | *P*<0.0001 |

List of up- and down-regulated cellular candidate genes selected from the Affymetrix HG U133 Plus 2.0 GeneChip™ array. Ranked by fold-change, where $P<0.05$ is considered statistically significant. Genes selected for further analysis (bold)

### 4.2.9 Validation of microarray data for 22 cellular candidate genes by real-time PCR

In order to verify the regulation of the candidate genes, and to what extent, prior to further analysis, real-time PCR using TaqMan gene expression assays was used to validate the microarray data for all 22 candidate genes. Samples were run in triplicate using cDNA (diluted 1/100) derived from pooled duplicate flasks; two biological replicates (replicates a and b) of induced and uninduced Raji cells were tested by real-time PCR and fold-changes calculated in Prism as described previously (section 2.4.9). The single-copy house-keeping *ACTB* gene was used as the internal reference control. The regulation of the cellular genes was consistent between real-time PCR and microarray results with fourteen up-regulated and eight down-regulated genes (Figures 4.5). A comparison of the fold-change for all 22 candidate genes derived from real-time PCR and microarray is presented in Table 4.3. Correlations between the microarray and PCR distributions were determined using pearson's correlation coefficient and determined to be highly significant (0.746; $P<0.00007$).

**(A)**

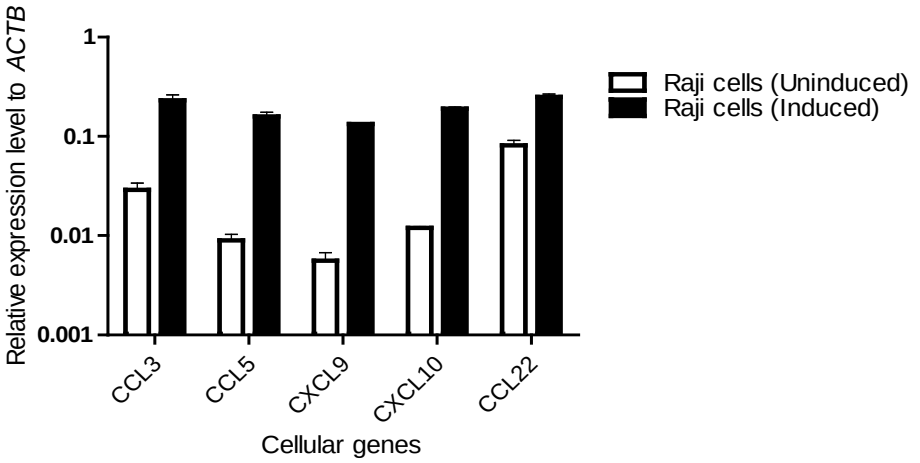
Relative expression level to ACTB
1
0.1
0.01
0.001
CCL3
CCL5
CXCL9
CXCL10
CCL22
Cellular genes
Raji cells (Uninduced)
Raji cells (Induced)

**(B)**

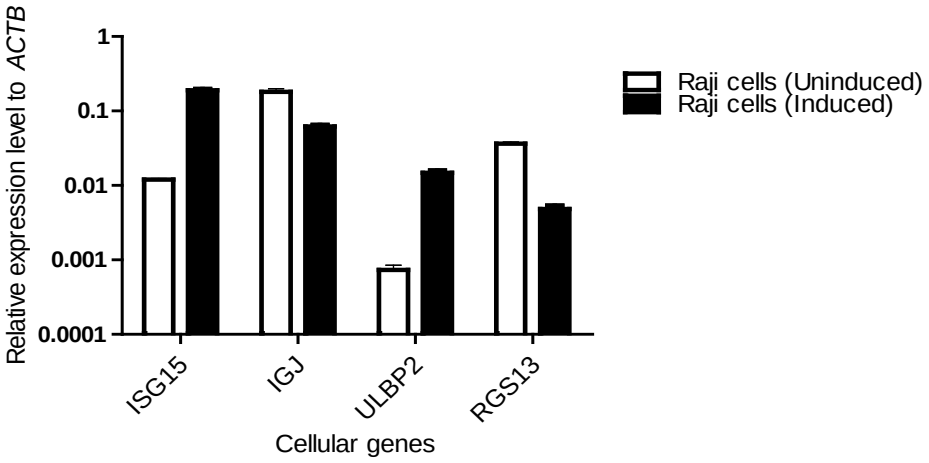
Relative expression level to ACTB
1
0.1
0.01
0.001
0.0001
ISG15
IGJ
ULBP2
RGS13
Cellular genes
Raji cells (Uninduced)
Raji cells (Induced)

**(C)**

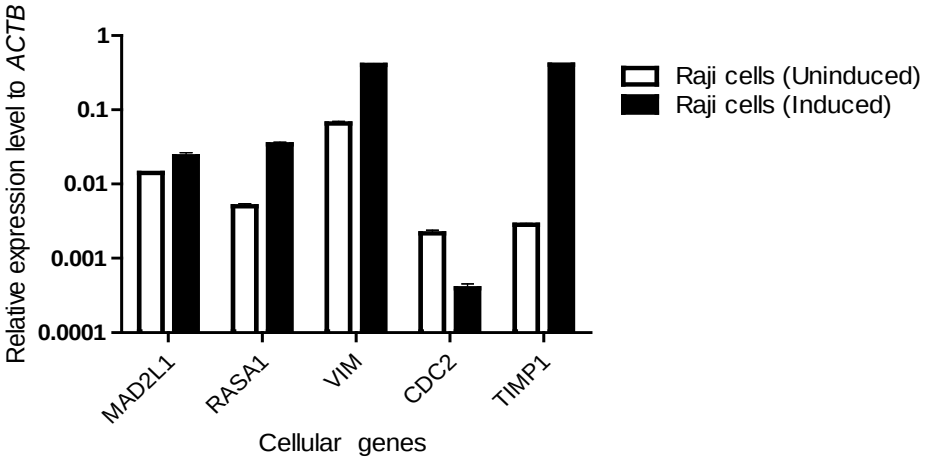
Relative expression level to ACTB
1
0.1
0.01
0.001
0.0001
MAD2L1
RASA1
VIM
CDC2
TIMP1
Cellular genes
Raji cells (Uninduced)
Raji cells (Induced)

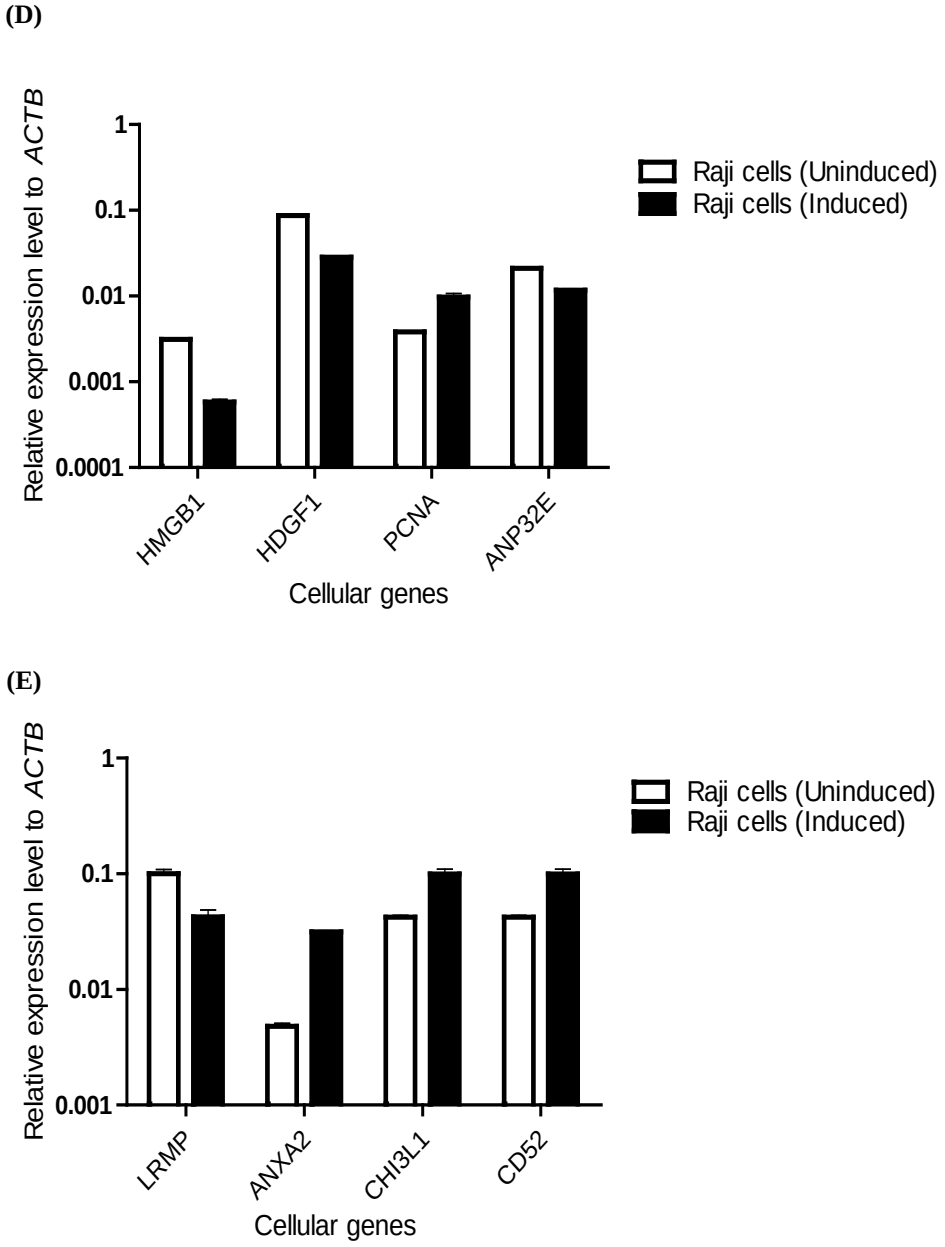


**Figure 4-5 Validation of microarray data for Cellular candidate genes by real-time PCR**

Bar charts showing relative expression levels for *CCL3*, *CCL5*, *CXCL9*, *CXCL10* and *CCL22* (chemokines) (**A**), *ISG15*, *IGJ*, *ULBP2* and *RGS13* (immune response and cell-cell signaling) (**B**), *MAD2L1*, *RASA1*, *VIM*, *CDC2* and *TIMP1* (cell cycle) (**C**) and *HMGB1*, *HDGF1*, *PCNA* and *ANP32E* (DNA replication and transcription) (**D**) and *LRMP*, *ANXA2*, *CHI3L1* and *CD52* (Other functions) (**E**) in response to EBV lytic induction in TPA/NaB induced Raji cells (closed bars) versus uninduced Raji cells (open bars) quantitated using real-time PCR. Total RNA was isolated from duplicate biological replicates of TPA/NaB induced and uninduced Raji cells using the Qiagen RNeasy Extraction Kit and 2 µg reverse-transcribed to cDNA using the Retroscript™ Kit. Real-time PCR was performed on serial 1/100 dilutions of cDNA using TaqMan gene expression assays and the TaqMan Gene Expression Master Mix. *ACTB* was used as the internal reference control. Data represents the mean fold-change ± SD for two independent experiments performed in triplicate.

### 4.2.10 Validation of microarray data for *TIMP1* by real-time PCR

Real-time PCR was used to validate microarray data for the *TIMP1* gene, which was up-regulated 14.7-fold ($P<0.00002$) and 15.2-fold ($P<0.001$) in induced Raji and Ramos cells, respectively (Table 7.2). This additional data was used to confirm that the regulation in Raji cells was a specific response to either TPA/NaB stimulus, as TIMP1 is known to be up-regulated regardless of EBV infection (Kim et al., 2008). Although *TIMP1* was up-regulated by EBV infection in uninduced EBV-positive Raji cells (Figure 4.6), it was notably up-regulated in TPA/NaB induced Raji cells. This pattern indicated that *TIMP1* is regulated by EBV infection and that this regulation is enhanced by TPA/NaB treatment. Similar regulation patterns were observed in *TIMP1* between induced and uninduced Ramos cells, although to a marginally higher level in the induced Ramos cells, indicating some regulation by TPA/NaB (Table 7.2). Given that *TIMP1* is regulated by EBV replication and its regulation has been shown to influence PTLD outcome, this gene was chosen as one of the 22 candidate genes (Craig et al., 2007).

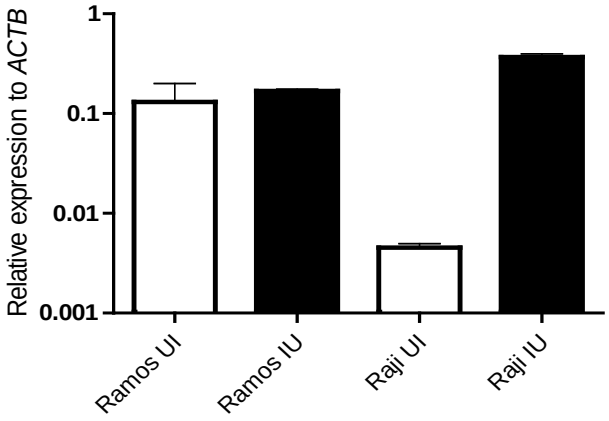


**Figure 4-6 Validation of microarray data for *TIMP1* by real-time PCR**

Bar charts showing relative expression levels for *TIMP1*, in response to EBV infection in TPA/NaB induced (closed bars) and uninduced Ramos cells (open bars), versus TPA/NaB induced (closed bars) and uninudced Raji cells, as determined using real-time PCR. Total RNA was isolated from duplicate biological replicates of TPA/NaB induced and uninduced Raji cells using the Qiagen RNeasy Extraction Kit and 2 µg reverse-transcribed to cDNA using the Retroscript™ Kit. Real-time PCR was performed on serial 1/100 dilutions of cDNA using TaqMan gene expression assays and the TaqMan Gene Expression Master Mix. *ACTB* was used as the internal reference control. Data represents the mean fold-change ±SD for two independent experiments performed in triplicate.

**Table 4-3 Validation of microarray data for cellular candidate genes by real-time PCR**

| Probe set ID | Gene | Biological process | Fold-change (Microarray) | Fold-change (Real-time PCR) |
|---|---|---|---|---|
| 205114_s_at | *CCL3* | Chemokines | 3.7 | 7.96 |
| 1405_i_at | *CCL5* | Chemokines | 9.6 | 17.81 |
| 207861_at | *CCL22* | Chemokines | 4.4 | 13.84 |
| 203915_at | *CXCL9* | Chemokines | 10.2 | 23.71 |
| 204533_at | *CXCL10* | Chemokines | 4.0 | 15.87 |
| 212592_at | *IGJ* | Immune response and cell signaling | -2.6 | -2.89 |
| 205483_s_at | *ISG15* | Immune response and cell signaling | 6.4 | 15.87 |
| 210258_at | *RGS13* | Immune response and cell signaling | -8.7 | -7.59 |
| 238542_at | *ULBP2* | Immune response and cell signaling | 8.0 | 20.20 |
| 203213_at | *CDC2* | Cell Cycle | -5.14 | 0.18 |
| 203362_s_at | *MAD2L1* | Cell Cycle | -5.3 | 1.67 |
| 210621_s_at | *RASA1* | Cell Cycle | 5.4 | 6.81 |
| 201666_at | *TIMP1* | Cell Cycle | 14.7 | 143.3 |
| 201426_s_at | *VIM* | Cell Cycle | 3.3 | 6.13 |
| 221505_at | *ANP32E* | DNA replication and transcription | -2.4 | -1.78 |
| 200896_x_at | *HDGF1* | DNA replication and transcription | -4.1 | -3.08 |
| 200680_x_at | *HMGF1* | DNA replication and transcription | -5.6 | -5.41 |
| 201202_at | *PCNA* | DNA replication and transcription | -2.9 | -2.53 |
| 201590_x_at | *ANXA2* | Other functions | 5.9 | 6.54 |
| 34210_at | *CD52* | Other functions | 3.0 | 2.36 |
| 209395_at | *CHI3L1* | Other functions | 18.1 | 236 |
| 204674_at | *LRMP* | Other functions | -3.4 | -2.35 |

### 4.2.11 Gene Ontology analysis of differentially expressed genes

Gene Ontology (GO) analysis was undertaken in MetaCore to determine the GO biological processes and disease biomarker processes, as well as canonical network pathways represented by data sets from replicates a) 6,157 probe sets and b) 5,437 probe sets, in response to EBV lytic induction. Both data sets were uploaded into MetaCore and enrichment analysis was used to identify the most representative functions altered in response to EBV lytic induction in Raji cells at a threshold of 1.5 and $P<0.05$.

### 4.2.11.1 Functional canonical pathway analysis

Pathway analysis revealed the ten most significantly represented ($P$<0.05) canonical pathways for both data sets as illustrated in Figure 4.7. Amongst these pathways, the three most significant pathways, in order of significance were the anaphase-promoting cycle (APC) in cell cycle regulation, the metaphase checkpoint, and the spindle assembly and chromosome separation.

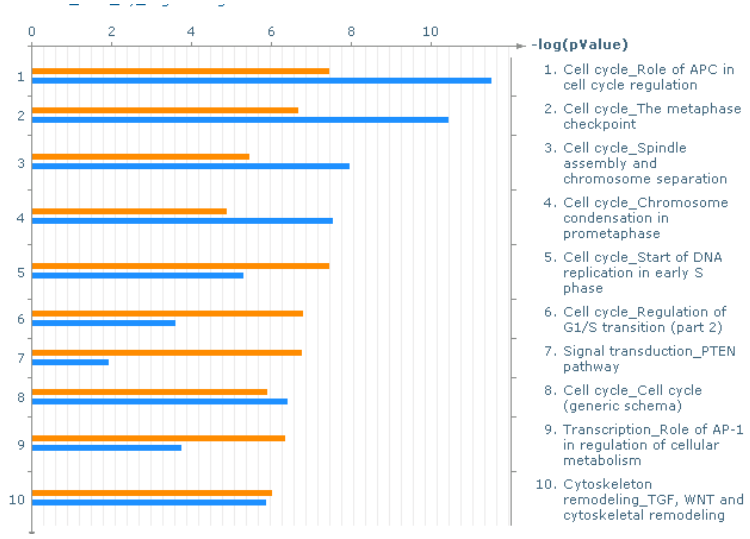


**Figure 4-7 Canonical network pathway analysis of differentially expressed cellular genes**

Histogram showing the top ten most significantly represented canonical network pathways, in probe sets derived from Affymetrix microarray gene expression data, altered in response to the EBV lytic phase in TPA/NaB induced Raji cells. Seven of ten pathways are involved in cell cycle. Gene expression data at a threshold of 1.5 and $P$<0.05 was subjected to Enrichment analysis using GeneGo MetaCore.

### 4.2.12 Functional biological processes network analysis

Analysis of GO biological network processes revealed the top ten most significantly represented biological processes altered in response to EBV lytic induction (Figure 4.8). Six of ten networks were involved in cell cycle regulation, with the top three most significantly regulated involved in cell cycle core, cell cycle synthesis (S) phase and cytoskeleton spindle microtubules. In order to identify additional potential candidate genes, further analysis is required to identify key gene interactions or genes highly differentially regulated within each

of the cell cycle core networks. Of interest, chemotaxis was also a highly representative biological process and relevant to EBV infection.

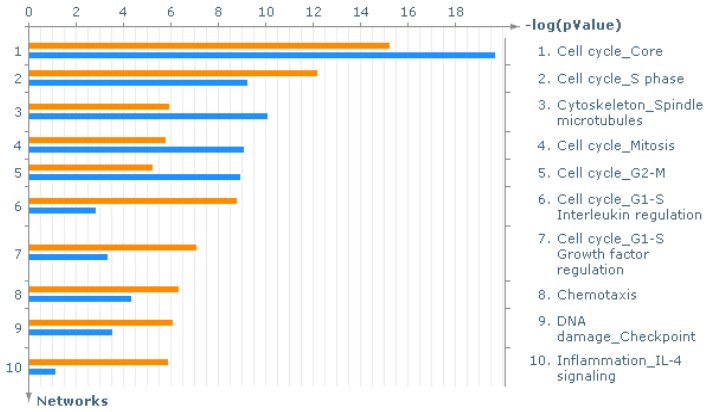


**Figure 4-8 Biological processes network analysis of differentially expressed cellular genes**

Histogram showing the top ten most significantly represented canonical network pathways, in probe sets derived from Affymetrix microarray gene expression data altered in response to the EBV lytic phase in TPA/NaB induced Raji cells. All ten pathways are involved in cell cycle. Gene expression data at a threshold of 1.5 and $P<0.05$ was subjected to Enrichment analysis using GeneGo MetaCore.

### 4.3.14 Functional biomarker network pathway analysis

In order to identify potential disease biomarkers in response to gene expression changes in lytic induced Raji cells, preliminary biomarker network processes were analysed within enrichment analysis in GeneGO MetaCore™. Figure 4.9 shows the ten most statistically significant pathways. As such, lymphoproliferative disorders were among the ten most significant networks represented by the Affymetrix data sets. Amongst these networks, the three most significant biomarker networks were lymphatic diseases, lymphoproliferative disorders and immunoproliferative disorders. Further analysis on functional gene interactions could reveal additional important candidate genes within lymphoproliferative disorders.

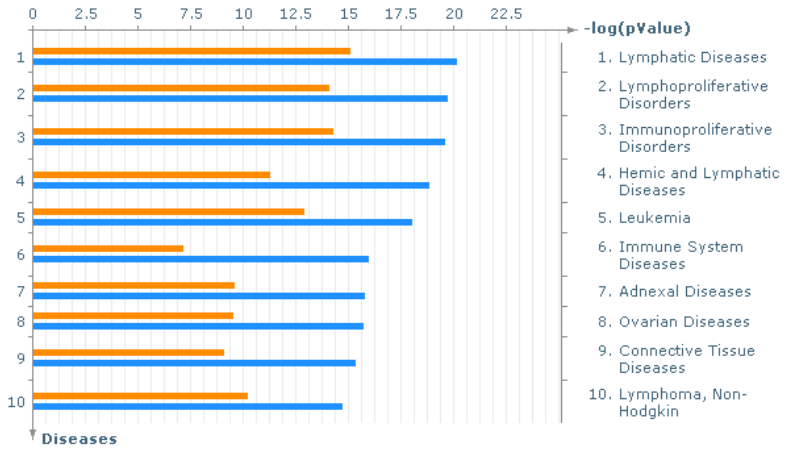


**Figure 4-9 Biomarker network pathway analysis of differentially expressed cellular genes**

Histogram showing the top ten most significantly represented biomarker network pathways, in probe sets derived from Affymetrix microarray gene expression data, altered in response to the EBV lytic phase in TPA/NaB induced Raji cells. Gene expression data was set at a threshold of 1.5 and $P<0.05$ and subjected to Enrichment analysis using GeneGo MetaCore.

## 4.3 DISCUSSION

In this chapter, we used Affymetrix HG U133 Plus 2.0 GeneChip$^{TM}$ arrays to identify highly differentially expressed and regulated cellular genes in response to EBV lytic induction. This was achieved by comparing the most highly differentially expressed probe sets from the TPA/NaB induced EBV-negative Ramos cells to the most highly regulated probe sets in the induced EBV-postivie Raji cells (Chapter 3). This microarray analysis, identified 5,437 and 6,517 probe sets that were differentially regulated over 2-fold in two induced biological replicates. Amongst the two replicates, 3,884 probe sets were commonly regulated in both; of which 191 were commonly regulated when the top 250 most highly differentially expressed probe sets were ranked (Table 7.2). These 191 probe sets were analysed further to identify any potential candidate genes that could serve as markers for PTLD. Given that phorbol esters, such as TPA, can induce uniform gene transcription (Fields et al., 2007), a further filter was performed to remove any genes that were up regulated in response to TPA induction alone. For this filter the most highly modulated genes in the TPA/NaB induced EBV negative Ramos cells were subtracted from the most modulated genes in the TPA/NaB induced EBV positive Raji cells. This analysis revealed 58 probe sets (57 genes) that were potentially regulated in response to TPA/NaB treatment, leaving 133 probe sets (112 genes) that were likely to be regulated specifically by EBV (Figures 4.4; Table 7.2). Within the 133 probe sets that were regulated in response to EBV reactivation, 77 probe sets (64 genes) were up-regulated (≥2-fold) and 56 probe sets (49 genes) down-regulated (≤2-fold) (Table 7.2).

For the preliminary investigation, a maximum of 17 cellular candidate genes could be evaluated per clinical sample in each real-time PCR run using limited cDNA template. To select the initial 17 genes, we devised criteria for identifying potential targets based on the

following: (i) no regulation in response to TPA/SB lytic inducers, (ii) previous regulation by EBV and/or PTLD, (iii) highly regulated cellular genes with other biological functions of interest, and (iv) Gene Ontology pathways. Our rationale was that any highly regulated cellular genes likely to be regulated in response to the EBV lytic phase could also drive PTLD pathogenesis.

**Analysis of cellular gene expression *in vitro***

In this study, TPA/NaB induced Raji cells were used to examine cellular gene regulation in response to EBV lytic induction. However, other studies have examined cellular gene regulation in response to EBV reactivation in other LCLs (Cahir-McFarland et al., 2004; Yuan et al., 2006). For instance, in a previous study, IgG cross-linking was used to mimic B-cell activation of the EBV-positive Akata cell line (Yuan et al., 2006). When we compared our findings to this study, several up-regulated genes overlapped, such as *DUSP5, EGR1, SQSTM1, OAS1, OASL* and *PLEK*. This overlap lends confidence to the hypothesis that the cellular genes that we have identified are being modulated in response to EBV expression. However, one gene, *LRMP*, was observed to be upregulated in this study, while being down regulated in our array. One potential reason for this discrepancy could be to differences in time-points between the two studies, as well as differences in the kinetics of EBV gene expression. Interestingly in the study by Yuan and colleagues, they noted that temporal difference influenced the magnitude and direction of modulation of particular genes. For instance, while *OASL* and *OAS1* were up-regulated between 24 to 48 hr time-points, they were down-regulated at earlier time-points (8-24 hrs). This suggests that differences in gene regulation may relate to temporal changes in EBV gene expression patterns following activation of viral replication (Yuan et al., 2006). Of note these temporal differences in EBV gene expression could also account for the discrepancies in another study that found *LRMP* to

be down-regulated 48 hrs after reactivation, using IgG cross-linking in Akata cells relative to EBV-negative AK31 cells (Broderick et al., 2009). Therefore, these findings suggest that the time-point (24 hrs) at which RNA was harvested in our array could potentially influence the level of expression of the EBV genes and also the cellular candidate genes chosen for further analysis.

In the study by Yuan and colleagues, the effects of EBV latent genes on cellular gene expression were also investigated (Yuan et al., 2006). When we compared their results to our analyses we identified several overlapping genes, including *SGK1*, *STAT-1*, *ANXA2*, *DUSP5*, *TIMP-1*, *ETV7* and *EGR1*, all of which were previously shown to be regulated in response to EBV LMP-1 (Cahir-McFarland et al., 2004) (Table 7.2). Moreover, *DUSP5* was shown to be up-regulated by latency III in two studies, suggesting that these highly regulated cellular genes could be regulated by latency III in our model system (Cahir-McFarland et al., 2004; Yuan et al., 2006). During latency III, all EBV latency proteins are expressed (Fields et al., 2007). Latency III expression has been demonstrated previously during lytic replication and is thought to facilitate viral replication (Yuan et al., 2006). In the previous chapter (Chapter 3) we demonstrated low fold-induction levels for certain EBV latent genes, the remainder of which were down-regulated. For instance, we demonstrated a 1.6-fold and 1.77-fold induction level of *LMP-1* and *EBNA-3B,* respectively at 24 hrs post-induction, whereas *EBNA-2* was induced <2-fold. This suggests that the highly differentially expressed and regulated cellular genes could be attributable to not only lytic, but latent gene expression. We also identified genes known to be up-regulated directly by the EBNA-2 protein in LCLs, including *JUND, CCL5, ILI41, PCNA* and *CD69* (Table 7.2) (Lucchesi et al., 2008; Spender et al., 2006; Zhao et al., 2006). Importantly, *ILI41* and *CD69* were also regulated in Ramos, whereas *PCNA, LRMP* and *CD69* that are involved in the cell cycle were down-regulated in

our model system. Since previous studies have demonstrated latent gene expression in a small proportion of IgG cross-linked Akata cells, it is uncertain which genes are truly regulated by EBV lytic replication alone (Yuan et al., 2006). However, both latency III coupled with lytic gene expression is documented in PTLD patients (Hopwood et al., 2002). Therefore, regardless of the discrepancy of our findings, the selection of candidate genes from this data set could still provide useful markers for PTLD. We selected five candidate genes (*RGS13*, *LRMP*, *TIMP-1*, *ISG15*, and *PCNA*) for further analysis. Our rationale for selecting these genes was that they were known to be regulated in response to EBV infection, and therefore, this would give us a good starting point for the clinical validation.

**Analysis of EBV gene expression in PTLD**

To assess how our results compared to microarray analysis carried out on PTLD biopsy tissue, we compared our findings to two previous studies (Baran-Marszak et al., 2002; Craig et al., 2007). The first study compared the gene expression profiles of EBV-positive M-PTLD relative to EBV-negative M-PTLD (Craig et al., 2007). The results the study were validated by an earlier study that investigated cellular gene expression profiles of EBV infected B cells versus uninfected cells, and further compared these to EBV-positive B cells in the context of PTLD (Baran-Marszak, 2002). Altogether, we identified two up-regulated genes (*HMGA1*, 2.2-fold and *TIMP1*, 14.7-fold) and seven down-regulated genes (*ANP32A*, -2.6-fold, *ANP32E*,-2.4-fold, *CDC2*, -5.4-fold; *HMGB1*, -5.6-fold; *MAD2L1*, -5.3-fold; *LRMP*, -3.4-fold and *PCNA*, -2.9-fold) (Table 4.3) that were consistent with both studies. Moreover, EBV latent genes are known to up-regulate four of these genes (*CDC2*, *HMGA1*, *LRMP* and *TIMP1*) from previous studies, indicating possible regulation by EBV infection or B cell regulation (Cahir-McFarland et al., 2004; Yuan et al., 2006). A further two genes were found to be modulated across studies (*MAD2L1*, -5.3-fold; *CDC2*, -5.4-fold). However, these genes

were also shown to be modulated in response to TPA/NaB treatment in our study in EBV-negative Ramos cells, although to lower levels (-2.6-fold vs. -2.2-fold; Table 7.2), indicating regulation independent of EBV infection. In contrast to these studies, *CD52*, which encodes the Campath1 antigen CD52 was up-regulated 3-fold in our array analysis (Table 7.2), but down-regulated in PTLD and in latency III expressing cells (Cahir-McFarland et al., 2004; Craig et al., 2007).

Eight genes (*ANP32E*, *CDC2*, *CD52*, *HDGF1*, *LRMP*, *MAD2L1*, *PCNA*, and *TIMP1*) were chosen as potential markers of PTLD, four (*CDC2*, *TIMP-1*, *LRMP* and *PCNA*) of which were also identified as regulated by EBV infection *in vitro*. Our rationale for selecting these candidate genes was to choose cellular genes that were regulated in relation to PTLD, since we were limited by the amount of material available for the clinical evaluation. Moreover, the products of the candidate genes appear to be involved in processes likely to be relevant to PTLD progression, such as anti-apoptosis (*ANP32E*), cell growth and apoptosis (*CDC2*; *CD52; MAD2L1*; *LRMP*) apoptosis, cell growth, cell invasion and apoptosis (*HDGF1*), regulation of transcription/anti-tumour immunity (*HMGB1*), cell proliferation (*PCNA*) and, cell proliferation, apoptosis, angiogenesis and cellular signaling (*TIMP1*) (Guo et al., 2010b; Kallakury et al., 1997; Lee et al., 2010; Liu et al., 2011; Malkas et al., 2006; Manenti et al., 2006; Peng et al., 2011; Rodig et al., 2006; Tsukamoto et al., 2008). In addition, *CHI3L1*, that encodes the chitinase-3-like 1 protein, was also chosen since it was the most up-regulated gene (18.1-fold) identified in our array, and has also been implicated in several cancers (Eurich et al., 2009). Therefore, overall nine cellular genes were selected for further analysis.

**GeneOntology Analysis**

We performed Gene Ontology analysis in MetaCore$^{TM}$ software on the differentially

expressed probe sets regulated over 2-fold in our array data (i.e., 5,437 and 6,517 probe sets from two biological replicates). This analysis allowed us to determine the overall functional, represented by the data sets following EBV lytic induction, and the potential microenvironment in which PTLD could develop.

We performed GO for functional biological processes, canonical pathway analysis and disease biomarkers using enrichment analysis in MetaCore software. We found the cell cycle to be the most highly represented biological process in response to EBV reactivation. The events in the cell cycle are an important factor in EBV biology, components of which are necessary for activating naive resting B cells into proliferating lymphoblasts. In particular, *EBNA-1, EBNA- 2, EBNA-3A, EBNA-3C, EBNA-LP* and *LMP-1* are known to regulate the cell cycle (Knight and Robertson, 2004; Sinclair et al., 1994). However, the IE gene *BZLF1* can also promote cell cycle arrest to facilitate EBV lytic replication (Zhou et al., 2010). Therefore, the identification of cell cycle as the most significant biological process during induction of EBV lytic replication could be of considerable importance. This, together with the identification of several cellular genes, involved in the cell cycle in our array and associated with PTLD in other studies, suggests a role for both latent and lytic gene expression in cell cycle dysregulation in PTLD (Craig et al., 2007).

Furthermore, we also identified chemotaxis as one of the ten most highly represented processes in the cell cycle. In particular, we identified four highly regulated chemokines including CXCL9 (MIG: monokine-induced by interferon-γ), CXCL10, the interferon-γ (IFN-γ)-inducible protein-10 (IP-10), CCL5 (regulated upon activation of the normal T cell express sequence, RANTES) and CCL3 (macrophage inflammatory protein-1 alpha, MIP-1α) (Table 7.2, Table 4.2). Chemokines are a class of cytokines with chemoattractant properties, including around 40 small soluble molecules (12-14 kDa) divided into 4 major families including the CXC-, CC-, C- and CX3C- families (Ohshima et al., 2002). All chemokine

receptors are integral membrane proteins linked to G-proteins, with seven membrane spanning domains. A key role for chemokines is the recruitment of blood leukocytes to sites of inflammation (Baggiolini et al., 1997; Schluger and Rom, 1997; Uchihara et al., 2005). At these sites, chemokines regulate leukocyte maturation, trafficking and homing, and the development of lymphoid tissues (Baggiolini, 1998; Nelson and Krensky, 1998; Uchihara et al., 2005). Chemokines are also important in cancers, where they are involved in processes such as homeostasis, cell proliferation, haematopoiesis, viral/cell interactions, angiogenesis, neovascularisation and metastasis (Ali and Lazennec, 2007). This category of pathways is of particular interest since chemokines are involved in the initial phases of the immune response against viruses; hence are known to be regulated by EBV, and are also known to regulate angiogenesis, a crucial event in the development of cancers (Ali and Lazennec, 2007; Baggiolini et al., 1997). Furthermore, they are soluble secreted proteins that are detectable in the circulation and therefore represent potentially viable and non-invasive diagnostic markers.

Previous studies have shown that the EBV latent genes, in particular *LMP-1* are capable of up-regulating chemokines, including CCL5, CCL3 (macrophage inflammatory protein-1 alpha, MIP-1α), CCL17 (thymus-associated regulatory chemokine, TARC), CCL19 (Epstein-Barr virus-induced molecule 1 ligand chemokine, ELC), CCL22 (macrophage-derived chemotactic factor, MDC), CXCL10 and interleukin-8 (IL-8) via the NF-kappa B pathway (NF-κB) (Buettner et al., 2007; Eliopoulos et al., 1999; Nakayama et al., 2004; Uchihara et al., 2005; Vockerodt et al., 2005).

In the previous chapter (chapter 3) we demonstrated a 1.6-fold induction of *LMP-1* in TPA/NaB induced Raji cells at 24 hrs. Therefore, it is possible that the highly up-regulated chemokine network identified is attributable to low-level *LMP-1* induction. However, it is possible that lytic gene expression could also be contributing to the up-regulation of these

chemokines. A previous study has demonstrated that the IE transactivator, BZLF1 can up-regulate cytokines (chemokine enhancers) interleukin (IL)-6 (IL-6), IL-10, IL-13 and the IL-8 mediated chemokine (CXCL8) (Hsu et al., 2008; Jones et al., 2007; Mahot et al., 2003; Tsai et al., 2009). Regulation of these latter cytokines is achieved through direct binding of BZLF1 to their promoters via a consensus AP-1 site (Hsu et al., 2008). *BZLF1* was induced 19-fold at 24 hrs in the model system. This suggests a potential role for EBV lytic gene products in enhancement of chemokine regulation in our array.

Both CXCL9 and CXCL10 are CXC chemokine ligands, produced by IFN-γ stimulated cells that signal through the G-protein coupled receptor CXCR3 on Th1 activated T cells and NK cells (Loetscher et al., 1996; Neville et al., 1997; Thapa et al., 2008). We found a 10-fold and 4-fold up- regulation of CXCL9 and CXCL10, respectively in our microarray analysis. While regulation of CXCL9 and CXCL10 by EBV lytic genes has not been demonstrated, direct correlations were found between EBV infection and increased up-regulation of CXCL9 and CXCL10 in EBV-positive HL tissue by RT-PCR (Teruya-Feldstein et al., 1999). Moreover, both CXCL9 and CXCL10 have anti-tumour properties and have been up-regulated in EBV-associated lymphoproliferative disorders *in vitro* (Setsuda et al., 1999; Sgadari et al., 1997; Teruya-Feldstein et al., 1997).

CCL3 and CCL5 both signal through the CCR1 and CCR5 receptors on monocytes and activated Th1 T cells, resulting in an inflammatory effect (Uchihara et al., 2005), presumably to control EBV infection. We found a 3.7- and 9.6-fold up-regulation of CCL3 and CCL5, respectively. Moreover, correlations between the presence of EBV and high levels of expression of CCL3 along with CXCL10 were demonstrated in Hodgkin's disease (Teruya-Feldstein et al., 1999; Teruya-Feldstein et al., 2000). A recent study employed the Affymetrix HG U133 Plus 2.0 GeneChipTM to investigate cellular gene expression in biopsy specimens from transplant recipients at high risk of PTLD (Allen et al., 2009). They showed up-

regulation of CCL5 and highlighted the importance of EBV modulation of Th1 and Th2 response on chemokine expression, suggesting a role for these proteins in PTLD development.

We also demonstrated a 4-fold up-regulation of CCL22 (Table 7.2), a CC chemokine that signals through the CCR4 receptor and activates Th2 CD4+ T cells and NK cells upon LMP-1 regulation (Nakayama et al., 2004). LMP-1 is known to regulate CCL3, CCL5 and CCL22 (Nakayama et al., 2004), whereas CCL3 and CCL5 are upregulated directly by EBNA-2 in EBV LCLs (Spender et al., 2006; Zhao et al., 2006). However, the role of the EBV lytic genes in the regulation of these chemokines is uncertain. Further, chemokines recruit either Th1 or Th2 responses based on the receptors they interact with. Hence, EBV infection is controlled by the CTL response, and the different inflammatory effects following differential chemokine regulation could be important in the immune response to infection, and in the development of PTLD (Allen et al., 2009).

These findings warrant further study on the contribution of chemokines to the development of PTLD, in particular the role of EBV lytic gene products in chemokine regulation during EBV reactivation.

In summary, we chose five genes (*CCL3*, *CCL5*, *CCL22*, *CXCL9* and *CXCL10*) that encode chemokines for further evaluation as markers of PTLD. Our rationale for selecting these genes was their known regulation by EBV and their implications in PTLD (Allen et al., 2009; Setsuda et al., 1999; Sgadari et al., 1997; Teruya-Feldstein et al., 1997).

**Overall summary of selected genes**

One of the main goals of this thesis was to identify potential markers for the early detection of PTLD. For this purpose, we analysed cellular gene expression in response to lytic

induction by microarray analysis, from which 191 highly regulated probe sets were identified (Table 7.2), representing 112 unique cellular genes. The 17 candidate genes can be further assigned to the following selection criteria: i) EBV infection and EBV-PTLD biopsy tissue (*RASA1*, *RGS13*, *ANP32E*, *MAD2L1*, *TIMP1*, *CDC2*, *CD52*, *LRMP*, *HDGF1*, *ISG15* and *PCNA*); and ii) highly regulated cellular genes (*CHI3L1*), and (iii) other biological functions, including chemotaxis in GeneOntology (*CCL3*, *CCL5*, *CCL22*, *CXCL9* and *CXCL10*). In addition, the majority of these genes had extracellular locations, increasing their likelihood of detection in whole blood.

Once chosen, we established that our genes were truly modulated, via real-time PCR validation and fold-changes derived from these analyses were compared to those derived from the microarray analysis. Our results showed increased sensitivity of real-time PCR over microarray analysis based on fold-change, and therefore, a suitable system to perform subsequent gene expression analyses. Further, we showed that the regulation pattern of all 17 genes was the same between real-time PCR and microarray analysis, confirming the validity of the microarray analysis.

# 5 CHAPTER 5. VALIDATION OF EBV AND CELLULAR GENE EXPRESSION IN WHOLE BLOOD FROM PAEDIATRIC AND ADULT TRANSPLANT RECIPIENTS

## 5.1 INTRODUCTION

In the previous chapters we employed real-time PCR and the Affymetrix Human Genome U133 Plus 2.0 GeneChip® to identify highly regulated EBV and cellular candidate genes during the EBV lytic induction phase, as potential markers for the early detection of PTLD. Altogether, 14 EBV and 17 cellular candidate genes were chosen for further analysis (Table 5.1). Preliminary investigations were undertaken to assess their potential as specific, non-invasive markers of early PTLD by screening RNA extracted from whole blood samples. However, three of the 17 EBV genes (*BMRF1, BPLF1* and *BVRF1*) were only identified as overlapping late lytic genes genes following preliminary screening. Therefore, any results for these genes have been excluded from the thesis, and data is presented for 14 EBV genes only. Early diagnosis and the prompt initiation of treatment is crucial for the prevention of PTLD, to improve patient survival, and prevent graft loss (Gulley and Tang, 2008). While elevated EBV DNA loads have proven useful as predictive markers for PTLD, they lack specificity, and there is some disagreement over the significance of elevated viral loads and the development of disorder (Scheenstra et al., 2004). Therefore, a better understanding of the correlation between EBV DNA load and the onset of PTLD was required in order to develop more specific assays for the early identification of patients at risk of PTLD (Gartner and Preiksaitis, 2010). Latency III patterns of EBV gene expression have been detected in PTLD positive biopsy tissue (Brink et al., 1997). Therefore, one of the aims of our study was to identify EBV latent gene expression profiles in PTLD and non-PTLD patients and identify potential markers for the early diagnosis of PTLD. Further, we wanted to investigate the role of the EBV lytic genes, since their role in PTLD was unclear (Rowe et al., 1998). EBV lytic gene expression has been demonstrated alongside latency III in PTLD biopsies and following lytic activation in LCLs, and latency III can enhance EBV replication (Yuan et al., 2006).

Therefore, one of the aims of our study was to monitor EBV lytic gene expression profiles in PTLD and non-PTLD patients and identify potential markers of PTLD (Yuan et al., 2006). Another aim was to analyse cellular gene expression profiles in PTLD and non PTLD patients, since EBV gene products are known to regulate cellular genes (Spender et al., 2001; Spender et al., 2006; Yuan et al., 2006). It was anticipated that any highly differentially expressed cellular genes could provide potential markers of PTLD as well as providing insight into the potential microenvironment in which PTLD could arise. A further aim was to examine EBV gene expression profiles in patients with variable EBV DNA loads to determine whether there was any association between EBV replication and viral load (Chang et al., 2006; Hahn et al., 2005; Morrison and Kenney, 2004; Morrison et al., 2004). It was also anticipated that any associations would facilitate further the identification of effective markers for the early detection of PTLD.

### 5.1.1 Objectives of Chapter 5

The primary objective of this study was to identify potential cellular and EBV gene markers for specific and early detection of PTLD. As part of this investigation, we developed and validated real-time two-step RT-PCR assays to evaluate EBV and cellular gene expression profiles in whole blood from paediatric solid organ transplant (SOT) and adult umbilical cord blood transplant (UCBT) recipients, with and without PTLD.

The specific aims of this chapter were to determine:

(i) To determine the EBV gene expression profiles in whole blood from PTLD and non-PTLD transplant patients, and determine whether these coincide with the latency III gene expression profile previously observed in PTLD biopsy tissue

(ii) To identify any differentially expressed cellular genes between PTLD and non PTLD patients

(iii) To determine if there was any association between EBV DNA load and specific EBV and cellular gene expression profiles or expression of individual genes

(iv) To establish whether the real-time PCR assays were sensitive and specific for EBV and cellular gene expression analysis in whole blood samples from PTLD and non-PTLD transplant patients

**Table 5-1 EBV and cellular genes for clinical validation in whole blood**

| EBV genes | Cellular genes |
|---|---|
| *EBNA-1* | *ANP32E* |
| *EBNA-2* | *CDC2* |
| *EBNA-3A* | *CD52* |
| *EBNA-3B* | *CHI3L1* |
| *EBNA-3C* | *CCL3* |
| *EBNA-LP* | *CCL5* |
| *LMP-1* | *CCL22* |
| *LMP-2* | *CXCL9* |
| *BALF5* | *CXCL10* |
| *BDLF4* | *HDGF1* |
| *BGLF4* | *ISG15* |
| *BRRF1* | *LRMP* |
| *BXLF1* | *MAD2L1* |
| *BZLF1* | *PCNA* |
| | *RASA1* |
| | *RGS13* |
| | *TIMP1* |

## 5.2 RESULTS

### 5.2.1 Determining EBV gene expression profiling by real-time PCR

To determine the expression of several EBV genes (*BALF5*, *BDLF3*, *BDLF4*, *BMRF1*, *EBNA-1* and *LMP-1*) and ensure that we had sufficient cDNA to complete the full testing of 17 candidate EBV genes, real-time TaqMan PCR was performed on cDNA (1/2 dilution) derived from 200 ng total RNA input from ten adult bone marrow transplant (BMT) controls (Ctrls). These samples carried varying EBV DNA loads ranging from 664 to 31,834 copies/ml (Table 5.2). In two controls with <10 copies/ml, no EBV genes were detected. For unknown reasons, in two controls (Ctrls. 6 and 8), with detectable viral loads of 16,028 and 5,709 copies/ml, respectively, no EBV gene expression was observed for the genes tested. In all other controls, at minimum, the expression of the viral DNA polymerase *BALF5* was detectable, with increasing amounts detected with increasing viral loads. Real-time PCR was performed on minus RT-controls from each patient and confirmed the absence of EBV gDNA in all EBV candidate genes tested.

**Table 5-2 Determining the expression of EBV gene targets in whole blood samples from ten adult controls by real-time PCR**

| Controls | EBV DNA load (Copies/ml) | *LMP-1* ($C_t$) | *EBNA-1* ($C_t$) | *BALF5* ($C_t$) | *BDLF3* (Ct) | *BDLF4* ($C_t$) | *BMRF1* ($C_t$) |
|---|---|---|---|---|---|---|---|
| Ctrl. 4 | <10 | | | | | | |
| Ctrl. 5 | <10 | | | | | | |
| Ctrl. 9 | 664 | | | 41.99 $^{(+/-)}$ | | | |
| Ctrl. 10 | 3,447 | | | 39.86 $^{(+/-)}$ | | | |
| Ctrl. 8 | 5,709 | | | | | | |
| Ctrl. 2 | 9,607 | 38.74 | 38.59 $^{(+/-)}$ | 38.8 | 37.14 $^{(+/-)}$ | | |
| Ctrl. 6 | 16,028 | | | | | | |
| Ctrl. 3 | 16,324 | 43.03 $^{(+/-)}$ | | 38.13 $^{(+/-)}$ | | | |
| Ctrl. 1 | 19,518 | 39.47 | | 37.65 | | 40.07 $^{(+/-)}$ | 38.85 |
| Ctrl. 7 | 31,834 | | | 36.00 | | | |

Ctrl, control; $^{+/-}$, Borderline detection Blank, not detectable; $C_t$, Threshold cycle; *LMP-1*, Latent membrane protein 1; *EBNA-1*, EBV nuclear antigen 1; *BALF5*, DNA polymerase; *BDLF3*, Structural capsid; *BDLF4*, Structural capsid; *BMRF1*, DNA polymerase processivity factor.

### 5.2.2 Determining the expression of *BALF5, CXCL9* and *VIM* by real-time PCR

Prior to using the full set of samples, preliminary tests were undertaken to identify the optimal cDNA quantity (maximising the number of genes that could be assessed) for the real-time PCR assays. In these preliminary tests, expression of the *BALF5* EBV gene, and two cellular genes (*CXCL9* and *VIM)*, was evaluated at 1/2, 1/3 and 1/5 dilutions of cDNA derived from 300 ng total RNA in four controls (Ctrls. 1, 2, 5 and 10). These results were analysed in combination with the previously described dilutions, for which a 1/2 dilution of cDNA derived from 200 ng total RNA gave high Ct values (section 5.2.1, Table 5.2).

Table 5.3 presents the EBV DNA loads for each target tested in triplicate for each control. Relative expression levels were derived by normalisation against the *ACTB* reference control. EBV DNA loads for the four test samples are presented in Table 5.3. Control no. 5 served as the EBV-negative control with an EBV DNA load <10 copies/ml. No expression of *BALF5* was detectable in this sample. In all other samples, *BALF5* was detected at all dilutions, with the exception of the 1/5 dilution for the control with the lowest viral load (Ctrl. 10; 3,447 copies/ml). Both cellular genes, *VIM* and *CXCL9*, were detectable at all dilutions in all

controls. *VIM* was consistently detectable at the same Ct for the two controls with the highest viral load (Ctrls. 1 and 2) and, at a slightly lower Ct value for the two controls with lower viral loads, including control no. 5, with <10 copies/ml. The detection of *VIM* was decreased by 1 log from dilutions of 1/2 to 1/5. Overall, 1/2 dilutions of cDNA provided the most reproducible data (Table 5.3). However, the 1/3 dilutions were also highly reproducible, maintained the required sensitivity, and enabled sufficient cDNA to investigate gene expression profiles for all 14 EBV and 17 cellular candidate genes. Therefore, a 1/3 dilution was chosen for further investigation. However, owing to the lack of ready access to a flow cytometer at the time of isolation of the non-RBC fraction, the fraction of tumour B cells was not assessed. Future work should incorporate this analysis into the study.

**Table 5-3 Determining the expression of *BALF5, CXCL9* and *VIM* over a range of dilutions by real-time PCR**

| Controls | EBV DNA load (copies/ml) | *BALF5* ($C_t$) | *CXCL9* ($C_t$) | *VIM* ($C_t$) | *ACTB* ($C_t$) |
|---|---|---|---|---|---|
| **cDNA (1/2 dilution)** | | | | | |
| no. 1 | 19,518 | 33.8 | 34.6 | 16.0 | 17.0 |
| no. 2 | 9,607 | 34.8 | 33.9 | 16.0 | 17.0 |
| no. 5 | <10 | | 29.5 | 17.0 | 17.0 |
| no. 10 | 3,447 | 36.1 | 27.2 | 16.0 | 17.0 |
| **cDNA (1/3 dilution)** | | | | | |
| no. 1 | 19,518 | 34.3 | 34.4 | 17.0 | 18.7 |
| no. 2 | 9,607 | 34.3 | 34.3 | 16.9 | 18.3 |
| no. 5 | <10 | | 29.5 | 18.0 | 19.0 |
| no. 10 | 3,447 | 36.4 | 27.4 | 17.4 | 18.5 |
| **cDNA (1/5 dilution)** | | | | | |
| no. 1 | 19,518 | 37.0 | 36.0 | 18.0 | 19.0 |
| no. 2 | 9,607 | 37.0 | 36.0 | 18.0 | 19.0 |
| no. 5 | <10 | | 30.0 | 19.0 | 19.0 |
| no. 10 | 3,447 | | 28.0 | 19.0 | 19.0 |

Blank, not detectable; $C_t$, Threshold cycle; *BALF5*, DNA polymerase; *CXCL9*, CXC chemokine 9; *VIM*, Vimentin; *ACTB*, Beta actin; *GAPDH*, Glyceraldehyde 3-dehydrogenase

### 5.2.3 Analysis of EBV gene expression in adult and paediatric transplant patients

Although EBV latent genes and the latency III pattern are frequently expressed in PTLD, the role of the lytic genes in the development of PTLD was unclear. Therefore, relative expression levels of 8 latent and 6 lytic genes were examined in 33 whole blood samples from 21 paediatric SOT patients (5 PTLD, 16 non-PTLD), and 12 samples from 2 adult UCBT recipients (1 PTLD, 1 non-PTLD) (Figure 2.3). To examine EBV gene expression in whole blood samples, EBV gene expression levels were measured relative to the reference control *ACTB* using real-time PCR assays. Gene expression was recorded as detectable (+), borderline detectable (+/-) or not detectable (blank). Samples were deemed borderline positive, if one or two of the three replicates were positive. The integrity of the cDNA was confirmed by consistent Ct values (Ct~16) for *ACTB.* Results of the EBV gene expression profiling for paediatric and adult transplant recipients are presented in Tables 5.4, 5.5, 5.6 5.7, and Tables 5.8 and 5.9, respectively.

#### 5.2.3.1 EBV gene expression analysis in paediatric transplant patients

Eight latent genes (*EBNA-1, EBNA-2, EBNA-3A, EBNA-3B, EBNA-3C, EBNA-LP, LMP-1* and *LMP-2A*) and six lytic genes (*BALF5, BDLF4, BGLF4, BRRF1, BXLF1,* and *BZLF1*) were assessed in whole blood from the paediatric transplant recipients. The relative expression levels of each EBV gene detected in samples from the paediatric PTLD and non-PTLD patients are represented in Figures 5.1 and 5.2, respectively.

Lytic gene expression was detected in 25/33 (76%) samples from 21 paediatric SOT patients, including 9/15 (60%) samples from 5 PTLD patients and 16/18 (89%) samples from 16 non-PTLD patients (Tables 5.4 and 5.5). As expected, no EBV latent or lytic gene expression was detected in the single EBV-seronegative patient with no EBV viraemia (no. 21; Table 5.5).

Notably, expression of *BALF5* was detected in 25/33 (76%) samples from paediatric patients, including 2 PTLD patients (no. 4, sample C and no. 5, samples C-D) with viral loads <10 copies/ml (Table 5.4).

In the PTLD group, lytic gene expression was detected in 9/15 (60%) samples from 5 PTLD patients, all of which were positive for *BALF5* (Table 5.4). *BDLF4* was expressed in 3/15 (20%) samples, *BGLF4* in 3/15 (20%) samples, *BRRF1* in 3/15 (20%) samples, *BXLF1* in 3/15 (20%) samples, and *BZLF1* in 4/15 (26.7%) samples. Therefore, *BZLF1* were the most frequently detected genes after *BALF5*. *BALF5* had the highest level of expression across samples (Figure 5.1). The mean relative expression level ±SD was 0.002984 (±0.005305) for *BALF5*.

In the non-PTLD group, aside from *BALF5*, lytic gene expression (*BRRF1*) was detected in 1/16 (6.25%) with elevated viral loads (Table 5.5). *BALF5* was detected in 16/18 (89%) samples from 16 patients, whereas 1/16 (6.25%) expressed *BRRF1* (Table 5.4). *BALF5* had the highest level of expression (Figure 5.2). The mean relative expression level ±SD was 0.0007910 (±0.0008665) for *BALF5*.

In the PTLD group, latent gene expression (*EBNA-1, EBNA-2, EBNA-3A, EBNA-3B, EBNA-3C, EBNA-LP, LMP-1* and *LMP-2A*) was detected in 7/15 (46.67%) samples (Table 5.6). Five of 15 samples (33%) expressed *EBNA-1*, 1/15 (6.6%) expressed *EBNA-2*, 1/15 (6.6%) expressed *EBNA-3A*, 1/15 (6.6%) expressed *-3B* and 1/15 (6.6%) expressed *3-C*, 5/15 (33%) expressed *EBNA-LP*, 4/15 (26.7%) expressed *LMP-1* and 4/15 (26.7%) *LMP-2* (Table 5.6). All latent genes were detected in one patient (no. 3). *EBNA-LP* had the highest level of expression across samples (Figure 5.1). The mean relative expression level ±SD for *EBNA-LP* was 0.0007825 (±0.001208).

In the non-PTLD group, latent gene expression (*EBNA-1*, *EBNA-2*, *EBNA-3A*, *EBNA-3B*, *EBNA-3C*, *EBNA-LP* and *LMP-1*) was detected in 8/16 (50%) samples from 18 patients (Table 5.7). Three of 16 (18.75%) patients expressed *EBNA-1*, 2/16 (12.5%) expressed *EBNA-2*, 1/16 (6.25%) expressed *EBNA-3A*, 1/16 (6.25%) expressed *EBNA-3B*, 2/16 (12.5%) expressed *EBNA-3C*, 1/16 (12.5%) expressed *EBNA-LP*, and 5/16 (31%) expressed *LMP-1*. Therefore, *LMP-1* was the most frequently detected latent gene. *EBNA-LP* had the highest level of expression across samples (Figure 5.2). The mean relative expression level for *EBNA-LP* was 0.00002565 (±0.0001026).

**Table 5-4 Summary of EBV lytic transcripts in paediatric PTLD patients as determined by real-time PCR (ranked by viral loads)**

| Patient no. (Sample) | Time from transplant (Days) | EBV load | EBV Serology | *BALF5* | *BDLF4* | *BGLF4* | *BRRF1* | *BXLF1* | *BZLF1* |
|---|---|---|---|---|---|---|---|---|---|
| no. 1 (sample A) | 73 | 197,629 | VCA IgG- | + | + | + | + | +/- | + |
| no. 1 (sample B) | 50 | 43,119 | VCA IgG- | + | + | + | + | + | + |
| no. 1 (sample C) | 143 | <10 | VCA IgG- | | | | | | |
| no. 1 (sample D) | 171 | <10 | VCA IgG- | | | | | | |
| no. 2 (sample A) | 157 | 9,792 | VCA IgG- | + | | | | | |
| no. 2 (sample B) | 131 | 452 | VCA IgG- | | | | | | |
| no. 2 (sample C) | 154 | 99 | VCA IgG- | | | | | | |
| no. 3 | 47 | 7,609 | VCA IgG- | + | + | + | + | + | + |
| no.4 (sample A) | 26 | 1,530 | VCA IgG Indet | + | | | | | + |
| no. 4 (sample B) | 89 | 1,033 | VCA IgG Indet | +/- | | | | | |
| no. 4 (sample C) | 68 | <10 | VCA IgG Indet | + | | | | | |
| no. 5 (sample A) | 124 | <10 | VCA IgG+ | | | | | | |
| no. 5 (sample B) | 107 | <10 | VCA IgG+ | | | | | | |
| no. 5 (sample C) | 128 | <10 | VCA IgG+ | +/- | | | | | |
| no. 5 (sample D) | 142 | <10 | VCA IgG+ | +/- | | | | | |

+, Positive; +/-, Borderline detectable; Blank, Not detectable; no, number; NK, not known; VCA IgG, Viral capsid Immunoglobulin; PTLD; post-transplant lymphoproliferative disorder; *BALF5*, DNA polymerase; *BDLF4*, Structural; *BGLF4*, Protein kinase; *BRRF1*, lytic cycle enhancer; *BXLF1*, Thymidine kinase; *BZLF1*, lytic cycle transactivator; ǂ, primary EBV infection

**Table 5-5 Summary of EBV lytic transcripts in paediatric non-PTLD patients as determined by real-time PCR (ranked by viral loads)**

| Patient no. (Sample) | Time from transplant (Days) | EBV load | EBV Serology | *BALF5* | *BDLF4* | *BGLF4* | *BRRF1* | *BXLF1* | *BZLF1* |
|---|---|---|---|---|---|---|---|---|---|
| no. 6 | NK | 68,278 | VCA IgG- | + | | | | | |
| no. 7 | NK | 52,351 | VCA IgG Indet | + | | | | | |
| no. 8 (sample A) | 33 | 41,512 | VCA IgG- | + | | | | | |
| no. 9 | NK | 40,377 | VCA IgG+ | + | | | | | |
| no. 10 | NK | 28,979 | VCA IgM+ | + | | | +/- | | |
| no. 11 | NK | 17,830 | VCA IgG- | + | | | | | |
| no. 12 | 85 | 15,343 | VCA IgG+ | + | | | | | |
| no. 13 | NK | 10,740 | VCA IgG+ | + | | | | | |
| no. 14 (sample A) | 602 | 10,392 | VCA IgG Indet | + | | | | | |
| no. 15 | NK | 7,587 | EBNA IgG+ | + | | | | | |
| no. 14 (sample B) | 618 | 7,219 | VCA IgG Indet | + | | | | | |
| no. 16 | NK | 4,709 | VCA IgG+ | +/- | | | | | |
| no. 8 (sample B) | 17 | 4,461 | VCA IgG- | + | | | | | |
| no. 17 | NK | 182 | VCA IgG+ | +/- | | | | | |
| no. 18 | NK | 158 | VCA IgG Indet | + | | | | | |
| no. 19 | NK | 48 | EBNA IgG- | +/- | | | | | |
| no. 20 | NK | 48 | VCA IgG- | | | | | | |
| no. 21* | 16 | <10 | VCA IgG- | | | | | | |

+, Positive; +/-, Borderline detectable; Blank, Not detectable; no, number; NK, not known; VCA IgG, Viral capsid Immunoglobulin; PTLD; post-transplant lymphoproliferative disorder; *BALF5*, DNA polymerase; *BDLF4*, Structural; *BGLF4*, Protein kinase; *BRRF1*, lytic cycle enhancer; *BXLF1*, Thymidine kinase; *BZLF1*, lytic cycle transactivator; ǂ, primary EBV infection; *Primary EBV infection with no EBV viraemia

**Table 5-6 Summary of EBV latent transcripts in paediatric PTLD patients as determined by real-time PCR (ranked by viral loads)**

| Patient no. (Sample) | Time from transplant (Days) | EBV load | EBV Serology | *EBNA-1* | *EBNA-2* | *EBNA-3A* | *EBNA-3B* | *EBNA-3C* | *EBNA-LP* | *LMP-1* | *LMP-2* |
|---|---|---|---|---|---|---|---|---|---|---|---|
| no. 1 (sample A) | 73 | 197,629 | VCA IgG- | | | | | | + | + | +/- |
| no. 1 (sample B) | 50 | 43,119 | VCA IgG- | + | | | | | + | +/- | + |
| no. 1 (sample C) | 143 | <10 | VCA IgG- | | | | | | | | |
| no. 1 (sample D) | 171 | <10 | VCA IgG- | | | | | | | | |
| no. 2 (sample A) | 157 | 9,792 | VCA IgG- | | | | | | | | |
| no. 2 (sample B) | 131 | 452 | VCA IgG- | | | | | | | | |
| no. 2 (sample C) | 154 | 99 | VCA IgG- | | | | | | | | |
| no. 3 | 47 | 7,609 | VCA IgG- | + | + | + | + | + | + | + | + |
| no.4 (sample A) | 26 | 1,530 | VCA IgG Indet | +/- | | | | | + | + | +/- |
| no. 4 (sample B) | 89 | 1,033 | VCA IgG Indet | | | | | | + | | |
| no. 4 (sample C) | 68 | <10 | VCA IgG Indet | +/- | | | | | | | |
| no. 5 (sample A) | 124 | <10 | VCA IgG+ | +/- | | | | | | | |
| no. 5 (sample B) | 107 | <10 | VCA IgG+ | | | | | | | | |
| no. 5 (sample C) | 128 | <10 | VCA IgG+ | | | | | | | | |
| no. 5 (smple D) | 142 | <10 | VCA IgG+ | | | | | | | | |

+, Positive; +/-, Borderline detectable; Blank, Not detectable; no, number; NK, not known; VCA IgG, Viral capsid Immunoglobulin; PTLD; post-transplant lymphoproliferative disorder; *EBNA*, EBV nuclear antigen; *LMP*, Latent membrane protein; ∓, primary EBV infection

**Table 5-7 Summary of EBV latent transcripts in paediatric non-PTLD patients as determined by real-time PCR (ranked by viral loads)**

| Patient no. (Sample) | Time from transplant (Days) | EBV load | EBV Serology | *EBNA-1* | *EBNA-2* | *EBNA-3A* | *EBNA-3B* | *EBNA-3C* | *EBNA-LP* | *LMP-1* | *LMP-2* |
|---|---|---|---|---|---|---|---|---|---|---|---|
| no. 6 | NK | 68,278 | VCA IgG- | | | | | | | +/- | |
| no. 7 | NK | 52,351 | VCA IgG Indet | + | + | | | +/- | | | |
| no. 8 (sample A) | 33 | 41,512 | VCA IgG- | | + | +/- | +/- | | | + | |
| no. 9 | NK | 40,377 | VCA IgG+ | | | | | | | +/- | |
| no. 10 | NK | 28,979 | VCA IgM+ | | | | | | | +/- | |
| no. 11 | NK | 17,830 | VCA IgG- | | | | | | | | |
| no. 12 | 85 | 15,343 | VCA IgG+ | +/- | | | | | | +/- | |
| no. 13 | NK | 10,740 | VCA IgG+ | +/- | | | | | | | |
| no. 14 (sample A) | 602 | 10,392 | VCA IgG Indet | | | | | | | | |
| no. 15 | NK | 7,587 | EBNA IgG+ | | | | | | | | |
| no. 14 (sample B) | 618 | 7,219 | VCA IgG Indet | | | | | | | | |
| no. 16 | NK | 4,709 | VCA IgG+ | | | | | | | | |
| no. 8 (sample B) | 17 | 4,461 | VCA IgG- | | | | | | | | |
| no. 17 | NK | 182 | VCA IgG+ | | | | | | | | |
| no. 18 | NK | 158 | VCA IgG Indet | | | | | +/- | + | | |
| no. 19 | NK | 48 | EBNA IgG- | | | | | | | | |
| no. 20 | NK | 48 | VCA IgG- | | | | | | | | |
| no. 21* | 16 | <10 | VCA IgG- | | | | | | | | |

+, Positive; +/-, Borderline detectable; Blank, Not detectable; no, number; NK, not known; VCA IgG, Viral capsid Immunoglobulin; PTLD; post-transplant lymphoproliferative disorder; *EBNA*, EBV nuclear antigen; *LMP*, Latent membrane protein

# el to *ACTB*

**Figure 5-1 Quantitative EBV gene expression patterns in paediatric PTLD transplant recipients**

Relative expression of EBV latent and lytic EBV genes in the whole blood of paediatric transplant patients with PTLD. The transcripts were analysed by real-time TaqMan PCR from total mRNA extracted from 7 whole blood samples of transplant patients with PTLD ($n$ = 5). Relative expression of the transcripts was normalised to the *ACTB* gene. Data represents the means ±SD of triplicates.

# el to *ACTB*

l to *ACTB*

**Figure 5-2 Quantitative EBV gene expression patterns in paediatric non-PTLD transplant recipients**

Relative expression of EBV latent and lytic EBV genes in whole blood samples of paediatric transplant patients without PTLD. The transcripts were analysed by real-time TaqMan PCR from total mRNA extracted from 16 whole blood samples of transplant patients without PTLD ($n$ = 8). Relative expression of the transcripts was normalised to the *ACTB* gene. Data represents the means ±SD of triplicates.

#### 5.2.3.2 Analysis of EBV gene expression in adult transplant patients

While the majority of EBV genes expressed in the paediatric group were lytic genes, particularly within PTLD diagnosed patients, the majority of EBV genes expressed in the adult group were latent genes and detectable in the single adult PTLD patient (no. 22, samples A-E) (Tables 5.8 and 5.9).

Table 5.8 summarises EBV lytic gene expression in 2 adult transplant recipients. *BALF5*, was detected in all samples from the single adult PTLD patient (no. 22, samples A-E), and 5/6 (83.33%) samples (no. 23, samples A-E) from the non-PTLD control (Table 5.8). Notably, all lytic genes were expressed in 1/6 (16.7%) samples (no. 22A), which also had the highest viral load (477,642 copies/ml). Lytic gene expression was sporadic in the remaining 5/6 (83.33%) samples; 8 transcripts were expressed in one sample, two transcripts in another, and three in a further sample. *BALF5* was the most highly expressed EBV gene detected in the PTLD versus non-PTLD patient (Figures 5.3 and 5.4, panels A). The mean relative expression levels ±SD for *BALF5* was 0.006298 (±0.01) and 0.0002945 (±0.0002) in samples from the PTLD and non-PTLD patient, respectively.

Table 5.9 summarises EBV latent gene expression in the 2 adult transplant recipients. No latent gene expression was detected in the non-PTLD patient (no. 23). In comparison, we detected latent gene expression in all samples from the PTLD patient (Table 5.9; no. 22, samples A-F). Further, all of the latent genes were detected in the sample (no. 22A) with the highest viral load (477,642 copies/ml). Notably, the most highly expressed latent gene detected was *EBNA-LP*, followed by *LMP-1* and *LMP-2* (Figure 5.3, panel B). The mean relative expression levels ±SD for *EBNA-LP, LMP1* and *LMP2* were 0.007024 (±0.01), 0.006298 (±0.01) and 0.005014 (±0.01), respectively.

**Table 5-8 Summary of EBV lytic transcripts in adult transplant recipients as determined by real-time PCR (ranked by viral loads)**

| Patient no. (Sample no.) | Time from transplant (Days) | EBV load | EBV serology | *BALF5* | *BDLF4* | *BGLF4* | *BRRF1* | *BXLF1* | *BZLF1* |
|---|---|---|---|---|---|---|---|---|---|
| *PTLD* | | | | | | | | | |
| no. 22 (sample A) | 126 | 477,642 | VCA IgG+ | + | + | + | + | + | + |
| no. 22 (sample B) | 139 | 14,170 | VCA IgG+ | + | | | + | | |
| no. 22 (sample C) | 111 | 10,209 | VCA IgG+ | + | | | +/- | | |
| no. 22 (sample D) | 92 | 7,589 | VCA IgG+ | + | | | | | |
| no. 22 (sample E) | 174 | 6,631 | VCA IgG+ | + | +/- | + | +/- | + /- | + |
| no. 22 (sample F) | 94 | 210 | VCA IgG+ | + | | | | | |
| *Non-PTLD* | | | | | | | | | |
| no. 23 (sample A) | 443 | 26,649 | VCA IgG+ | + | | | | | |
| no. 23 (sample B) | 601 | 1,535 | VCA IgG+ | + | | | | | |
| no. 23 (sample C) | 519 | 1,149 | VCA IgG+ | +/- | | | | | |
| no. 23 (sample D) | 517 | 1,208 | VCA IgG+ | + | | | | | |
| no. 23 (sample E) | 524 | 339 | VCA IgG+ | + | | | | | |
| no. 23 (sample F) | 545 | <10 | VCA IgG+ | | | | | | |

+, Positive; +/-, Borderline detectable; Blank, Not detectable; VCA IgG, Viral capsid Immunoglobulin; PTLD; post-transplant lymphoproliferative disorder; *BALF5*, DNA polymerase; *BDLF4*, Structural; *BGLF4*, Protein kinase; *BRRF1*, lytic cycle enhancer; *BXLF1*, Thymidine kinase; *BZLF1*, lytic cycle transactivator.

**Table 5-9 Summary of EBV latent transcripts in adult transplant recipients as determined by real-time PCR (ranked by viral loads)**

| Patient no. (Sample no.) | Time from transplant (Days) | EBV load | EBV serology | *EBNA-1* | *EBNA-2* | *EBNA-3A* | *EBNA-3B* | *EBNA-3C* | *EBNA-LP* | *LMP-1* | *LMP-2* |
|---|---|---|---|---|---|---|---|---|---|---|---|
| *PTLD* | | | | | | | | | | | |
| no. 22 (sample A) | 126 | 477,642 | VCA IgG+ | + | + | + | + | + | + | + | + |
| no. 22 (sample B) | 139 | 14,170 | VCA IgG+ | + | + | +/- | +/- | | + | + | + |
| no. 22 (sample C) | 111 | 10,209 | VCA IgG+ | +/- | +/- | +/- | | +/- | + | +/- | +/- |
| no. 22 (sample D) | 92 | 7,589 | VCA IgG+ | +/- | + | | +/- | | + | +/- | +/- |
| no. 22 (sample E) | 174 | 6,631 | VCA IgG+ | +/- | + | + | + | | + | + | + |
| no. 22 (sample F) | 94 | 210 | VCA IgG+ | +/- | +/- | | | | + | | +/- |
| *Non-PTLD* | | | | | | | | | | | |
| no. 23 (sample A) | 443 | 26,649 | VCA IgG+ | | | | | | | | |
| no. 23 (sample B) | 601 | 1,535 | VCA IgG+ | | | | | | | | |
| no. 23 (sample C) | 519 | 1,149 | VCA IgG+ | | | | | | | | |
| no. 23 (sample D) | 517 | 1,208 | VCA IgG+ | | | | | | | | |
| no. 23 (sample E) | 524 | 339 | VCA IgG+ | | | | | | | | |
| no. 23 (sample F) | 545 | <10 | VCA IgG+ | | | | | | | | |

+, Positive; +/-, Borderline detectable; Blank, Not detectable; VCA IgG, Viral capsid Immunoglobulin; PTLD; post-transplant lymphoproliferative disorder; *EBNA-1, -2, -3A, -3B, 3-C* and *–LP*, EBV nuclear antigens *-1, -2, -3A, 3B* and *-3C; LMP-1*, Latent membrane protein 1*; LMP2A/B*, Latent membrane protein 2

**(A)**

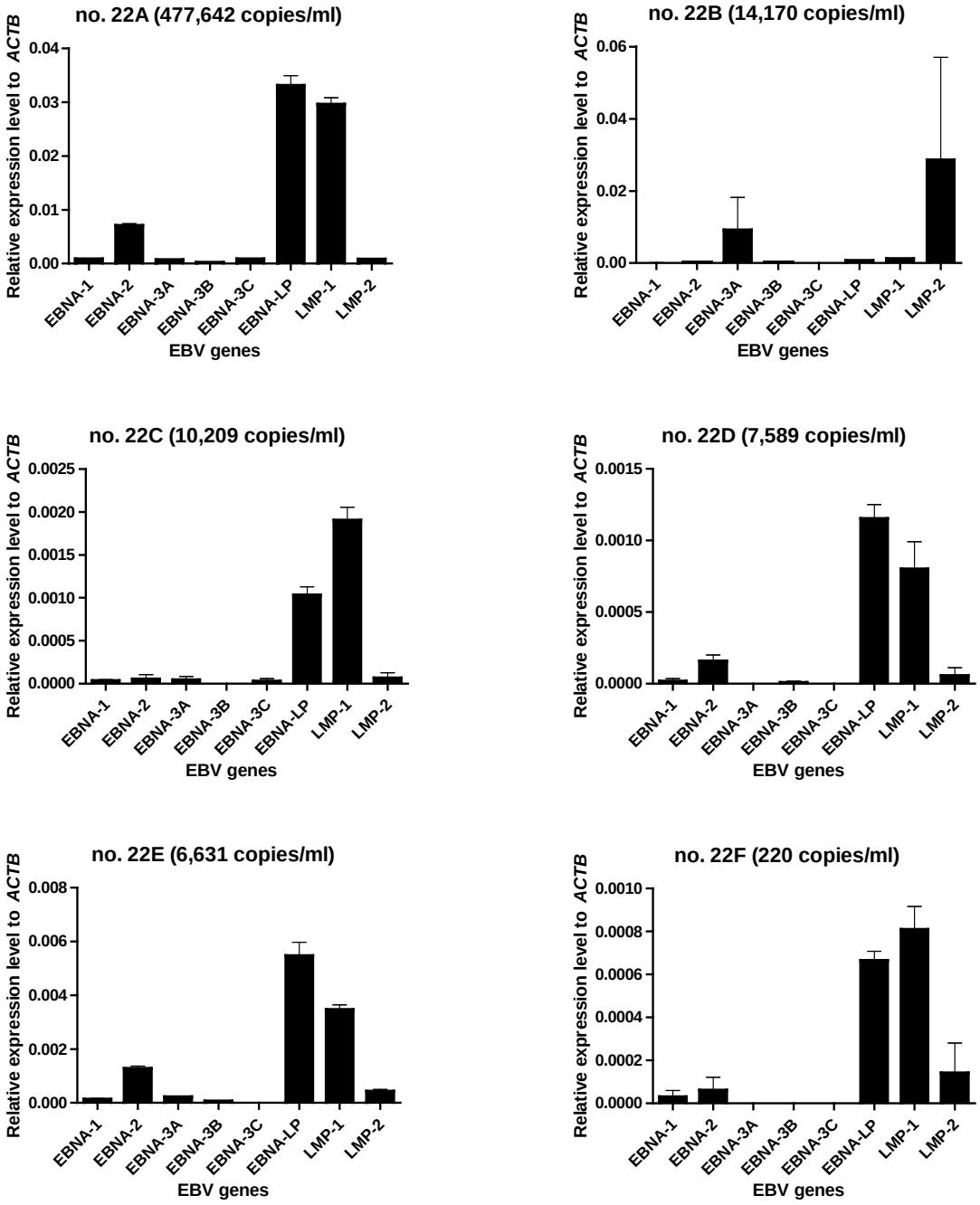


**(B)**

**Figure 5-3 Quantitative EBV gene expression patterns in adult PTLD and non-PTLD transplant recipients**

Relative expression levels of EBV latent and lytic EBV genes in whole blood from a single adult UCBT recipient with PTLD. Relative expression levels of EBV lytic (*BALF5*, *BDLF4*, *BGLF4*, *BRRF1*, *BXLF1* and *BZLF1*) (**A**) and latent (*EBNA-1*, *EBNA-2*, *EBNA-3A*, *EBNA-3B*, *EBNA-3C*, *EBNA-LP*, *LMP-1* and *LMP-2*) (**B**) transcripts were analysed by real-time TaqMan PCR. Relative expression of the transcripts was normalised to the *ACTB* gene. Data represents the means ±SD of triplicates.

**Figure 5-4 Quantitative EBV gene expression patterns in a single adult non-PTLD transplant recipient**

Relative expression of the EBV *BALF5* transcript in a single adult UCBT recipient without PTLD; Data represents the mean of triplicates ±SD. Relative expression of EBV lytic (*BALF5*, *BDLF4*, *BGLF4*, *BRRF1*, *BXLF1* and *BZLF1*) (**A**) transcripts were analysed by real-time TaqMan PCR; EBV latent gene expression was not observed in this patient. Relative expression of the transcripts was normalised to the *ACTB* gene. Data represents the means ±SD of triplicates.

### 5.2.4 Analysis of EBV latency patterns

In our earlier analysis of EBV gene expression within adult and paediatric transplant patients, we observed a larger number of latent and lytic genes expressed in PTLD positive versus non-PTLD patients (Tables 5.4-5.9).

The EBV latency patterns are detailed in Table 1.3. Latency III is defined by the expression of all latent EBV genes, in particular *EBNA-2* and *LMP-1* (Young et al., 1989). We next examined EBV latency patterns in the PTLD versus non-PTLD patients, since latency III was demonstrated in tumour cells in PTLD (Brink et al., 1997). Eight EBV latency genes were assessed (Tables 5.3-5.8).

Table 5.10 details latent EBV gene expression in the PTLD groups only, ranked by viral load. We detected gene expression patterns typical of latency III (*EBNA-2*$^{(+)}$, *LMP-1*$^{(+)}$) in 2/5 (40%) paediatric PTLD patients (no. 3 and no. 4, sample A), and all samples from the single adult PTLD patient (no. 22). In addition, we demonstrated latency III with discrepancy for *EBNA-2* in two samples from one paediatric PTLD patient (no. 1, samples A and B). When we examined the 15 paediatric non-PTLD patients, we detected latency III in 1/15 (6.7%) patient genes (no. 8 sample A) (Table 5.7). The remaining PTLD and non-PTLD patients exhibited variations in the patterns of EBV latent gene expression, not typical of latency III (*EBNA-2*$^{(-)}$, *LMP-1*$^{(-)}$) (Tables 5.6 and 5.7).

We next examined lytic gene expression in patients displaying latency III, since both have been demonstrated in tumour cells of PTLD (Rea et al., 1994a; Rea et al., 1994b). We detected latency III coupled with lytic gene expression in the two paediatric PTLD patients (no. 3 and no. 4, sample A) and the adult PTLD patient (no. 22), including the full spectrum of lytic gene expression in 2 patients (no. 3 and no. 22) (Table 5.11).

**Table 5-10 Summary of EBV latent transcripts in whole blood from five cases of paediatric and one case of adult PTLD as determined by real-time PCR (Ranked by EBV viral loads)**

| Patient no. (Sample no.) | Time from transplant (Days) | EBV viral load (copies/mL) | *EBNA-1* | *EBNA-2* | *EBNA-3A* | *EBNA-3B* | *EBNA-3C* | *EBNA-LP* | *LMP-1* | *LMP-2* |
|---|---|---|---|---|---|---|---|---|---|---|
| *Paediatric* | | | | | | | | | | |
| no. 1 (sample A) | 73 | 197,629 | + | | | | | + | + | + |
| no. 1 (sample B) | 50 | 43,119 | + | | | | | + | + | + |
| no. 2 (sample A) | 157 | 9,792 | | | | | | | | |
| no. 3 | 47 | 7,609 | + | + | + | + | + | + | + | + |
| no. 4 (sample A) | 26 | 1,530 | | +/- | | | | + | + | +/- |
| no. 4 (sample B) | 89 | 1,033 | | | | | | | | |
| no. 2 (sample B) | 131 | 452 | | | | | | | | |
| no. 2 (sample C) | 154 | 99 | | | | | | | | |
| no. 1 (sample C) | 143 | <10 | | | | | | | | |
| no. 1 (sample D) | 171 | <10 | | | | | | | | |
| no. 4 (sample C) | 68 | <10 | | + | | | | | | |
| no. 5 (sample A) | 124 | <10 | | | | | | | | |
| no. 5 (sample B) | 107 | <10 | | | | | | | | |
| no. 5 (sample C) | 128 | <10 | | | | | | | | |
| no. 5 (sample D) | 142 | <10 | | | | | | | | |
| *Adults* | | | | | | | | | | |
| no. 22 (sample A) | 126 | 477,642 | + | + | + | + | + | + | + | + |
| no. 22 (sample B) | 139 | 14,170 | + | + | +/- | +/- | | + | + | + |
| no. 22 (sample C) | 111 | 10,209 | +/- | +/- | +/- | | +/- | + | +/- | +/- |
| no. 22 (sample D) | 92 | 7,589 | +/- | + | | +/- | | + | +/- | +/- |
| no. 22 (sample E) | 174 | 6,631 | +/- | + | + | + | | + | + | + |
| no. 22 (sample F) | 94 | 210 | +/- | +/- | | | | + | | +/- |

+, positive; +/-, Borderline detectable; Blank, Not detectable; VCA IgG, Viral capsid Immunoglobulin; PTLD; post-transplant lymphoproliferative disorder; *EBNA-1, -2, -3A, -3B, 3-C and –LP*, EBV nuclear antigens *-1, -2, -3A, 3B and -3C; LMP-1*, Latent membrane protein 1*; LMP2A/B*, Latent membrane protein 2.

**Table 5-11 Summary of EBV lytic transcripts in whole blood from five cases of paediatric and one case of adult PTLD as determined by real-time PCR (Ranked by EBV viral loads)**

| Patient no. (Sample no.) | Time from transplant (Days) | EBV viral load (copies/ml) | *BALF5* | *BDLF4* | *BGLF4* | *BRRF1* | *BXLF1* | *BZLF1* |
|---|---|---|---|---|---|---|---|---|
| *Paediatric* | | | | | | | | |
| no. 1 (sample A) | 73 | 197,629 | + | + | + | + | +/- | + |
| no. 1 (sample B) | 50 | 43,119 | + | + | + | + | + | + |
| no. 2 (sample A) | 157 | 9,792 | + | | | | | |
| no. 3 | 47 | 7,609 | + | + | + | + | + | + |
| no. 4 (sample A) | 26 | 1,530 | + | | | | | + |
| no. 4 (sample B) | 89 | 1,033 | | | | | | |
| no. 2 (sample B) | 131 | 452 | +/- | | | | | |
| no. 2 (sample C) | 154 | 99 | | | | | | |
| no. 1 (sample C) | 143 | <10 | | | | | | |
| no. 1 (sample D) | 171 | <10 | | | | | | |
| no. 4 (sample C) | 68 | <10 | + | | | | | |
| no. 5 (sample A) | 124 | <10 | | | | | | |
| no. 5 (sample B) | 107 | <10 | | | | | | |
| no. 5 (sample C) | 128 | <10 | +/- | | | | | |
| no. 5 (sample D) | 142 | <10 | +/- | | | | | |
| *Adults* | | | | | | | | |
| no. 22 (sample A) | 126 | 477,642 | + | + | + | + | + | + |
| no. 22 (sample B) | 139 | 14,170 | + | | | | | |
| no. 22 (sample C) | 111 | 10,209 | + | | | + | | |
| no. 22 (sample D) | 92 | 7,589 | + | | | | | |
| no. 22 (sample E) | 174 | 6,631 | + | +/- | + | +/- | +/- | + |
| no. 22 (sample F) | 94 | 210 | + | | | | | |

+, positive; +/-, Borderline detectable; Blank, Not detectable; VCA IgG, Viral capsid Immunoglobulin; PTLD; post-transplant lymphoproliferative disorder; *BALF5*, DNA polymerase; *BDLF4*, Structural; *BGLF4*, Protein kinase; *BRRF1*, lytic cycle enhancer; *BXLF1*, Thymidine kinase; *BZLF1*, lytic cycle transactivator.

### 5.2.5 Analysis of EBV gene expression and viral load

Overall, the majority of EBV latent and lytic genes expressed were from PTLD positive patients, with more latent genes expressed in samples from the adult PTLD patient, and more lytic genes expressed in samples from the paediatric PTLD patients. As the viral loads varied across these patients, we next addressed whether there was any indication of an association between EBV gene expression levels and viral load amongst the PTLD and non-PTLD groups. We detected some association between EBV gene expression and viral loads in the PTLD groups (Tables 5.4, 5.6, 5.8, 5.9, 5.10 and 5.11). In the non-PTLD paediatric group, we detected EBV lytic and latent EBV gene expression in samples with high viral loads (Tables 5.5 and 5.7). Moreover, higher mean relative expression levels were demonstrated for two genes (*BALF5* and *EBNA-LP*) in samples with higher viral loads in both PTLD and non-PTLD groups (Figures 5.1, 5.2 and 5.3).

### 5.2.6 Analysis of cellular gene expression profiles in the peripheral blood

Seventeen cellular genes were assessed to examine gene expression profiles in the peripheral blood of all samples from paediatric PTLD and non-PTLD patients. The mean relative expression levels for all 17 genes, tested in each sample for all paediatric transplant patients are summarised in Figures 7.1. All 17 cellular genes were expressed. Scatter group column analysis was performed in the earliest and most closely matched samples from 5 paediatric PTLD and 5 non-PTLD patients to identify statistically differentially expressed cellular genes (Figure 5.5). Comparisons between the mean relative expression levels for each gene in each group were evaluated using the Mann Whitney *U*-test. Statistical significance was determined at the 5% threshold. Table 5.12 details the mean relative expression levels with standard deviation (SD) for all 17 genes. None of the 17 cellular genes showed statistically significant differences ($P <$ ns; data not shown).

In addition, the ratio of the mean relative expression levels were compared for each gene in each group (Table 5.12). A 2-fold difference was considered significant. With the exception of *CHI3L1*, that was differentially expressed by approximately 3-fold between the PTLD and non-PTLD controls, no differences (≥2-fold) were found for any of the remaining 16 cellular genes. None of the differences were statistically significant ($P <$ ns; data not shown).

**Table 5-12 Mean relative expression levels of cellular gene transcripts in paediatric solid organ transplant patients as determined by real-time TaqMan PCR**

| Cellular gene | Mean relative expression level in non-PTLD subjects (±SD) | Mean relative expression level in PTLD subjects (±SD) | Comparison of expression values between PTLD and non-PTLD patients |
|---|---|---|---|
| *ANP32E* | 0.2051 (±0.44) | 0.01783 (±0.02) | 0.09 |
| *CDC2* | 0.0007935 (±0.0004) | 0.0007671 (±0.0006) | 0.96 |
| *CD52* | 0.4268 (±0.58) | 0.2261 (±0.21) | 0.53 |
| ***CHI3L1*** | 0.03085 (±0.04) | 0.08823 (±0.11) | 2.86 |
| *CCL3* | 0.01712 (±0.02) | 0.009373 (±0.006) | 0.55 |
| *CCL5* | 0.2516 (±0.29) | 0.1385 (±0.13) | 0.55 |
| *CCL22* | 0.0002115 (±0.0002) | 0.0001500 (±8.951e-005) | 0.71 |
| *CXCL9* | 0.002246 (±0.002) | 0.0007526 (±0.0002) | 0.33 |
| *CXCL10* | 0.009595 (±0.02) | 0.006038 (±0.008) | 0.63 |
| *HDGF1* | 0.05835 (±0.06) | 0.04582 (±0.05) | 0.79 |
| *ISG15* | 0.09131 (±0.09) | 0.1122 (±0.10) | 1.23 |
| *LRMP* | 0.03302 (±0.05) | 0.04378 (±0.07) | 1.33 |
| *MAD2L1* | 0.02403 (±0.02) | 0.01958 (±0.02) | 0.81 |
| *PCNA* | 0.001314 (±0.0008) | 0.001383 (±0.001) | 1.05 |
| *RASA1* | 0.006034 (±0.007) | 0.008621 (±0.01) | 1.43 |
| *RGS13* | 0.0004639 (±0.0004) | 0.0002916 (±0.0003) | 0.63 |
| *TIMP1* | 0.1092 (±0.1) | 0.1277 (±0.15) | 1.17 |

Mean relative expression levels (±SD, standard deviation) were calculated for each gene. Fold-differenecs (*P*-value) were calculated for the PTLD group ($n = 15$) compared to the non-PTLD group ($n = 16$) from the 2-delta delta Ct formula. Cellular gene in bold were differentially regulated by 2-fold.

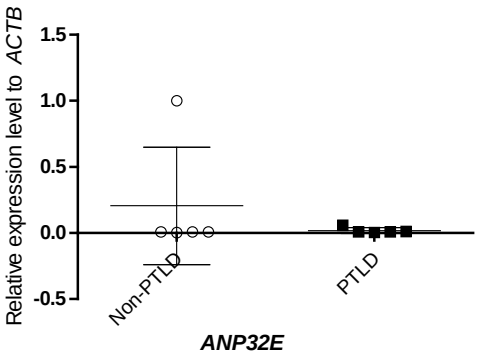


***ANP32E***

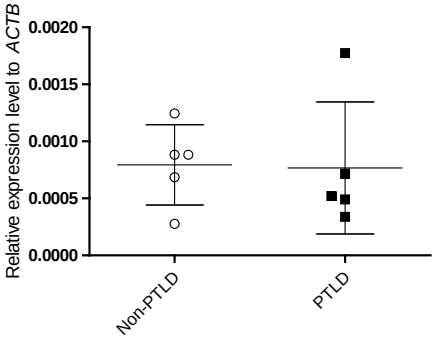


***CDC2***

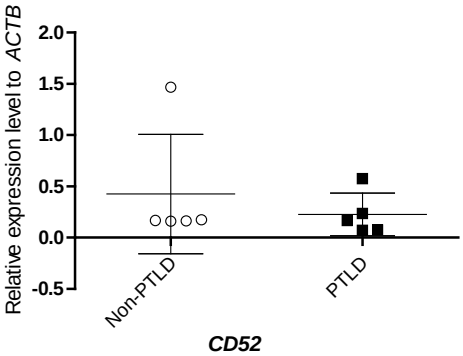


***CD52***

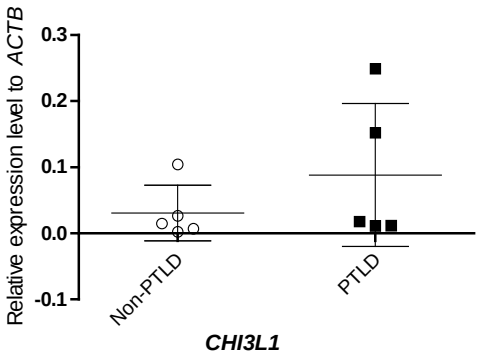


***CHI3L1***

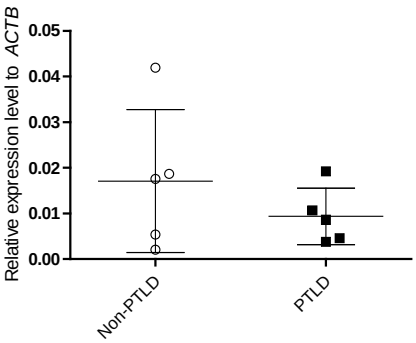


***CCL3***

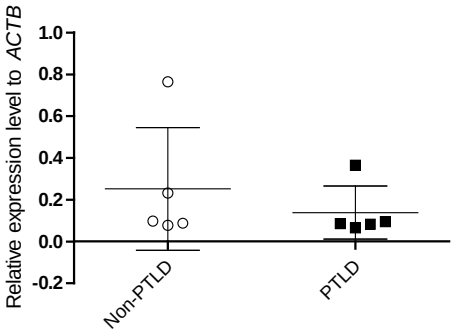


***CCL5***

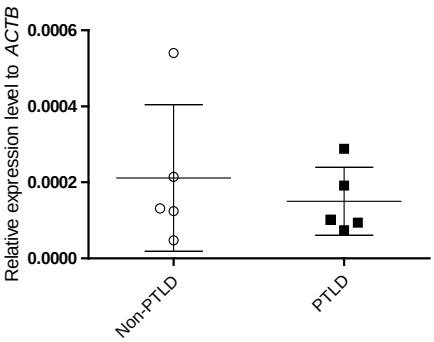


***CCL22***

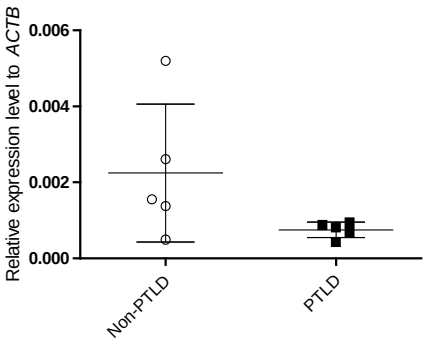


***CXCL9***

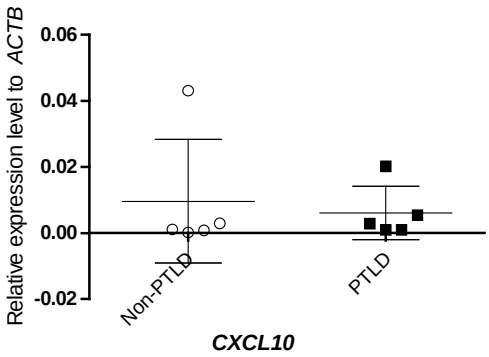


***CXCL10***

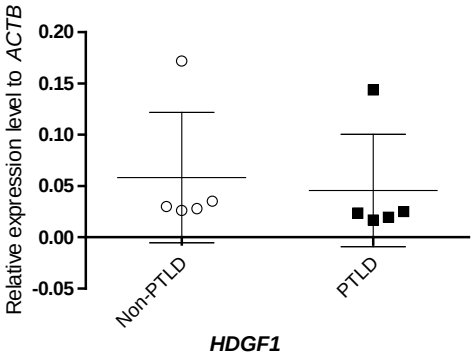


***HDGF1***

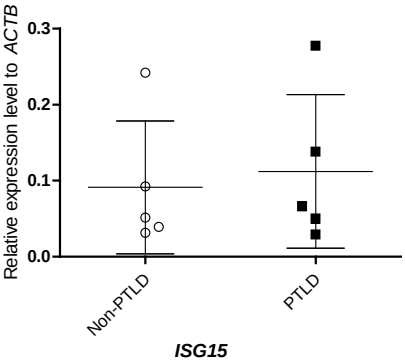


***ISG15***

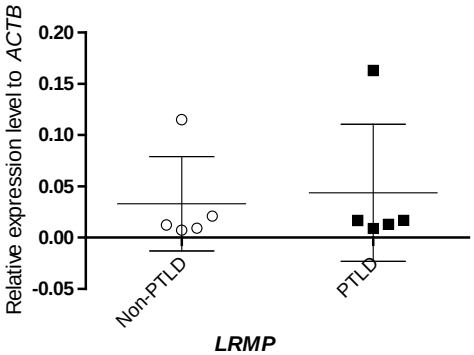


***LRMP***

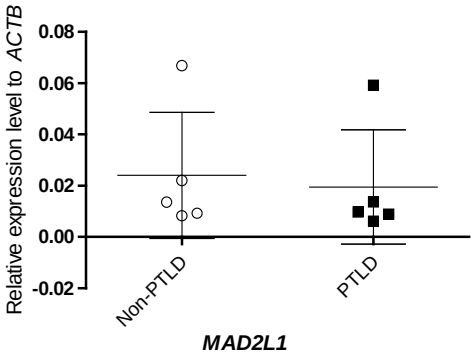


***MAD2L1***

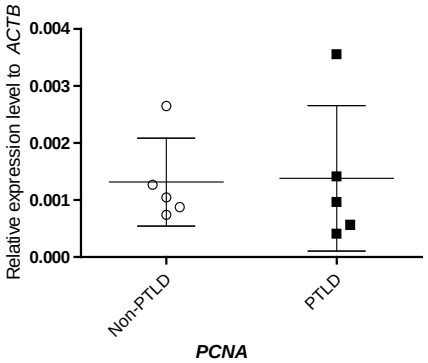


***PCNA***

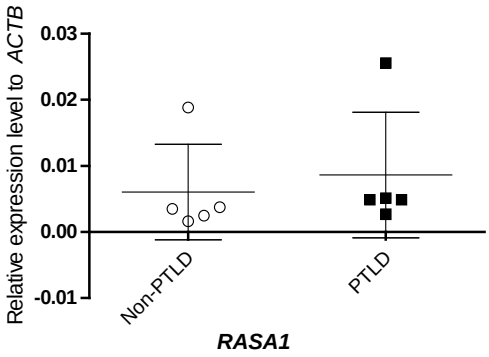


***RASA1***

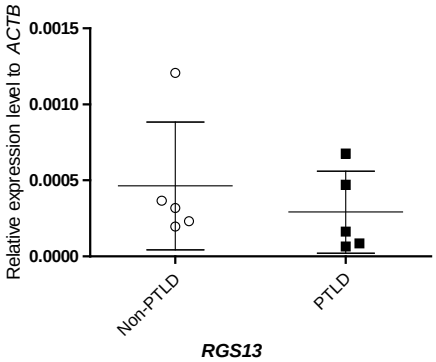


***RGS13***

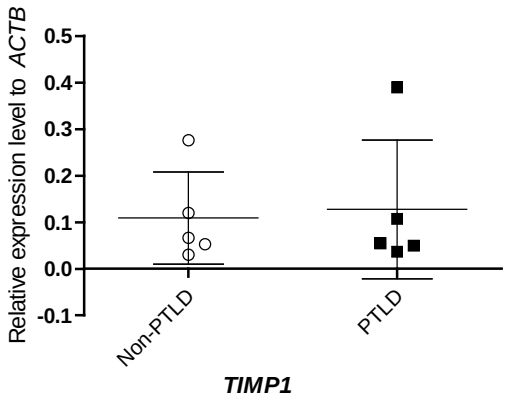


**Figure 5-5 Comparison of relative expression levels of 17 cellular candidate genes in the peripheral blood of paediatric PTLD and non-PTLD patients**

Relative expression levels were quantified relative to the *ACTB* gene using real-time TaqMan PCR. Graphs refer to the relative expression level of each cellular gene in whole blood from paediatric transplant patients (PTLD [*black squares*]; *n*=5]) (non-PTLD [*white circles*]; *n*=5). Horizontal lines denote the mean relative expression level in each group of transplant patients. Each circle/square represents the means of triplicates.

We next examined cellular gene expression profiles between the adult PTLD and non-PTLD patient (Figure 5.6). The mean relative expression levels for the 17 genes, tested in each sample (*n*=6) for both patients are summarised in Figure 7.2. Table 5.13 details the mean relative expression levels with SD for all 17 cellular genes as determined using the Mann-Whitney *U*-test. None of the 17 genes showed statistically significant differences ($P <$ ns; data not shown). In addition, the ratios between mean relative expression levels for each gene between each group were determined in Prism. We identified four genes (*CXCL9, CXCL10, CDC2* and *CHI3L1*) as differentially expressed (>2-fold) between the adult PTLD and non-PTLD patient. Notably, *CXCL9* was the most highly differentially expressed gene (9-fold), followed by *CXCL10* (7-fold), *CDC2* (3-fold) and *CHI3L1* (2-fold). None of the differences were statistically significant ($P <$ ns; data not shown).

**Table 5-13 Mean relative expression levels of cellular genes in adult transplant patients as determined by real-time PCR**

| Cellular gene | Mean relative expression level in a non-PTLD patient (±SD) | Mean relative expression level in a PTLD patient (±SD) | Ratio of mean relative expression levels between PTLD and non-PTLD patients |
|---|---|---|---|
| *ANP32E* | 0.01482 (±0.02) | 0.03924 (±0.02) | 1.02 |
| ***CDC2*** | 0.0003592 (±0.0003) | 0.001051 (±0.001) | 2.93 |
| *CD52* | 0.1431 (±0.14 ) | 0.1776 (±0.18) | 1.24 |
| *CCL3* | 0.02560 (±0.03 ) | 0.02202 (±0.02) | 0.86 |
| *CCL5* | 0.1112 (±0.09) | 0.08657 (±0.08) | 0.78 |
| *CCL22* | 0.0003287 (±0.0001) | 0.0002974 (±0.0003) | 0.91 |
| *CHI3L1* | 0.01898 (±0.012) | 0.03789 (±0.023) | 1.99 |
| ***CXCL9*** | 0.001646 (±0.002) | 0.01512 (±0.023) | 9 |
| ***CXCL10*** | 0.0004847 (±0.0008) | 0.003509 (±0.004 | 7.24 |
| *HDGF1* | 0.04127 (±0.04) | 0.04363 (±0.04) | 1.06 |
| *ISG15* | 0.1165 (±0.07) | 0.1581 (±0.05) | 1.36 |
| *LRMP* | 0.03327 (±0.04) | 0.01569 (±0.01) | 0.47 |
| *MAD2L1* | 0.01778 (±0.02) | 0.01687 (±0.01) | 0.95 |
| *PCNA* | 0.0006464 (±0.0004) | 0.0007058 (±0.0006) | 1.09 |
| *RASA1* | 0.00751(±0.01) | 0.006366 (±0.01) | 0.84 |
| *RGS13* | 0.0003935 (±0.0002) | 0.0004944 (±0.001) | 1.26 |
| *TIMP1* | 0.1372 (±0.13) | 0.1387 (±0.11) | 1.01 |

Mean relative expression levels (±SD, standard deviation) were calculated for each gene. Fold-differences were calculated for the PTLD group ($n$ = 1) compared to the non-PTLD group ($n$ = 1) from the 2-delta delta Ct formula. Cellular genes in bold were differentially regulated by 2-fold.

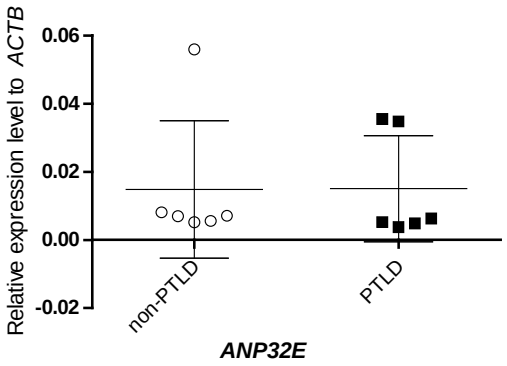


***ANP32E***

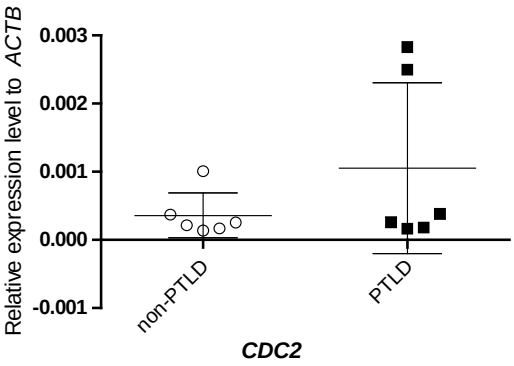


***CDC2***

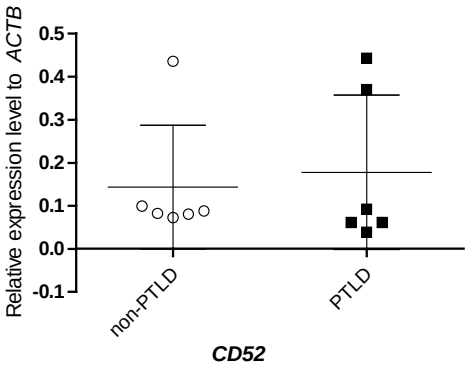


***CD52***

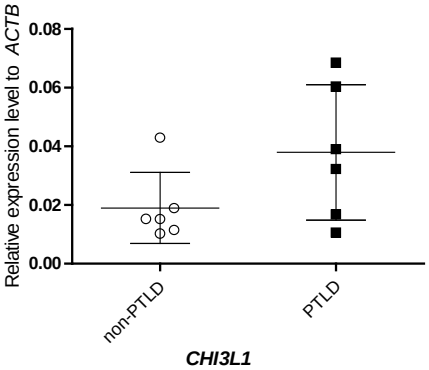


***CHI3L1***

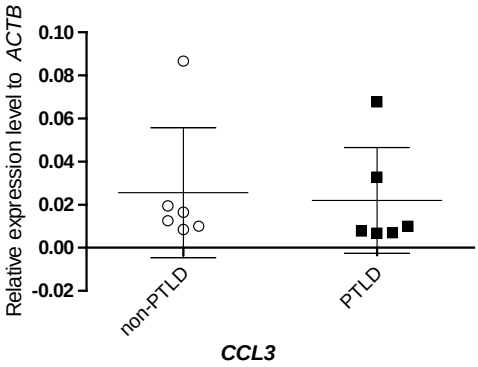


***CCL3***

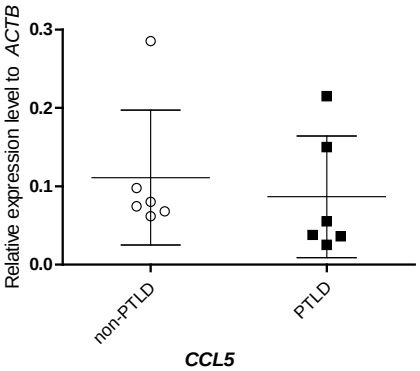


***CCL5***

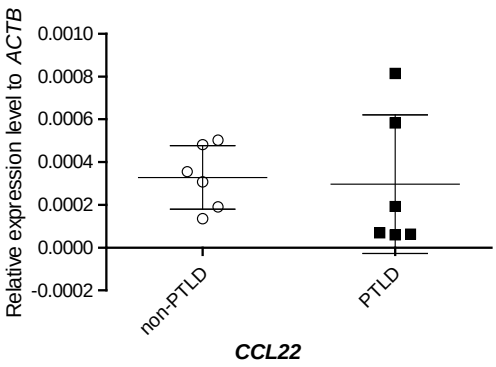


***CCL22***

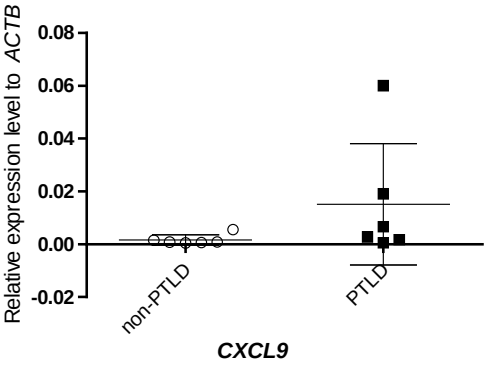


***CXCL9***

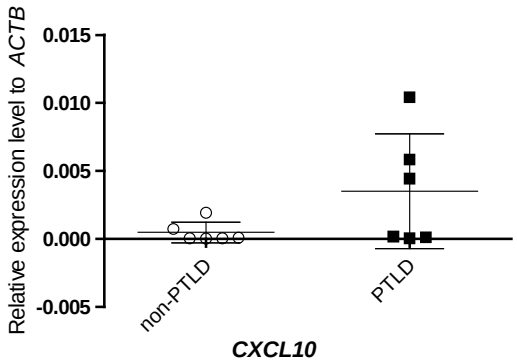


***CXCL10***

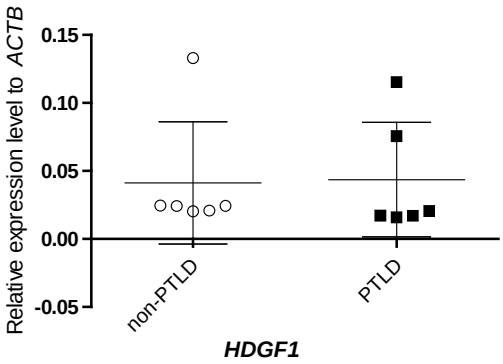


***HDGF1***

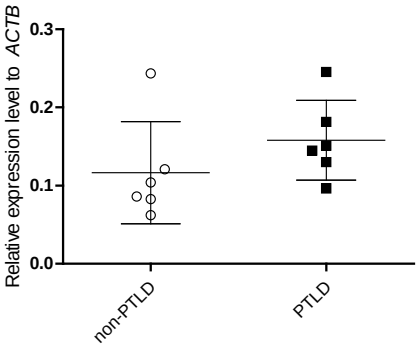


***ISG15***

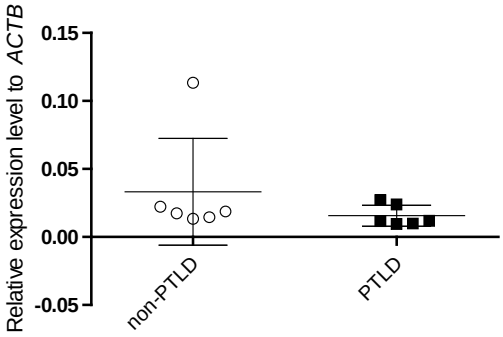


***LRMP***

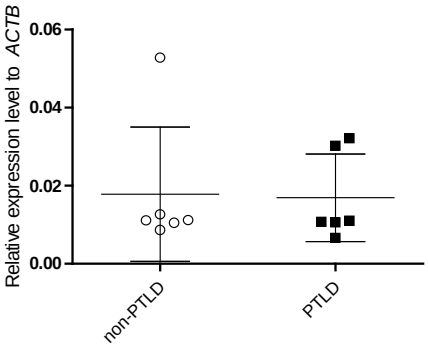


***MAD2L1***

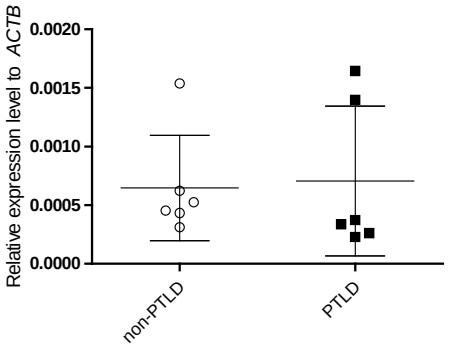


***PCNA***

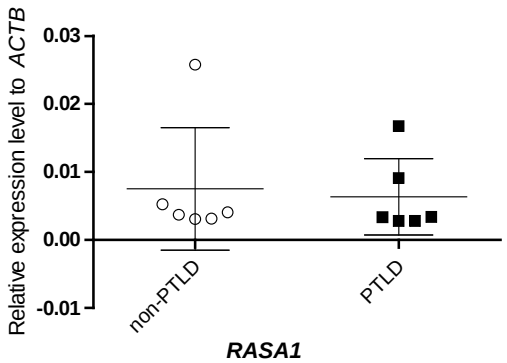


***RASA1***

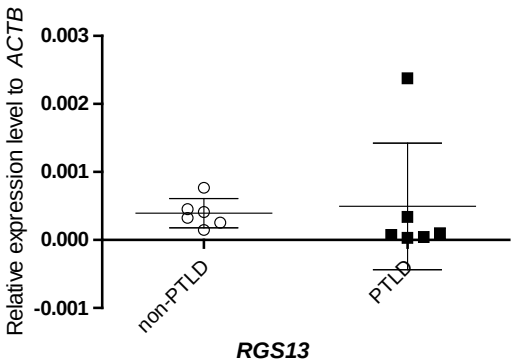


***RGS13***

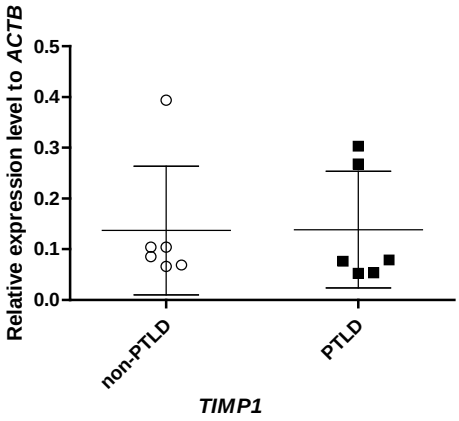


**Figure 5-6 Comparison of relative expression levels of 17 cellular candidate genes in the peripheral blood of multiple samples from a single adult PTLD and non-PTLD patient**

Relative expression levels were quantified relative to the *ACTB* gene using real-time TaqMan PCR. Graphs refer to the relative expression level of each cellular gene in multiple whole blood samples from 2 adult UCBT recipients (PTLD [*black squares*]; *n*=1]) (non-PTLD [*white circles*]; *n*=1). Horizontal lines denote the mean relative expression level in each group of transplant patients. Each circle/square represents the means of triplicates.

## 5.3 DISCUSSION

Differentially expressed genes between PTLD and non-PTLD patients provide the identification of potential early markers of PTLD. In this study, 17 EBV (9 lytic, 8 latent) and 17 cellular candidate genes were assessed in the whole blood of paediatric and adult transplant recipients. However, data has been excluded for three lytic genes (*BMRF1*, *BPLF1* and *BVRF1*), since these were subsequently realised to be overlapping genes, late lytic genes following analysis, and their expression levels may be overestimated. Therefore, data has been presented for 14 EBV genes (6 lytic, 8 latent). We determined that a 1/3 dilution of 300 ng cDNA template derived from whole blood was sufficient and reliable for full testing of the candidate genes in triplicate. We used real-time PCR to evaluate EBV gene expression profiles in PTLD versus non-PTLD paediatric ($n$ = 21) and adult ($n$ = 2) transplant recipients as markers for PTLD. Alongside these groups, we tested an EBV-seronegative patient (no. 21), with no EBV viraemia, and who showed no detectable EBV latent or lytic gene expression (Tables 5.5 and 5.7), which ensured validity of our results. The main findings of this study included: (i) the detection of a higher number of EBV latent and lytic genes in the PTLD versus non-PTLD patients, (ii) the detection of higher levels of gene expression in the PTLD versus non-PTLD patient, (iii) the detection of EBV latency III in PTLD patients, and (iv) the identification of several differentially expressed cellular genes between the PTLD and non-PTLD patients. The main findings of the EBV and cellular gene expression analysis and their potential utility as PTLD markers are discussed here.

### EBV gene expression analysis in paediatric SOT patients

EBV lytic gene expression was detected in 9/15 (60%) samples from 5 paediatric PTLD patients and 16/18 (89%) samples from 16 paediatric non-PTLD patients, indicating

productive infection. Overall in the paediatric PTLD group, we detected varying degrees of lytic gene expression, with some association with viral load. In contrast, fewer lytic genes were detected in the paediatric non-PTLD group, and in association with viral load. We next examined individual EBV lytic gene expression in paediatric PTLD and non-PTLD patients. We first assessed the utility of *BALF5* as a potential marker of PTLD. *BALF5* is an early gene that encodes the viral DNA polymerase, BALF5, essential for lytic DNA replication (Tsurumi, 1991). We detected expression of *BALF5* in the majority (60%) of paediatric patients, including samples from two PTLD patients with viral loads <10 copies/ml. This finding indicates that EBV lytic replication was ongoing, and supports further the sensitivity of the two-step real-time PCR approach for gene expression analysis over a range of viral loads.

With the exception of *BALF5*, EBV lytic gene expression was detected in only 3/18 (16%) samples from 16 paediatric non-PTLD patients, indicating that the majority of lytic gene expression was attributable to *BALF5*. Furthermore, *BALF5* was also the most highly expressed lytic gene detected in the PTLD and non-PTLD group, although a higher level of expression was detected in the PTLD patients. Since *BALF5* was expressed highly in both groups, in association with lytic DNA replication, its use as a marker of PTLD needs to be investigated further since its expression could be associated with a role in lytic replication alone.

Alongside *BALF5*, we detected the expression of *BRRF1*, an inducer of the lytic cycle (Hong et al., 2004) in one non-PTLD patient with elevated viral loads. No other EBV lytic genes were detected in this group. Based on their biological functions, this finding suggests further that active lytic replication is ongoing in these patients. Although both genes were the most

highly expressed lytic genes in this group, their amplifications were all borderline positive, suggesting expression at very low-levels. Both genes (*BALF5* and *BRRF1*) were also expressed in the paediatric PTLD patients, however at higher levels.

The immediate-early (IE) gene *BZLF1* encodes the transcription factor, BZLF1, that is expressed prior to viral replication, and essential for lytic cycle activation (Fields et al., 2007). Therefore, we were interested in assessing its potential as a marker of PTLD. We detected no expression of *BZLF1* in the non-PTLD group, in contrast to an earlier study, where 9/27 (33%) paediatric transplant patients without PTLD, and with primary EBV infection were positive for *BZLF1*, 21/27 (78%) positive for *BALF2* and 19/27 (70%) positive for *BcLF1* (Bergallo et al., 2007). However, we did demonstrate *BZLF1* expression in three paediatric PTLD patients, two of which also had primary EBV infection. An earlier study detected *BZLF1* expression in 13/18 (72%) paediatric liver transplant recipients with primary EBV infection. No association with risk of PTLD development was found, and viral load, not *BZLF1* expression was determined as a more sensitive predictor for PTLD (Vajro et al., 2000). Further, in a recent study, which assessed productive infection based on lytic gene expression (*BALF2* and *BZLF1*), *BALF2* alone was detected in the majority of non-PTLD HSCT patients, including asymptomatics (Zawilinska et al., 2008). Therefore, our findings and that of others, suggest that *BZLF1* is probably expressed highly during primary EBV since it has a role in activating the lytic cycle. Therefore, the detection of *BZLF1* in these patients could reflect lytic replication, possibly in association with primary EBV infection, and when assessed alone, is unlikely to be a specific marker of PTLD.

Previous studies have suggested that the EBV late lytic genes are detected less frequently in tumour cells found in PTLD (Rea et al., 1994a; Rea et al., 1994b), and NPC biopsy tissue

(Martel-Renoir et al., 1995), and that activation of the lytic cycle may not always result in productive infection. Indeed, it has been suggested that an abortive lytic cycle occurs in tumours of several EBV-associated malignancies, resulting in survival of the infected host cells (Martel-Renoir et al., 1995). We did however detect EBV late lytic gene expression (*BPLF1* and *BVRF1*) in the whole blood of paediatric PTLD patients only. Therefore, further analysis is required to identify their utility as markers for PTLD.

**EBV latent gene expression in paediatric transplant recipients**

We next examined EBV latent gene expression in paediatric PTLD and non-PTLD patients. While latent gene expression was detected mostly at higher viral loads (>10,740 copies/ml) in non-PTLD patients, it was also detected sporadically in samples from 4/5 (80%) PTLD patients, with viral loads ranging from <10 to 197,629 copies/ml. Overall, a higher level and frequency of latent gene expression was confirmed in PTLD versus non-PTLD patients (47% versus 44%, respectively).

We detected expression of *EBNA-3A, EBNA3B* and *EBNA3C* in two non-PTLD patients, with elevated viral loads, and also primary EBV infection. However, these amplifications were all borderline positive. Similarly, these genes were expressed in the single paediatric PTLD patient who exhibited the full spectrum of latent genes. The EBNA3s act as transcriptional regulators of latency by modulating *EBNA-2* up-regulation of cellular and viral promoters as well as having oncogenic properties, and could be important markers for PTLD (Tomkinson et al., 1993). We also detected expression of both *EBNA-LP* and *3C* in a non-PTLD patient with a low viral load (158 copies/ml). *EBNA-LP* was also expressed in 3 PTLD patients, and at a higher level of expression than the non-PTLD group. Moreover, *EBNA-LP* was the most highly expressed latent gene detected in PTLD patients, suggesting a potential role in PTLD.

*EBNA-LP* is one of the first latency genes to be expressed following EBV infection, and acts as a transcriptional co-activator of EBNA-2 that plays a crucial role in EBV-induced B-cell transformation (Mannick et al., 1991; Sinclair et al., 1994).

In addition, we detected expression of *LMP-1*, *EBNA-1* and *EBNA-2* in non-PTLD patients with elevated viral loads (>10,000 copies/ml). In the PTLD group, we detected sporadic expression of *LMP-1*, *LMP-2A*, *EBNA-1* and *EBNA-2* in viral loads ranging from <10 to 197,629 copies/ml. *LMP-1* is considered to be the primary EBV oncogene and encodes the LMP-1 protein that is essential for EBV-induced B-cell transformation *in vitro,* as demonstrated in both rodent fibroblast and epithelial cells (Kilger et al., 1998; Kim et al., 2000; Kulwichit et al., 1998; Wang et al., 1985). LMP-1 also inhibits apoptosis and can induce B cell lymphomas in transgenic mice (Kulwichit et al., 1998). Indeed, up-regulation of LMP-1 is implicated in Hodgkin's lymphoma (Herbst et al., 1991). The majority of the effects of LMP-1 occur through activaton of the nuclear-factor kappa B (NF-κB) pathway (Kaye et al., 1993; Rowe, 1999). EBNA-2 functions as the key transcriptional activator of latency (Wang et al., 1991). However, EBNA-1 is not required for B-cell transformation but is essential for replication and maintenance of the EBV genome (Yates et al., 1984). Notably, EBNA-2 and LMP-1 are characteristic of latency III and essential for B-cell transformation, suggesting that their expression could lead to PTLD (Thorley-Lawson and Gross, 2004).

In summary, we detected EBV latent and lytic gene expression in both PTLD and non-PTLD patients, however a higher number of lytic genes in the PTLD group. In addition, a higher level of lytic gene expression was detected in the PTLD group, suggestive of an important role in PTLD. While the majority of studies have evaluated EBV gene expression in paediatric liver transplant recipients with chronic high EBV loads (CHL) (Gotoh et al., 2010; Qu et al., 2000), fewer studies have been conducted in paediatric SOT patients who are not

CHL carriers. Therefore, further studies are warranted to evaluate latent and lytic gene expression in PTLD in transplant recipients in order to determine EBV gene expression patterns predictive of PTLD in this setting.

**EBV gene expression in adult transplant recipients**

The environment for the onset of EBV-associated PTLD in adults appears to differ slightly from that in paediatric transplant recipients. In the case of UCBT, donor cells are considered to EBV negative, whereas adult recipients are usually EBV seropositive. Therefore, EBV infection in adult UCBT recipients is likely to arise in one of two ways: (i) reactivation of the endogenous EBV strain and (ii) infection with a new exogenous EBV strain (Kawa et al., 2011). PTLD is likely to arise from reactivation of EBV latently infected B cells or uncontrolled proliferation of the EBV positive B cell pool.

Only 2 adult patients were examined, both with multiple samples ranging between <10 to 477,642 copies/ml, respectively. On examination of EBV latent gene expression profiles in the adult PTLD patient, we confirmed transcripts in all 6 samples. Notably, the entire set of latent genes was observed in one sample, and almost the entire set was observed in four samples. Furthermore, the transcriptional co-activator, *EBNA-LP* was expressed in all triplicates tested from this patient, regardless of viral load. This finding supports the earlier observation of high *EBNA-LP* gene expression in the paediatric PTLD patients, indicating a potential role in PTLD. In contrast, no latent gene expression was detected in samples from the adult non-PTLD patient, the reasons of which are unclear.

We next examined lytic gene expression patterns in the adult patients. The full set of lytic genes was also detected in two samples from the PTLD patient. However, sporadic lytic gene

expression was detected in other sequential samples with higher viral loads. As with the paediatric cohort, we detected expression of *BALF5* in both patients, indicating active EBV lytic DNA replication. Previous studies have reported EBV latent and lytic gene expression in the peripheral blood of adult transplant recipients with and without PTLD (Bergallo et al., 2007; Zawilinska et al., 2008). Together, both studies assessed four latent genes (*EBNA1*, *EBNA2*, *LMP1* and *LMP2*) and two lytic genes (*BZLF1*, *BALF2*). EBV latency and lytic gene expression was confirmed in adult HSCT transplant patients without PTLD, indicating a high risk for PTLD (Zawilinska et al., 2008). Notably, *EBNA-2* and *LMP-1* were associated with higher viral loads. Consistent with our study where *BALF5* was detected in samples from the single adult non-PTLD patient, productive infection was also confirmed in the adult HSCT patients as detected by the expression of *BZLF1* and *BALF2* in 19% and 83% of samples, respectively (Zawilinska et al., 2008). However, we detected no latent gene expression in this patient, suggestive of the stage of engraftment. While latent and lytic gene expression were detected in the single adult PTLD patient, no lytic gene expression was detected in the four adult SOT patients with PTLD in the study by Bergallo and colleagues, suggestive of higher levels of EBV reactivation in HSCT transplant recipients (Zawilinska et al., 2008). In summary, EBV latent and lytic gene expression was detected in all samples from the adult PTLD patient. *BALF5* gene expression was also confirmed in most samples from the adult non-PTLD patient however none of the other genes were detected.

**Analysis of EBV latency III profiles**

In order to determine the type of latency found in whole blood, and to determine any associations between latency III and PTLD, we analysed EBV latent gene expression patterns in the whole blood of PTLD and non-PTLD patients. Latency III is defined by the expression of all latency genes, notably *EBNA-2* and *LMP-1*, and is frequently detected in EBV-positive

B cells within PTLD biopsy tissue (Brink et al., 1997; Gratama et al., 1991; Knowles, 1999; Young et al., 1989). Therefore, a latency III profile is considered to be high risk for PTLD development. However, latency III is also associated, although less frequently, with infectious mononucleosis (Farrell, 1995; Tierney et al., 1994). Previous studies have examined a limited set of latent genes and confirmed latency type III based on the demonstration of *EBNA-2* and *LMP-1* genes in the peripheral blood of adult HSCT patients without PTLD (Zawilinska et al., 2008). However, latency III was not detected in any of the four adult SOT patients with PTLD examined using the same targets (Bergallo, 2007). As mentioned earlier, both EBNA-2 and LMP-1 function in B-cell transformation, suggestive of their importance to latency III (Thorley-Lawson and Gross, 2004).

We assessed the full set of EBV latent genes however none of the latent RNAs were examined. Firstly, we detected latent gene expression patterns typical of latency III (*EBNA-2*$^{(+)}$, *LMP-1*$^{(+)}$) in 2/5 (40%) paediatric PTLD patients, and all samples (100%) from the adult PTLD patient, indicating some associations between latency III and PTLD. Notably, the full spectrum of latent genes was detected in one of the paediatric PTLD patients and in 3/5 (60%) samples from the adult patient. However, we also detected a type III latency profile (*EBNA-2*$^{(+)}$, *EBNA-3A*$^{(+)}$, *EBNA-3B*$^{(+)}$, *LMP-1*$^{(+)}$) in 1/16 (6%) paediatric non-PTLD patients suggesting that latency III is not always specific to PTLD. Secondly, we detected more varied EBV latent gene expression patterns, not typical of latency III in the remaining PTLD and non-PTLD patients, the reasons for which are unclear. For instance, in one paediatric PTLD patient, *EBNA-1*, *EBNA-LP*, *LMP-1* and *LMP-2A* were expressed and *EBNA-2* was absent. Taken together, these findings suggest that latency III is not always specific to PTLD, and that variations in latent gene expression patterns are found in whole blood from PTLD patients. This is consistent with the earlier study by Bergallo and colleaugues where latency

III was detected in the peripheral blood, although in only 1/4 (25%) adult SOT patients with PTLD (Bergallo et al., 2007).

Possible reasons for our findings may be technical rather than biological (i.e. transient or low-level expression of the transcripts). Such factors may include (i) variations in sampling times, (ii) delays in blood at collection, (iii) number of tumour B cells, (iv) presence of inhibitors of PCR in the sample, (v) poor quality RNA due to freeze-thawing and storage, (vi) inefficient cDNA synthesis. All of these could have affected the detection of the mRNA transcripts. Secondly, other factors that could result in the absence of the transcripts could be the robustness of the PCR, including amplification efficiency and variations in TaqMan PCR assays or cDNA template. Also, the sensitivity of detection of target transcripts in each sample, since this was not validated during the PCR runs.

Another possible explanation for the observed variations in EBV latent gene expression may be the origin of B cells in which gene expression was measured. Earlier studies have suggested that latency III can be heterogeneous at the single cell level, owing to a potential switch between different latency types, or a reflection of the different phases in the cell cycle of the EBV-infected B cells (Brink et al., 1997; Niedobitek et al., 1995; Oudejans et al., 1995; Pallesen et al., 1993; Rea et al., 1994b). Therefore, changes in cellular morphology can be attributable to such heterogeneity (Brink et al., 1997). Moreover, Brink and colleaugues also suggested that latency III cells appeared to represent an intermediary stage between EBNA-$2^{(+)}$/LMP-$1^{(-)}$ and EBNA-$2^{(-)}$/LMP-$1^{(+)}$ expressing cells. Further, a more recent study found that late onset PTLD was often associated with more restricted latency types (*EBNA-*$2^{(-)}$, *LMP-*$1^{(+)}$ and *LMP-*$1^{(+)}$, *EBNA-*$2^{(-)}$) (Timms et al., 2003). Therefore, this heterogeneity in latency profiles could explain our findings, and further work is required to clarify the latency

profiles detected in EBV-positive B cells present in whole blood. For instance, latency II (*EBNA-2*$^{(-)}$, *LMP-1*$^{(+)}$) was detected in two paediatric PTLD cases, however not in all samples (Table 5.6). Since we detected latency III in some cases, as described above, it is likely that the latency II profile represents borderline detection of latency III, as not all samples exhibited latency II. Therefore, the detection efficiency of the RT-PCR could be limiting. Although we assessed the sensitivity of the PCR assays in a range of cDNA dilutions by amplification of several EBV targets, no target cDNA controls were used to validate the sensitivity during the PCR runs. Owing to the absence of such controls, the detection of latency II could be attributable to the absence of *EBNA-2*, due to poor amplification efficiency of this target. However, more than one transcript was detected in the latency II positive samples (i.e., *LMP-1* and *LMP-2*), and the latency II profile was specific to two of five PTLD cases, independent of viral load. *EBNA-1* was also detectable in samples of low viral load (<10 copies/ml), indicating that sensitivity and efficiency of detection was not a limiting factor, and that *EBNA-2* was genuinely not expressed. Further, the β-actin reference control (*ACTB*) was amplified in each PCR run and gave similar Ct values (~17 cycles), indicating that the RT-PCR was efficient. Therefore, it is likely that the latency II profile observed is genuine, and a number of factors could account for the absence of this profile in the remainder samples/patients. Firstly, aside from the lower viral load samples, differences in sampling times post-transplant could account for the latency II profile. For instance, latency III is characteristic of the lymphoblast stage of early EBV infection, whereas latency II is characteristic of B cells that have entered the GC, suggesting that the gene expression we have measured reflects the stage of B cell infection.

Again, this finding highlights the fact that heterogeneity of gene expression is a characteristic feature of B cells in whole blood from PTLD patients. We also detected EBV latent gene expression patterns typical of latency III in one paediatric non-PTLD patient. Moreover, this

patient also had primary EBV infection, indicating that the latency III profile could reflect the lymphoblastoid stage of the infected B cells. Taken together, this suggests firstly that latency III is also found in transplant recipients without PTLD, and secondly that this profile could be predictive for PTLD. Further, the detection of latency III in adult HSCT patients without PTLD in a recent study, supports further that latency III is not specific to PTLD, but may be predictive of PTLD (Bergallo et al., 2007; Zawilinska et al., 2008).

Earlier studies also detected lytic replication in a small proportion of cells in PTLD tumours expressing latency III (Rea et al., 1994a; Rea et al., 1994b; Thomas et al., 1990). We detected latency III accompanied by lytic gene expression in all patients investigated, except for the paediatric non-PTLD patient, suggesting a role for the lytic genes in PTLD. These observations concur with a previous study where both latency III and lytic gene expression were detected in 5/11 (45%) cardiothoracic PTLD patients (Hopwood et al., 2002). However, in contrast to these observations, in another study, no lytic gene expression was detected in any of the adult SOT PTLD patients, possibly owing to transient or low-level expression (Bergallo et al., 2007). Previous work detected both latency III and lytic gene expression in non-PTLD HSCT patients (Zawilinska et al., 2008), supporting further the previous suggestion that isolated detection of unrestricted latent gene expression together with lytic gene expression is not specifically indicative of PTLD development (Hopwood et al., 2002). Interestingly, latency III coupled with lytic gene expression has been reported in astronauts during flight, suggesting further that these gene expression patterns are characteristic of the immunosuppressed state (Stowe et al., 2011). Notably, we observed that all paediatric patients exhibiting latency III also had primary EBV infection, indicating that the latency III pattern observed in the non-PTLD patient could represent infectious mononucleosis or the early stages of PTLD, as lymphoblasts in both scenarios can express latency III (Thorley-

Lawson et al., 1999). In summary, although the study size was small, our findings suggest that although latency III coupled with lytic gene expression is more frequently detected in PTLD. However, it is not necessarily associated with the condition as it can be exhibited in other conditions such as primary EBV infection.

**Associations between EBV gene expression and viral load**

Several studies have identified associations between high EBV DNA load in the peripheral blood and risk of PTLD development in both SOT and HSCT recipents (Baldanti et al., 2000; Kenagy et al., 1995; Lucas et al., 1998; Riddler et al., 1994; Savoie et al., 1994; Wagner et al., 2002; Wagner et al., 2001). Further, associations between EBV gene expression, viral loads and PTLD have also been reported (Bergallo et al., 2007; Hopwood et al., 2002). However, this correlation is not perfect, indicating that, in addition to total viral DNA load, other factors influence PTLD development. Moreover, only a limited panel of EBV genes were assessed in these studies. We suspected that the expression levels of one or more viral proteins might influence the onset of PTLD. To further evaluate the correlation between the aforementioned variables in a broader set of EBV genes, EBV gene expression profiles were analysed in both groups with varying viral loads. We detected some association between the expression of two EBV lytic genes (*BALF5* and *BRRF1*) and viral load in three paediatric non-PTLD patients. Similarly, in the paediatric PTLD group two genes (*BALF5* and *EBNA-LP*) were highly expressed in association with viral load. In the adult PTLD patient, five genes (*EBNA-LP, BRRF1*, *BALF5*, *LMP-1* and *LMP-2*), were highly expressed in association with viral loads, whereas *BALF5* was highly expressed in the non-PTLD patient. Notably, *BALF5* was highly expressed in both PTLD and non-PTLD groups, however *EBNA-LP* was highly expressed in samples with higher viral loads in the majority of PTLD patients, suggestive of its potential as a marker of PTLD.

*EBNA-LP* is a co-transcriptional activator of EBNA-2 that functions to up-regulate factors necessary for B-cell growth. Except for one sample with a low viral load from a paediatric non-PTLD patient, *EBNA-LP* detected markedly high expression in PTLD patients with higher viral loads, indicating its involvement in B-cell proliferation (Figure 5.5) (McCann et al., 2001). Furthermore, EBNA-LP is known to regulate the thymus activated responsive chemokine (TARC), a Th2-responsive chemokine that leads to a Th2 response (Kanamori et al., 2004). Previous studies have demonstrated that a Th2-predominant response, may lead to the development of cancers such as PTLD as a consequence of a less potent T-cell response to EBV-latently infected B-cells, and a Th2-like cytokine environment (Burke et al., 1992; Mathur et al., 1994; Nalesnik et al., 1999; Yuling et al., 2009); Moreover, CD4+ T-cells, which are primarily active against the EBV lytic genes, are known to induce a Th2 response (Ma et al., 2010). Therefore, the overexpression of EBNA-LP may contribute to the development of PTLD through the induction of EBNA-LP-induced TARC, whereas EBV lytic replication could induce this response further. In summary, we showed that more EBV latent genes were associated with viral load in the adult PTLD patients compared to the paediatric PTLD patients. In particular, we identified *EBNA-LP* as highly expressed in association with viral load in PTLD patients only. An earlier study demonstrated detection of circular and linear genomes in the peripheral blood representing latent and lytic infection, respectively (Babcock et al., 1999). Therefore, possible reasons as to why viral loads do not correlate with PTLD include: (i) high viral loads could be attributable to viral lytic DNA replication not just latent DNA replication and (ii) the combination of both could cumulatively contribute to overall viral burden, however in the case of PTLD the proportion of one versus the other could be a significant factor in the onset of PTLD (Babcock et al., 1999). This could account for increased viral loads in the peripheral blood, suggesting that lytic gene expression contributes to total viral DNA burden in transplant patients. Therefore,

by measuring a single EBV gene target in a real-time PCR assay, an accurate assessment as to how much latent or lytic infection could be contributing to the onset of PTLD, is not possible.

**Cellular gene expression analysis**

EBV lytic genes are known to regulate cellular gene expression (Carter et al., 2002; Chang et al., 2006; Hahn et al., 2005; Morrison and Kenney, 2004; Morrison et al., 2004). PTLD stems from an inability to control the proliferation of EBV transformed B cells, however it has been shown that viral loads and therefore, EBV infection per se is not solely responsible for the development of PTLD. Our next set of results show how the host cell response could, potentially, be contributing to the onset of PTLD through a complex interplay between viral and cellular gene products.

We used real-time PCR to identify differentially expressed cellular genes between PTLD and non-PTLD patients. We assessed 17 cellular genes that were highly differentially expressed in a model system of lytic-induced Raji LCLs. Owing to the availability of multiple samples for some PTLD patients, but not for others, we examined gene expression profiles in 5 of the earliest and most closely matched samples from 5 PTLD patients. The main findings of the cellular gene expression analysis was the identification of four genes (*CDC2*, *CXCL9*, *CXCL10* and *CHI3L1*) that were differentially expressed between multiple samples from the adult PTLD and non-PTLD patient (Table 5.13). Similarly, no significant differences were detected in the paediatric group for any of the 17 cellular genes, although *CHI3L1* was differentially expressed (Table 5.12). Of the genes identified in the adult group, *CXCL9* was the most highly differentially regulated (9-fold), followed by *CXCL10* (7-fold), *CDC2* (4-fold) and *CHI3L1* (2-fold). Previous studies have reported up-regulation of CXCL9 and

CXCL10 in PTLD (Teruya-Feldstein et al., 1997). CXCL10 has also been reported in EBV-positive cases of classical Hodgkin lymphoma (HL), where EBV genes regulate this chemokine, suggesting further that EBV regulation of chemokines can influence tumour-host interactions (Maggio et al., 2002; Setsuda et al., 1999; Teruya-Feldstein et al., 1997; Vockerodt et al., 2005).

CXCL9 (Monokine-induced chemokine, MIG) and CXCL10 (interferon-inducible IP chemokine, IP-10) are interferon-γ (IFN-γ) responsive Th1-chemokines that share a CXCR3 receptor and chemoattract CXCR3+ Th1 cells and NK T-cells, leading to a Th1-predominant response (Loetscher et al., 1996; Teichmann et al., 2005). LMP-1 can lead to up-regulation of various inflammatory factors, such as cytokines and chemokines that mediate proliferation, angiogenesis and inflammation *in vivo* (Hannigan et al., 2011; Morris et al., 2008). Furthermore, previous studies have demonstrated that LMP-1 can up-regulate the expression of various chemokines, including CXCL9 and CXCL10, through LMP-1-mediated NF-κB induction (Kaye et al., 1993). Hence, the NK-κB pathway is important in cancer progression. We detected EBV LMP-1 expression in the PTLD patient, however not from the non-PTLD patient. Therefore, it is likely that the increased levels of *CXCL9* and *CXCL10* in this patient are attributable to LMP-1**.** Moreover, previous studies have demonstrated that both chemokines have anti-tumor properties (Arenberg et al., 1996; Brunda et al., 1993; Luster and Leder, 1993; Sgadari et al., 1996; Sgadari et al., 1997)**.** For instance, up-regulation of CXCL10 and CXCL9 has been reported to promote PTLD tumour regression in T-cell deficient athymic mice models (Setsuda et al., 1999; Sgadari et al., 1996; Sgadari et al., 1997). However, an earlier study demonstrated that CXCL10 does not have anti-neoplastic functions as demonstrated *in vitro* (Teichmann et al., 2005). Therefore, through the LMP-1-activated (NF-κB) induction, we postulate that these chemokines probably contribute to

processes relevant to the regression and/or progression of PTLD. Therefore, further studies are required to determine the significance of these chemokines in PTLD.

*CDC2* (cell division cycle 2) encodes CDC2, a protein kinase that is essential for G1/S and G2/M phase transitions of cell cycle. Previous studies have shown that *EBNA-2* can induce up-regulation of cell-cycle regulating proteins including CDC2, however, whether the effects are direct or indirect is uncertain (Spender et al., 2001). As a result of its role in cell cycle proliferation, CDC2 has been associated with progression in lung cancer patients and diffuse large B cell lymphoma (Bai et al., 2005; Zhao and Gartenhaus, 2009), and *CDC2* regulation has been reported in EBV-positive monomorphic (MP) PTLD patients in a previous study (Craig et al., 2007). In the study, *CDC2* showed decreased levels of expression in EBV-positive MP relative to EBV-negative MP, suggesting down-regulation by EBV. *CHI3L1* encodes the chitinase 3-like 1 protein CHI3L1 (also called YKL-40 or HC-gp39), a member of the mammalian chitinase-like protein (CLPs) family, which lack enzymatic activity and have carbohydrate binding proteins (Qureshi et al., 2011). CHI3L1 functions as a lectin that binds heparin, chitin and collagen, and is secreted by many cell types, including leucocytes and macrophages (Biggar et al., 2008). Although the exact biological function of CHI3L1 is largely unknown, CHI3L1 appears to be important in host defense mechanisms, where it is suggested to play an important role in proliferation and differentiation of tumour cells, angiogenesis, antiapoptosis, invasion and extracellular tissue remodeling (Biggar et al., 2008; Johansen, 2006; Lee et al., 2009). Indeed, CHI3L1 has been linked to both autoimmune and inflammatory diseases, as well as various solid cancers (Eurich et al., 2009; Johansen et al., 2008). Furthermore, elevated levels of CHI3L1 have been found in the serum and/or plasma of patients with these conditions, and are associated with poor prognosis (Eurich et al., 2009; Kucur et al., 2008). Therefore, serum levels of CHI3L1 have been suggested as a reliable and

sensitive biomarker of cancer progression, such as Hodgkin's lymphoma (Biggar et al., 2008; Johansen et al., 2009; Qin et al., 2007).

In addition, although the association of CHI3L1 with EBV is unclear, its isoform, *CHI2L1* is known to be up-regulated by *EBNA-2* in LCLs (Spender et al., 2006). Indeed, CHI3L1 is up-regulated in Hodgkin's lymphoma and multiple sclerosis, of which a previous EBV infection is a risk factor (Ascherio and Munger, 2010; Brune et al., 2008). Therefore, further studies are required to identify the use of CHI3L1 as a potential marker for PTLD. Moreover, except for *CDC2* and *CHI3L1*, the differences in expression of CXCL9 and CXCL10 were similar to those found in the lytic induced Raji LCLs where *CDC2*, *CXCL9, CXCL10* and *CHI3L1* were regulated to -5.4-, 10-, 4- and 18.1-fold, respectively, compared to control LCLs. This suggests that CXCL9 and CXCL10 might be regulated further by EBV lytic replication during PTLD, and that CDC2 that functions in anti-apoptosis and cell cycle might be up-regulated by EBV latent proteins in PTLD to sustain B-cell proliferation. However, the exact contribution of these genes to the development of PTLD needs to be investigated further. One possible explanation for the up-regulation in the single adult PTLD patient could be due to its involvement in cell cycle, proliferation and anti-apoptosis, respectively and could be regulated in response to EBV infection to ensure an optimised environment for B-cell transformation. This also implies that such processes are regulated by EBV and might be relevant to PTLD. Despite these preliminary findings, one of the major limitations of the host gene expression analysis in the adult group was the small number of PTLD cases and controls investigated. Therefore, further work is needed to investigate these four genes as possible markers of PTLD. Whilst a larger sample number is required to assess this differential gene expression further, differences in gene expression in PTLD might provide further information on the processes involved in PTLD. Further work is required to clarify whether these genes

are beneficial for use as markers of PTLD, and whether EBV lytic replication is involved in the development of PTLD.

In summary, we have detected the following: (i) a higher number and level of latent and lytic gene expression in PTLD versus non-PTLD patients, (ii) variations in latent gene expression patterns, including profiles typical of latency III in three PTLD patients and one paediatric non-PTLD patient; (iii) no significant differences in cellular gene expression between the groups, however >2-fold fold-differences in expression of four cellular genes (*CXCL9*, *CXCL10*, *CDC2* and *CHI3L1*), and (iv) demonstrated that the real-time PCR assays are sensitive enough for evaluation of EBV and cellular candidate genes the whole blood of these patients.

# 6 CHAPTER 6. GENERAL DISCUSSION

## Importance of study

The identification of specific markers for the development of PTLD is crucial for the early diagnosis of PTLD. This study was important since previous investigations have resulted in conflicting evidence for the association between viral loads and the development of PTLD (Scheenstra et al., 2004). The findings of this thesis provide several potential candidate genes, both viral and cellular, which could be investigated further as markers for the early detection of PTLD. In addition, it was important to gain insight into the potential microenvironment in which PTLD could arise during EBV infection.

## Objectives of study

In order to identify potential candidate genes as markers for PTLD, we carried out an analysis of EBV and cellular gene expression in an *in vitro* model system of TPA/NaB lytic induced Raji cells, using real-time PCR and whole genome microarrays, respectively. This was followed by a preliminary analysis of EBV and cellular gene expression in whole blood from PTLD versus non-PTLD patients, to evaluate the candidate genes as suitable markers for PTLD.

## Summary of main findings

In our *in vitro* model system, we detected firstly, successful lytic cycle activation by the induction of the *BZLF1* gene, followed by the identification of several highly induced EBV early and late genes, at 24 and 48 hrs, respectively. Secondly, we detected low-level induction of several latent genes. In the microarray experiment, we detected 133 highly differentially expressed and regulated probe sets, of which 112 genes were found to be

induced in response to EBV alone. From these experiments, we selected 17 EBV (9 lytic, 8 latent) and 17 cellular genes as candidate markers for the clinical evaluation. However, three genes (*BMRF1, BPLF1* and *BVRF1*) were overlapping and/or late lytic genes and data for these genes were subsequently excluded from the thesis since their expression levels may be overestimated. So, only 14 EBV genes (6 lytic, 8 latent) were analysed. These genes were highly induced in response to the EBV lytic induction phase. The cellular genes were previously implicated with EBV and/or PTLD and likely to be involved in processes relevant to PTLD, including anti-apoptosis, cell proliferation, angiogenesis and chemotaxis. In addition, Gene Ontology analysis of cellular genes regulated in response to lytic cycle induction, revealed highly significantly representative pathways for canonical networks (cell cycle), biological processes (chemotaxis), and biomarkers (lymphoproliferative disorders), from which additional candidate genes can be selected for further investigation. These pathways also indicate the potential microenvironment found in the induced EBV lytic phase in Raji cells.

In the preliminary analysis of the EBV candidate genes in whole blood, firstly, we detected higher numbers and levels of EBV latent and lytic gene expression in the PTLD versus non-PTLD group, including higher levels of latent and lytic gene expression for two genes *BALF5* and *EBNA-LP*. Notably, *BALF5* was detected in the vast majority of PTLD and non-PTLD patients, suggesting it was necessary for viral DNA replication, and therefore a potential target for antivirals in the prevention of PTLD. Secondly, we detected EBV latent gene expression patterns typical of latency III (*EBNA-2*$^{(+)}$, *LMP-1*$^{(+)}$) in three PTLD patients (1 adult, 2 paediatric) and one non PTLD patient, however, more varied EBV latent gene expression patterns in the remaining patients, the reasons for which are unclear. In addition, we detected latency III together with lytic gene expression, consistent with earlier studies,

suggesting an important role for the EBV lytic genes in PTLD (Hopwood et al., 2002). Latency III is often associated with EBV-positive B cells in PTLD, although more restricted latency profiles have been found (Brink et al., 1997), particularly in late onset PTLDs (Timms et al., 2003). It is possible that the observed variations in latent gene expression are due to heterogeneity of the latency types, and therefore, further studies are necessary to clarify the latency profiles found within tumour cells in whole blood. Such a profile might be useful to determine those patients at most risk of developing PTLD. Finally, we detected some associations between EBV gene expression and viral loads, including *BALF5* and *BRRF1* in the PTLD and non-PTLD groups, and *EBNA-LP*, *LMP-1*, and *LMP-2* in the adult PTLD patient. This finding was important since there is a disagreement over the significance of increasing viral loads and the development of PTLD (Gulley and Tang, 2008). This difficulty is that while an association between high EBV DNA viral loads and PTLD can be demonstrated, the condition can also arise in patients with low viral loads (Gotoh et al., 2010; Qu et al., 2000). In the preliminary analysis of cellular gene candidates, we identified four differentially expressed cellular genes between the PTLD and non-PTLD groups, including (*CXCL9, CXCL10, CDC2* and *CHI3L1*), of which their potential implications with PTLD are discussed below. Finally, we demonstrated the successful development and validation of a two-step real-time RT-PCR approach for gene expression analysis in routinely collected whole blood samples.

**Potential contributions of viral and cellular candidate genes to PTLD**

Our findings suggest potential markers for the early detection of PTLD, and their potential contributions to PTLD are discussed here. We identified *BALF5* as the most highly expressed EBV lytic gene between PTLD and non-PTLD groups and, in association with viral load. BALF5 is necessary for viral DNA lytic replication, suggesting ongoing EBV lytic

replication. We also identified *EBNA-LP* as the most highly expressed latent gene in both PTLD groups, indicating an important role for this gene. *EBNA-LP* functions in B-cell transformation and is known to up-regulate TARC, which attracts a Th2 response (Lee et al., 1997; Sinclair et al., 1994). A Th2 response is predominant amongst malignancies, including PTLD, and associated with a poor outcome (Holley-Guthrie et al., 2005; Lee et al., 1997; Nalesnik et al., 1999; Sinclair et al., 1994). Our findings suggest potential roles for *BALF5* and *EBNA-LP* in the development of PTLD, and the possible contribution of an EBV-induced Th2 microenvironment.

Chemokines function in the recruitment of T cells and NK cells and their involvement in cancer are well established (Allavena et al., 2011; Rollins, 2006). CXCL9 and CXCL10 attract a Th1 response that has anti-neoplastic properties *in vivo* and have been implicated in the regression of PTLD (Sgadari et al., 1996; Sgadari et al., 1997; Teruya-Feldstein et al., 1999)**.** However, CXCL10 is also suggested to have pro-invasive properties (Zipin-Roitman et al., 2007). In addition, CDC2 functions in cell cycle progression in several cancers (Bai et al., 2005), whereas CHI3L1 functions in metastasis and is associated with poor prognosis (Qureshi et al., 2011), and could both contribute to the development of PTLD. Therefore, all four genes could serve as potential markers for progression to PTLD.

**Broader implications of our findings**

Earlier studies have proposed a model of EBV persistence (Figure 1.5). This model suggests that in the absence of immunosuppressive drugs, EBV infects naive resting B cells to become lymphoblasts that reside in the lymph nodes and behave as normal antigen activated B cells (Figure 1.5) (Thorley-Lawson, 2001). These activated B cells proliferate and differentiate into resting memory B cells that migrate into the peripheral blood to establish a persistent

infection (Thorley-Lawson, 2001; Thorley-Lawson and Babcock, 1999; Thorley-Lawson and Gross, 2004). Occasionally, memory B cells will differentiate into plasma cells that undergo EBV reactivation to release infectious virus (Laichalk and Thorley-Lawson, 2005). The earlier studies propose further that increasing levels of infectious virus derived from either newly infected B cells or re-infections from reactivated memory B cells not only drives the formation of activated lymphoblasts exhibiting latency III, but increases the likelihood of infection of B cells other than naive B cells, known as 'bystander' B cells into an intermediate state of activation (Thorley-Lawson and Gross, 2004). Rarely, these bystander cells escape from the lymph nodes into the peripheral circulation where they accumulate genetic changes resulting in extra nodal PTLD (Babcock et al., 1999). Such a rare event is more likely to occur during immunosuppression when uncontrolled proliferation of lymphoblasts arises.

We detected varied latent EBV gene expression patterns in the PTLD patients, including latency III in two cases. Since latency III is associated not only with the lymphoblastic stage of B cells, but epithelial cells and even germinal centre (GC) and post-GC B cells, this suggests that PTLD can arise from a variety of different bystander B cell types (Rowe et al., 1998; Siemer et al., 2008). Therefore, the detection of latency III-expressing cells could be derived from either of these cell types found in whole blood. In addition, we detected lytic gene expression patterns in most cases of PTLD, possibly derived from lytically infected/reactivating B cells, dead cells (necrotic tumours), and active EBV replication from epithelial cells in the oropharynx (Laichalk and Thorley-Lawson, 2005; Prang et al., 1997). We know that EBV-reactivation arises as a consequence of increased B cell proliferation following T cell immunosuppression in transplant recipients. This results in an increased level of viral shedding and consequently an increased number of newly infected B cells in the

peripheral blood (Thorley-Lawson and Babcock, 1999). Thus, any increase in B cell proliferation in the absence of a functional cytotoxic T cell (CTL) response ultimately leads to uncontrolled proliferation, with eventual progression to PTLD. Indeed, an earlier study has suggested that in healthy individuals, a fully functional CTL response targeting lytic rather than latent genes explains why expression of latency III alone does not predispose to PTLD development and that lytic reactivation is an important risk factor for PTLD development during immunosuppression (Hopwood et al., 2002).

Therefore, in the context of our findings, we postulate that the demonstration of latency III coupled with lytic gene expression probably resulted from an impaired CTL response directed against EBV lytic replication. This impairment could have lead to an increased production of infectious virus from an expansion of GC memory B cells, expressing latency III, or alternatively, from the expansion of newly infected primary B cells exhibiting latency III. Any newly infected naive B cells exhibiting latency III and any pre-existing GC B cells could then proliferate into PTLD (Hopwood et al., 2002). Furthermore, the concomitant EBV reactivation and lytic infection could accelerate either approach through increased horizontal spread between B cells, increasing the total number of latently infected B cells and increasing the likelihood of bystander B cells (Hong et al., 2005).

Taken together, this overall increase in EBV lytic reactivation and enhanced proliferation of lymphoblasts could account for the higher levels of latent and lytic gene expression in the PTLD as compared to non-PTLD patients. Furthermore, the up-regulation of EBV-induced cellular genes, such as EBNA-LP-induced TARC and the various chemokines could enhance any progression to PTLD.

**Comparison with other studies**

While latency III was detected in only 1/4 (25%) PTLD SOT patients, no lytic gene expression was detected (Bergallo et al., 2007). The absence of lytic gene expression in PTLD patients exhibiting latency III in this study could be due to a number of reasons including the low sensitivity of their assay. While these earlier studies tested one, two and three lytic genes, respectively (Bergallo et al., 2007; Hopwood et al., 2002; Zawilinska et al., 2008), we extended this analysis further by examining nine lytic genes, which increases the number of lytic genes detected. While we detected some lytic gene expression in adult and paediatric non-PTLD patients with high viral loads, the level of expression was not as high as in the PTLD patients, indicating that lytic gene expression is important for PTLD regardless of viral load, where the full set of lytic genes analysed were expressed in two PTLD patients. Notably, the viral DNA polymerase, BALF5 was detected consistently in PTLD and non-PTLD patients, including those with viral loads ≤10 copies/ml, providing further evidence for active EBV lytic DNA replication. Our study is limited by the lack of matched controls and a prospective longitudinal analysis in patients at high risk for PTLD. However, limitations of the earlier studies include the use of semi-quantitative PCR, which is both prone to contamination and also time-consuming. Real-time PCR occurs in a closed system, and offers an alternative method for measurement of gene expression levels which is sensistive and rapid and highly specific when TaqMan probes are used. Further, only two or three lytic genes were evaluated. This is compared to nine lytic genes investigated in our study, which more broadly detected active EBV lytic infection, in doing so we could better account for transient or temporal expression of these genes. We also tested twice as many latent genes, rather than the four latent (*EBNA-1*, *EBNA-2*, *LMP-1* and *LMP-2*) examined in each of the studies (Bergallo et al., 2007; Zawilinska et al., 2008). This allowed us to analyse the

different latency profiles exhibited in whole blood. In addition all gene targets were tested in triplicate to increase the confidence of any expression.

**Discussion of study limitations**

Limitations of this study were primarily the small study size, including the number of PTLD cases, particularly in the adult group, where only 1 patient was available at follow-up post-transplant. As a consequence, we were unable to draw definitive conclusions on the findings. In addition, due to the small number of matched controls to draw from, the majority of controls in the paediatric group were unmatched based on age and sex and matching was based primarily on sampling time post-transplant (<1 yr). Furthermore the infrequent follow-up for the majority of patients meant that few sequential samples were available and that matched controls (sex/age) were hard to draw from the available paediatric transplant population for testing. Furthermore, while we wanted to identify non-invasive markers of PTLD, in the paediatric group, a limited whole blood volume (0.5 ml) and the frequency of samples received in our laboratory was often unpredictable for both PTLD and non-PTLD groups. A larger volume is ideal for isolation of WBCs, particularly for the extraction of high yields of total RNA. As a consequence, few EBV-seronegative paediatric patients were available for analysis that gave sufficient total RNA yields and a prospective longitudinal analysis was not undertaken. More importantly, the fraction of tumour B cells in whole blood was not assessed by i.e. flow cytometry analysis, which would have been useful for the interpretation of our data, particularly in cases where no transcripts were detectable in samples with high viral loads. Other limitations include the number of replicates analysed and consequently the reliability of the data, in particular for the model system of lytic induction in Raji cells, where only one bioloigal replicate was analysed for EBV gene expression. Additional replicates are necessary to validate the highly induced EBV genes identified in our

system. Consequently, only two replicates were analysed in the microarray analysis, however probe sets were regulated similarly between the arrays and significant *P*-values ($P<0.05$) determined. Further, Ramos cells were used to assess the effects of the inducing agents, since a Raji EBV-negative cell line is not available. The caveat is that there are many genetic differences between Ramos and Raji cells independent of EBV and the effects of the inducing agents cannot be assessed reliably. The reliability of the data could be increased by increasing the numbers of replicates used since only two replicates were analysed for each cell line in the genome-wide analysis. Further, the reliability of the data could be confirmed by analysis in an alternative EBV-positive cell line such as the Akata cell line, for which an EBV-negative counterpart is available. However, strengths of our study include the large number of EBV and cellular gene targets assessed.

**Future work**

Owing to the limitations encountered in this study, the focus of future work should be to assemble a large prospective study in a well-defined cohort of PTLD and non-PTLD controls, and to use the RT-PCR approach to examine any contributions of the genes evaluated in our study to PTLD. Further, an evaluation of more genes is needed to validate our findings and to identify other potentially interesting candidate genes. Any differentially expressed genes could be useful as markers in real-time RT-PCR assays for the early detection of PTLD. In addition, longitudinal studies should also be carried out to determine significant correlations between viral loads and any differentially expressed genes as markers for routine testing alongside viral load monitoring.

## Conclusion

In conclusion, the findings made in this study are important since specific markers of PTLD are lacking. Further, these findings have provided insight into the types of EBV gene expression patterns found in whole blood of transplant recipients monitored routinely in our laboratory, and the potential microenvironment in which PTLD could develop. Any future studies will be valuable in identifying viral and host factors predictive of PTLD development as well as developing our understanding of the EBV biology and the exact role of EBV gene products in the pathogenesis of PTLD.

# 7 APPENDIX

**Table 7-1 Fold change for 88 EBV genes at early time-points following TPA/NaB induction in Raji cells**

| Gene | 0 hr | 2 hr | 6 hr |
|---|---|---|---|
| *BZLF1* | 1.01 | 0.56 | 2.21 |
| *BRLF1* | 1.5 | 1.06 | 0.5 |
| *BALF1* | - | - | - |
| *BALF2* | - | - | - |
| *BALF3* | 1.12 | 0.71 | 1.17 |
| *BALF5* | 1.01 | 0.81 | 0.91 |
| *BaRF1* | 1.11 | 0.36 | 0.96 |
| *BARF1* | - | - | - |
| *BBLF2/BBLF3* | 0.87 | 0.23 | 1.03 |
| *BBLF3/ BBLF2* | 0.97 | 0.32 | 0.68 |
| *BBLF4* | 1.14 | 0.77 | 1.07 |
| *BcRF1* | 0.64 | 0.78 | 0.72 |
| *BDLF4* | 0.63 | 0.31 | 1.20 |
| *BFRF1* | 0.96 | 0.60 | 1.59 |
| *BFRF2* | 0.18 | 0.29 | 0.04 |
| *BGLF5* | 0.95 | 0.39 | 0.29 |
| *BGLF4* | 1.08 | 1.02 | 1.05 |
| *BGRF1/ BDRF1* | 0.65 | 0.77 | 0.24 |
| *BHRF1* | 0.74 | 0.76 | 0.73 |
| *BKRF3* | 1.11 | 0.49 | 0.39 |
| *BLLF2* | 1.02 | 0.52 | 0.90 |
| *BLLF3* | 1.33 | 1.14 | 1.34 |
| *BSMLF1* | 0.16 | 0.08 | 0.33 |
| *BMRF1* | 0.85 | 1.15 | 1.32 |
| *BNLF2a* | 0.32 | 0.07 | 0.12 |
| *BNLF2b* | 0.86 | 0.89 | 1.40 |
| *BORF2* | 0.56 | 0.87 | 0.99 |
| *BRRF1* | 0.76 | 0.90 | 76.84 |
| *BSLF1* | 0.02 | 0.17 | 297.1 |
| *BXLF1* | 0.99 | 0.32 | 1.30 |
| *BXRF1* | 0.73 | 1.24 | 1.60 |
| *LF1* | 1.62 | 0.44 | 1.42 |
| *LF2* | 0.98 | 0.47 | 1.02 |
| *LF3* | 0.55 | 0.43 | 0.74 |
| *BALF4* | 1.15 | 0.40 | 0.76 |
| *BBLF1* | 0.79 | 0.49 | 0.27 |
| *BBRF1* | 0.31 | 0.43 | 0.28 |
| *BBRF2* | 0.99 | 0.41 | 0.11 |
| *BBRF3* | 0.83 | 0.37 | 0.32 |
| *BcLF1* | 0.69 | 1.11 | 0.51 |
| *BCRF1* | 0.65 | 0.76 | 1.06 |
| *BDLF1* | 1.99 | 1.09 | 0.22 |
| *BDLF2* | 0.89 | 1.29 | 1.19 |
| *BDLF3.5* | 1.10 | 0.18 | 0.16 |
| *BDLF3* | 1.08 | 1.02 | 1.20 |
| *BDRF1/ BGRF1* | 0.85 | 0.49 | 0.92 |
| *BdRF1* | - | - | - |
| *BFLF1* | 1.29 | 0.33 | 0.44 |
| *BFLF2* | 0.36 | 0.55 | 0.89 |
| *BFRF1A* | 0.80 | 0.32 | 1.10 |
| *BFRF3* | 0.14 | 1.35 | 0.76 |
| *BGLF1* | 1.32 | 0.30 | 0.56 |
| *BGLF2* | 1.09 | 0.36 | 0.53 |

| | | | |
|---|---|---|---|
| *BGLF3.5* | 0.76 | 0.41 | 0.28 |
| *BGLF3* | 0.41 | 0.25 | 0.26 |
| *BGRF1/BDRF1* | 0.65 | 0.77 | 0.24 |
| *BILF1-gp64* | 1.01 | 0.53 | 0.81 |
| *BILF2-gp78/55* | 0.49 | 0.89 | 1.33 |
| *BKRF2-gp25* | 0.75 | 0.86 | 0.65 |
| *BKRF4* | 1.33 | 1.14 | 1.34 |
| *BLLF1a* | 1.11 | 0.19 | 0.56 |
| *BLLF1b* | - | - | - |
| *BLRF1* | 1.15 | 0.30 | 0.49 |
| *BLRF2* | 3.67 | 0.48 | 0.92 |
| *BMRF2* | 0.68 | 0.26 | 2.95 |
| *BNRF1* | 0.38 | 1.17 | 0.32 |
| *BOLF1* | | | |
| *BORF1* | 1.12 | 1.31 | - |
| *BPLF1* | 10.83 | 0.64 | 1.48 |
| *BRRF2* | 1.12 | 0.49 | 0.61 |
| *BSRF1* | 1.13 | 0.55 | 0.67 |
| *BTRF1* | 0.65 | 0.72 | 0.43 |
| *BVRF1* | 1.11 | 0.87 | 2.48 |
| *BVRF2* | 0.85 | 0.94 | 0.46 |
| *BWRF1* | 2.06 | 0.56 | 0.32 |
| *BXLF2* | 1.17 | 1.88 | 4.55 |
| *BVLF1* | 0.86 | 0.71 | 0.54 |
| *BZLF2-gp42 ** | - | - | - |
| *A73/ RPMS1 splice* | - | - | - |
| *BARF0* | - | - | - |
| *EBER-1* | 0.68 | 1.03 | 1.29 |
| *EBNA-1* | 0.79 | 1.29 | 0.80 |
| *EBNA-2* | 1.01 | 1.55 | 0.59 |
| *EBNA-3A* | 1.49 | 0.58 | 0.23 |
| *EBNA-3B* | 1.55 | 0.49 | 0.43 |
| *EBNA-3C* | - | - | - |
| *EBNA-LP* | 1.25 | 0.54 | 0.72 |
| *LMP-1* | 1.01 | 0.88 | 1.37 |
| *LMP-2A / 2B* | 1.03 | 0.85 | 0.96 |

-, not detected

**Table 7-2 Summary of the top 191 highly differentially expressed and regulated probe sets identified from the Affymetrix HG U133 Plus 2.0 GeneChip® array in response to EBV lytic induction in Raji cells (ranked by fold-change)**

| Probe set ID | Gene name & symbol | GO biological | GO molecular function | GO cellular component | Fold-change | Regulation in TPA/NaB treated Ramos cells (*n*=58) |
|---|---|---|---|---|---|---|
| 209395_at | chitinase 3-like 1 (cartilage glycoprotein-39) (CHI3L1) | Carbohydrate metabolic process Chitin catabolic process | Catalytic activity | Extracellular | 18.1 | |
| 201105_at | lectin, galactoside-binding, soluble, 1 (LGALS1) | Apoptosis; regulation of apoptosis; positive regulation of NF-kappaB cascade | Glycoprotein binding; signal transducer activity | Extracellular region | 17 | 17.2 |
| 220468_at | ADP-ribosylation factor-like 14 (ARL14) | Small GTPase mediated signal transduction | Nucleotide binding/GTP binding | Intracellular | 16.1 | |
| 205249_at | early growth response 2 (EGR2) | Transcription/regulation of transcription | Nucleic acid binding | Intracellular/nucleus | 15.7 | 14.6 |
| 224225_s_at | ets variant 7 (ETV7) | Regulation of transcription | DNA binding/Transcription factor activity | nucleus | 15.2 | |
| 201666_at | TIMP metallopeptidase inhibitor 1 (TIMP1) | Positive regulation of cell proliferation/Negative regulation of membrane protein | Enzyme inhibitor activity/protein binding/metalloendopeptidase inhibitor activity | Extracellular region/proteinaceous extracellular matrix | 14.7 | 15.2 |
| 220513_at | hypothetical protein LOC100129128 (RP11-257K9.7) | n/a | n/a | n/a | 14.6 | |
| 204179_at | myoglobin (MG) | Response to hypoxia/transport | Oxygen transporter activity/iron, oxygen, heme and metal ion binding | n/a | 13.2 | 15.1 |
| 225842_at | pleckstrin homology-like domain, family A, member 1(PHLDA1) | Apoptosis/Induction of apoptosis; FasL biosynthetic process | Protein binding | nucleus | 13.1 | |
| 213112_s_at | sequestosome 1 (SQSTM1) | Ubiquitin-dependent protein catabolic | Protein kinase C binding | Nucleus/cytoplasm/endosome | 12.4 | |

| | | | | | | |
|---|---|---|---|---|---|---|
| | | process/apoptosis/response to stress/intracellular signaling | | | | |
| 217996_at | pleckstrin homology-like domain, family A, member 1 (PHLDA1) | Apoptosis/Induction of apoptosis; FasL biosynthetic process | Protein binding | nucleus | 11.8 | |
| 206632_s_at | apolipoprotein B mRNA editing enzyme, catalytic polypeptide-like 3B (APOBEC3B) | n/a | RNA binding/Catalytic binding | mitochondrion | 11.4 | 5.3 |
| 201694_s_at | early growth response 1(EGR1) | Positive and negative regulation of transcription from RNA polymerase II promoter | Nucleic acid binding | Intracellular nucleus | 11.2 | 12.9 |
| 230966_at | interleukin 4 induced 1 (IL4I1) | Oxidation reduction | L-amino acid oxidase activity | cytosol | 11 | 12.2 |
| 202252_at | RAB13, member RAS oncogene family (RAB13) | Transport/Cell adhesion/Small GTPase mediated signal transduction | nucleotide binding/GTPase activity/GTP binding | Cytoplasm/Golig body/Cell junction | 10.9 | 11.4 |
| 209969_s_at | signal transducer and activator of transcription 1, 91kDa (STAT1) | Regulation of transcription/signal transduction/response to virus/induction of apoptosis/DNA dependent RNA transcription from polymerase II promoter/ I-kappaB kinase/NF-kappaB cascade JAK-STAT cascade | DNA binding transcription factor activity signal transducer activity hematopoietin/interferon-class (D200-domain) cytokine receptor signal transducer activity calcium ion binding protein binding sequence-specific DNA binding | Nucleus/nucleolus/cytoplasm/axon/dendrite | 10.3 | |
| 201693_s_at | early growth response 1 (EGR1) | Positive and negative regulation of transcription from RNA polymerase II promoter | Nucleic acid binding | Intracellular nucleus | 10.3 | |
| 203915_at | chemokine (C-X-C motif) ligand 9 (CXCL9) | Chemotaxis/defense/inflammatory response/immune response/signal transduction/cell-cell signaling | Chemokine activity/ cytokine activity | extracellular region/extracellular space | 10.2 | |
| 202497_x_at | solute carrier | Carbohydrate metabolic | Transporter | Cytoplasm/plasma membrane | 10 | |

| | | | | | | |
|---|---|---|---|---|---|---|
| | family 2 (facilitated glucose transporter), member 3 (SLC2A3) | process/transport/ | activity/glucose transmembrane transporter activity | | | |
| 205352_at | serpin peptidase inhibitor, clade I (neuroserpin), member 1 (SERPINI1) | Central nervous system development/regulation of cell adhesion | Serine-type endopeptidase inhibitor activity/peptidase inhibitor activity | Extracellular region | 10 | 3.5 |
| 218986_s_at | DEAD (Asp-Glu-Ala-Asp) box polypeptide 60 (DDX60) | n/a | Nucleotide binding/ATP-dependent helicase activity | n/a | 9.7 | |
| 1405_i_at | chemokine (C-C motif) ligand 5 (CCL5) | Chronic inflammatory response/chemotaxis/cell adhesion/signal transduction/response to tumour necrosis factor/ negative regulation of viral genome replication | signal transducer activity/receptor binding/cytokine, chemokine and chemoattractant activity | Extracellular region/soluble fraction/cytoplasm | 9.6 | |
| 205660_at | 2'-5'-oligoadenylate synthetase-like (OASL) | Immune response | Nucleic acid binding/ATP binding/transferase activity/thyroid hormone receptor binding | Nucleolus/cytoplasm | 9.5 | |
| AFFX-HUMISGF3A/M97935_MB_at | signal transducer and activator of transcription 1, 91kDa (STAT1) | Regulation of transcription/signal transduction/response to virus/induction of apoptosis/DNA dependent RNA transcription from polymerase II promoter/ I-kappaB kinase/NF-kappaB cascade JAK-STAT cascade | nucleic acid binding/signal transducer activity/calcium, ion and DNA binding | Nucleus/nucleolus/cytoplasm/axon/dendrite | 9.1 | |
| 1555759_a_at | chemokine (C-C motif) ligand 5 (CCL5) (RANTES) | chronic inflammatory response/chemotaxis/cell adhesion/signal transduction/response to tumour necrosis factor/ negative regulation of viral genome replication | signal transducer activity/receptor binding/cytokine, chemokine and chemoattractant activity | extracellular region/soluble fraction/cytoplasm | 9 | |
| 202499_s_at | solute carrier family 2 (facilitated | carbohydrate metabolic process/glucose, carbohydrate and | transporter activity | Cytoplasm/plasma membrane/membrane/integral | 8.9 | |

| | | | | | | |
|---|---|---|---|---|---|---|
| | glucose transporter), member 3 (SLC2A3) | transmembrane transport | | to membrane | | |
| 209457_at | dual specificity phosphatase 5 (DUSP5) | protein amino acid dephosphorylation | phosphoprotein phosphatase activity/ MAP kinase tyrosine/serine/threonine phosphatise | Nucleus | 8.6 | 13.8 |
| 203868_s_at | vascular cell adhesion molecule 1 (VCAM1) | cell adhesion/cell-cell adhesion/leukocyte adhesion/membrane-membrane docking/B-cell differentiation/positive regulation of T cell proliferation | integrin binding/protein binding/cell adhesion molecule binding | Extracellular space/external side of plasma membrane | 8.6 | |
| 204655_at | chemokine (C-C motif) ligand 5 (CCL5) (RANTES) | chronic inflammatory response/chemotaxis/cell adhesion/signal transduction/response to tumour necrosis factor/ negative regulation of viral genome replication | signal transducer activity/receptor binding/cytokine, chemokine and chemoattractant activity | extracellular region/soluble fraction/cytoplasm | 8.4 | |
| 238542_at | UL16 binding protein 2 (ULBP2) | Immune response/antigen processing and presentation/natural killer cell activation | MHC class I receptor activity | Extracellular region/extracellular space./plasma membrane/cell surface/anchored to membrane/MHC class I protein complex | 8 | |
| 203153_at | interferon-induced protein with tetratricopeptide repeats 1 (IFIT1) | n/a | Binding | cytoplasm | 7.9 | |
| 204415_at | interferon, alpha-inducible protein 6 (IFI6) | Release of cytochrome c from mitochondria/anti-apoptosis/immune response/nregative regulation of caspase activity/negative regulation of mitochondrial depolarization | Protein binding | Mitochondrion/membrane/integral to membrane | 7.9 | |
| 202967_at | glutathione S-transferase alpha 4 | Metabolic process | Glutathione transferase activity/transferase activity | cytoplasm | 7.8 | |
| AFFX-HUMISGF3A/M9793 | signal transducer and activator of | Regulation of transcription/signal transduction/response to | nucleic acid binding/signal | Nucleus/nucleolus/cytoplasm/axon/dendrite | 7.6 | |

| | | | | | | |
|---|---|---|---|---|---|---|
| 5_3_at | transcription 1, 91kDa (STAT1) | virus/induction of apoptosis/DNA dependent RNA transcription from polymerase II promoter/ I-kappaB kinase/NF-kappaB cascade JAK-STAT cascade | transducer activity/calcium, ion and DNA binding | | | |
| 201531_at | zinc finger protein 36, C3H type, homolog (mouse) (ZFP36) | Nuclear-transcribed mRNA catabolic process/deadenylation-dependent decay/nuclear-transcribed mRNA poly(A) tail shortening/protein kinase C binding/regulation of mRNA stability/negative regulation of inflammatory response | Nucleic acid binding/zinc ion binding/AU-rich binding/metal ion binding | Nucleus/cytoplasm/cytosol | 7.3 | 5 |
| 204747_at | interferon-induced protein with tetratricopeptide repeats 3 (IFIT3) | n/a | Binding | n/a | 7 | |
| 208581_x_at | metallothionein 1X (MT1X) | Response to metal ion | Copper, zinc, cadmium and metal ion binding | n/a | 6.8 | |
| 204326_x_at | metallothionein 1X (MT1X) | Response to metal ion | Copper, zinc, cadmium and metal ion binding | n/a | 6.5 | |
| 229450_at | interferon-induced protein with tetratricopeptide repeats 3 (IFIT3) | n/a | Binding | n/a | 6.5 | |
| 201471_s_at | sequestosome 1(SQSTM1) | Ubiquitin-dependent protein catabolic process/apoptosis/response to stress/immune response/intracellular signalling cascade/cell differentiation/regulation of I-kappaB kinase/NF-kappaB cascade/positive regulation of transcription from RNA polymerase II promoter | Protein kinase C binding/protein binding/zinc ion binding/receptor tyrosine kinase binding/SH2 domain binding/uniquitin binding/metal ion binding | Nucleus/cytoplasm/endosome/ cytosol | 6.5 | |
| 205483_s_at | ISG15 ubiquitin-like modifier (ISG15) | Cell-cell signalling/response to virus/modification-dependent protein catabolic process/ISG15-protein conjugation interspecies interaction between organisms | Protein binding/protein tag | extracellular region, space/cytoplasm | 6.4 | |

| | | | | | | |
|---|---|---|---|---|---|---|
| 202388_at | regulator of G-protein signaling 2, 24kDa (RGS2) | Cell cycle/regulation of G-protein coupled receptor/signaling pathway/negative regulation of signal transduction | Signal transducer activity/GTPase activator activity/protein binding/calmodulin binding | n/a | 6.3 | RGS2 (202388_at) 3.8 |
| 200887_s_at | signal transducer and activator of transcription 1, 91kDa (STAT1) | ? | antigen binding | ? | 6.1 | |
| 212185_x_at | metallothionein 2A (MT2A) | Cellular copper ion homeostasis | Protein, zinc and metal ion binding | n/a | 6.1 | |
| 211456_x_at | metallothionein 1 pseudogene 2 (MT1P2) | n/a | n/a | n/a | 6.1 | |
| 201590_x_at | annexin A2 (ANXA2) | Skeletal system development/angiogenesis/body fluid secretion/collagen fibril/organisation/fibrinolysis | Phospholipase inhibitor activity/Binding etc | extracellular region/proteinasceous extracellular matrix/basement membrane/soluble fraction/cytoplasm etc | 5.9 | |
| 206461_x_at | metallothionein 1H (MT1H) | Cellular zinc ion homeostasis/nitric oxide mediated signal transduction/detoxification of copper ion | Copper, protein, zinc ion, cadmium ion and metal ion binding | n/a | 5.6 | |
| 204794_at | dual specificity phosphatase 2 (DUSP2) | | protein binding | endoplasmic reticulum | 5.6 | 7.6 |
| 202869_at | 2',5'-oligoadenylate synthetase 1, 40/46kDa (OAS1) | Inactivation of MAPK activity/protein amino acid dephosphorylation | Phosphoprotein phosphotase activity/MAP kinase tyrosine/serine/threonine phosphatase activity | Nucleus | 5.6 | |
| 210621_s_at | RAS p21 protein activator (GTPase activating protein) 1 | Cytokinesis/negative regulation of cell-matrix adhesion/signal transduction/intracellular signalling cascade/positive regulation of anti-apoptosis/regulation of small GTPase mediated signal transduction//regulation of RNA metabolic process | Glycoprotein binding/GTPase activator activity/Ras GTPase activator activity/receptor binding/protein binding/GTPase binding/potassium channel inhibitor | Ruffle/intracellular/cytoplasm/ ’plasma membrane | 5.4 | |
| 202677_at | RAS p21 protein | Cytokinesis/negative regulation of | Glycoprotein | Ruffle/intracellular/cytoplasm/ | 5.3 | |

| | | | | | | |
|---|---|---|---|---|---|---|
| | activator (GTPase activating protein) 1(RASA1) | cell-matrix adhesion/signal transduction/intracellular signalling cascade/positive regulation of anti-apoptosis/regulation of small GTPase mediated signal transduction//regulation of RNA metabolic process | binding/GTPase activator activity/Ras GTPase activator activity/receptor binding/protein binding/GTPase binding/potassium channel inhibitor | ’plasma membrane | | |
| 204141_at | tubulin, beta 2A (TUBB2) | Microtubule based process and movement/neuron differentiation/protein polymerisation | Nucleotide binding/GTPase activity/structural molecular activity/protein binding/GTP binding | Microtubule protein complex | 5.3 | |
| 209911_x_at | histone cluster 1, H2bd (HIST1H2BD) | Nucleosome assembly/defense response to bacterium | DNA binding/protein binding | Nucleosome/nucleus/chromosome | 5.3 | |
| 222572_at | pyruvate dehyrogenase phosphatase catalytic subunit 1 (PDP1) | Protein amino acid dephosphorylation | Magnesium ion binding/catalytic activity/phosphoprotein phosphatase /protein-serine threonine phosphatase activity/Binding | Mitochondrion/mitochondrial matrix/protein-serine threonine phosphatase complex | 5 | |
| 209795_at | CD69 molecule (CD69) | n/a | Transmembrane receptor activity/binding/calcium ion binding/sugar binding | Integral to plasma membrane/external side of plasma membrane/integral to membrane | 5 | 7.5 |
| 202446_s_at | phospholipid scramblase 1 (PLSCR1) | Response to virus/phospholipids scrambling/platelet activation | Calcium ion, protein and SH3 binding/phospholipid scramblase activity | Plasma membrane/membrane/integral to membrane | 5 | |
| 35820_at | GM2 ganglioside activator (GM2A) | Lipid, sphingolipid and ganglioside metabolic process/lipid transport/oligosaccharide, glycolipid, and sphingolipid process/neurological process/positive regulation of hydrolase activity | Beta-N-acetlyhexosaminidase activity/lipid transporter activity/enzyme activator activity/phospholipase activator activity/sphingolipid activator protein | Cytoplasm/mitochondrion/lysosome/hydrogen:potassium-exchanging ATPase complex/internal side of plasma membrane/apical cortex | 4.9 | |

| | | | | | | |
|---|---|---|---|---|---|---|
| | | | activity/beta-N-acetylgalactosaminidase activity | | | |
| 200866_s_at | prosaposin (PSAP) | Lipid metabolic protein/sphingolipid metabolic process/glycosphingolipid process/lipid transport | Enzyme activator activity/lipid binding | Extracellular space/mitochondrion/lysosome /golgi apparatus/integral to membrane/intracellular membrane-bounded organelle | 4.8 | 5.3 |
| 214211_at | ferritin, heavy polypeptide 1(FTH1) | Iron ion transport/cellular iron ion homeostasis/intracellular sequestering of iron ion/immune response/cell proliferation/negative regulation of cell proliferation/response to stimulus/oxidation reduction | Ferroxidase activity/ion channel activity/chloride channel activity/iron ion, calcium, protein, chloride, metal ion, transition metal ion and ferric iron binding/oxidoreductase activity | Membrane fraction/cytosol/plasma membrane/intracellular ferritin complex/integral to membrane/basolateral plasma membrane | 4.7 | |
| 216834_at | regulator of G-protein signaling 1(RGS1) | | phosphoprotein phosphatase activity | nucleus | 4.4 | 8.1 |
| 202081_at | immediate early response 2 (IER2) | n/a | n/a | cytoplasm | 4.4 | 3.1 |
| 207861_at | chemokine (C-C motif) ligand 22 (CCL22) | Chemotaxis/inflammatory response/immune response/signal transduction/cell-cell signalling/response to virus/cell migration | Cytokine and chemokine activity | Extracellular region and space | 4.4 | |
| 212573_at | endonuclease domain containing 1 (ENDOD1) | n/a | Nucleic acid binding, nuclease activity, endonuclease activity, hydrolase activity, metal ion binding | Extracellular region | 4.4 | |
| 207826_s_at | inhibitor of DNA binding 3, dominant negative helix-loop-helix protein (ID3) | Negative regulation of transcription from RNA polymerase II promoter/regulation of DNA replication/positive regulation of apoptosis/negative regulation of transcription factor activity/regulation of cell cycle/response to protein stimulus | Transcription/co-repressor activity/protein and transcription factor binding/transcription regulator activity | nucleus | 4.3 | |
| 201739_at | serum/glucocorticoi | Protein amino acid | Nucleotide | Nucleus/cytoplasm/endoplasmi | 4.2 | 11.4 |

| | | | | | | |
|---|---|---|---|---|---|---|
| | d regulated kinase 1 (SGK1) | phosphorylation/sodium ion transport/apoptosis/response to stress/response to DNA damage stimulus | binding/protein kinase activity/protein serine-threonine kinase activity/protein binding/ATP binding/transferase activity | c reticulum/plasma membrane/membrane | | |
| 212737_at | GM2 ganglioside activator (GM2A) | Lipid metabolic process/sphingolipid metabolic process/ganglioside metabolic process/lipid transport/lipid and sphingolipid catabolic process | Beta-N-acetylhexosaminidase activity/lipid transporter activity/enzyme activator activity/phospholipase activator activity/sphingolipid activator protein activity/ | Cytoplasm/mitochondrion/lysosome/hydrogen:potassium-exchanging ATPase complex internal side plasma membrane/apical cortex | 4.2 | 2.5 |
| 210592_s_at | spermidine/spermine N1-acetyltransferase 1(SAT1) | Polyamine/metabolic process/regulation of cell proliferation | Diamine N-acetyltransferase activity/protein binding/spermidine binding | Intracellular/soluble fraction/cytoplasm | 4.2 | |
| 205681_at | BCL2-related protein A1(BCL2A1) | Apoptosis/anti-apoptosis/regulation of apoptosis | Protein binding | cytoplasm | 4.2 | 10.6 |
| 201625_s_at | insulin induced gene 1 (INSIG1) | Lipid metabolic process/cell proliferation/ER-nuclear sterol response/metabolic response/ | Protein binding | Endoplasmic reticulum/integral membrane | 4.2 | |
| 200871_s_at | prosaposin (PSAP) | lipid metabolic process sphingolipid metabolic process glycosphingolipid metabolic process lipid transport | Enzyme activator activity/lipid binding | Extracellular space/mitochondrion/lysosome /golgi apparatus/integral to membrane/intracellular membrane-bounded organelle | 4.1 | 4.5 |
| 204533_at | chemokine (C-X-C motif) ligand 10 (CXCL10) | Chemotaxis/inflammatory response/signal transduction/cell surface receptor linked signal transduction/cell-cell signalling/positive regulation of cell proliferation | Receptor binding/cytokine activity/chemokine activity/cAMP-dependent protein kinase regulator activity | Extracellular region/space | 4 | |
| 221269_s_at | SH3 domain | Cell redox/homeostasis | Electron carrier | Nucleus/cytoplasm | 4 | 4.9 |

| | | | | | | |
|---|---|---|---|---|---|---|
| | binding glutamic acid-rich protein like 3 (SH3BGRL3) | | activity/protein disulfide/oxidoreductase activity | | | |
| 212907_at | Solute carrier family 30 (zinc transporter), member 1 (SLC30A1) | Transport | Zinc ion transmembrane transporter activity/zinc ion binding/cation transmembrane transporter activity | Plasma membrane/integral to membrane/intracellular membrane-bounded organelle | 4 | |
| 201845_s_at | RING1 and YY1 binding protein (RYBP) | Negative regulation of transcription from RNA polymerase II promoter/transcription/apoptosis | DNA binding/transcription/co-repressor activity/protein, zinc ion and metal ion binding | Intracellular/nucleus/nucleoplasm/cytoplasm | 4 | |
| 225083_at | general transcription factor IIIC, polypeptide 6, alpha 35kDa (GTF3C6) | Transcription/DNA-dependent 5S class rRNA transcription/tRNA transcription from RNA polymerase II promoter | DNA binding/RNA polymerase III transcription factor activity/protein binding | Transcription factor/TFIIIC complex,nucleus | 3.9 | |
| 201393_s_at | insulin-like growth factor 2 receptor (IGF2R) | Transport/receptor mediated-endocytosis/signal transduction/regulation of apoptosis | Glycoprotein binding/G-protein alpha-subunit binding/receptor activity/insulin-like growth factor receptor activity | Membrane fraction/nucleus/nuclear envelope lumen/cytoplasm/lysosome/endosome/golgi apparatus/integral to plasma membrane | 3.9 | |
| 225799_at | hypothetical LOC541471 non-protein coding RNA 152 LOC541471/NCRNA00152 | n/a | n/a | n/a | 3.8 | 10.4 |
| 203455_s_at | spermidine/spermine N1-acetyltransferase 1 (SAT1) | Polyamine/metabolic process/regulation of cell proliferation | diamine N-acetyltransferase activity | Intracellular soluble fraction/cytoplasm | 3.8 | |
| 205114_s_at | chemokine (C-C motif) ligand 3 (CCL3, | Cellular calcium ion homeostasis/exocytosis/chemotaxis/ inflammatory response/signal | Signal transducer activity/cytokine activity/chemokine | Extracellular region/extracellular space | 3.7 | |

| | | | | | | |
|---|---|---|---|---|---|---|
| | CCL3L1,CCL3L3) | transduction/G-protein coupled receptor/protein signalling pathway/cell-cell signalling/negative regulation of cell proliferation/regulation of viral genome replication | activity/chemoaatractant activity | | | |
| 224565_at | nuclear paraspeckle assembly transcript 1 (non-protein coding) (NEAT1) | n/a | n/a | n/a | 3.7 | 4.1 |
| 217732_s_at | integral membrane protein 2B (ITIM2B) | Apoptosis/induction of apoptosis | Protein and ATP binding | Golgi apparatus/integral to membrane | 3.5 | 3.6 |
| 204205_at | apolipoprotein B mRNA editing enzyme, catalytic polypeptide-like 3G (APOBEC3G) | Positive regulation of defense response to virus by host transcription/RNA dependent response to virus/innate immune response/negative regulation of retroviral genome replication/negative regulation of viral reproduction | RNA binding catalytic activitiy/cytidine deaminase activity/protein, zinc ion and metal ion binding/hydrolase activity/protein homodimerization activity | Nucleus/cytoplasm/nucleolus/ mitochondrion/cytosol/apolipoprotein B mRNA editing enzyme | 3.4 | |
| 201847_at | lipase A, lysosomal acid, cholesterol esterase (LIPA) | Cell morphogenesis/cytokine production/protein amino acid N-linked glycosylation/lipid metabolic process/fatty acid metabolic process/inflammatory response/cell proliferation/tissue remodelling | Sterole esterase activity/lipase activity/hydrolase activity | Extracellular region/lysosome | 3.3 | 4 |
| 201426_s_at | vimentin (VIM) | Cell motion/interspecies interaction between organisms/intermediate filament-based process | Structural molecule activity/structural constituent of cytoskeleton/protein binding/protein C-terminus binding/protein kinase binding | Cytoplasm/cytosol/cytoskeleton/intermediate filament/plasma membrane/axon | 3.3 | |
| 203752_s_at | jun D proto-oncogene (JUND) | Regulation of transcription/DNA-dependent regulation of transcription from RNA polymerase II promoter/ | DNA binding/transcription factor activity/RNA polymerase II transcription factor activity/protein binding sequence-specific | Chromatin/nucleus | 3.2 | 3.6 |

| | | | | | | |
|---|---|---|---|---|---|---|
| | | | DNA binding/protein dimerization activity | | | |
| 206310_at | serine peptidase inhibitor, Kazal type 2 (acrosin-trypsin inhibitor) (SPINK2) | n/a | Endopeptidase inhibitor activity/serine-type endopeptidase inhibitor activity/peptidase activity/peptidase inhibitor activity | Extracellular region | 3.2 | 11.2 |
| 211962_s_at | zinc finger protein 36, C3H type-like 1 (ZFP36L1) | Nuclear transcribed mRNA catabolic process/deadenylation-dependent decay/mRNA catabolic process/regulation of translation/regulation of mRNA stability | Nucleic acid binding/DNA binding transcription factor activity/mRNA binding/protein binding/zinc ion binding/AU-rich element binding/metal ion binding | Nucleus/cytoplasm/cytosol | 3.2 | 4.3 |
| 201627_s_at | insulin induced gene 1 (INSIG1) | Lipid metabolic process/response to sterol depletion/metabolic process/cell proliferation/ER-nuclear sterol response pathway | Protein binding | ER/membrane/integral to membrane | 3 | |
| 34210_at | CD52 molecule | Elevation of cytosolic calcium ion concentration/respiratory burst | n/a | Membrane fraction/plasma membrane/integral to plasma membrane/membrane anchored to membrane | 3 | |
| 212094_at | paternally expressed 10 (PEG10) | Proteolysis/apoptosis/cell differentiation/negative regulation of transforming growth factor beta receptor signalling pathway | Nucleic acid binding/DNA binding/aspartic-type endopeptidase activity/protein, zinc ion, and metal ion binding | Nucleus/cytoplasm | 3 | |
| 229872_s_at | hypothetical protein LOC100132999 | n/a | n/a | n/a | 3 | |
| 204661_at | CD52 molecule | Elevation of cytosolic calcium ion concentration/respiratory burst | n/a | Membrane fraction/plasma membrane/integral to plasma membrane/membrane anchored to membrane | 2.9 | |
| 201251_at | pyruvate kinase, muscle (PKM2) | Glycolysis programmed cell death | Nucleotide binding/magnesium ion binding/catalytic | Nucleus/cytoplasm/cytosol | 2.8 | |

| | | | | | |
|---|---|---|---|---|---|
| | | | activity/pyruvate kinase activity/protein binding/ATP binding/kinase activity/transferase activity/potassium ion binding/metal ion binding | | |
| 213164_at | solute carrier family 5 (sodium/myo-inositol cotransporter), member 3 (SLC5A3) | Inositol metabolic process/transport (ion, sodium ion, myo inositol), transmembrane transport | transporter activity/myo-inositol:sodium symporter activity/sodium ion binding | integral to plasma membrane/integral to membrane | 2.8 |
| AFFX-M27830_M_at | | n/a | n/a | n/a | 2.7 |
| 212944_at | solute carrier family 5 (sodium/myo-inositol cotransporter), member 3 (SLGA3) | Inositol metabolic process/transport (ion, sodium ion, myo inositol), transmembrane transport | transporter activity/myo-inositol:sodium symporter activity/sodium ion binding | integral to plasma membrane/integral to membrane | 2.6 |
| 202362_at | RAP1A, member of RAS oncogene family (RAP1A) | Signal transduction/small GTPase mediated signal transduction | nucleotide binding/GTPase activity/protein binding/GTP binding/Ras GTPase binding | Intracellular/cytosol/plasma membrane/anchored to membrane/guanyl-nucleotide exchange factor complex | 2.4 |
| 208881_x_at | isopentenyl-diphosphate delta isomerase 1 (IDI1) | Steroid, lipid, cholesterol, carotenoid and isoprenoid biosynthetic process | magnesium ion binding isopentenyl-diphosphate delta-isomerase activity hydrolase activity isomerase activity metal ion binding ... | Peroxisome/cytosol | 2.4 |
| 204897_at | prostaglandin E receptor 4 (subtype EP4) (PTGER4) | Immune response/signal transduction/G-protein coupled receptor protein signaling pathway/G-protein signaling/coupled to cAMP | Signal transducer activity/receptor activity/G-protein coupled receptor activity/ | Plasma membrane/membrane/integral to membrane | 2.4 |

| | | | | | | |
|---|---|---|---|---|---|---|
| | | nucleotide second messenger | | | | |
| 202693_s_at | serine/threonine kinase 17a (STK17A) | Protein amino acid phosphorylation/apoptosis/induction of apoptosis/protein kinase cascade | Nucleotide binding/protein kinase activity/protein serine/threonine kinase activity/ATP binding/kinase activity/transferase activity | nucleus | 2.4 | |
| 201626_at | insulin induced gene 1(INSIG1) | Lipid metabolic process/response to sterol depletion/metabolic process/cell proliferation/ER-nuclear sterol response pathway | Protein binding | ER/membrane/integral to membrane | 2.3 | |
| 200748_s_at | ferritin, heavy polypeptide 1(FTH1) | Iron ion transport/cellular iron ion homeostasis/intracellular sequestering of iron ion/immune response/cell proliferation/negative regulation of cell proliferation/response to stimulus/oxidation reduction | Ferroxidase activity/ion channel activity/chloride channel activity/iron ion, calcium, protein, chloride, metal ion, transition metal ion and ferric iron binding/oxidoreductase activity | Membrane fraction/cytosol/plasma membrane/intracellular ferritin complex/integral to membrane/basolateral plasma membrane | 2.25 | |
| 200046_at | defender against cell death 1 (DAD1) | Apoptosis/antiapoptosis/response to nutrient protein amino acid N-linked glycosylation via asparagine/response to drug | dolichyl-diphosphooligosaccharide-protein glycotransferase activity transferase activity | oligosaccharyltransferase complex membrane integral to membrane | 2.25 | 2.5 |
| 201201_at | cystatin B (stefin B) (CSTB) | Negative regulation of peptidase activity/regulation of apoptosis | Protease binding/endopeptidase inhibitor activity/cysteine-type endopeptodase inhibitor activity/peptidase inhibitor activity | Intracellular/nucleus/nucleolus /cytoplasm | 2.25 | |
| 36553_at | acetylserotonin O-methyltransferase-like (ASMTL) | Melatonin/biosynthetic process | methyltransferase activity O-methyltransferase activity transferase activity acetylserotonin O- | cytoplasm | 2.25 | |

| | | | | | | |
|---|---|---|---|---|---|---|
| | | | methyltransferase activity | | | |
| 206074_s_at | high mobility group AT-hook 1 (HMGA1) | DNA unwinding during replication/nucleosome disassembly/loss of chromatin silencing/regulation of transcription/DNA-dependent protein complex assembly/provirus integration/initiation of viral infection/interspecies interaction between organisms/ | DNA binding/AT DNA binding/transcription factor activity/protein binding/transcription factor binding/enzyme binding/retinoic acid receptor binding | Chromatin/nucleus/transcription factor complex/chromosome/cytosol | 2.2 | |
| 200905_x_at | major histocompatibility complex, class I, E (HLA-E) | Antigen processing and presentation of peptide antigen via MHC class I/immune response/antigen processing and presentation | MHC class I receptor activity | Plasma membrane/membrane/integral to membrane/MHC class I protein complex | 2.1 | 4.2 |
| 201106_at | glutathione peroxidase 4 (phospholipid hydroperoxidase) (GPX4) | Chromatin organisation/phospholipid and glutathione metabolic process/response to oxidative stress/regulation of inflammatory response | Peroxidise activity/glutathione peroxidise activity/selenium binding/oxidoreductase activity/glutathione binding/phospholipid hydroperoxidase/glutathione peroxidise activity | Soluble fraction/nucleus/nuclear envelope/cytoplasm/mitochondiron/cytosol | 2.1 | |
| 200004_at | eukaryotic translation initiation factor 4 gamma, 2 (EIF4G2) | Translation/regulation of translational initiation/cell cycle arrest/cell death/RNA metabolic process | Translation initiation factor activity/protein binding/nucleic acid binding | Cytoplasm/eukaryotic translation/intitiation factor 4F complex | -2 | -2.3 |
| 200772_x_at | prothymosin, alpha (PTMA) | Transcription | n/a | nucleus | -2.1 | |
| 208672_s_at | splicing factor, arginine/serine-rich 3 (SFRS3) | Nuclear mRNA splicing via spliceosome/mRNA processing/RNA splicing | nucleotide binding/nucleic acid binding/RNA and protein binding | nucleus | -2.2 | |
| 208956_x_at | deoxyuridine triphosphatase (DU2) | nucleobase, nucleoside, nucleotide and nucleic acid metabolic process DNA replication nucleotide metabolic process dUTP metabolic process | magnesium ion binding dUTP diphosphatase activity protein binding hydrolase activity | Nucleus/mitochondrion/cytosol | -2.25 | |

| | | | | | | |
|---|---|---|---|---|---|---|
| 201930_at | minichromosome maintenance complex component 6 (MCM6) | DNA replication/DNA unwinding during replication/DNA replication inititation/transcription/cell cycle/regulation of transcription | Nucleotide binding/DNA binding/DNA helicase activity/ssDNA binding/protein binding/ATP binding/identical protein binding | Nucleus/cytoplasm | -2.25 | |
| 205133_s_at | heat shock 10kDa protein 1 (chaperonin 10) (HSPE1) | Protein folding/activation of caspase activity/response to stress/response to unfolded protein | Protein binding/ATP binding/unfolded protein binding/chaperone binding | Cytoplasm/mitochondrion/mitochondrial matrix | -2.25 | -2.4 |
| 211714_x_at | tubulin, beta (TUBB) | Cell motion/microtubule based movement/mitosis/natural killer cell mediated cytotoxicity/spindle assemble/protein polymerisation | Nucleotide binding/GTPase activity/structural molecule activity/structural constituent of cytoskeleton/GTP binding/MHC class I protein binding | Cytoskeleton/microtubule/flotillin complex/protein complex | -2.3 | |
| 40189_at | SET nuclear oncogene (SET) | DNA replication/nucleosome assembly/nucleosome disassembly/nucleocytoplasmic transport/negative regulation of histone acetylation | Phosphoprotein phosphatise inhibitor activity/protein binding/protein phosphatise type 2A regulator activity/histone binding | Nucleus/nucleoplasm/cytoplasm/ER/cytosol/perinuclear region of cytosol | -2.3 | |
| 211921_x_at | prothymosin, alpha (PTMA) | Transcription | n/a | nucleus | -2.4 | |
| 221952_x_at | TRM5 tRNA methyltransferase 5 homolog (S. cerevisiae) (TRM5) | tRNA processing | methyltransferase activity tRNA (guanine-N1-)-methyltransferase activity transferase activity | cytoplasm | -2.4 | -3.1 |
| 213047_x_at | SET nuclear oncogene (SET) | DNA replication/nucleosome assembly/nucleosome disassembly/nucleocytoplasmic transport/negative regulation of histone acetylation | Phosphoprotein phosphatise inhibitor activity/protein binding/protein phosphatise type 2A | Nucleus/nucleoplasm/cytoplasm/ER/cytosol/perinuclear region of cytosol | -2.4 | |

| | | | | | | |
|---|---|---|---|---|---|---|
| | | | regulator activity/histone binding | | | |
| 221505_at | acidic (leucine-rich) nuclear phosphoprotein 32 family, member E (ANP32E) | | Protein binding phosphatase inhibitor activity | Nucleus/cytoplasm/cytoplasmic membrane-bounded vesicle | -2.4 | |
| 206976_s_at | heat shock 105kDa/110kDa protein 1 (HSPH1) | Response to stress/response to unfolded protein/chaperone mediated protein folding requiring cofactor | Nucleotide binding/protein binding/ATP binding | cytoplasm | -2.5 | |
| 214938_x_at | high-mobility group box 1 (HMGB1) | DNA unwinding during replication/DNA repair/base-excision repair/DNA ligation/DNA recombination/chromatin organisation/regulation of transcription from RNA polymerase II promoter/anti-apoptosis/signal transduction/negative regulation of transcriptional preinitiation complex assembly | DNA binding/protein binding/transcription factor binding/DNA bending activity | Condensed chromosome/nucleus/chromosome/nucleolus | -2.6 | |
| 212592_at | immunoglobulin J polypeptide, linker protein for immunoglobulin alpha and mu polypeptides (IGJ) | Immune response | antigen binding | Extracellular | -2.6 | |
| 209026_x_atD | tubulin, beta (TUBB) | Cell motion/microtubule based movement/mitosis/natural killer cell mediated cytotoxicity/spindle assemble/protein polymerisation | Nucleotide binding/GTPase activity/structural molecule activity/structural constituent of cytoskeleton/GTP binding/MHC class I protein binding | Cytoskeleton/microtubule/flotillin complex/protein complex | -2.6 | -2.0 |
| 212330_at | transcription factor Dp-1 (TFDP1) | Transcription/regulation of transcription/DNA-dependent regulation of transcription from RNA polymerase II promoter/cell cycle/cell proliferation/regulation of transcription | DNA binding/transcription factor activity/transcription coactivator activity/transcription | Nucleus/nucleoplasm/transcription factor complex | -2.6 | |

| | | | | | | |
|---|---|---|---|---|---|---|
| | | | factor binding/protein domain/specific binding | | | |
| 201051_at | acidic (leucine-rich) nuclear phosphoprotein 32 family, member (ANP32A) | Transcription/nucleocytoplasmic transport/intracellular signalling cascade/regulation of transcription | Protein binding | Nucleus/cytoplasm/ER/perinuclear region of cytoplasm | -2.6 | -2.4 |
| 202413_s_at | ubiquitin specific peptidase 1 (USP1) | DNA repair/regulation of DNA repair/ubiquitin-dependent protein catabolic process | Cysteine-type endopeptidase activity/protein binding/ | nucleus | -2.7 | -2.1 |
| 212320_at | Tubulin, beta (TUBB) | Cell motion/microtubule based movement/mitosis/natural killer cell mediated cytotoxicity/spindle assemble/protein polymerisation | Nucleotide binding/GTPase activity/structural molecule activity/structural constituent of cytoskeleton/GTP binding/MHC class I protein binding | Cytoskeleton/microtubule/flotillin complex/protein complex | -2.7 | -2.3 |
| 223062_s_at | phosphoserine aminotransferase 1 (PSAT1) | L-serine biosynthetic process/metabolic process/pyridoxine biosynthetic process/cellular amino acid biosynthetic process | catalytic activity O-phospho-L-serine:2-oxoglutarate aminotransferase activity transaminase activity transferase activity pyridoxal phosphate binding | kinetochore | -2.7 | -2.0 |
| 200754_x_at | splicing factor, arginine/serine-rich 2 (SFSR2) | Nuclear mRNA splicing, via spliceosome/mRNA processing/RNA splicing | Nucleotide binding/nucleic acid binding/transcription/co-repressor activity/RNA binding/protein binding | Nucleus/PML body/nuclear speck | -2.8 | |
| 201202_at | proliferating cell nuclear antigen (PCNA) | DNA replication/regulation of DNA replication/DNA repair/base-excision repair, gap-filling nucleotide-excision repair/DNA gap filling/mismatch repair/intracellular protein | purine-specific mismatch base pair DNA N-glycosylase activity DNA binding protein binding | cyclin-dependent protein kinase holoenzyme complex nucleus nuclear lamina nucleoplasm replication fork | -2.9 | |

| | | | | | | |
|---|---|---|---|---|---|---|
| | | transport/cell proliferation/phosphoinositide-mediated signaling | DNA polymerase processivity factor activity dinucleotide insertion or deletion binding MutLalpha complex binding | DNA replication factor C complex PCNA complex | | |
| 214882_s_at | splicing factor, arginine/serine-rich 2 | Nuclear mRNA splicing via spliceosome mRNA processing/RNA splicing | nucelotide binding/nucleic acid binding/transcription/corepressor activity/RNA binding/protein binding | nucleus/PML body/nuclear speck | -2.9 | |
| 227517_s_at | growth arrest-specific 5 (non-protein coding) (GAS5) | n/a | n/a | n/a | -2.9 | |
| 202546_at | vesicle-associated membrane protein 8 (endobrevin) (VAMP8) | Protein complex assembly/membrane fusion/vesicle-mediated transport | Protein binding | Membrane fraction/early endosome/membrane/integral to membrane/SNARE complex | -2.9 | |
| 201112_s_at | CSE1 chromosome segregation 1-like (yeast)(CSE1L) | Protein import into nucleus/docking transport/intracellular protein transport/apoptosis/cell proliferation/protein transport | Binding/protein binding/importin-alpha export/receptor activity/protein transporter activity | Nucleus/nuclear pore/cytoplasm | -3 | CSE1L (201112_s_at) -2.2 |
| 200875_s_at | NOP56 ribonucleoprotein homolog (yeast) (NOP56) | rRNA processing/ribosome biogenesis | RNA binding/protein binding/snoRNA binding | Nucleus/nucleolus/small nuclear ribonucleoprotein complex box C/D snoRNP complex/pre-snoRNP complex | -3 | -2.5 |
| 211929_at | heterogeneous nuclear ribonucleoprotein A3 (HNRNPA3) | Nuclear mRNA splicing via spliceosome/mRNA processing/RNA splicing | Nucleotide binding/nucleic acid binding/RNA binding/protein binding | Nucleus/spliceosomal complex/nucleolus/cytoplasm/ribonucleoprotein complex | -3 | |
| 200680_x_at | high-mobility group box 1 (HMGB1) | DNA unwinding during replication/DNA repair/base-excision repair/DNA ligation/DNA recombination/chromatin organisation/regulation of transcription from RNA polymerase | DNA binding/protein binding/transcription factor binding/DNA bending activity | Condensed chromosome/nucleus/chromosome/nucleolus | -3.1 | |

| | | | | | |
|---|---|---|---|---|---|
| | | II promoter/anti-apoptosis/signal transduction/negative regulation of transcriptional preinitiation complex assembly | | | |
| 201306_s_at | acidic (leucine-rich) nuclear phosphoprotein 32 family, member B (ANP32B) | n/a | Protein binding | nucleus | -3.1 |
| 224578_at | regulator of chromosome condensation 2 (RCC2) | Cell cycle/mitosis/cell division | n/a | Chromosome/centromeric region/nucleus/nucleolus/spindle/microtubule | -3.1 |
| 224731_at | high-mobility group box 1 (HMGB1) | DNA unwinding during replication/DNA repair/base-excision repair/DNA ligation/DNA recombination/chromatin organisation/regulation of transcription from RNA polymerase II promoter/anti-apoptosis/signal transduction/negative regulation of transcriptional preinitiation complex assembly | DNA binding/protein binding/transcription factor binding/DNA bending activity | Condensed chromosome/nucleus/chromosome/nucleolus | -3.2 |
| 201305_x_at | acidic (leucine-rich) nuclear phosphoprotein 32 family, member B (ANP32B) | n/a | Protein binding | nucleus | -3.3 |
| 216250_s_at | leupaxin (LPXN) | Protein complex assembly/cell adhesion/signal transduction | Zinc ion binding/metal ion binding | cytoplasm | -3.3 |
| 201277_s_at | heterogeneous nuclear ribonucleoprotein A/B (HNRNPAB) | Epithelial to mesenchymal transition/positive regulation of gene-specific transcription/negative regulation of transcription, DNA-dependent | Nucleotide binding/nucleic acid binding/DNA replicaion origin binding transcription factor activity/RNA binding/mRNA binding/protein binding sequence-specific DNA binding | Nucleus/cytoplasm/ribonucleoprotein complex | ? |
| 204674_at | lymphoid-restricted membrane protein | Vesicle targeting/vesicle fusion | n/a | Cytoplasm/ER/ER membrane/integral to | -3.4 |

| | | | | | | |
|---|---|---|---|---|---|---|
| | (LRMP) | | | plasmamembrane/membrane/integral to membrane | | |
| 209773_s_at | ribonucleotide reductase M2 (RRM2) | DNA replication/deoxyribonucleotide metabolic process/oxidation reduction | Ribonucleotide-diphosphate reductase activity/iron ion binding/protein binding/oxidoreductase activity/metal ion binding/transition metal ion binding | Cytoplasm/cytosol | -3.4 | -2.4 |
| 1555812_a_at | Rho GDP dissociation inhibitor (GDI) beta (ARHGDIB) | Cell motion/immune response/negative regulation of cell adhesion/Rho protein signal transduction/actin cytoskeleton organization | Rho GDP-dissociation inhibitor activity/GTPase activator activity/protein binding | Cytoplasm/cytoskeleton/cytoplasmic membrane-bounded vesicle | -3.4 | |
| 215780_s_at | SET translocation (myeloid leukemia-associated) pseudogene (hCG_1644608 SET) | DNA replication/nucleosome assembly/nucleosome disassembly/nucleocytoplasmic transport/negative regulation of histone acetylation | Phosphoprotein/phosphatase inhibitor activity/protein binding/protein phosphatise type 2A regulator activity histone binding | Nucleus/nucleoplasm/cytoplasm/ER/cytosol/perinuclear region of cytoplasm | -3.4 | |
| 200806_s_at | heat shock 60kDa protein 1 (chaperonin) (HSPD1) | B cell cytokine production (IL-6, 10, 12)/MyD88-dependent toll-like receptor signalling pathway positive regulation of T cell mediated immune response to tumour cell/protein folding/B-cell proliferation/positive and negative regulation of apoptosis | Nucleotide binding/lipopolysaccharide binding/p53 binding/DNA replication origin binding/ssDNA binding/protein binding/ATP binding/ATPase activity/cell surface binding/unfolded protein binding/chaperone binding | Extracellular space/cytoplasm/mitochondrion/cytosol/cell surface | -3.5 | -3.1 |
| 201516_at | spermidine synthase (SRM) | Spermidine biosynthetic process | Catalytic activity/spermidine synthase activity/transferase activity | n/a | -3.5 | -3.3 |
| 209932_s_at | deoxyuridine triphosphatase | nucleobase, nucleoside, nucleotide and nucleic acid metabolic process | magnesium ion binding dUTP diphosphatase | Nucleus/mitochondrion/cytosol | -3.6 | |

| | | | | | | |
|---|---|---|---|---|---|---|
| | (DU2) | DNA replication<br>nucleotide metabolic process<br>dUTP metabolic process | activity<br>protein binding<br>hydrolase activity | | | |
| 35974_at | lymphoid-restricted membrane protein (LRMP) | Vesicle targeting/vesicle fusion | n/a | Cytoplasm/ER/ER membrane/integral to plasmamembrane/membrane/integral to membrane | -3.6 | |
| 214141_x_at | splicing factor, arginine/serine-rich 7, 35kDa (SFRS7) | Nuclear mRNA splicing, via spliceosome/mRNA processing/RNA splicing | nucelotide binding/nucleic acid binding/RNA binding/protein binding/zinc ion binding/metal ion binding | nucleus | -3.7 | -2.0 |
| 228273_at | No gene symbol | n/a | n/a | n/a | -3.7 | |
| 210448_s_at | purinergic receptor P2X, ligand-gated ion channel, 5 (P2RX5) | Transport/ion transport/signal transduction/positive regulation of calcium ion transport into cytosol | Purinergic nucleotide receptor activity/transmembrane receptor activity/ATP-gated cation channel activity | Integral to plasmamembrane/integral to membrane | -3.7 | |
| 202503_s_at | KIAA0101 | n/a | nucelotide binding | Nucleus/mitochondrion | -3.8 | |
| 219117_s_at | FK506 binding protein 11, 19 kDa (FKBP11) | Protein folding | peptidyl-prolyl cis-trans isomerase activity<br>isomerase activity | Membrane/integral to membrane | -3.8 | |
| 202899_s_at | splicing factor, arginine/serine-rich 3 (SFRS3) | Nuclear mRNA splicing, via spliceosome/mRNA processing/RNA splicing | Nucleotide binding/nucleic acid binding/RNA binding/protein binding | nucleus | -3.8 | |
| 217301_x_at | retinoblastoma binding protein 4 (RBBP4) | DNA replication/chromatin remodelling/transcription/cell cycle/negative regulation of cell proliferation/chromatin modification/regulation of transcription | protein binding<br>DNA-dependent ATPase activity<br>histone binding<br>histone deacetylase binding | Nucleus/sin3/Nu3D complex | -3.8 | |
| 201664_at | structural maintenance of chromosomes 4 (SMC4) | Mitotic sister chromatid segregation/cell cycle/mitosis/cell division | Nucleotide binding/protein binding/ATP binding/protein heterodimerization activity | Condensing complex/nucleus/chromosome/cytoplasm | -4 | |

| | | | | | | |
|---|---|---|---|---|---|---|
| 200896_x_at | hepatoma-derived growth factor (high-mobility group protein 1-like (HDGF1) | Transcription/signal transduction/cell proliferation/regulation of transcription | nucelotide binding/DNA binding/growth factor activity/heparin binding | Extracellular space/nucleus/cytoplasm | -4 | |
| 202483_s_at | RAN binding protein 1 (RANBP1) | Spindle organization/signal transduction/positive regulation of mitotic centrosome separation/intracellular transport | GDP-dissociation inhibitor activity/GTPase activator activity/protein binding/Ran GTPase binding | Nucleus/cytoplasm/centrosome | -4.1 | -2.4 |
| 201897_s_at | CDC28 protein kinase regulatory subunit 1B (CKS1B) | Regulation of cyclin-dependent protein kinase activity/cell cycle/cell proliferation/cell division | Protein binding kinase activity/cyclin-dependent protein kinase regulator activity | nucleoplasm | -4.1 | -2.8 |
| 203302_at | deoxycytidine kinase (DCK) | Deoxycytidine metabolic process | Nucleotide binding/magnesium ion binding/ATP binding/drug binding/deoxycytidine kinase activity | Nucleus/cytosol | -4.1 | |
| 201477_s_at | ribonucleotide reductase M1 (RRM1) | DNA replication/deoxyribonucleotide biosynthetic process/protein oligomerization/oxidation reduction | Nucleotide binding/ribonucleoside-diphosphate reductase activity/protein binding/ATP binding/oxidoreductase activity/purine nucleotide binding | Cytoplasm/cytosol/ribonucleoside-diphosphate reductase complex | -4.2 | -2.7 |
| 218039_at | nucleolar and spindle associated protein 1 (NUSAP1) | Mitotic sister chromatid segregation/cell cycle/cell division/positive regulation of mitosis | DNA binding/microtubule binding | Nucleus/nucleolus/cytoplasm/spindle/microtubule/spindle microtubule | -4.2 | |
| 219014_at | placenta-specific 8 (PLAC8) | n/a | n/a | n/a | -4.7 | |
| 225310_at | RNA binding motif protein, X-linked (RBMX) | Nuclear mRNA splicing via spliceosome/mRNA processing/RNA splicing | Nucleotide binding/nucleic acid binding/RNA binding/protein binding | Nucleus/spliceosomal complex/ribonucleoprotein complex/heterogeneous nuclear ribonucleoprotein complex | -4.8 | -3.6 |

| | | | | | | |
|---|---|---|---|---|---|---|
| 228153_at | ring finger protein 144B (RNF144B) | Apoptosis/modification-dependent protein catabolic process/protein ubiquination during ubiquitin-dependent protein catabolic process | Ubiquitin-protein ligase activity/protein binding/zinc ion binding ligase activity/metal ion binding | Ubiquitin ligase complex/membrane/integral to membrane | -5 | -3.3 |
| 226319_s_at | THO complex 4 (THOC4) | Nuclear mRNA splicing via spliceosome/mRNA processing/RNA splicing/mRNA export from nucleus transport/RNA splicing/intronless viral mRNA export from host nucleus/mRNA transport | Nucleotide binding/nucleic acid binding/RNA binding/protein binding | Transcription export complex/nucleus/spliceosomal complex/cytoplasm/nuclear speck | -5.1 | -3.4 |
| 225834_at | family with sequence similarity 72, member A | n/a | n/a | n/a | -5.2 | |
| 208808_s_at | high-mobility group box 2 (HMGB2) | DNA unwinding during replication/DNA repair/base-excision repair/DNA ligation/DNA recombination/chromatin organisation/regulation of transcription from RNA polymerase II promoter/anti-apoptosis/signal transduction/negative regulation of transcriptional preinitiation complex assembly | DNA binding/protein binding/transcription factor binding/DNA bending activity | Condensed chromosome/nucleus/chromosome/nucleolus | -5.3 | |
| 203362_s_at | MAD2 mitotic arrest deficient-like 1 (yeast) (MAD2L1) | Mitotic sister chromatid segregation/cell cycle/mitosis/mitotic cell cycle checkpoint/cell division | Protein binding/protein homodimerization activity | Chromosome/centromeric region/kineotochore/nucleus/cytoplasm | -5.3 | -2.6 |
| 203213_at | cell division cycle 2, G1 to S and G2 to M (CDC2) | Protein amino acid phosphorylation/anti-apoptosis/cell cycle/mitosis/anaphase-promoting complex-dependent proteasomal ubiquitin-dependent protein catabolic process/cell division/ | nucelotide binding/protein kinase activity/protein serine-threonine kinase activity/cyclin-dependent protein kinase activity/protein binding/ATP binding/RNA polymerase II carboxy-terminal domain kinase activity/ | Nucleus/cytoplasm/cytosol/spindle/microtubule midbody | -5.4 | -2.2 |
| 203755_at | budding | Apoptosis/cell cycle/spindle | nucelotide | Kinetochore/condensed | -5.5 | |

| | | | | | | |
|---|---|---|---|---|---|---|
| | uninhibited by benzimidazoles 1 homolog beta (yeast) (BUB1B) | organization/mitosis | binding/protein kinase activity/protein serine-threonine kinase activity/protein binding/ATP binding/ | chromosome/cytosol/centrosome | | |
| 202107_s_at | minichromosome maintenance complex component 2 (MCM2) | DNA replication/DNA unwinding during replication/DNA replication initiation/nucleosome assembly/transcription/cell cycle/regulation of transcription | Nucleotide binding/DNA binding/DNA replication origin binding/protein binding/ATP binding/zinc ion binding/metal ion binding | Chromatin/nucleus/nucleoplasm/nuclear origin of replication recognition complex | -5.5 | |
| 200679_x_at | high-mobility group box 1 (HMGB1) | | protein binding | nucleus | -5.6 | |
| 48808_at | dihydrofolate reductase (DHFR) | Glycine biosynthetic process/nucleotide biosynthetic process/oxidation reduction | Dihydrofolate reductase activity/oxidoreductase activity/NADP or NADPH binding | n/a | -5.6 | -3.3 |
| 201292_at | topoisomerase (DNA) II alpha 170kDa (TOP2A) | DNA replication/DNA topological change/DNA ligation and repair/response to DNA damage/chromosome segregation/positive regulation of apoptosis/positive regulation of viral genome replication | Nucleotide binding/DNA binding/chromatin binding/DNA topoisomerase activity/protein kinase c binding/ATP binding/protein c-terminus binding | Nucleus/nuclear chromosome/nucleoplasm/chromosome/nucleolus/DNA topoisomerase complex/cytoplasm | -5.6 | |
| 204026_s_at | ZW10 interactor (ZWINT) | Mitotic sister chromatid segregation/cell cycle/spindle organization/mitosis/mitotic cell cycle checkpoint | Protein binding/protein N-terminus binding | Kinetochore/condensed chromosome/kinetochore/nucleus | -5.6 | -2.3 |
| 202589_at | thymidylate synthetase (TYMS) | DNA replication/DNA repair/dTMP biosynthetic process/ | Nucleotide binding/thymidylate synthase/methyltransferase activity/transferase activity/cofactor binding | nucleus | -5.7 | -4.1 |

| | | | | | | |
|---|---|---|---|---|---|---|
| 210258_at | regulator of G-protein signaling 13 (RGS13) | G-protein coupled receptor protein signalling pathway/negative regulation of signal transduction/negative regulation of G-protein coupled receptor protein signalling pathway | Signal transducer activity/protein binding | Nucleus/cytosol/plasma membrane | -5.7 | |
| 207165_at | hyaluronan-mediated motility receptor (RHAMM) (HMMR) | n/a | Receptor activity/hyaluronic activity | Cytoplasm/cell surface | -5.7 | |
| 221286_s_at | hypothetical protein MGC29506 | apoptosis | serine-type endopeptidase | extracellular region/cytoplasm | -5.7 | |
| 206150_at | CD27 molecule (CD27) | Apoptosis/antiapoptosis/induction of apoptosis/immune response/signal transduction/release of cytoplasmic sequestered NF-kappa-B/immunoglobulin-mediated immune response | Receptor activity/transmembrane receptor activity/protein binding/caspase inhibitor activity | Extracellular region/membrane fraction/integral to plasmamembrane/integral to membrane | -5.8 | -7.2 |
| 229147_at | n/a | n/a | n/a | n/a | -6.6 | |
| 210559_s_at | cell division cycle 2, G1 to S and G2 to M (CDC2) | Protein amino acid phosphorylation/anti-apoptosis/cell cycle/mitosis/anaphase-promoting complex-dependent proteasomal ubiquitin-dependent protein catabolic process/cell division/ | nucelotide binding/protein kinase activity/protein serine-threonine kinase activity/cyclin-dependent protein kinase activity/protein binding/ATP binding/RNA polymerase II carboxy-terminal domain kinase activity/ | Nucleus/cytoplasm/cytosol/spindle/microtubule midbody | -6.6 | |
| 1554768_a_at | MAD2 mitotic arrest deficient-like 1 (yeast) (MAD2L1) | Mitotic sister chromatid segregation/cell cycle/mitosis/mitotic cell cycle checkpoint/cell division | Protein binding/protein homodimerization activity | Chromosome/centromeric region/kineotochore/nucleus/cytoplasm | -6.8 | |
| 202954_at | ubiquitin-conjugating enzyme E2C (UBE2C) | Ubiquitin-dependent protein catabolic process cell cycle/spindle organization/mitosis/protein ubiquitination/positive regulation of exit from mitosis | Nucleotide binding/ubiquitin-protein ligase activity/ATP binding/ligase activity/small | Nucleoplasm/cytosol | -7 | |

| | | | | | | |
|---|---|---|---|---|---|---|
| | | | conjugating protein ligase activity | | | |
| 1554696_s_at | thymidylate synthetase (TYMS) | Nucleobase, nucleoside, nucleotide, and nucleio acid metabolic process/dTMP biosynthetic process/DNA replication/DNA repair/ | nucelotide binding/thymidylate synthase activity/methyltransfer ase activity/cofactor binding | cytosol | -7.3 | |
| 1568752_s_at | regulator of G-protein signaling 13 (RGS13) | G-protein coupled receptor protein signalling pathway/negative regulation of signal transduction/negative regulation of G-protein coupled receptor protein signalling pathway | Signal transducer activity/protein binding | Nucleus/cytosol/plasma membrane | -8.7 | -3.8 |

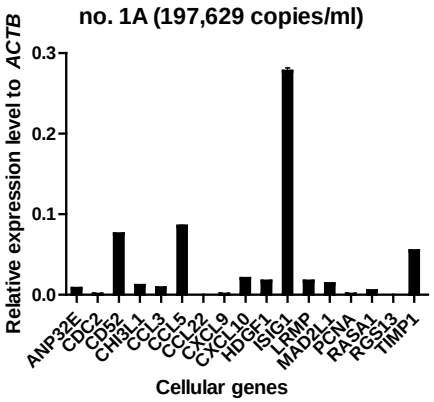
no. 1A (197,629 copies/ml)
Relative expression level to ACTB
0.3
0.2
0.1
0.0
ANP32E
CDC2
CD52
CHI3L1
CCL3
CCL5
CCL22
CXCL9
CXCL10
HDGF1
ISIG1
LRMP
MAD2L1
PCNA
RASA1
RGS13
TIMP1
Cellular genes

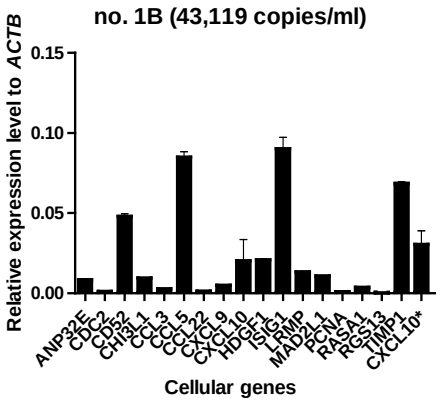
no. 1B (43,119 copies/ml)
Relative expression level to ACTB
0.15
0.10
0.05
0.00
ANP32E
CDC2
CD52
CHI3L1
CCL3
CCL5
CCL22
CXCL9
CXCL10
HDGF1
ISIG1
LRMP
MAD2L1
PCNA
RASA1
RGS13
TIMP1
CXCL10*
Cellular genes

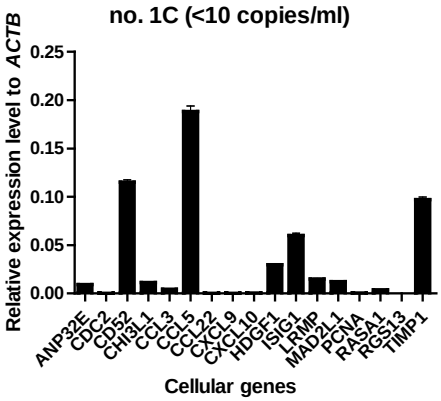
no. 1C (<10 copies/ml)
Relative expression level to ACTB
0.25
0.20
0.15
0.10
0.05
0.00
ANP32E
CDC2
CD52
CHI3L1
CCL3
CCL5
CCL22
CXCL9
CXCL10
HDGF1
ISIG1
LRMP
MAD2L1
PCNA
RASA1
RGS13
TIMP1
Cellular genes

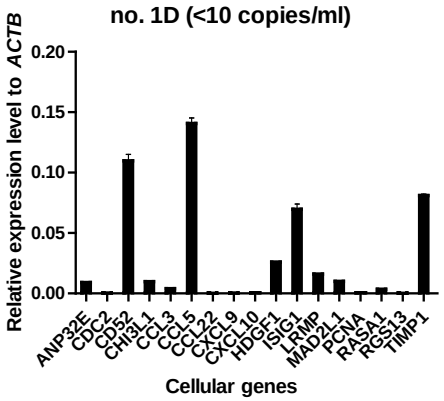
no. 1D (<10 copies/ml)
Relative expression level to ACTB
0.20
0.15
0.10
0.05
0.00
ANP32E
CDC2
CD52
CHI3L1
CCL3
CCL5
CCL22
CXCL9
CXCL10
HDGF1
ISIG1
LRMP
MAD2L1
PCNA
RASA1
RGS13
TIMP1
Cellular genes

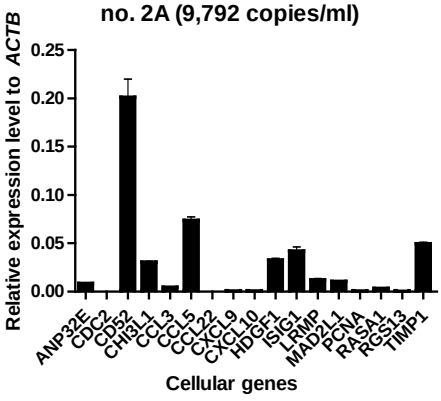
no. 2A (9,792 copies/ml)
Relative expression level to ACTB
0.25
0.20
0.15
0.10
0.05
0.00
ANP32E
CDC2
CD52
CHI3L1
CCL3
CCL5
CCL22
CXCL9
CXCL10
HDGF1
ISIG1
LRMP
MAD2L1
PCNA
RASA1
RGS13
TIMP1
Cellular genes

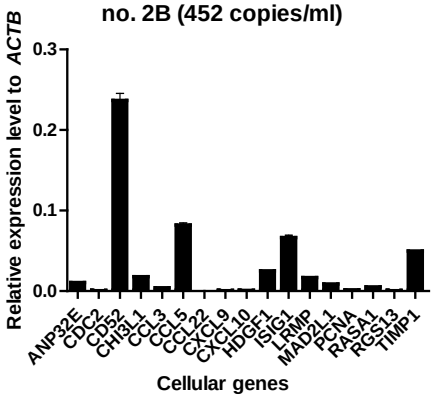
no. 2B (452 copies/ml)
Relative expression level to ACTB
0.3
0.2
0.1
0.0
ANP32E
CDC2
CD52
CHI3L1
CCL3
CCL5
CCL22
CXCL9
CXCL10
HDGF1
ISIG1
LRMP
MAD2L1
PCNA
RASA1
RGS13
TIMP1
Cellular genes

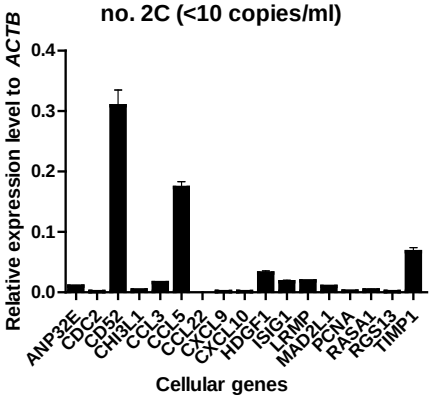
no. 2C (<10 copies/ml)
Relative expression level to ACTB
0.4
0.3
0.2
0.1
0.0
ANP32E
CDC2
CD52
CHI3L1
CCL3
CCL5
CCL22
CXCL9
CXCL10
HDGF1
ISIG1
LRMP
MAD2L1
PCNA
RASA1
RGS13
TIMP1
Cellular genes

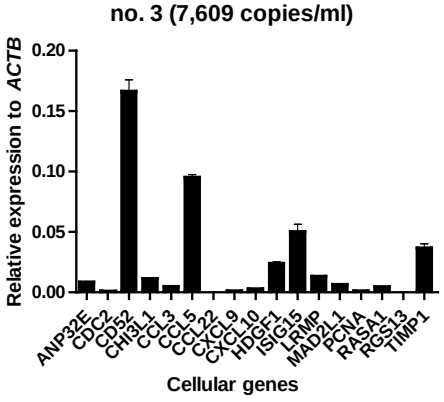
no. 3 (7,609 copies/ml)
Relative expression to ACTB
0.20
0.15
0.10
0.05
0.00
ANP32E
CDC2
CD52
CHI3L1
CCL3
CCL5
CCL22
CXCL9
CXCL10
HDGF1
ISIG15
LRMP
MAD2L1
PCNA
RASA1
RGS13
TIMP1
Cellular genes

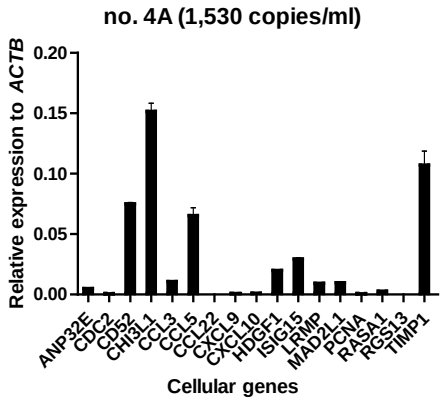
no. 4A (1,530 copies/ml)
Relative expression to ACTB
0.20
0.15
0.10
0.05
0.00
ANP32E
CDC2
CD52
CHI3L1
CCL3
CCL5
CCL22
CXCL9
CXCL10
HDGF1
ISIG15
LRMP
MAD2L1
PCNA
RASA1
RGS13
TIMP1
Cellular genes

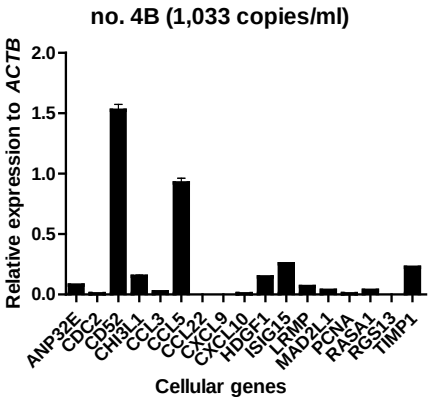
no. 4B (1,033 copies/ml)
Relative expression to ACTB
2.0
1.5
1.0
0.5
0.0
ANP32E
CDC2
CD52
CHI3L1
CCL3
CCL5
CCL22
CXCL9
CXCL10
HDGF1
ISIG15
LRMP
MAD2L1
PCNA
RASA1
RGS13
TIMP1
Cellular genes

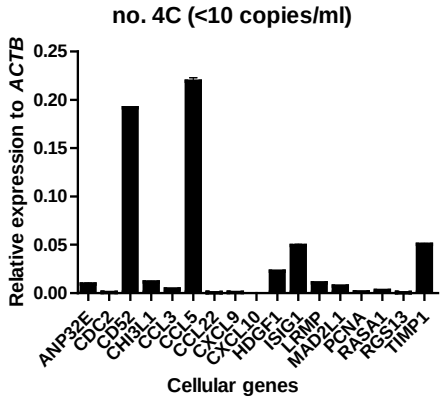
no. 4C (<10 copies/ml)
Relative expression to ACTB
0.25
0.20
0.15
0.10
0.05
0.00
ANP32E
CDC2
CD52
CHI3L1
CCL3
CCL5
CCL22
CXCL9
CXCL10
HDGF1
ISIG1
LRMP
MAD2L1
PCNA
RASA1
RGS13
TIMP1
Cellular genes

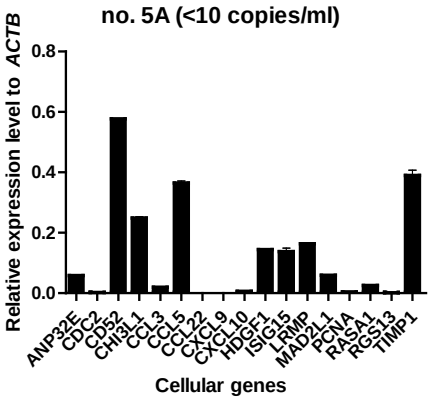
no. 5A (<10 copies/ml)
Relative expression level to ACTB
0.8
0.6
0.4
0.2
0.0
ANP32E
CDC2
CD52
CHI3L1
CCL3
CCL5
CCL22
CXCL9
CXCL10
HDGF1
ISIG15
LRMP
MAD2L1
PCNA
RASA1
RGS13
TIMP1
Cellular genes

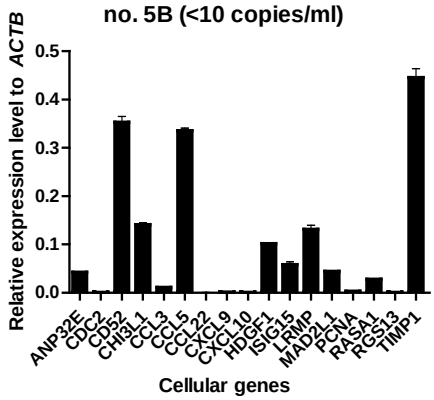
no. 5B (<10 copies/ml)
Relative expression level to ACTB
0.5
0.4
0.3
0.2
0.1
0.0
ANP32E
CDC2
CD52
CHI3L1
CCL3
CCL5
CCL22
CXCL9
CXCL10
HDGF1
ISIG15
LRMP
MAD2L1
PCNA
RASA1
RGS13
TIMP1
Cellular genes

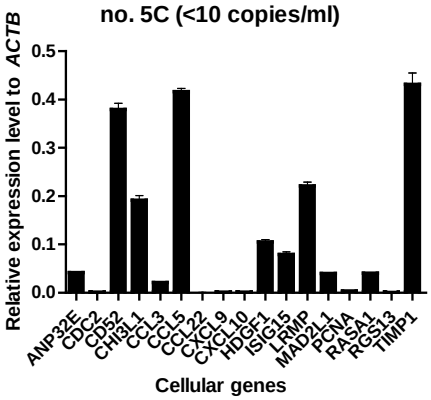
no. 5C (<10 copies/ml)
Relative expression level to ACTB
0.5
0.4
0.3
0.2
0.1
0.0
ANP32E
CDC2
CD52
CHI3L1
CCL3
CCL5
CCL22
CXCL9
CXCL10
HDGF1
ISIG15
LRMP
MAD2L1
PCNA
RASA1
RGS13
TIMP1
Cellular genes

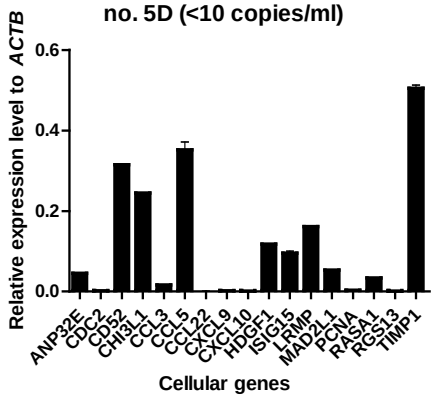
no. 5D (<10 copies/ml)
Relative expression level to ACTB
0.6
0.4
0.2
0.0
ANP32E
CDC2
CD52
CHI3L1
CCL3
CCL5
CCL22
CXCL9
CXCL10
HDGF1
ISIG15
LRMP
MAD2L1
PCNA
RASA1
RGS13
TIMP1
Cellular genes

**(C)**

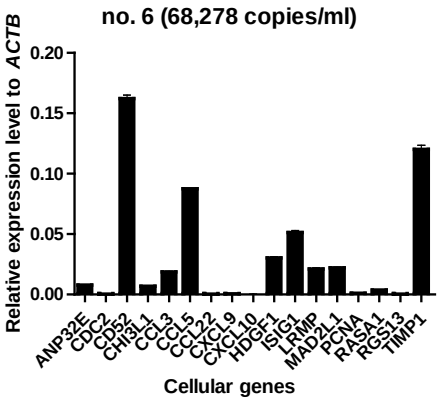
no. 6 (68,278 copies/ml)
Relative expression level to ACTB
0.20
0.15
0.10
0.05
0.00
ANP32E CDC2 CD52 CHI3L1 CCL3 CCL5 CCL22 CXCL9 CXCL10 HDGF1 ISIG1 LRMP MAD2L1 PCNA RASA1 RGS13 TIMP1
Cellular genes

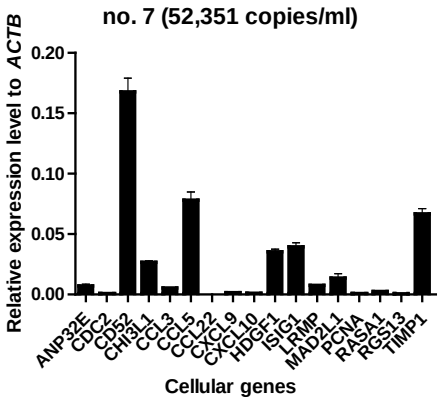
no. 7 (52,351 copies/ml)
Relative expression level to ACTB
0.20
0.15
0.10
0.05
0.00
ANP32E CDC2 CD52 CHI3L1 CCL3 CCL5 CCL22 CXCL9 CXCL10 HDGF1 ISIG1 LRMP MAD2L1 PCNA RASA1 RGS13 TIMP1
Cellular genes

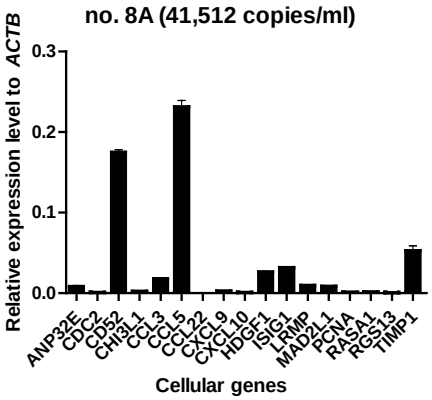
no. 8A (41,512 copies/ml)
Relative expression level to ACTB
0.3
0.2
0.1
0.0
ANP32E CDC2 CD52 CHI3L1 CCL3 CCL5 CCL22 CXCL9 CXCL10 HDGF1 ISIG1 LRMP MAD2L1 PCNA RASA1 RGS13 TIMP1
Cellular genes

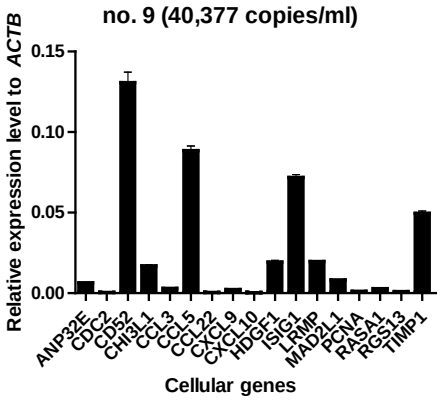
no. 9 (40,377 copies/ml)
Relative expression level to ACTB
0.15
0.10
0.05
0.00
ANP32E CDC2 CD52 CHI3L1 CCL3 CCL5 CCL22 CXCL9 CXCL10 HDGF1 ISIG1 LRMP MAD2L1 PCNA RASA1 RGS13 TIMP1
Cellular genes

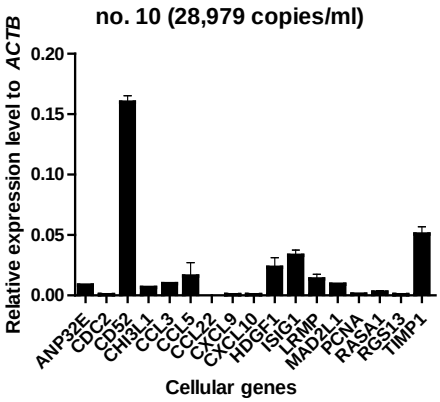
no. 10 (28,979 copies/ml)
Relative expression level to ACTB
0.20
0.15
0.10
0.05
0.00
ANP32E CDC2 CD52 CHI3L1 CCL3 CCL5 CCL22 CXCL9 CXCL10 HDGF1 ISIG1 LRMP MAD2L1 PCNA RASA1 RGS13 TIMP1
Cellular genes

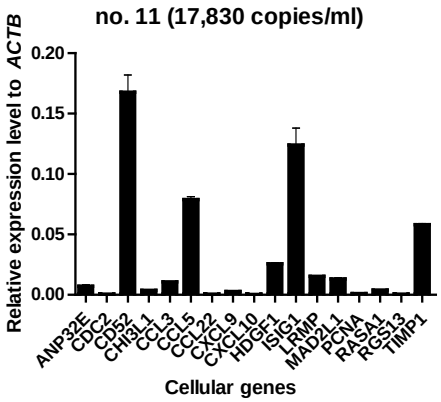
no. 11 (17,830 copies/ml)
Relative expression level to ACTB
0.20
0.15
0.10
0.05
0.00
ANP32E CDC2 CD52 CHI3L1 CCL3 CCL5 CCL22 CXCL9 CXCL10 HDGF1 ISIG1 LRMP MAD2L1 PCNA RASA1 RGS13 TIMP1
Cellular genes

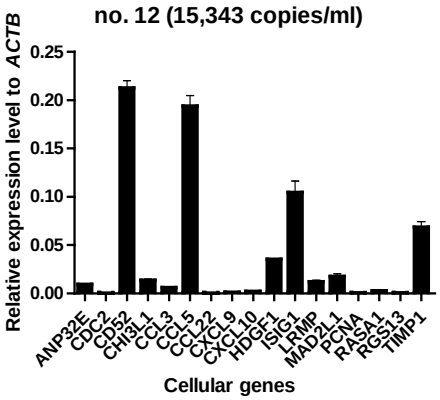
no. 12 (15,343 copies/ml)
Relative expression level to ACTB
0.25
0.20
0.15
0.10
0.05
0.00
ANP32E CDC2 CD52 CHI3L1 CCL3 CCL5 CCL22 CXCL9 CXCL10 HDGF1 ISIG1 LRMP MAD2L1 PCNA RASA1 RGS13 TIMP1
Cellular genes

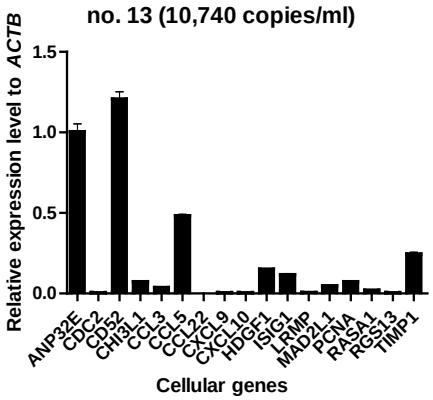
no. 13 (10,740 copies/ml)
Relative expression level to ACTB
1.5
1.0
0.5
0.0
ANP32E CDC2 CD52 CHI3L1 CCL3 CCL5 CCL22 CXCL9 CXCL10 HDGF1 ISIG1 LRMP MAD2L1 PCNA RASA1 RGS13 TIMP1
Cellular genes

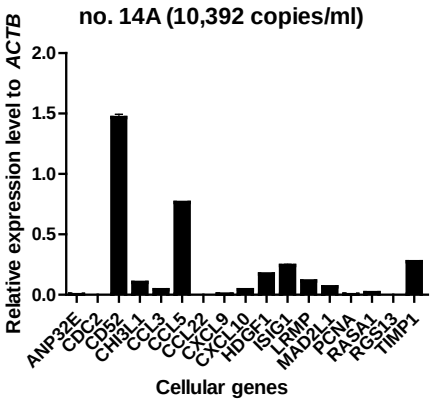
no. 14A (10,392 copies/ml)
Relative expression level to ACTB
2.0
1.5
1.0
0.5
0.0
ANP32E CDC2 CD52 CHI3L1 CCL3 CCL5 CCL22 CXCL9 CXCL10 HDGF1 ISIG1 LRMP MAD2L1 PCNA RASA1 RGS13 TIMP1
Cellular genes

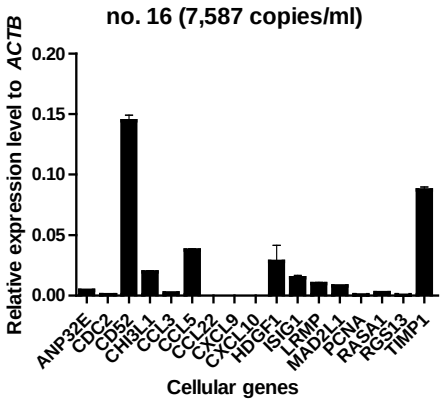
no. 16 (7,587 copies/ml)
Relative expression level to ACTB
0.20
0.15
0.10
0.05
0.00
ANP32E CDC2 CD52 CHI3L1 CCL3 CCL5 CCL22 CXCL9 CXCL10 HDGF1 ISIG1 LRMP MAD2L1 PCNA RASA1 RGS13 TIMP1
Cellular genes

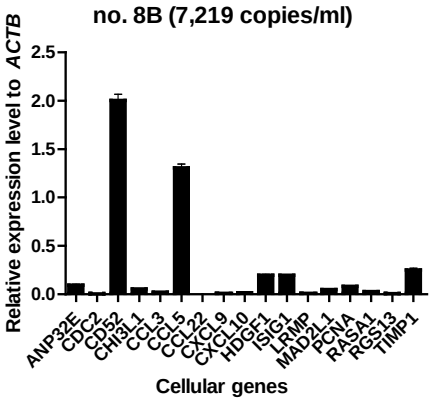
no. 8B (7,219 copies/ml)
Relative expression level to ACTB
2.5
2.0
1.5
1.0
0.5
0.0
ANP32E CDC2 CD52 CHI3L1 CCL3 CCL5 CCL22 CXCL9 CXCL10 HDGF1 ISIG1 LRMP MAD2L1 PCNA RASA1 RGS13 TIMP1
Cellular genes

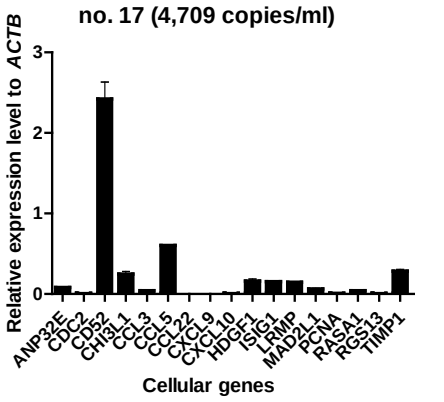
no. 17 (4,709 copies/ml)
Relative expression level to ACTB
3
2
1
0
ANP32E CDC2 CD52 CHI3L1 CCL3 CCL5 CCL22 CXCL9 CXCL10 HDGF1 ISIG1 LRMP MAD2L1 PCNA RASA1 RGS13 TIMP1
Cellular genes

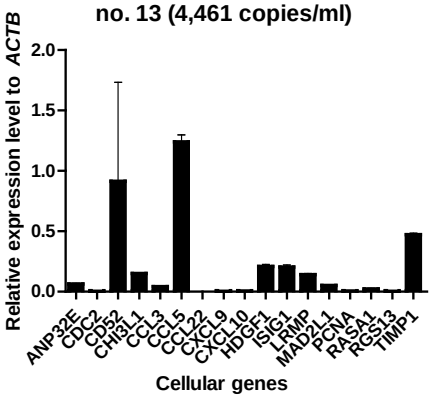
no. 13 (4,461 copies/ml)
Relative expression level to ACTB
2.0
1.5
1.0
0.5
0.0
ANP32E CDC2 CD52 CHI3L1 CCL3 CCL5 CCL22 CXCL9 CXCL10 HDGF1 ISIG1 LRMP MAD2L1 PCNA RASA1 RGS13 TIMP1
Cellular genes

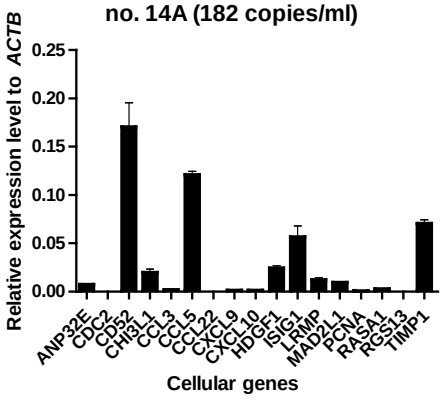
no. 14A (182 copies/ml)
Relative expression level to ACTB
0.25
0.20
0.15
0.10
0.05
0.00
ANP32E CDC2 CD52 CHI3L1 CCL3 CCL5 CCL22 CXCL9 CXCL10 HDGF1 ISIG1 LRMP MAD2L1 PCNA RASA1 RGS13 TIMP1
Cellular genes

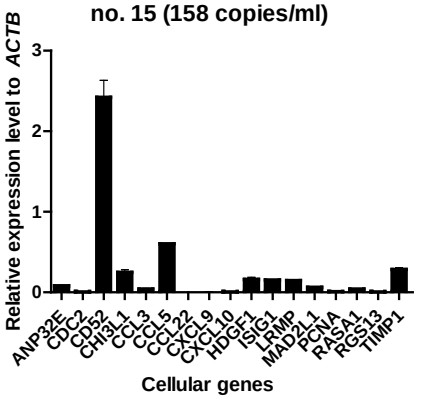
no. 15 (158 copies/ml)
Relative expression level to ACTB
3
2
1
0
ANP32E CDC2 CD52 CHI3L1 CCL3 CCL5 CCL22 CXCL9 CXCL10 HDGF1 ISIG1 LRMP MAD2L1 PCNA RASA1 RGS13 TIMP1
Cellular genes

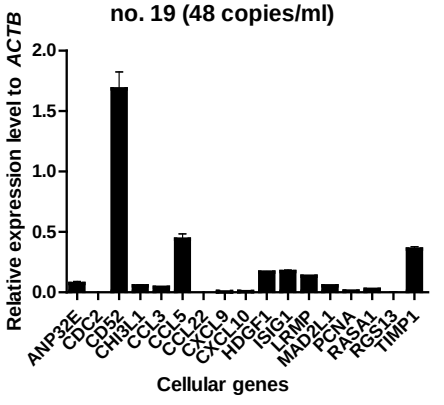
no. 19 (48 copies/ml)
Relative expression level to ACTB
2.0
1.5
1.0
0.5
0.0
ANP32E CDC2 CD52 CHI3L1 CCL3 CCL5 CCL22 CXCL9 CXCL10 HDGF1 ISIG1 LRMP MAD2L1 PCNA RASA1 RGS13 TIMP1
Cellular genes

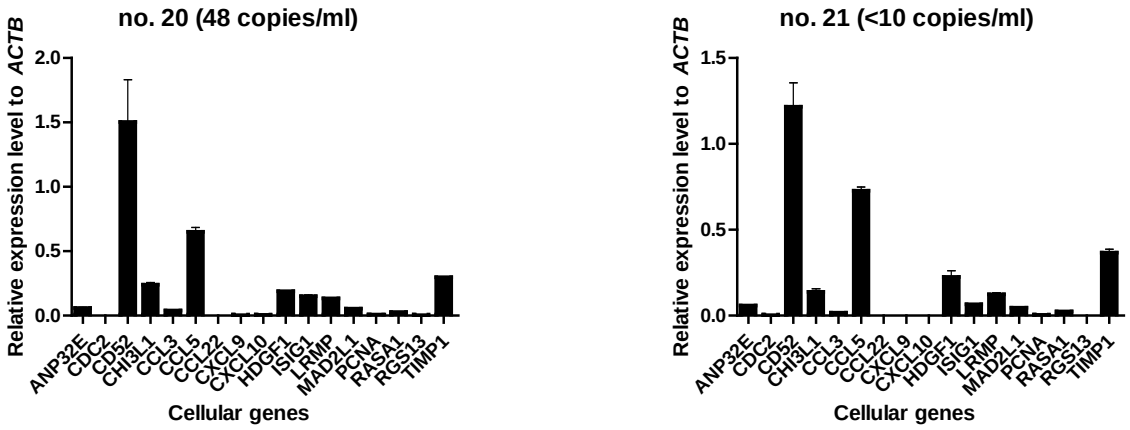


(**B**)

**Figure 7-1 Gene expression levels for 17 cellular candidate genes in the peripheral blood of PTLD and non-PTLD paediatric patients**

Relative expression levels were quantified relative to the *ACTB* gene using real-time TaqMan PCR. (**A**) Relative expression levels in 15 samples from 5 PTLD patients (Black bars); (**B**) Relative expression levels in 18 samples from 16 non-PTLD patients (Grey bars). Horizontal lines denote the mean relative expression level in each group of transplant patients. Each bar represents the mean relative expression level ±S.D of triplicates for each gene.

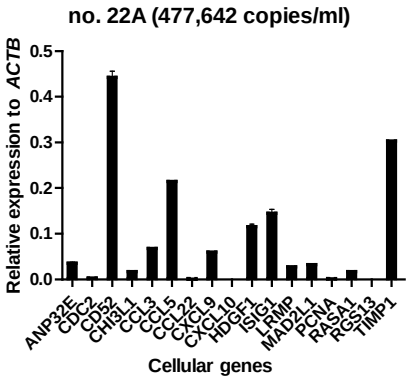
no. 22A (477,642 copies/ml)
Relative expression to ACTB
0.5
0.4
0.3
0.2
0.1
0.0
ANP32E
CDC2
CD52
CHI3L1
CCL3
CCL5
CCL22
CXCL9
CXCL10
HDGF1
ISIG1
LRMP
MAD2L1
PCNA
RASA1
RGS13
TIMP1
Cellular genes

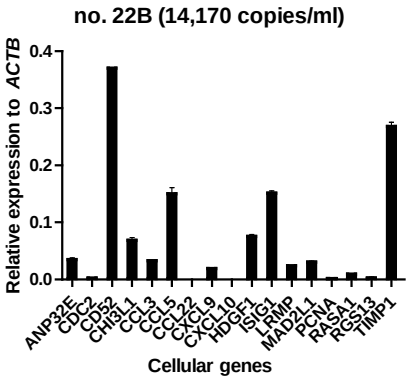
no. 22B (14,170 copies/ml)
Relative expression to ACTB
0.4
0.3
0.2
0.1
0.0
ANP32E
CDC2
CD52
CHI3L1
CCL3
CCL5
CCL22
CXCL9
CXCL10
HDGF1
ISIG1
LRMP
MAD2L1
PCNA
RASA1
RGS13
TIMP1
Cellular genes

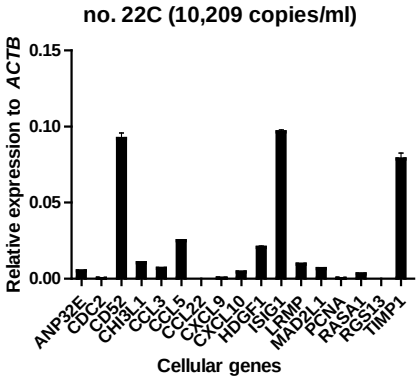
no. 22C (10,209 copies/ml)
Relative expression to ACTB
0.15
0.10
0.05
0.00
ANP32E
CDC2
CD52
CHI3L1
CCL3
CCL5
CCL22
CXCL9
CXCL10
HDGF1
ISIG1
LRMP
MAD2L1
PCNA
RASA1
RGS13
TIMP1
Cellular genes

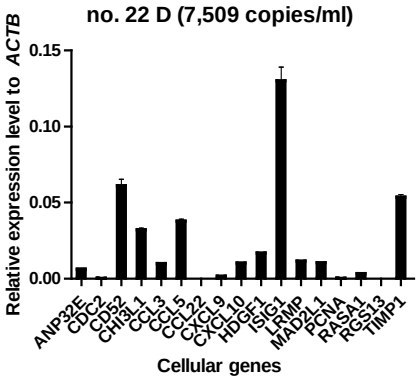
no. 22 D (7,509 copies/ml)
Relative expression level to ACTB
0.15
0.10
0.05
0.00
ANP32E
CDC2
CD52
CHI3L1
CCL3
CCL5
CCL22
CXCL9
CXCL10
HDGF1
ISIG1
LRMP
MAD2L1
PCNA
RASA1
RGS13
TIMP1
Cellular genes

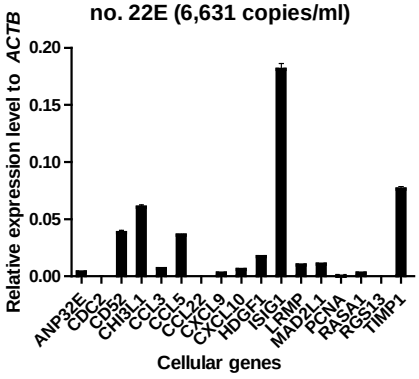
no. 22E (6,631 copies/ml)
Relative expression level to ACTB
0.20
0.15
0.10
0.05
0.00
ANP32E
CDC2
CD52
CHI3L1
CCL3
CCL5
CCL22
CXCL9
CXCL10
HDGF1
ISIG1
LRMP
MAD2L1
PCNA
RASA1
RGS13
TIMP1
Cellular genes

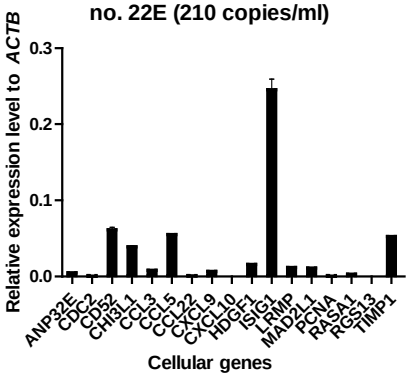
no. 22E (210 copies/ml)
Relative expression level to ACTB
0.3
0.2
0.1
0.0
ANP32E
CDC2
CD52
CHI3L1
CCL3
CCL5
CCL22
CXCL9
CXCL10
HDGF1
ISIG1
LRMP
MAD2L1
PCNA
RASA1
RGS13
TIMP1
Cellular genes

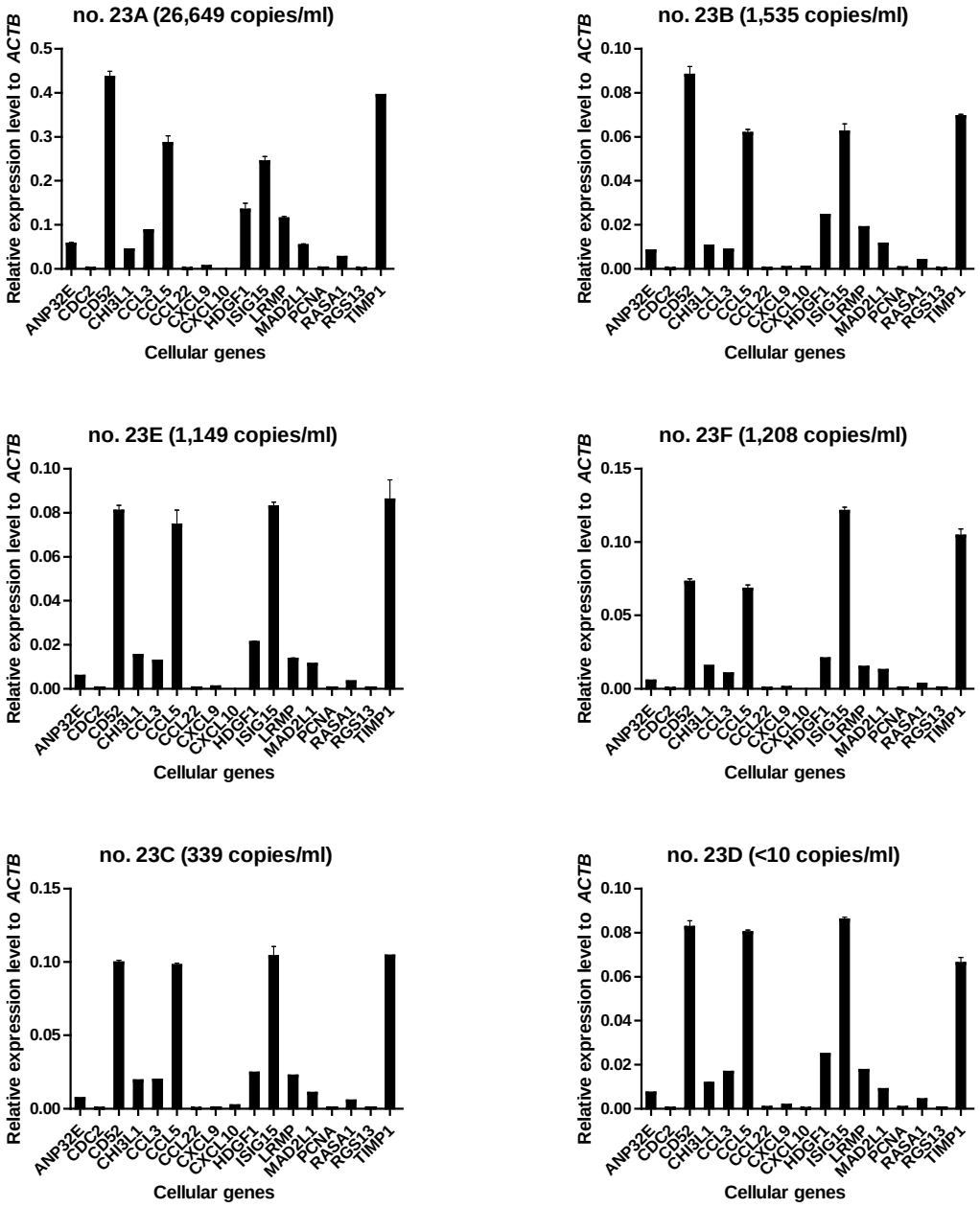


**Figure 7-2 Gene expression levels for 17 cellular candidate genes in the peripheral blood of adult PTLD and non-PTLD patients**

Relative expression levels were quantified relative to the *ACTB* gene using real-time TaqMan PCR. Relative expression levels in 6 samples from 1 PTLD (Black bars) and 6 samples from 1 non-PTLD patients. Each bar represents the mean relative expression level ±SD of triplicates for gene.

## *8 REFERENCES*


Adams, A., 1987. Replication of latent Epstein-Barr virus genomes in Raji cells. J Virol 61, 1743-1746.
Adamson, A.L., Kenney, S.C., 1998. Rescue of the Epstein-Barr virus BZLF1 mutant, Z(S186A), early gene activation defect by the BRLF1 gene product. Virology 251, 187-197.
Ali, S., Lazennec, G., 2007. Chemokines: novel targets for breast cancer metastasis. Cancer Metastasis Rev 26, 401-420.
Allavena, P., Germano, G., Marchesi, F., Mantovani, A., 2011. Chemokines in cancer related inflammation. Exp Cell Res 317, 664-673.
Allday, M.J., Crawford, D.H., Griffin, B.E., 1989. Epstein-Barr virus latent gene expression during the initiation of B cell immortalization. J Gen Virol 70 ( Pt 7), 1755-1764.
Allen, U., Barton, M., Beyene, J., Hu, P., Khodai-Booran, N., Hebert, D., Dipchand, A., Ng, V., Solomon, M., Grant, D., Fecteau, A., Ngan, B., Read, S., Zielenska, M., Weitzman, S., 2009. Gene expression using microarrays in transplant recipients at risk of EBV lymphoproliferation after organ transplantation: preliminary proof-of-concept. Pediatr Transplant 13, 990-998.
Allen, U., Hebert, D., Moore, D., Dror, Y., Wasfy, S., 2001. Epstein-Barr virus-related post-transplant lymphoproliferative disease in solid organ transplant recipients, 1988-97: a Canadian multi-centre experience. Pediatr Transplant 5, 198-203.
Allen, U.D., Farkas, G., Hebert, D., Weitzman, S., Stephens, D., Petric, M., Tellier, R., Ngan, B., Fecteau, A., West, L., Wasfy, S., 2005. Risk factors for post-transplant lymphoproliferative disorder in pediatric patients: a case-control study. Pediatr Transplant 9, 450-455.
Amon, W., Binne, U.K., Bryant, H., Jenkins, P.J., Karstegl, C.E., Farrell, P.J., 2004a. Lytic cycle gene regulation of Epstein-Barr virus. J Virol 78, 13460-13469.
Amon, W., Binne, U.K., Bryant, H., Jenkins, P.J., Karstegl, C.E., Farrell, P.J., 2004b. Lytic cycle gene regulation of Epstein-Barr virus. J Virol 78, 13460-13469.
Amon, W., White, R.E., Farrell, P.J., 2006a. Epstein-Barr virus origin of lytic replication mediates association of replicating episomes with promyelocytic leukaemia protein nuclear bodies and replication compartments. J Gen Virol 87, 1133-1137.
Amon, W., White, R.E., Farrell, P.J., 2006b. Epstein-Barr virus origin of lytic replication mediates association of replicating episomes with promyelocytic leukaemia protein nuclear bodies and replication compartments. J Gen Virol 87, 1133-1137.
Anderton, E., Yee, J., Smith, P., Crook, T., White, R.E., Allday, M.J., 2008. Two Epstein-Barr virus (EBV) oncoproteins cooperate to repress expression of the proapoptotic tumour-suppressor Bim: clues to the pathogenesis of Burkitt's lymphoma. Oncogene 27, 421-433.
Arenberg, D.A., Kunkel, S.L., Polverini, P.J., Morris, S.B., Burdick, M.D., Glass, M.C., Taub, D.T., Iannettoni, M.D., Whyte, R.I., Strieter, R.M., 1996. Interferon-gamma-inducible protein 10 (IP-10) is an angiostatic factor that inhibits human non-small cell lung cancer (NSCLC) tumorigenesis and spontaneous metastases. J Exp Med 184, 981-992.
Arrand, J.R., Young, L.S., Tugwood, J.D., 1989. Two families of sequences in the small RNA-encoding region of Epstein-Barr virus (EBV) correlate with EBV types A and B. J Virol 63, 983-986.
Arumugaswami, V., Wu, T.T., Martinez-Guzman, D., Jia, Q., Deng, H., Reyes, N., Sun, R., 2006. ORF18 is a transfactor that is essential for late gene transcription of a gammaherpesvirus. J Virol 80, 9730-9740.
Asai, R., Kato, A., Kato, K., Kanamori-Koyama, M., Sugimoto, K., Sairenji, T., Nishiyama, Y., Kawaguchi, Y., 2006. Epstein-Barr virus protein kinase BGLF4 is a virion tegument protein that dissociates from virions in a phosphorylation-dependent process and phosphorylates the viral immediate-early protein BZLF1. J Virol 80, 5125-5134.
Asai, R., Kato, A., Kawaguchi, Y., 2009. Epstein-Barr virus protein kinase BGLF4 interacts with viral transactivator BZLF1 and regulates its transactivation activity. J Gen Virol 90, 1575-1581.

Ascherio, A., Munger, K.L., 2010. Epstein-barr virus infection and multiple sclerosis: a review. J Neuroimmune Pharmacol 5, 271-277.
Babcock, G.J., Decker, L.L., Freeman, R.B., Thorley-Lawson, D.A., 1999. Epstein-barr virus-infected resting memory B cells, not proliferating lymphoblasts, accumulate in the peripheral blood of immunosuppressed patients. J Exp Med 190, 567-576.
Babcock, G.J., Decker, L.L., Volk, M., Thorley-Lawson, D.A., 1998. EBV persistence in memory B cells in vivo. Immunity 9, 395-404.
Babcock, G.J., Hochberg, D., Thorley-Lawson, A.D., 2000. The expression pattern of Epstein-Barr virus latent genes in vivo is dependent upon the differentiation stage of the infected B cell. Immunity 13, 497-506.
Badley, A.D., Portela, D.F., Patel, R., Kyle, R.A., Habermann, T.M., Strickler, J.G., Ilstrup, D.M., Wiesner, R.H., de Groen, P., Walker, R.C., Paya, C.V., 1996. Development of monoclonal gammopathy precedes the development of Epstein-Barr virus-induced posttransplant lymphoproliferative disorder. Liver Transpl Surg 2, 375-382.
Baer, R., Bankier, A.T., Biggin, M.D., Deininger, P.L., Farrell, P.J., Gibson, T.J., Hatfull, G., Hudson, G.S., Satchwell, S.C., Seguin, C., et al., 1984. DNA sequence and expression of the B95-8 Epstein-Barr virus genome. Nature 310, 207-211.
Baggiolini, M., 1998. Chemokines and leukocyte traffic. Nature 392, 565-568.
Baggiolini, M., Dewald, B., Moser, B., 1997. Human chemokines: an update. Annu Rev Immunol 15, 675-705.
Bai, M., Papoudou-Bai, A., Kitsoulis, P., Horianopoulos, N., Kamina, S., Agnantis, N.J., Kanavaros, P., 2005. Cell cycle and apoptosis deregulation in classical Hodgkin lymphomas. In Vivo 19, 439-453.
Bai, X., Hosler, G., Rogers, B.B., Dawson, D.B., Scheuermann, R.H., 1997. Quantitative polymerase chain reaction for human herpesvirus diagnosis and measurement of Epstein-Barr virus burden in posttransplant lymphoproliferative disorder. Clin Chem 43, 1843-1849.
Baldanti, F., Grossi, P., Furione, M., Simoncini, L., Sarasini, A., Comoli, P., Maccario, R., Fiocchi, R., Gerna, G., 2000. High levels of Epstein-Barr virus DNA in blood of solid-organ transplant recipients and their value in predicting posttransplant lymphoproliferative disorders. J Clin Microbiol 38, 613-619.
Baran-Marszak, F., Fagard, R., Girard, B., Camilleri-Broet, S., Zeng, F., Lenoir, G.M., Raphael, M., Feuillard, J., 2002. Gene array identification of Epstein Barr virus-regulated cellular genes in EBV-converted Burkitt lymphoma cell lines. Lab Invest 82, 1463-1479.
Baumann, M., Mischak, H., Dammeier, S., Kolch, W., Gires, O., Pich, D., Zeidler, R., Delecluse, H.J., Hammerschmidt, W., 1998a. Activation of the Epstein-Barr virus transcription factor BZLF1 by 12-O-tetradecanoylphorbol-13-acetate-induced phosphorylation. J Virol 72, 8105-8114.
Baumann, M., Mischak, H., Dammeier, S., Kolch, W., Gires, O., Pich, D., Zeidler, R., Delecluse, H.J., Hammerschmidt, W., 1998b. Activation of the Epstein-Barr virus transcription factor BZLF1 by 12-O-tetradecanoylphorbol-13-acetate-induced phosphorylation. J Virol 72, 8105-8114.
Baumforth, K.R., Young, L.S., Flavell, K.J., Constandinou, C., Murray, P.G., 1999. The Epstein-Barr virus and its association with human cancers. Mol Pathol 52, 307-322.
Bechtel, D., Kurth, J., Unkel, C., Kuppers, R., 2005. Transformation of BCR-deficient germinal-center B cells by EBV supports a major role of the virus in the pathogenesis of Hodgkin and posttransplantation lymphomas. Blood 106, 4345-4350.
Benden, C., Aurora, P., Burch, M., Cubitt, D., Lloyd, C., Whitmore, P., Neligan, S.L., Elliott, M.J., 2005. Monitoring of Epstein-Barr viral load in pediatric heart and lung transplant recipients by real-time polymerase chain reaction. J Heart Lung Transplant 24, 2103-2108.
Bentz, G.L., Liu, R., Hahn, A.M., Shackelford, J., Pagano, J.S., 2010. Epstein-Barr virus BRLF1 inhibits transcription of IRF3 and IRF7 and suppresses induction of interferon-beta. Virology 402, 121-128.
Bergallo, M., Costa, C., Baro, S., Musso, T., Balbo, L., Merlino, C., Cavallo, R., 2007. Multiplex-nested RT-PCR to evaluate latent and lytic Epstein Barr virus gene expression. J Biotechnol 128, 462-476.

Bernasconi, M., Berger, C., Sigrist, J.A., Bonanomi, A., Sobek, J., Niggli, F.K., Nadal, D., 2006. Quantitative profiling of housekeeping and Epstein-Barr virus gene transcription in Burkitt lymphoma cell lines using an oligonucleotide microarray. Virol J 3, 43.
Beveridge, T., Krupp, P., McKibbin, C., 1984. Lymphomas and lymphoproliferative lesions developing under cyclosporin therapy. Lancet 1, 788.
Bhatia, S., Ramsay, N.K., Steinbuch, M., Dusenbery, K.E., Shapiro, R.S., Weisdorf, D.J., Robison, L.L., Miller, J.S., Neglia, J.P., 1996. Malignant neoplasms following bone marrow transplantation. Blood 87, 3633-3639.
Bhende, P.M., Seaman, W.T., Delecluse, H.J., Kenney, S.C., 2004. The EBV lytic switch protein, Z, preferentially binds to and activates the methylated viral genome. Nat Genet 36, 1099-1104.
Bhende, P.M., Seaman, W.T., Delecluse, H.J., Kenney, S.C., 2005. BZLF1 activation of the methylated form of the BRLF1 immediate-early promoter is regulated by BZLF1 residue 186. J Virol 79, 7338-7348.
Biggar, R.J., Johansen, J.S., Smedby, K.E., Rostgaard, K., Chang, E.T., Adami, H.O., Glimelius, B., Molin, D., Hamilton-Dutoit, S., Melbye, M., Hjalgrim, H., 2008. Serum YKL-40 and interleukin 6 levels in Hodgkin lymphoma. Clin Cancer Res 14, 6974-6978.
Biggin, M., Bodescot, M., Perricaudet, M., Farrell, P., 1987. Epstein-Barr virus gene expression in P3HR1-superinfected Raji cells. J Virol 61, 3120-3132.
Boeckmann, B., Bairoch, A., Apweiler, R., Blatter, M.C., Estreicher, A., Gasteiger, E., Martin, M.J., Michoud, K., O'Donovan, C., Phan, I., Pilbout, S., Schneider, M., 2003. The SWISS-PROT protein knowledgebase and its supplement TrEMBL in 2003. Nucleic Acids Res 31, 365-370.
Bolstad, B.M., Irizarry, R.A., Astrand, M., Speed, T.P., 2003. A comparison of normalization methods for high density oligonucleotide array data based on variance and bias. Bioinformatics 19, 185-193.
Borza, C.M., Hutt-Fletcher, L.M., 2002. Alternate replication in B cells and epithelial cells switches tropism of Epstein-Barr virus. Nat Med 8, 594-599.
Brauninger, A., Spieker, T., Mottok, A., Baur, A.S., Kuppers, R., Hansmann, M.L., 2003. Epstein-Barr virus (EBV)-positive lymphoproliferations in post-transplant patients show immunoglobulin V gene mutation patterns suggesting interference of EBV with normal B cell differentiation processes. Eur J Immunol 33, 1593-1602.
Brink, A.A., Dukers, D.F., van den Brule, A.J., Oudejans, J.J., Middeldorp, J.M., Meijer, C.J., Jiwa, M., 1997. Presence of Epstein-Barr virus latency type III at the single cell level in post-transplantation lymphoproliferative disorders and AIDS related lymphomas. J Clin Pathol 50, 911-918.
Broderick, P., Hubank, M., Sinclair, A., 2009. [Effects of Epstein-Barr virus on host gene expression in Burkitt's lymphoma cell lines]. Ai Zheng 28, 813-821.
Brunda, M.J., Luistro, L., Warrier, R.R., Wright, R.B., Hubbard, B.R., Murphy, M., Wolf, S.F., Gately, M.K., 1993. Antitumor and antimetastatic activity of interleukin 12 against murine tumors. J Exp Med 178, 1223-1230.
Brune, V., Tiacci, E., Pfeil, I., Doring, C., Eckerle, S., van Noesel, C.J., Klapper, W., Falini, B., von Heydebreck, A., Metzler, D., Brauninger, A., Hansmann, M.L., Kuppers, R., 2008. Origin and pathogenesis of nodular lymphocyte-predominant Hodgkin lymphoma as revealed by global gene expression analysis. J Exp Med 205, 2251-2268.
Buettner, M., Meyer, B., Schreck, S., Niedobitek, G., 2007. Expression of RANTES and MCP-1 in epithelial cells is regulated via LMP1 and CD40. Int J Cancer 121, 2703-2710.
Burke, G.W., Cirocco, R., Hensley, G., Reddy, R., Jeffers, L., Schiff, E., Miller, J., 1992. The rapid development of a fatal, disseminated B cell lymphoma following liver transplantation--serial changes in levels of soluble serum interleukin 2 and interleukin 4 (B cell growth factor). Transplantation 53, 1148-1150.
Bustin, S.A., Nolan, T., 2004. Pitfalls of quantitative real-time reverse-transcription polymerase chain reaction. J Biomol Tech 15, 155-166.
Cahir-McFarland, E.D., Carter, K., Rosenwald, A., Giltnane, J.M., Henrickson, S.E., Staudt, L.M., Kieff, E., 2004. Role of NF-kappa B in cell survival and transcription of latent membrane protein 1-expressing or Epstein-Barr virus latency III-infected cells. J Virol 78, 4108-4119.

Callan, M.F., Steven, N., Krausa, P., Wilson, J.D., Moss, P.A., Gillespie, G.M., Bell, J.I., Rickinson, A.B., McMichael, A.J., 1996. Large clonal expansions of CD8+ T cells in acute infectious mononucleosis. Nat Med 2, 906-911.
Capello, D., Cerri, M., Muti, G., Berra, E., Oreste, P., Deambrogi, C., Rossi, D., Dotti, G., Conconi, A., Vigano, M., Magrini, U., Ippoliti, G., Morra, E., Gloghini, A., Rambaldi, A., Paulli, M., Carbone, A., Gaidano, G., 2003. Molecular histogenesis of posttransplantation lymphoproliferative disorders. Blood 102, 3775-3785.
Capello, D., Rasi, S., Oreste, P., Veronese, S., Cerri, M., Ravelli, E., Rossi, D., Minola, E., Colosimo, A., Gambacorta, M., Muti, G., Morra, E., Gaidano, G., 2009. Molecular characterization of post-transplant lymphoproliferative disorders of donor origin occurring in liver transplant recipients. J Pathol 218, 478-486.
Carter, K.L., Cahir-McFarland, E., Kieff, E., 2002. Epstein-barr virus-induced changes in B-lymphocyte gene expression. J Virol 76, 10427-10436.
Cen, H., Williams, P.A., McWilliams, H.P., Breinig, M.C., Ho, M., McKnight, J.L., 1993. Evidence for restricted Epstein-Barr virus latent gene expression and anti-EBNA antibody response in solid organ transplant recipients with posttransplant lymphoproliferative disorders. Blood 81, 1393-1403.
Cerri, M., Capello, D., Muti, G., Rambaldi, A., Paulli, M., Gloghini, A., Berra, E., Deambrogi, C., Rossi, D., Franceschetti, S., Conconi, A., Morra, E., Pasqualucci, L., Carbone, A., Gaidano, G., 2004. Aberrant somatic hypermutation in post-transplant lymphoproliferative disorders. Br J Haematol 127, 362-364.
Cesarman, E., Chadburn, A., Liu, Y.F., Migliazza, A., Dalla-Favera, R., Knowles, D.M., 1998. BCL-6 gene mutations in posttransplantation lymphoproliferative disorders predict response to therapy and clinical outcome. Blood 92, 2294-2302.
Chang, Y., Lee, H.H., Chen, Y.T., Lu, J., Wu, S.Y., Chen, C.W., Takada, K., Tsai, C.H., 2006. Induction of the early growth response 1 gene by Epstein-Barr virus lytic transactivator Zta. J Virol 80, 7748-7755.
Chang, Y.N., Dong, D.L., Hayward, G.S., Hayward, S.D., 1990. The Epstein-Barr virus Zta transactivator: a member of the bZIP family with unique DNA-binding specificity and a dimerization domain that lacks the characteristic heptad leucine zipper motif. J Virol 64, 3358-3369.
Chen, C., Li, D., Guo, N., 2009. Regulation of cellular and viral protein expression by the Epstein-Barr virus transcriptional regulator Zta: implications for therapy of EBV associated tumors. Cancer Biol Ther 8, 987-995.
Chen, F., Zou, J.Z., di Renzo, L., Winberg, G., Hu, L.F., Klein, E., Klein, G., Ernberg, I., 1995. A subpopulation of normal B cells latently infected with Epstein-Barr virus resembles Burkitt lymphoma cells in expressing EBNA-1 but not EBNA-2 or LMP1. J Virol 69, 3752-3758.
Chen, M.R., Chang, S.J., Huang, H., Chen, J.Y., 2000. A protein kinase activity associated with Epstein-Barr virus BGLF4 phosphorylates the viral early antigen EA-D in vitro. J Virol 74, 3093-3104.
Cheung, A., Kieff, E., 1982. Long internal direct repeat in Epstein-Barr virus DNA. J Virol 44, 286-294.
Chevallier-Greco, A., Manet, E., Chavrier, P., Mosnier, C., Daillie, J., Sergeant, A., 1986a. Both Epstein-Barr virus (EBV)-encoded trans-acting factors, EB1 and EB2, are required to activate transcription from an EBV early promoter. Embo J 5, 3243-3249.
Chevallier-Greco, A., Manet, E., Chavrier, P., Mosnier, C., Daillie, J., Sergeant, A., 1986b. Both Epstein-Barr virus (EBV)-encoded trans-acting factors, EB1 and EB2, are required to activate transcription from an EBV early promoter. EMBO J 5, 3243-3249.
Clave, E., Agbalika, F., Bajzik, V., Peffault de Latour, R., Trillard, M., Rabian, C., Scieux, C., Devergie, A., Socie, G., Ribaud, P., Ades, L., Ferry, C., Gluckman, E., Charron, D., Esperou, H., Toubert, A., Moins-Teisserenc, H., 2004. Epstein-Barr virus (EBV) reactivation in allogeneic stem-cell transplantation: relationship between viral load, EBV-specific T-cell reconstitution and rituximab therapy. Transplantation 77, 76-84.
Cohen, J.I., 2000. Epstein-Barr virus infection. N Engl J Med 343, 481-492.
Cohen, J.I., Wang, F., Mannick, J., Kieff, E., 1989. Epstein-Barr virus nuclear protein 2 is a key determinant of lymphocyte transformation. Proc Natl Acad Sci U S A 86, 9558-9562.

Constant, S.L., Bottomly, K., 1997. Induction of Th1 and Th2 CD4+ T cell responses: the alternative approaches. Annu Rev Immunol 15, 297-322.
Corsi, M.M., Ruscica, M., Passoni, D., Scarmozzino, M.G., Gulletta, E., 2004. High Th1-type cytokine serum levels in patients with infectious mononucleosis. Acta Virol 48, 263-266.
Countryman, J., Gradoville, L., Bhaduri-McIntosh, S., Ye, J., Heston, L., Himmelfarb, S., Shedd, D., Miller, G., 2009. Stimulus duration and response time independently influence the kinetics of lytic cycle reactivation of Epstein-Barr virus. J Virol 83, 10694-10709.
Countryman, J., Miller, G., 1985. Activation of expression of latent Epstein-Barr herpesvirus after gene transfer with a small cloned subfragment of heterogeneous viral DNA. Proc Natl Acad Sci U S A 82, 4085-4089.
Cox, K.L., Lawrence-Miyasaki, L.S., Garcia-Kennedy, R., Lennette, E.T., Martinez, O.M., Krams, S.M., Berquist, W.E., So, S.K., Esquivel, C.O., 1995. An increased incidence of Epstein-Barr virus infection and lymphoproliferative disorder in young children on FK506 after liver transplantation. Transplantation 59, 524-529.
Craig, F.E., Johnson, L.R., Harvey, S.A., Nalesnik, M.A., Luo, J.H., Bhattacharya, S.D., Swerdlow, S.H., 2007. Gene expression profiling of Epstein-Barr virus-positive and -negative monomorphic B-cell posttransplant lymphoproliferative disorders. Diagn Mol Pathol 16, 158-168.
Crawford, D.H., 2001. Biology and disease associations of Epstein-Barr virus. Philos Trans R Soc Lond B Biol Sci 356, 461-473.
Crawford, D.H., Macsween, K.F., Higgins, C.D., Thomas, R., McAulay, K., Williams, H., Harrison, N., Reid, S., Conacher, M., Douglas, J., Swerdlow, A.J., 2006. A cohort study among university students: identification of risk factors for Epstein-Barr virus seroconversion and infectious mononucleosis. Clin Infect Dis 43, 276-282.
Curtis, R.E., Travis, L.B., Rowlings, P.A., Socie, G., Kingma, D.W., Banks, P.M., Jaffe, E.S., Sale, G.E., Horowitz, M.M., Witherspoon, R.P., Shriner, D.A., Weisdorf, D.J., Kolb, H.J., Sullivan, K.M., Sobocinski, K.A., Gale, R.P., Hoover, R.N., Fraumeni, J.F., Jr., Deeg, H.J., 1999. Risk of lymphoproliferative disorders after bone marrow transplantation: a multi-institutional study. Blood 94, 2208-2216.
Daikoku, T., Kudoh, A., Fujita, M., Sugaya, Y., Isomura, H., Shirata, N., Tsurumi, T., 2005. Architecture of replication compartments formed during Epstein-Barr virus lytic replication. J Virol 79, 3409-3418.
Dambaugh, T., Hennessy, K., Chamnankit, L., Kieff, E., 1984. U2 region of Epstein-Barr virus DNA may encode Epstein-Barr nuclear antigen 2. Proc Natl Acad Sci U S A 81, 7632-7636.
Davies, A.H., Grand, R.J., Evans, F.J., Rickinson, A.B., 1991. Induction of Epstein-Barr virus lytic cycle by tumor-promoting and non-tumor-promoting phorbol esters requires active protein kinase C. J Virol 65, 6838-6844.
Davis, R.E., Staudt, L.M., 2002. Molecular diagnosis of lymphoid malignancies by gene expression profiling. Curr Opin Hematol 9, 333-338.
de Jesus, O., Smith, P.R., Spender, L.C., Elgueta Karstegl, C., Niller, H.H., Huang, D., Farrell, P.J., 2003a. Updated Epstein-Barr virus (EBV) DNA sequence and analysis of a promoter for the BART (CST, BARF0) RNAs of EBV. J Gen Virol 84, 1443-1450.
de Jesus, O., Smith, P.R., Spender, L.C., Elgueta Karstegl, C., Niller, H.H., Huang, D., Farrell, P.J., 2003b. Updated Epstein-Barr virus (EBV) DNA sequence and analysis of a promoter for the BART (CST, BARF0) RNAs of EBV. J Gen Virol 84, 1443-1450.
Decaussin, G., Leclerc, V., Ooka, T., 1995. The lytic cycle of Epstein-Barr virus in the nonproducer Raji line can be rescued by the expression of a 135-kilodalton protein encoded by the BALF2 open reading frame. J Virol 69, 7309-7314.
di Renzo, L., Altiok, A., Klein, G., Klein, E., 1994. Endogenous TGF-beta contributes to the induction of the EBV lytic cycle in two Burkitt lymphoma cell lines. Int J Cancer 57, 914-919.
Dolcetti, R., 2007. B lymphocytes and Epstein-Barr virus: the lesson of post-transplant lymphoproliferative disorders. Autoimmun Rev 7, 96-101.

Dotti, G., Fiocchi, R., Motta, T., Mammana, C., Gotti, E., Riva, S., Cornelli, P., Gridelli, B., Viero, P., Oldani, E., Ferrazzi, P., Remuzzi, G., Barbui, T., Rambaldi, A., 2002. Lymphomas occurring late after solid-organ transplantation: influence of treatment on the clinical outcome. Transplantation 74, 1095-1102.
Edelman, D.C., 2005. Human herpesvirus 8--a novel human pathogen. Virol J 2, 78.
El-Guindy, A.S., Miller, G., 2004. Phosphorylation of Epstein-Barr virus ZEBRA protein at its casein kinase 2 sites mediates its ability to repress activation of a viral lytic cycle late gene by Rta. J Virol 78, 7634-7644.
Eliopoulos, A.G., Gallagher, N.J., Blake, S.M., Dawson, C.W., Young, L.S., 1999. Activation of the p38 mitogen-activated protein kinase pathway by Epstein-Barr virus-encoded latent membrane protein 1 coregulates interleukin-6 and interleukin-8 production. J Biol Chem 274, 16085-16096.
Ernberg, I., Falk, K., Minarovits, J., Busson, P., Tursz, T., Masucci, M.G., Klein, G., 1989. The role of methylation in the phenotype-dependent modulation of Epstein-Barr nuclear antigen 2 and latent membrane protein genes in cells latently infected with Epstein-Barr virus. J Gen Virol 70 ( Pt 11), 2989-3002.
Eurich, K., Segawa, M., Toei-Shimizu, S., Mizoguchi, E., 2009. Potential role of chitinase 3-like-1 in inflammation-associated carcinogenic changes of epithelial cells. World J Gastroenterol 15, 5249-5259.
Fahraeus, R., Fu, H.L., Ernberg, I., Finke, J., Rowe, M., Klein, G., Falk, K., Nilsson, E., Yadav, M., Busson, P., et al., 1988. Expression of Epstein-Barr virus-encoded proteins in nasopharyngeal carcinoma. Int J Cancer 42, 329-338.
Fahraeus, R., Jansson, A., Ricksten, A., Sjoblom, A., Rymo, L., 1990. Epstein-Barr virus-encoded nuclear antigen 2 activates the viral latent membrane protein promoter by modulating the activity of a negative regulatory element. Proc Natl Acad Sci U S A 87, 7390-7394.
Farrell, P.J., 1995. Epstein-Barr virus immortalizing genes. Trends Microbiol 3, 105-109.
Farrell, P.J., 2002. Cell-switching and kissing. Nat Med 8, 559-560.
Farrell, P.J., Bankier, A., Seguin, C., Deininger, P., Barrell, B.G., 1983. Latent and lytic cycle promoters of Epstein-Barr virus. EMBO J 2, 1331-1338.
Farrell, P.J., Rowe, D.T., Rooney, C.M., Kouzarides, T., 1989. Epstein-Barr virus BZLF1 trans-activator specifically binds to a consensus AP-1 site and is related to c-fos. EMBO J 8, 127-132.
Feederle, R., Haar, J., Bernhardt, K., Linnstaedt, S.D., Bannert, H., Lips, H., Cullen, B.R., Delecluse, H.J., 2011. The members of an Epstein-Barr virus microRNA cluster cooperate to transform B lymphocytes. J Virol 85, 9801-9810.
Feederle, R., Kost, M., Baumann, M., Janz, A., Drouet, E., Hammerschmidt, W., Delecluse, H.J., 2000a. The Epstein-Barr virus lytic program is controlled by the co-operative functions of two transactivators. Embo J 19, 3080-3089.
Feederle, R., Kost, M., Baumann, M., Janz, A., Drouet, E., Hammerschmidt, W., Delecluse, H.J., 2000b. The Epstein-Barr virus lytic program is controlled by the co-operative functions of two transactivators. EMBO J 19, 3080-3089.
Feederle, R., Mehl-Lautscham, A.M., Bannert, H., Delecluse, H.J., 2009. The Epstein-Barr virus protein kinase BGLF4 and the exonuclease BGLF5 have opposite effects on the regulation of viral protein production. J Virol 83, 10877-10891.
Fields, B.N., Knipe, D.M., Howley, P.M., Ovid Technologies Inc., 2007. Fields' virology, 5th ed. Wolters kluwer/Lippincott Williams & Wilkins, Philadelphia.
Fixman, E.D., Hayward, G.S., Hayward, S.D., 1992. trans-acting requirements for replication of Epstein-Barr virus ori-Lyt. J Virol 66, 5030-5039.
Fixman, E.D., Hayward, G.S., Hayward, S.D., 1995. Replication of Epstein-Barr virus oriLyt: lack of a dedicated virally encoded origin-binding protein and dependence on Zta in cotransfection assays. J Virol 69, 2998-3006.
Flemington, E., Speck, S.H., 1990. Autoregulation of Epstein-Barr virus putative lytic switch gene BZLF1. J Virol 64, 1227-1232.

Flemington, E.K., Goldfeld, A.E., Speck, S.H., 1991. Efficient transcription of the Epstein-Barr virus immediate-early BZLF1 and BRLF1 genes requires protein synthesis. J Virol 65, 7073-7077.
Francis, A., Ragoczy, T., Gradoville, L., Heston, L., El-Guindy, A., Endo, Y., Miller, G., 1999. Amino acid substitutions reveal distinct functions of serine 186 of the ZEBRA protein in activation of early lytic cycle genes and synergy with the Epstein-Barr virus R transactivator. J Virol 73, 4543-4551.
Francis, A.L., Gradoville, L., Miller, G., 1997. Alteration of a single serine in the basic domain of the Epstein-Barr virus ZEBRA protein separates its functions of transcriptional activation and disruption of latency. J Virol 71, 3054-3061.
Gamadia, L.E., Rentenaar, R.J., van Lier, R.A., ten Berge, I.J., 2004. Properties of CD4(+) T cells in human cytomegalovirus infection. Hum Immunol 65, 486-492.
Gao, M., Knipe, D.M., 1991. Potential role for herpes simplex virus ICP8 DNA replication protein in stimulation of late gene expression. J Virol 65, 2666-2675.
Gao, Z., Krithivas, A., Finan, J.E., Semmes, O.J., Zhou, S., Wang, Y., Hayward, S.D., 1998. The Epstein-Barr virus lytic transactivator Zta interacts with the helicase-primase replication proteins. J Virol 72, 8559-8567.
Gargouri, B., Nasr, R., Ben Mansour, R., Lassoued, S., Mseddi, M., Attia, H., El Feki, A.E., Van Pelt, J., 2011a. Reactive Oxygen Species Production and Antioxidant Enzyme Expression after Epstein-Barr Virus Lytic Cycle Induction in Raji Cell Line. Biol Trace Elem Res.
Gargouri, B., Nasr, R., Mseddi, M., Benmansour, R., Lassoued, S., 2011b. Induction of Epstein-Barr virus (EBV) lytic cycle in vitro causes lipid peroxidation, protein oxidation and DNA damage in lymphoblastoid B cell lines. Lipids Health Dis 10, 111.
Gartner, B., Preiksaitis, J.K., 2010. EBV viral load detection in clinical virology. J Clin Virol 48, 82-90.
Gartner, B.C., Schafer, H., Marggraff, K., Eisele, G., Schafer, M., Dilloo, D., Roemer, K., Laws, H.J., Sester, M., Sester, U., Einsele, H., Mueller-Lantzsch, N., 2002. Evaluation of use of Epstein-Barr viral load in patients after allogeneic stem cell transplantation to diagnose and monitor posttransplant lymphoproliferative disease. J Clin Microbiol 40, 351-358.
Gotoh, K., Ito, Y., Ohta, R., Iwata, S., Nishiyama, Y., Nakamura, T., Kaneko, K., Kiuchi, T., Ando, H., Kimura, H., 2010. Immunologic and virologic analyses in pediatric liver transplant recipients with chronic high Epstein-Barr virus loads. J Infect Dis 202, 461-469.
Gradoville, L., Kwa, D., El-Guindy, A., Miller, G., 2002. Protein kinase C-independent activation of the Epstein-Barr virus lytic cycle. J Virol 76, 5612-5626.
Gratama, J.W., Ernberg, I., 1995. Molecular epidemiology of Epstein-Barr virus infection. Adv Cancer Res 67, 197-255.
Gratama, J.W., Zutter, M.M., Minarovits, J., Oosterveer, M.A., Thomas, E.D., Klein, G., Ernberg, I., 1991. Expression of Epstein-Barr virus-encoded growth-transformation-associated proteins in lymphoproliferations of bone-marrow transplant recipients. Int J Cancer 47, 188-192.
Green, M., Bueno, J., Rowe, D., Mazariegos, G., Qu, L., Abu-Almagd, K., Reyes, J., 2000. Predictive negative value of persistent low Epstein-Barr virus viral load after intestinal transplantation in children. Transplantation 70, 593-596.
Green, M., Cacciarelli, T.V., Mazariegos, G.V., Sigurdsson, L., Qu, L., Rowe, D.T., Reyes, J., 1998. Serial measurement of Epstein-Barr viral load in peripheral blood in pediatric liver transplant recipients during treatment for posttransplant lymphoproliferative disease. Transplantation 66, 1641-1644.
Green, M., Webber, S.A., 2002. EBV viral load monitoring: unanswered questions. Am J Transplant 2, 894-895.
Green, M., Webber, S.A., 2007. Persistent increased Epstein-Barr virus loads after solid organ transplantation: truth and consequences? Liver Transpl 13, 321-322.
Gruffat, H., Kadjouf, F., Mariame, B., Manet, E., 2012. The Epstein-Barr virus BcRF1 gene product is a TBP-like protein with an essential role in late gene expression. J Virol.
Gulley, M.L., Pulitzer, D.R., Eagan, P.A., Schneider, B.G., 1996. Epstein-Barr virus infection is an early event in gastric carcinogenesis and is independent of bcl-2 expression and p53 accumulation. Hum Pathol 27, 20-27.

Gulley, M.L., Tang, W., 2008. Laboratory assays for Epstein-Barr virus-related disease. J Mol Diagn 10, 279-292.
Guo, Q., Qian, L., Guo, L., Shi, M., Chen, C., Lv, X., Yu, M., Hu, M., Jiang, G., Guo, N., 2010a. Transactivators Zta and Rta of Epstein-Barr virus promote G0/G1 to S transition in Raji cells: a novel relationship between lytic virus and cell cycle. Mol Immunol 47, 1783-1792.
Guo, Y., Zhang, X., Yang, M., Miao, X., Shi, Y., Yao, J., Tan, W., Sun, T., Zhao, D., Yu, D., Liu, J., Lin, D., 2010b. Functional evaluation of missense variations in the human MAD1L1 and MAD2L1 genes and their impact on susceptibility to lung cancer. J Med Genet 47, 616-622.
Gustafsson, A., Levitsky, V., Zou, J.Z., Frisan, T., Dalianis, T., Ljungman, P., Ringden, O., Winiarski, J., Ernberg, I., Masucci, M.G., 2000. Epstein-Barr virus (EBV) load in bone marrow transplant recipients at risk to develop posttransplant lymphoproliferative disease: prophylactic infusion of EBV-specific cytotoxic T cells. Blood 95, 807-814.
Hackstadt, A.J., Hess, A.M., 2009. Filtering for increased power for microarray data analysis. BMC Bioinformatics 10, 11.
Hadinoto, V., Shapiro, M., Greenough, T.C., Sullivan, J.L., Luzuriaga, K., Thorley-Lawson, D.A., 2008. On the dynamics of acute EBV infection and the pathogenesis of infectious mononucleosis. Blood 111, 1420-1427.
Hahn, A.M., Huye, L.E., Ning, S., Webster-Cyriaque, J., Pagano, J.S., 2005. Interferon regulatory factor 7 is negatively regulated by the Epstein-Barr virus immediate-early gene, BZLF-1. J Virol 79, 10040-10052.
Hammerschmidt, W., Sugden, B., 1988. Identification and characterization of oriLyt, a lytic origin of DNA replication of Epstein-Barr virus. Cell 55, 427-433.
Han, Z., Marendy, E., Wang, Y.D., Yuan, J., Sample, J.T., Swaminathan, S., 2007. Multiple roles of Epstein-Barr virus SM protein in lytic replication. J Virol 81, 4058-4069.
Hannigan, A., Qureshi, A.M., Nixon, C., Tsimbouri, P.M., Jones, S., Philbey, A.W., Wilson, J.B., 2011. Lymphocyte deficiency limits Epstein-Barr virus latent membrane protein 1 induced chronic inflammation and carcinogenic pathology in vivo. Mol Cancer 10, 11.
Hardwick, J.M., Lieberman, P.M., Hayward, S.D., 1988. A new Epstein-Barr virus transactivator, R, induces expression of a cytoplasmic early antigen. J Virol 62, 2274-2284.
Harris, N.L., 1997. Principles of the revised European-American Lymphoma Classification (from the International Lymphoma Study Group). Ann Oncol 8 Suppl 2, 11-16.
Harris, N.L., Ferry, J.A., Swerdlow, S.H., 1997. Posttransplant lymphoproliferative disorders: summary of Society for Hematopathology Workshop. Semin Diagn Pathol 14, 8-14.
Harrison, A.P., Johnston, C.E., Orengo, C.A., 2007. Establishing a major cause of discrepancy in the calibration of Affymetrix GeneChips. BMC Bioinformatics 8, 195.
Hatfull, G., Bankier, A.T., Barrell, B.G., Farrell, P.J., 1988. Sequence analysis of Raji Epstein-Barr virus DNA. Virology 164, 334-340.
Heineman, T., Gong, M., Sample, J., Kieff, E., 1988. Identification of the Epstein-Barr virus gp85 gene. J Virol 62, 1101-1107.
Henle, G., Henle, W., Clifford, P., Diehl, V., Kafuko, G.W., Kirya, B.G., Klein, G., Morrow, R.H., Munube, G.M., Pike, P., Tukei, P.M., Ziegler, J.L., 1969. Antibodies to Epstein-Barr virus in Burkitt's lymphoma and control groups. J Natl Cancer Inst 43, 1147-1157.
Henwood, M., Clarke, P.A., Smith, A.M., Watson, S.A., 2001. Expression of gastrin in developing gastric adenocarcinoma. Br J Surg 88, 564-568.
Herbst, H., Dallenbach, F., Hummel, M., Niedobitek, G., Pileri, S., Muller-Lantzsch, N., Stein, H., 1991. Epstein-Barr virus latent membrane protein expression in Hodgkin and Reed-Sternberg cells. Proc Natl Acad Sci U S A 88, 4766-4770.
Hertle, M.L., Popp, C., Petermann, S., Maier, S., Kremmer, E., Lang, R., Mages, J., Kempkes, B., 2009. Differential gene expression patterns of EBV infected EBNA-3A positive and negative human B lymphocytes. PLoS Pathog 5, e1000506.

Hickabottom, M., Parker, G.A., Freemont, P., Crook, T., Allday, M.J., 2002. Two nonconsensus sites in the Epstein-Barr virus oncoprotein EBNA3A cooperate to bind the co-repressor carboxyl-terminal-binding protein (CtBP). J Biol Chem 277, 47197-47204.
Ho, M., Jaffe, R., Miller, G., Breinig, M.K., Dummer, J.S., Makowka, L., Atchison, R.W., Karrer, F., Nalesnik, M.A., Starzl, T.E., 1988. The frequency of Epstein-Barr virus infection and associated lymphoproliferative syndrome after transplantation and its manifestations in children. Transplantation 45, 719-727.
Holley-Guthrie, E.A., Seaman, W.T., Bhende, P., Merchant, J.L., Kenney, S.C., 2005. The Epstein-Barr virus protein BMRF1 activates gastrin transcription. J Virol 79, 745-755.
Holmes, R.D., Orban-Eller, K., Karrer, F.R., Rowe, D.T., Narkewicz, M.R., Sokol, R.J., 2002. Response of elevated Epstein-Barr virus DNA levels to therapeutic changes in pediatric liver transplant patients: 56-month follow up and outcome. Transplantation 74, 367-372.
Holmes, R.D., Sokol, R.J., 2002. Epstein-Barr virus and post-transplant lymphoproliferative disease. Pediatr Transplant 6, 456-464.
Hong, G.K., Delecluse, H.J., Gruffat, H., Morrison, T.E., Feng, W.H., Sergeant, A., Kenney, S.C., 2004. The BRRF1 early gene of Epstein-Barr virus encodes a transcription factor that enhances induction of lytic infection by BRLF1. J Virol 78, 4983-4992.
Hong, G.K., Gulley, M.L., Feng, W.H., Delecluse, H.J., Holley-Guthrie, E., Kenney, S.C., 2005. Epstein-Barr virus lytic infection contributes to lymphoproliferative disease in a SCID mouse model. J Virol 79, 13993-14003.
Hopwood, P., Crawford, D.H., 2000. The role of EBV in post-transplant malignancies: a review. J Clin Pathol 53, 248-254.
Hopwood, P.A., Brooks, L., Parratt, R., Hunt, B.J., Bokhari, M., Thomas, J.A., Yacoub, M., Crawford, D.H., 2002. Persistent Epstein-Barr virus infection: unrestricted latent and lytic viral gene expression in healthy immunosuppressed transplant recipients. Transplantation 74, 194-202.
Hoshikawa, Y., Satoh, Y., Murakami, M., Maeta, M., Kaibara, N., Ito, H., Kurata, T., Sairenji, T., 2002. Evidence of lytic infection of Epstein-Barr virus (EBV) in EBV-positive gastric carcinoma. J Med Virol 66, 351-359.
Hoshino, Y., Kimura, H., Tanaka, N., Tsuge, I., Kudo, K., Horibe, K., Kato, K., Matsuyama, T., Kikuta, A., Kojima, S., Morishima, T., 2001. Prospective monitoring of the Epstein-Barr virus DNA by a real-time quantitative polymerase chain reaction after allogenic stem cell transplantation. Br J Haematol 115, 105-111.
Hsu, M., Wu, S.Y., Chang, S.S., Su, I.J., Tsai, C.H., Lai, S.J., Shiau, A.L., Takada, K., Chang, Y., 2008. Epstein-Barr virus lytic transactivator Zta enhances chemotactic activity through induction of interleukin-8 in nasopharyngeal carcinoma cells. J Virol 82, 3679-3688.
Hsu, W.L., Chung, P.J., Tsai, M.H., Chang, C.L., Liang, C.L., 2012. A role for Epstein-Barr viral BALF1 in facilitating tumor formation and metastasis potential. Virus Res 163, 617-627.
Hubbell, E., Liu, W.M., Mei, R., 2002. Robust estimators for expression analysis. Bioinformatics 18, 1585-1592.
Hutt-Fletcher, L.M., 2007. Epstein-Barr virus entry. J Virol 81, 7825-7832.
Inman, G.J., Binne, U.K., Parker, G.A., Farrell, P.J., Allday, M.J., 2001. Activators of the Epstein-Barr virus lytic program concomitantly induce apoptosis, but lytic gene expression protects from cell death. J Virol 75, 2400-2410.
Irizarry, R.A., Bolstad, B.M., Collin, F., Cope, L.M., Hobbs, B., Speed, T.P., 2003. Summaries of Affymetrix GeneChip probe level data. Nucleic Acids Res 31, e15.
Jabs, W.J., Hennig, H., Kittel, M., Pethig, K., Smets, F., Bucsky, P., Kirchner, H., Wagner, H.J., 2001. Normalized quantification by real-time PCR of Epstein-Barr virus load in patients at risk for posttransplant lymphoproliferative disorders. J Clin Microbiol 39, 564-569.
Jain, A., Nalesnik, M., Reyes, J., Pokharna, R., Mazariegos, G., Green, M., Eghtesad, B., Marsh, W., Cacciarelli, T., Fontes, P., Abu-Elmagd, K., Sindhi, R., Demetris, J., Fung, J., 2002. Posttransplant

lymphoproliferative disorders in liver transplantation: a 20-year experience. Ann Surg 236, 429-436; discussion 436-427.
Jenson, H.B., Farrell, P.J., Miller, G., 1987. Sequences of the Epstein-Barr Virus (EBV) large internal repeat form the center of a 16-kilobase-pair palindrome of EBV (P3HR-1) heterogeneous DNA. J Virol 61, 1495-1506.
Johannsen, E., Luftig, M., Chase, M.R., Weicksel, S., Cahir-McFarland, E., Illanes, D., Sarracino, D., Kieff, E., 2004. Proteins of purified Epstein-Barr virus. Proc Natl Acad Sci U S A 101, 16286-16291.
Johansen, J.S., 2006. Studies on serum YKL-40 as a biomarker in diseases with inflammation, tissue remodelling, fibroses and cancer. Dan Med Bull 53, 172-209.
Johansen, J.S., Bojesen, S.E., Mylin, A.K., Frikke-Schmidt, R., Price, P.A., Nordestgaard, B.G., 2009. Elevated plasma YKL-40 predicts increased risk of gastrointestinal cancer and decreased survival after any cancer diagnosis in the general population. J Clin Oncol 27, 572-578.
Johansen, J.S., Pedersen, A.N., Schroll, M., Jorgensen, T., Pedersen, B.K., Bruunsgaard, H., 2008. High serum YKL-40 level in a cohort of octogenarians is associated with increased risk of all-cause mortality. Clin Exp Immunol 151, 260-266.
Jones, R.J., Seaman, W.T., Feng, W.H., Barlow, E., Dickerson, S., Delecluse, H.J., Kenney, S.C., 2007. Roles of lytic viral infection and IL-6 in early versus late passage lymphoblastoid cell lines and EBV-associated lymphoproliferative disease. Int J Cancer 121, 1274-1281.
Joseph, A.M., Babcock, G.J., Thorley-Lawson, D.A., 2000. EBV persistence involves strict selection of latently infected B cells. J Immunol 165, 2975-2981.
Kalla, M., Schmeinck, A., Bergbauer, M., Pich, D., Hammerschmidt, W., 2010. AP-1 homolog BZLF1 of Epstein-Barr virus has two essential functions dependent on the epigenetic state of the viral genome. Proc Natl Acad Sci U S A 107, 850-855.
Kallakury, B.V., Sheehan, C.E., Ambros, R.A., Fisher, H.A., Kaufman, R.P., Jr., Ross, J.S., 1997. The prognostic significance of p34cdc2 and cyclin D1 protein expression in prostate adenocarcinoma. Cancer 80, 753-763.
Kanamori, M., Watanabe, S., Honma, R., Kuroda, M., Imai, S., Takada, K., Yamamoto, N., Nishiyama, Y., Kawaguchi, Y., 2004. Epstein-Barr virus nuclear antigen leader protein induces expression of thymus- and activation-regulated chemokine in B cells. J Virol 78, 3984-3993.
Kato, K., Yokoyama, A., Tohya, Y., Akashi, H., Nishiyama, Y., Kawaguchi, Y., 2003. Identification of protein kinases responsible for phosphorylation of Epstein-Barr virus nuclear antigen leader protein at serine-35, which regulates its coactivator function. J Gen Virol 84, 3381-3392.
Katz, B.Z., Pahl, E., Crawford, S.E., Kostyk, M.C., Rodgers, S., Seshadri, R., Proytcheva, M., Pophal, S., 2007. Case-control study of risk factors for the development of post-transplant lymphoproliferative disease in a pediatric heart transplant cohort. Pediatr Transplant 11, 58-65.
Katz, B.Z., Raab-Traub, N., Miller, G., 1989. Latent and replicating forms of Epstein-Barr virus DNA in lymphomas and lymphoproliferative diseases. J Infect Dis 160, 589-598.
Kawa, K., Sawada, A., Sato, M., Okamura, T., Sakata, N., Kondo, O., Kimoto, T., Yamada, K., Tokimasa, S., Yasui, M., Inoue, M., 2011. Excellent outcome of allogeneic hematopoietic SCT with reduced-intensity conditioning for the treatment of chronic active EBV infection. Bone Marrow Transplant 46, 77-83.
Kawaguchi, Y., Kato, K., Tanaka, M., Kanamori, M., Nishiyama, Y., Yamanashi, Y., 2003. Conserved protein kinases encoded by herpesviruses and cellular protein kinase cdc2 target the same phosphorylation site in eukaryotic elongation factor 1delta. J Virol 77, 2359-2368.
Kaye, K.M., Izumi, K.M., Kieff, E., 1993. Epstein-Barr virus latent membrane protein 1 is essential for B-lymphocyte growth transformation. Proc Natl Acad Sci U S A 90, 9150-9154.
Kempkes, B., Spitkovsky, D., Jansen-Durr, P., Ellwart, J.W., Kremmer, E., Delecluse, H.J., Rottenberger, C., Bornkamm, G.W., Hammerschmidt, W., 1995. B-cell proliferation and induction of early G1-regulating proteins by Epstein-Barr virus mutants conditional for EBNA2. EMBO J 14, 88-96.

Kenagy, D.N., Schlesinger, Y., Weck, K., Ritter, J.H., Gaudreault-Keener, M.M., Storch, G.A., 1995. Epstein-Barr virus DNA in peripheral blood leukocytes of patients with posttransplant lymphoproliferative disease. Transplantation 60, 547-554.
Kennedy, G., Komano, J., Sugden, B., 2003. Epstein-Barr virus provides a survival factor to Burkitt's lymphomas. Proc Natl Acad Sci U S A 100, 14269-14274.
Kenney, S., Holley-Guthrie, E., Mar, E.C., Smith, M., 1989. The Epstein-Barr virus BMLF1 promoter contains an enhancer element that is responsive to the BZLF1 and BRLF1 transactivators. J Virol 63, 3878-3883.
Kienzle, N., Sculley, T.B., Poulsen, L., Buck, M., Cross, S., Raab-Traub, N., Khanna, R., 1998. Identification of a cytotoxic T-lymphocyte response to the novel BARF0 protein of Epstein-Barr virus: a critical role for antigen expression. J Virol 72, 6614-6620.
Kilger, E., Kieser, A., Baumann, M., Hammerschmidt, W., 1998. Epstein-Barr virus-mediated B-cell proliferation is dependent upon latent membrane protein 1, which simulates an activated CD40 receptor. EMBO J 17, 1700-1709.
Kim, D.B., Zabierowski, S., DeLuca, N.A., 2002. The initiator element in a herpes simplex virus type 1 late-gene promoter enhances activation by ICP4, resulting in abundant late-gene expression. J Virol 76, 1548-1558.
Kim, K.R., Yoshizaki, T., Miyamori, H., Hasegawa, K., Horikawa, T., Furukawa, M., Harada, S., Seiki, M., Sato, H., 2000. Transformation of Madin-Darby canine kidney (MDCK) epithelial cells by Epstein-Barr virus latent membrane protein 1 (LMP1) induces expression of Ets1 and invasive growth. Oncogene 19, 1764-1771.
Kim, Y.S., Seo, D.W., Kong, S.K., Lee, J.H., Lee, E.S., Stetler-Stevenson, M., Stetler-Stevenson, W.G., 2008. TIMP1 induces CD44 expression and the activation and nuclear translocation of SHP1 during the late centrocyte/post-germinal center B cell differentiation. Cancer Lett 269, 37-45.
Kimura, H., Morita, M., Yabuta, Y., Kuzushima, K., Kato, K., Kojima, S., Matsuyama, T., Morishima, T., 1999. Quantitative analysis of Epstein-Barr virus load by using a real-time PCR assay. J Clin Microbiol 37, 132-136.
Kirchmaier, A.L., Sugden, B., 1995. Plasmid maintenance of derivatives of oriP of Epstein-Barr virus. J Virol 69, 1280-1283.
Knight, J.S., Robertson, E.S., 2004. Epstein-Barr virus nuclear antigen 3C regulates cyclin A/p27 complexes and enhances cyclin A-dependent kinase activity. J Virol 78, 1981-1991.
Knowles, D.M., 1999. Immunodeficiency-associated lymphoproliferative disorders. Mod Pathol 12, 200-217.
Knowles, D.M., Cesarman, E., Chadburn, A., Frizzera, G., Chen, J., Rose, E.A., Michler, R.E., 1995. Correlative morphologic and molecular genetic analysis demonstrates three distinct categories of posttransplantation lymphoproliferative disorders. Blood 85, 552-565.
Kolman, J.L., Taylor, N., Marshak, D.R., Miller, G., 1993. Serine-173 of the Epstein-Barr virus ZEBRA protein is required for DNA binding and is a target for casein kinase II phosphorylation. Proc Natl Acad Sci U S A 90, 10115-10119.
Kucur, M., Isman, F.K., Balci, C., Onal, B., Hacibekiroglu, M., Ozkan, F., Ozkan, A., 2008. Serum YKL-40 levels and chitotriosidase activity as potential biomarkers in primary prostate cancer and benign prostatic hyperplasia. Urol Oncol 26, 47-52.
Kulwichit, W., Edwards, R.H., Davenport, E.M., Baskar, J.F., Godfrey, V., Raab-Traub, N., 1998. Expression of the Epstein-Barr virus latent membrane protein 1 induces B cell lymphoma in transgenic mice. Proc Natl Acad Sci U S A 95, 11963-11968.
Kurilla, M.G., Heineman, T., Davenport, L.C., Kieff, E., Hutt-Fletcher, L.M., 1995. A novel Epstein-Barr virus glycoprotein gp150 expressed from the BDLF3 open reading frame. Virology 209, 108-121.
Kusano, S., Raab-Traub, N., 2001. An Epstein-Barr virus protein interacts with Notch. J Virol 75, 384-395.
Laichalk, L.L., Thorley-Lawson, D.A., 2005. Terminal differentiation into plasma cells initiates the replicative cycle of Epstein-Barr virus in vivo. J Virol 79, 1296-1307.

Landgren, O., Gilbert, E.S., Rizzo, J.D., Socie, G., Banks, P.M., Sobocinski, K.A., Horowitz, M.M., Jaffe, E.S., Kingma, D.W., Travis, L.B., Flowers, M.E., Martin, P.J., Deeg, H.J., Curtis, R.E., 2009. Risk factors for lymphoproliferative disorders after allogeneic hematopoietic cell transplantation. Blood 113, 4992-5001.
Laux, G., Freese, U.K., Fischer, R., Polack, A., Kofler, E., Bornkamm, G.W., 1988. TPA-inducible Epstein-Barr virus genes in Raji cells and their regulation. Virology 162, 503-507.
Leblond, V., Choquet, S., 2004. Lymphoproliferative disorders after liver transplantation. J Hepatol 40, 728-735.
Leblond, V., Davi, F., Charlotte, F., Dorent, R., Bitker, M.O., Sutton, L., Gandjbakhch, I., Binet, J.L., Raphael, M., 1998. Posttransplant lymphoproliferative disorders not associated with Epstein-Barr virus: a distinct entity? J Clin Oncol 16, 2052-2059.
Lee, C.G., Hartl, D., Lee, G.R., Koller, B., Matsuura, H., Da Silva, C.A., Sohn, M.H., Cohn, L., Homer, R.J., Kozhich, A.A., Humbles, A., Kearley, J., Coyle, A., Chupp, G., Reed, J., Flavell, R.A., Elias, J.A., 2009. Role of breast regression protein 39 (BRP-39)/chitinase 3-like-1 in Th2 and IL-13-induced tissue responses and apoptosis. J Exp Med 206, 1149-1166.
Lee, K.H., Choi, E.Y., Kim, M.K., Lee, S.H., Jang, B.I., Kim, T.N., Kim, S.W., Song, S.K., Kim, J.R., Jung, B.C., 2010. Hepatoma-derived growth factor regulates the bad-mediated apoptotic pathway and induction of vascular endothelial growth factor in stomach cancer cells. Oncol Res 19, 67-76.
Lee, P.P., Zeng, D., McCaulay, A.E., Chen, Y.F., Geiler, C., Umetsu, D.T., Chao, N.J., 1997. T helper 2-dominant antilymphoma immune response is associated with fatal outcome. Blood 90, 1611-1617.
Lee, T.C., Savoldo, B., Barshes, N.R., Rooney, C.M., Heslop, H.E., Gee, A.P., Caldwell, Y., Scott, J.D., Goss, J.A., 2006. Use of cytokine polymorphisms and Epstein-Barr virus viral load to predict development of post-transplant lymphoproliferative disorder in paediatric liver transplant recipients. Clin Transplant 20, 389-393.
Lee, T.C., Savoldo, B., Rooney, C.M., Heslop, H.E., Gee, A.P., Caldwell, Y., Barshes, N.R., Scott, J.D., Bristow, L.J., O'Mahony, C.A., Goss, J.A., 2005. Quantitative EBV viral loads and immunosuppression alterations can decrease PTLD incidence in pediatric liver transplant recipients. Am J Transplant 5, 2222-2228.
Lester, J.T., DeLuca, N.A., 2011. Herpes simplex virus 1 ICP4 forms complexes with TFIID and mediator in virus-infected cells. J Virol 85, 5733-5744.
Li, Q.X., Young, L.S., Niedobitek, G., Dawson, C.W., Birkenbach, M., Wang, F., Rickinson, A.B., 1992. Epstein-Barr virus infection and replication in a human epithelial cell system. Nature 356, 347-350.
Lieberman, P.M., Hardwick, J.M., Sample, J., Hayward, G.S., Hayward, S.D., 1990. The zta transactivator involved in induction of lytic cycle gene expression in Epstein-Barr virus-infected lymphocytes binds to both AP-1 and ZRE sites in target promoter and enhancer regions. J Virol 64, 1143-1155.
Liebowitz, D., 1994. Nasopharyngeal carcinoma: the Epstein-Barr virus association. Semin Oncol 21, 376-381.
Lin, J.C., Sista, N.D., Besencon, F., Kamine, J., Pagano, J.S., 1991. Identification and functional characterization of Epstein-Barr virus DNA polymerase by in vitro transcription-translation of a cloned gene. J Virol 65, 2728-2731.
Lipshutz, R.J., Fodor, S.P., Gingeras, T.R., Lockhart, D.J., 1999. High density synthetic oligonucleotide arrays. Nat Genet 21, 20-24.
Littler, E., Zeuthen, J., McBride, A.A., Trost Sorensen, E., Powell, K.L., Walsh-Arrand, J.E., Arrand, J.R., 1986. Identification of an Epstein-Barr virus-coded thymidine kinase. EMBO J 5, 1959-1966.
Liu, P., Speck, S.H., 2003. Synergistic autoactivation of the Epstein-Barr virus immediate-early BRLF1 promoter by Rta and Zta. Virology 310, 199-206.
Liu, W.M., Mei, R., Di, X., Ryder, T.B., Hubbell, E., Dee, S., Webster, T.A., Harrington, C.A., Ho, M.H., Baid, J., Smeekens, S.P., 2002. Analysis of high density expression microarrays with signed-rank call algorithms. Bioinformatics 18, 1593-1599.

Liu, Z., Falo, L.D., Jr., You, Z., 2011. Knockdown of HMGB1 in tumor cells attenuates their ability to induce regulatory T cells and uncovers naturally acquired CD8 T cell-dependent antitumor immunity. J Immunol 187, 118-125.
Livak, K.J., Schmittgen, T.D., 2001. Analysis of relative gene expression data using real-time quantitative PCR and the 2(-Delta Delta C(T)) Method. Methods 25, 402-408.
Loetscher, M., Gerber, B., Loetscher, P., Jones, S.A., Piali, L., Clark-Lewis, I., Baggiolini, M., Moser, B., 1996. Chemokine receptor specific for IP10 and mig: structure, function, and expression in activated T-lymphocytes. J Exp Med 184, 963-969.
Lones, M.A., Shintaku, I.P., Weiss, L.M., Thung, S.N., Nichols, W.S., Geller, S.A., 1997. Posttransplant lymphoproliferative disorder in liver allograft biopsies: a comparison of three methods for the demonstration of Epstein-Barr virus. Hum Pathol 28, 533-539.
Loren, A.W., Porter, D.L., Stadtmauer, E.A., Tsai, D.E., 2003. Post-transplant lymphoproliferative disorder: a review. Bone Marrow Transplant 31, 145-155.
Lu, C.C., Jeng, Y.Y., Tsai, C.H., Liu, M.Y., Yeh, S.W., Hsu, T.Y., Chen, M.R., 2006. Genome-wide transcription program and expression of the Rta responsive gene of Epstein-Barr virus. Virology 345, 358-372.
Lucas, K.G., Filo, F., Heilman, D.K., Lee, C.H., Emanuel, D.J., 1998. Semiquantitative Epstein-Barr virus polymerase chain reaction analysis of peripheral blood from organ transplant patients and risk for the development of lymphoproliferative disease. Blood 92, 3977-3978.
Lucchesi, W., Brady, G., Dittrich-Breiholz, O., Kracht, M., Russ, R., Farrell, P.J., 2008. Differential gene regulation by Epstein-Barr virus type 1 and type 2 EBNA2. J Virol 82, 7456-7466.
Luka, J., Kallin, B., Klein, G., 1979. Induction of the Epstein-Barr virus (EBV) cycle in latently infected cells by n-butyrate. Virology 94, 228-231.
Luo, B., Murakami, M., Fukuda, M., Fujioka, A., Yanagihara, K., Sairenji, T., 2004. Characterization of Epstein-Barr virus infection in a human signet ring cell gastric carcinoma cell line, HSC-39. Microbes Infect 6, 429-439.
Luster, A.D., Leder, P., 1993. IP-10, a -C-X-C- chemokine, elicits a potent thymus-dependent antitumor response in vivo. J Exp Med 178, 1057-1065.
Lyngaa, R., Norregaard, K., Kristensen, M., Kubale, V., Rosenkilde, M.M., Kledal, T.N., 2010. Cell transformation mediated by the Epstein-Barr virus G protein-coupled receptor BILF1 is dependent on constitutive signaling. Oncogene 29, 4388-4398.
Ma, S.D., Hegde, S., Young, K.H., Sullivan, R., Rajesh, D., Zhou, Y., Jankowska-Gan, E., Burlingham, W.J., Sun, X., Gulley, M.L., Tang, W., Gumperz, J.E., Kenney, S.C., 2010. A new model of EBV infection reveals an important role for early lytic viral protein expression in the development of lymphomas. J Virol.
MacMahon, E.M., Glass, J.D., Hayward, S.D., Mann, R.B., Becker, P.S., Charache, P., McArthur, J.C., Ambinder, R.F., 1991. Epstein-Barr virus in AIDS-related primary central nervous system lymphoma. Lancet 338, 969-973.
Maggio, E.M., Van Den Berg, A., Visser, L., Diepstra, A., Kluiver, J., Emmens, R., Poppema, S., 2002. Common and differential chemokine expression patterns in rs cells of NLP, EBV positive and negative classical Hodgkin lymphomas. Int J Cancer 99, 665-672.
Mahot, S., Sergeant, A., Drouet, E., Gruffat, H., 2003. A novel function for the Epstein-Barr virus transcription factor EB1/Zta: induction of transcription of the hIL-10 gene. J Gen Virol 84, 965-974.
Malkas, L.H., Herbert, B.S., Abdel-Aziz, W., Dobrolecki, L.E., Liu, Y., Agarwal, B., Hoelz, D., Badve, S., Schnaper, L., Arnold, R.J., Mechref, Y., Novotny, M.V., Loehrer, P., Goulet, R.J., Hickey, R.J., 2006. A cancer-associated PCNA expressed in breast cancer has implications as a potential biomarker. Proc Natl Acad Sci U S A 103, 19472-19477.
Maloy, K.J., Burkhart, C., Junt, T.M., Odermatt, B., Oxenius, A., Piali, L., Zinkernagel, R.M., Hengartner, H., 2000. CD4(+) T cell subsets during virus infection. Protective capacity depends on effector cytokine secretion and on migratory capability. J Exp Med 191, 2159-2170.

Manenti, G., Galbiati, F., Pettinicchio, A., Spinola, M., Piconese, S., Leoni, V.P., Conti, B., Ravagnani, F., Incarbone, M., Pastorino, U., Dragani, T.A., 2006. A V141L polymorphism of the human LRMP gene is associated with survival of lung cancer patients. Carcinogenesis 27, 1386-1390.
Manez, R., Kusne, S., Abu-Elmagd, K., Reyes, J., Irish, W., Green, M., Furukawa, H., Kadry, Z., Tzakis, A., Todo, S., et al., 1994. Factors associated with recurrent cytomegalovirus disease after small bowel transplantation. Transplant Proc 26, 1422-1423.
Mannick, J.B., Cohen, J.I., Birkenbach, M., Marchini, A., Kieff, E., 1991. The Epstein-Barr virus nuclear protein encoded by the leader of the EBNA RNAs is important in B-lymphocyte transformation. J Virol 65, 6826-6837.
Martel-Renoir, D., Grunewald, V., Touitou, R., Schwaab, G., Joab, I., 1995. Qualitative analysis of the expression of Epstein-Barr virus lytic genes in nasopharyngeal carcinoma biopsies. J Gen Virol 76 ( Pt 6), 1401-1408.
Mathur, A., Kamat, D.M., Filipovich, A.H., Steinbuch, M., Shapiro, R.S., 1994. Immunoregulatory abnormalities in patients with Epstein-Barr virus-associated B cell lymphoproliferative disorders. Transplantation 57, 1042-1045.
McAulay, K.A., Higgins, C.D., Macsween, K.F., Lake, A., Jarrett, R.F., Robertson, F.L., Williams, H., Crawford, D.H., 2007. HLA class I polymorphisms are associated with development of infectious mononucleosis upon primary EBV infection. J Clin Invest 117, 3042-3048.
McCann, E.M., Kelly, G.L., Rickinson, A.B., Bell, A.I., 2001. Genetic analysis of the Epstein-Barr virus-coded leader protein EBNA-LP as a co-activator of EBNA2 function. J Gen Virol 82, 3067-3079.
McWilliams, J.K., Fields, R.C., Broehm, C.J., Gibbs, T., Texas. Dept. of Transportation. Archeology Studies Program., Prewitt and Associates., Texas Antiquities Committee., 2006. Archeological impact evaluations and surveys in the Texas Department of Transportation's Abilene, Brownwood, Fort Worth, and Waco districts, 2003-2006. Texas Dept. of Transportation Prewitt and Associates, Austin, Tex.
Meij, P., van Esser, J.W., Niesters, H.G., van Baarle, D., Miedema, F., Blake, N., Rickinson, A.B., Leiner, I., Pamer, E., Lowenberg, B., Cornelissen, J.J., Gratama, J.W., 2003. Impaired recovery of Epstein-Barr virus (EBV)--specific CD8+ T lymphocytes after partially T-depleted allogeneic stem cell transplantation may identify patients at very high risk for progressive EBV reactivation and lymphoproliferative disease. Blood 101, 4290-4297.
Middeldorp, J.M., Brink, A.A., van den Brule, A.J., Meijer, C.J., 2003. Pathogenic roles for Epstein-Barr virus (EBV) gene products in EBV-associated proliferative disorders. Crit Rev Oncol Hematol 45, 1-36.
Miller, I.G., Jr., El-Guindy, A., 2002. Regulation of Epstein-Barr virus lytic cycle activation in malignant and nonmalignant disease. J Natl Cancer Inst 94, 1733-1735.
Minarovits, J., Minarovits-Kormuta, S., Ehlin-Henriksson, B., Falk, K., Klein, G., Ernberg, I., 1991. Host cell phenotype-dependent methylation patterns of Epstein-Barr virus DNA. J Gen Virol 72 ( Pt 7), 1591-1599.
Miyashita, E.M., Yang, B., Babcock, G.J., Thorley-Lawson, D.A., 1997. Identification of the site of Epstein-Barr virus persistence in vivo as a resting B cell. J Virol 71, 4882-4891.
Molesworth, S.J., Lake, C.M., Borza, C.M., Turk, S.M., Hutt-Fletcher, L.M., 2000. Epstein-Barr virus gH is essential for penetration of B cells but also plays a role in attachment of virus to epithelial cells. J Virol 74, 6324-6332.
Montone, K.T., Hodinka, R.L., Salhany, K.E., Lavi, E., Rostami, A., Tomaszewski, J.E., 1996. Identification of Epstein-Barr virus lytic activity in post-transplantation lymphoproliferative disease. Mod Pathol 9, 621-630.
Morris, M.A., Dawson, C.W., Wei, W., O'Neil, J.D., Stewart, S.E., Jia, J., Bell, A.I., Young, L.S., Arrand, J.R., 2008. Epstein-Barr virus-encoded LMP1 induces a hyperproliferative and inflammatory gene expression programme in cultured keratinocytes. J Gen Virol 89, 2806-2820.
Morrison, T.E., Kenney, S.C., 2004. BZLF1, an Epstein-Barr virus immediate-early protein, induces p65 nuclear translocation while inhibiting p65 transcriptional function. Virology 328, 219-232.

Morrison, T.E., Mauser, A., Klingelhutz, A., Kenney, S.C., 2004. Epstein-Barr virus immediate-early protein BZLF1 inhibits tumor necrosis factor alpha-induced signaling and apoptosis by downregulating tumor necrosis factor receptor 1. J Virol 78, 544-549.
Mylonas, I., Bergauer, F., 2011. Diagnosis of vaginal discharge by wet mount microscopy: a simple and underrated method. Obstet Gynecol Surv 66, 359-368.
Nakayama, T., Hieshima, K., Nagakubo, D., Sato, E., Nakayama, M., Kawa, K., Yoshie, O., 2004. Selective induction of Th2-attracting chemokines CCL17 and CCL22 in human B cells by latent membrane protein 1 of Epstein-Barr virus. J Virol 78, 1665-1674.
Nalesnik, M.A., Zeevi, A., Randhawa, P.S., Faro, A., Spichty, K.J., Demetris, A.J., Fung, J.J., Whiteside, T.L., Starzl, T.E., 1999. Cytokine mRNA profiles in Epstein-Barr virus-associated post-transplant lymphoproliferative disorders. Clin Transplant 13, 39-44.
Nelson, B.P., Nalesnik, M.A., Bahler, D.W., Locker, J., Fung, J.J., Swerdlow, S.H., 2000. Epstein-Barr virus-negative post-transplant lymphoproliferative disorders: a distinct entity? Am J Surg Pathol 24, 375-385.
Nelson, P.J., Krensky, A.M., 1998. Chemokines, lymphocytes and viruses: what goes around, comes around. Curr Opin Immunol 10, 265-270.
Neuhierl, B., Delecluse, H.J., 2006. The Epstein-Barr virus BMRF1 gene is essential for lytic virus replication. J Virol 80, 5078-5081.
Neville, L.F., Mathiak, G., Bagasra, O., 1997. The immunobiology of interferon-gamma inducible protein 10 kD (IP-10): a novel, pleiotropic member of the C-X-C chemokine superfamily. Cytokine Growth Factor Rev 8, 207-219.
Niedobitek, G., Agathanggelou, A., Herbst, H., Whitehead, L., Wright, D.H., Young, L.S., 1997a. Epstein-Barr virus (EBV) infection in infectious mononucleosis: virus latency, replication and phenotype of EBV-infected cells. J Pathol 182, 151-159.
Niedobitek, G., Agathanggelou, A., Rowe, M., Jones, E.L., Jones, D.B., Turyaguma, P., Oryema, J., Wright, D.H., Young, L.S., 1995. Heterogeneous expression of Epstein-Barr virus latent proteins in endemic Burkitt's lymphoma. Blood 86, 659-665.
Niedobitek, G., Mutimer, D.J., Williams, A., Whitehead, L., Wilson, P., Rooney, N., Young, L.S., Hubscher, S.G., 1997b. Epstein-Barr virus infection and malignant lymphomas in liver transplant recipients. Int J Cancer 73, 514-520.
Niesters, H.G., van Esser, J., Fries, E., Wolthers, K.C., Cornelissen, J., Osterhaus, A.D., 2000. Development of a real-time quantitative assay for detection of Epstein-Barr virus. J Clin Microbiol 38, 712-715.
Nikolsky, Y., Ekins, S., Nikolskaya, T., Bugrim, A., 2005. A novel method for generation of signature networks as biomarkers from complex high throughput data. Toxicol Lett 158, 20-29.
Ohashi, M., Horie, K., Hoshikawa, Y., Nagata, K., Osaki, M., Ito, H., Sairenji, T., 2007. Accumulation of Epstein-Barr virus (EBV) BMRF1 protein EA-D during latent EBV activation of Burkitt's lymphoma cell line Raji. Microbes Infect 9, 150-159.
Ohshima, K., Tutiya, T., Yamaguchi, T., Suzuki, K., Suzumiya, J., Kawasaki, C., Haraoka, S., Kikuchi, M., 2002. Infiltration of Th1 and Th2 lymphocytes around Hodgkin and Reed-Sternberg (H&RS) cells in Hodgkin disease: Relation with expression of CXC and CC chemokines on H&RS cells. Int J Cancer 98, 567-572.
Opelz, G., Dohler, B., 2004. Lymphomas after solid organ transplantation: a collaborative transplant study report. Am J Transplant 4, 222-230.
Oudejans, J.J., Jiwa, M., van den Brule, A.J., Grasser, F.A., Horstman, A., Vos, W., Kluin, P.M., van der Valk, P., Walboomers, J.M., Meijer, C.J., 1995. Detection of heterogeneous Epstein-Barr virus gene expression patterns within individual post-transplantation lymphoproliferative disorders. Am J Pathol 147, 923-933.
Pallesen, G., Hamilton-Dutoit, S.J., Zhou, X., 1993. The association of Epstein-Barr virus (EBV) with T cell lymphoproliferations and Hodgkin's disease: two new developments in the EBV field. Adv Cancer Res 62, 179-239.

Pan, Y.R., Fang, C.Y., Chang, Y.S., Chang, H.Y., 2005. Analysis of Epstein-Barr virus gene expression upon phorbol ester and hydroxyurea treatment by real-time quantitative PCR. Arch Virol 150, 755-770.
Papesch, M., Watkins, R., 2001. Epstein-Barr virus infectious mononucleosis. Clin Otolaryngol Allied Sci 26, 3-8.
Parker, B.D., Bankier, A., Satchwell, S., Barrell, B., Farrell, P.J., 1990. Sequence and transcription of Raji Epstein-Barr virus DNA spanning the B95-8 deletion region. Virology 179, 339-346.
Parker, G.A., Crook, T., Bain, M., Sara, E.A., Farrell, P.J., Allday, M.J., 1996. Epstein-Barr virus nuclear antigen (EBNA)3C is an immortalizing oncoprotein with similar properties to adenovirus E1A and papillomavirus E7. Oncogene 13, 2541-2549.
Paulson, E.J., Speck, S.H., 1999. Differential methylation of Epstein-Barr virus latency promoters facilitates viral persistence in healthy seropositive individuals. J Virol 73, 9959-9968.
Paya, C.V., Fung, J.J., Nalesnik, M.A., Kieff, E., Green, M., Gores, G., Habermann, T.M., Wiesner, P.H., Swinnen, J.L., Woodle, E.S., Bromberg, J.S., 1999. Epstein-Barr virus-induced posttransplant lymphoproliferative disorders. ASTS/ASTP EBV-PTLD Task Force and The Mayo Clinic Organized International Consensus Development Meeting. Transplantation 68, 1517-1525.
Peng, L., Yanjiao, M., Ai-guo, W., Pengtao, G., Jianhua, L., Ju, Y., Hongsheng, O., Xichen, Z., 2011. A fine balance between CCNL1 and TIMP1 contributes to the development of breast cancer cells. Biochem Biophys Res Commun 409, 344-349.
Peng, R., Moses, S.C., Tan, J., Kremmer, E., Ling, P.D., 2005. The Epstein-Barr virus EBNA-LP protein preferentially coactivates EBNA2-mediated stimulation of latent membrane proteins expressed from the viral divergent promoter. J Virol 79, 4492-4505.
Penn, I., 1991. The changing pattern of posttransplant malignancies. Transplant Proc 23, 1101-1103.
Pepper, S.D., Saunders, E.K., Edwards, L.E., Wilson, C.L., Miller, C.J., 2007. The utility of MAS5 expression summary and detection call algorithms. BMC Bioinformatics 8, 273.
Pfeffer, S., Zavolan, M., Grasser, F.A., Chien, M., Russo, J.J., Ju, J., John, B., Enright, A.J., Marks, D., Sander, C., Tuschl, T., 2004. Identification of virus-encoded microRNAs. Science 304, 734-736.
Prang, N.S., Hornef, M.W., Jager, M., Wagner, H.J., Wolf, H., Schwarzmann, F.M., 1997. Lytic replication of Epstein-Barr virus in the peripheral blood: analysis of viral gene expression in B lymphocytes during infectious mononucleosis and in the normal carrier state. Blood 89, 1665-1677.
Preiksaitis, J.K., Diaz-Mitoma, F., Mirzayans, F., Roberts, S., Tyrrell, D.L., 1992. Quantitative oropharyngeal Epstein-Barr virus shedding in renal and cardiac transplant recipients: relationship to immunosuppressive therapy, serologic responses, and the risk of posttransplant lymphoproliferative disorder. J Infect Dis 166, 986-994.
Preiksaitis, J.K., Keay, S., 2001. Diagnosis and management of posttransplant lymphoproliferative disorder in solid-organ transplant recipients. Clin Infect Dis 33 Suppl 1, S38-46.
Qin, W., Zhu, W., Schlatter, L., Miick, R., Loy, T.S., Atasoy, U., Hewett, J.E., Sauter, E.R., 2007. Increased expression of the inflammatory protein YKL-40 in precancers of the breast. Int J Cancer 121, 1536-1542.
Qu, L., Green, M., Webber, S., Reyes, J., Ellis, D., Rowe, D., 2000. Epstein-Barr virus gene expression in the peripheral blood of transplant recipients with persistent circulating virus loads. J Infect Dis 182, 1013-1021.
Quinlivan, E.B., Holley-Guthrie, E.A., Norris, M., Gutsch, D., Bachenheimer, S.L., Kenney, S.C., 1993. Direct BRLF1 binding is required for cooperative BZLF1/BRLF1 activation of the Epstein-Barr virus early promoter, BMRF1. Nucleic Acids Res 21, 1999-2007.
Qureshi, A.M., Hannigan, A., Campbell, D., Nixon, C., Wilson, J.B., 2011. Chitinase-like proteins are autoantigens in a model of inflammation-promoted incipient neoplasia. Genes Cancer 2, 74-87.
Raab-Traub, N., 2002. Epstein-Barr virus in the pathogenesis of NPC. Semin Cancer Biol 12, 431-441.
Ragoczy, T., Heston, L., Miller, G., 1998. The Epstein-Barr virus Rta protein activates lytic cycle genes and can disrupt latency in B lymphocytes. J Virol 72, 7978-7984.
Ragoczy, T., Miller, G., 1999. Role of the epstein-barr virus RTA protein in activation of distinct classes of viral lytic cycle genes. J Virol 73, 9858-9866.

Randhawa, P., Nalesnik, M., Demetris, J., Zeevi, A., 1995. Interleukin-10 production by a B-cell line derived from human post-transplant lymphoproliferative disease. Hematol Oncol 13, 13-18.
Rea, D., Delecluse, H.J., Hamilton-Dutoit, S.J., Marelle, L., Joab, I., Edelman, L., Finet, J.F., Raphael, M., 1994a. Epstein-Barr virus latent and replicative gene expression in post-transplant lymphoproliferative disorders and AIDS-related non-Hodgkin's lymphomas. French Study Group of Pathology for HIV-associated Tumors. Ann Oncol 5 Suppl 1, 113-116.
Rea, D., Fourcade, C., Leblond, V., Rowe, M., Joab, I., Edelman, L., Bitker, M.O., Gandjbakhch, I., Suberbielle, C., Farcet, J.P., et al., 1994b. Patterns of Epstein-Barr virus latent and replicative gene expression in Epstein-Barr virus B cell lymphoproliferative disorders after organ transplantation. Transplantation 58, 317-324.
Reisman, D., Yates, J., Sugden, B., 1985. A putative origin of replication of plasmids derived from Epstein-Barr virus is composed of two cis-acting components. Mol Cell Biol 5, 1822-1832.
Rek, O., Czescik, A., Trzcinska, A., Siennicka, J., 2010. [Raji, P3HR-1 and Namalwa cells as a model for the study of Epstein-Barr virus (EBV) reactivation]. Med Dosw Mikrobiol 62, 263-269.
Rentenaar, R.J., Gamadia, L.E., van DerHoek, N., van Diepen, F.N., Boom, R., Weel, J.F., Wertheim-van Dillen, P.M., van Lier, R.A., ten Berge, I.J., 2000. Development of virus-specific CD4(+) T cells during primary cytomegalovirus infection. J Clin Invest 105, 541-548.
Rice, S.A., Knipe, D.M., 1990. Genetic evidence for two distinct transactivation functions of the herpes simplex virus alpha protein ICP27. J Virol 64, 1704-1715.
Rickinson, A.B., Finerty, S., Epstein, M.A., 1978. Inhibition by phosphonoacetate of the in vitro outgrowth of Epstein-Barr virus genome-containing cell lines from the blood of infectious mononucleosis patients. IARC Sci Publ, 721-728.
Rickinson, A.B., Young, L.S., Rowe, M., 1987. Influence of the Epstein-Barr virus nuclear antigen EBNA 2 on the growth phenotype of virus-transformed B cells. J Virol 61, 1310-1317.
Riddler, S.A., Breinig, M.C., McKnight, J.L., 1994. Increased levels of circulating Epstein-Barr virus (EBV)-infected lymphocytes and decreased EBV nuclear antigen antibody responses are associated with the development of posttransplant lymphoproliferative disease in solid-organ transplant recipients. Blood 84, 972-984.
Riley, K.J., Rabinowitz, G.S., Yario, T.A., Luna, J.M., Darnell, R.B., Steitz, J.A., 2012. EBV and human microRNAs co-target oncogenic and apoptotic viral and human genes during latency. Embo J.
Robertson, E.S., 2005. Epstein-Barr virus. Caister Academic Press, Wymondham, Norfolk, England.
Robertson, E.S., Ooka, T., Kieff, E.D., 1996. Epstein-Barr virus vectors for gene delivery to B lymphocytes. Proc Natl Acad Sci U S A 93, 11334-11340.
Robertson, K.D., Ambinder, R.F., 1997. Methylation of the Epstein-Barr virus genome in normal lymphocytes. Blood 90, 4480-4484.
Rodig, S.J., Abramson, J.S., Pinkus, G.S., Treon, S.P., Dorfman, D.M., Dong, H.Y., Shipp, M.A., Kutok, J.L., 2006. Heterogeneous CD52 expression among hematologic neoplasms: implications for the use of alemtuzumab (CAMPATH-1H). Clin Cancer Res 12, 7174-7179.
Rollins, B.J., 2006. Inflammatory chemokines in cancer growth and progression. Eur J Cancer 42, 760-767.
Rooney, C., Howe, J.G., Speck, S.H., Miller, G., 1989a. Influence of Burkitt's lymphoma and primary B cells on latent gene expression by the nonimmortalizing P3J-HR-1 strain of Epstein-Barr virus. J Virol 63, 1531-1539.
Rooney, C.M., Loftin, S.K., Holladay, M.S., Brenner, M.K., Krance, R.A., Heslop, H.E., 1995. Early identification of Epstein-Barr virus-associated post-transplantation lymphoproliferative disease. Br J Haematol 89, 98-103.
Rooney, C.M., Rowe, D.T., Ragot, T., Farrell, P.J., 1989b. The spliced BZLF1 gene of Epstein-Barr virus (EBV) transactivates an early EBV promoter and induces the virus productive cycle. J Virol 63, 3109-3116.
Rooney, C.M., Smith, C.A., Ng, C.Y., Loftin, S.K., Sixbey, J.W., Gan, Y., Srivastava, D.K., Bowman, L.C., Krance, R.A., Brenner, M.K., Heslop, H.E., 1998. Infusion of cytotoxic T cells for the prevention

and treatment of Epstein-Barr virus-induced lymphoma in allogeneic transplant recipients. Blood 92, 1549-1555.
Rowe, C.L., Matsuura, H., Jardetzky, T.S., Longnecker, R., 2011. Investigation of the function of the putative self-association site of Epstein-Barr virus (EBV) glycoprotein 42 (gp42). Virology 415, 122-131.
Rowe, D.T., 1999. Epstein-Barr virus immortalization and latency. Front Biosci 4, D346-371.
Rowe, D.T., Qu, L., Reyes, J., Jabbour, N., Yunis, E., Putnam, P., Todo, S., Green, M., 1997. Use of quantitative competitive PCR to measure Epstein-Barr virus genome load in the peripheral blood of pediatric transplant patients with lymphoproliferative disorders. J Clin Microbiol 35, 1612-1615.
Rowe, D.T., Webber, S., Schauer, E.M., Reyes, J., Green, M., 2001. Epstein-Barr virus load monitoring: its role in the prevention and management of post-transplant lymphoproliferative disease. Transpl Infect Dis 3, 79-87.
Rowe, M., Lear, A.L., Croom-Carter, D., Davies, A.H., Rickinson, A.B., 1992. Three pathways of Epstein-Barr virus gene activation from EBNA1-positive latency in B lymphocytes. J Virol 66, 122-131.
Rowe, M., Niedobitek, G., Young, L.S., 1998. Epstein-Barr virus gene expression in post-transplant lymphoproliferative disorders. Springer Semin Immunopathol 20, 389-403.
Rowe, M., Rowe, D.T., Gregory, C.D., Young, L.S., Farrell, P.J., Rupani, H., Rickinson, A.B., 1987. Differences in B cell growth phenotype reflect novel patterns of Epstein-Barr virus latent gene expression in Burkitt's lymphoma cells. EMBO J 6, 2743-2751.
Rowe, M., Young, L.S., Cadwallader, K., Petti, L., Kieff, E., Rickinson, A.B., 1989. Distinction between Epstein-Barr virus type A (EBNA 2A) and type B (EBNA 2B) isolates extends to the EBNA 3 family of nuclear proteins. J Virol 63, 1031-1039.
Sample, J., Hummel, M., Braun, D., Birkenbach, M., Kieff, E., 1986. Nucleotide sequences of mRNAs encoding Epstein-Barr virus nuclear proteins: a probable transcriptional initiation site. Proc Natl Acad Sci U S A 83, 5096-5100.
Sample, J., Young, L., Martin, B., Chatman, T., Kieff, E., Rickinson, A., 1990. Epstein-Barr virus types 1 and 2 differ in their EBNA-3A, EBNA-3B, and EBNA-3C genes. J Virol 64, 4084-4092.
Savoie, A., Perpete, C., Carpentier, L., Joncas, J., Alfieri, C., 1994. Direct correlation between the load of Epstein-Barr virus-infected lymphocytes in the peripheral blood of pediatric transplant patients and risk of lymphoproliferative disease. Blood 83, 2715-2722.
Schaefer, B.C., Strominger, J.L., Speck, S.H., 1995. Redefining the Epstein-Barr virus-encoded nuclear antigen EBNA-1 gene promoter and transcription initiation site in group I Burkitt lymphoma cell lines. Proc Natl Acad Sci U S A 92, 10565-10569.
Schaefer, B.C., Woisetschlaeger, M., Strominger, J.L., Speck, S.H., 1991. Exclusive expression of Epstein-Barr virus nuclear antigen 1 in Burkitt lymphoma arises from a third promoter, distinct from the promoters used in latently infected lymphocytes. Proc Natl Acad Sci U S A 88, 6550-6554.
Scheenstra, R., Verschuuren, E.A., de Haan, A., Slooff, M.J., The, T.H., Bijleveld, C.M., Verkade, H.J., 2004. The value of prospective monitoring of Epstein-Barr virus DNA in blood samples of pediatric liver transplant recipients. Transpl Infect Dis 6, 15-22.
Schepers, A., Pich, D., Hammerschmidt, W., 1996. Activation of oriLyt, the lytic origin of DNA replication of Epstein-Barr virus, by BZLF1. Virology 220, 367-376.
Schlager, S., Speck, S.H., Woisetschlager, M., 1996. Transcription of the Epstein-Barr virus nuclear antigen 1 (EBNA1) gene occurs before induction of the BCR2 (Cp) EBNA gene promoter during the initial stages of infection in B cells. J Virol 70, 3561-3570.
Schluger, N.W., Rom, W.N., 1997. Early responses to infection: chemokines as mediators of inflammation. Curr Opin Immunol 9, 504-508.
Schmittgen, T.D., Livak, K.J., 2008. Analyzing real-time PCR data by the comparative C(T) method. Nat Protoc 3, 1101-1108.
Sebelin-Wulf, K., Nguyen, T.D., Oertel, S., Papp-Vary, M., Trappe, R.U., Schulzki, A., Pezzutto, A., Riess, H., Subklewe, M., 2007. Quantitative analysis of EBV-specific CD4/CD8 T cell numbers, absolute CD4/CD8 T cell numbers and EBV load in solid organ transplant recipients with PLTD. Transpl Immunol 17, 203-210.

Segouffin-Cariou, C., Farjot, G., Sergeant, A., Gruffat, H., 2000. Characterization of the epstein-barr virus BRRF1 gene, located between early genes BZLF1 and BRLF1. J Gen Virol 81, 1791-1799.
Serio, T.R., Cahill, N., Prout, M.E., Miller, G., 1998a. A functionally distinct TATA box required for late progression through the Epstein-Barr virus life cycle. J Virol 72, 8338-8343.
Serio, T.R., Cahill, N., Prout, M.E., Miller, G., 1998b. A functionally distinct TATA box required for late progression through the Epstein-Barr virus life cycle. J Virol 72, 8338-8343.
Serio, T.R., Kolman, J.L., Miller, G., 1997a. Late gene expression from the Epstein-Barr virus BcLF1 and BFRF3 promoters does not require DNA replication in cis. J Virol 71, 8726-8734.
Serio, T.R., Kolman, J.L., Miller, G., 1997b. Late gene expression from the Epstein-Barr virus BcLF1 and BFRF3 promoters does not require DNA replication in cis. J Virol 71, 8726-8734.
Setsuda, J., Teruya-Feldstein, J., Harris, N.L., Ferry, J.A., Sorbara, L., Gupta, G., Jaffe, E.S., Tosato, G., 1999. Interleukin-18, interferon-gamma, IP-10, and Mig expression in Epstein-Barr virus-induced infectious mononucleosis and posttransplant lymphoproliferative disease. Am J Pathol 155, 257-265.
Sgadari, C., Angiolillo, A.L., Cherney, B.W., Pike, S.E., Farber, J.M., Koniaris, L.G., Vanguri, P., Burd, P.R., Sheikh, N., Gupta, G., Teruya-Feldstein, J., Tosato, G., 1996. Interferon-inducible protein-10 identified as a mediator of tumor necrosis in vivo. Proc Natl Acad Sci U S A 93, 13791-13796.
Sgadari, C., Farber, J.M., Angiolillo, A.L., Liao, F., Teruya-Feldstein, J., Burd, P.R., Yao, L., Gupta, G., Kanegane, C., Tosato, G., 1997. Mig, the monokine induced by interferon-gamma, promotes tumor necrosis in vivo. Blood 89, 2635-2643.
Shannon-Lowe, C.D., Neuhierl, B., Baldwin, G., Rickinson, A.B., Delecluse, H.J., 2006. Resting B cells as a transfer vehicle for Epstein-Barr virus infection of epithelial cells. Proc Natl Acad Sci U S A 103, 7065-7070.
Sheng, W., Decaussin, G., Ligout, A., Takada, K., Ooka, T., 2003. Malignant transformation of Epstein-Barr virus-negative Akata cells by introduction of the BARF1 gene carried by Epstein-Barr virus. J Virol 77, 3859-3865.
Shimizu, N., Takada, K., 1993a. Analysis of the BZLF1 promoter of Epstein-Barr virus: identification of an anti-immunoglobulin response sequence. J Virol 67, 3240-3245.
Shimizu, N., Takada, K., 1993b. Analysis of the BZLF1 promoter of Epstein-Barr virus: identification of an anti-immunoglobulin response sequence. J Virol 67, 3240-3245.
Shroff, R., Rees, L., 2004. The post-transplant lymphoproliferative disorder-a literature review. Pediatr Nephrol 19, 369-377.
Siemer, D., Kurth, J., Lang, S., Lehnerdt, G., Stanelle, J., Kuppers, R., 2008. EBV transformation overrides gene expression patterns of B cell differentiation stages. Mol Immunol 45, 3133-3141.
Sinclair, A.J., Palmero, I., Peters, G., Farrell, P.J., 1994. EBNA-2 and EBNA-LP cooperate to cause G0 to G1 transition during immortalization of resting human B lymphocytes by Epstein-Barr virus. EMBO J 13, 3321-3328.
Sixbey, J.W., Nedrud, J.G., Raab-Traub, N., Hanes, R.A., Pagano, J.S., 1984. Epstein-Barr virus replication in oropharyngeal epithelial cells. N Engl J Med 310, 1225-1230.
Smets, F., Latinne, D., Bazin, H., Reding, R., Otte, J.B., Buts, J.P., Sokal, E.M., 2002. Ratio between Epstein-Barr viral load and anti-Epstein-Barr virus specific T-cell response as a predictive marker of posttransplant lymphoproliferative disease. Transplantation 73, 1603-1610.
Smith, A.M., Watson, S.A., 2000. Review article: gastrin and colorectal cancer. Aliment Pharmacol Ther 14, 1231-1247.
Smith, P.R., de Jesus, O., Turner, D., Hollyoake, M., Karstegl, C.E., Griffin, B.E., Karran, L., Wang, Y., Hayward, S.D., Farrell, P.J., 2000. Structure and coding content of CST (BART) family RNAs of Epstein-Barr virus. J Virol 74, 3082-3092.
Spear, P.G., Longnecker, R., 2003. Herpesvirus entry: an update. J Virol 77, 10179-10185.
Speck, S.H., Chatila, T., Flemington, E., 1997. Reactivation of Epstein-Barr virus: regulation and function of the BZLF1 gene. Trends Microbiol 5, 399-405.

Spender, L.C., Cornish, G.H., Rowland, B., Kempkes, B., Farrell, P.J., 2001. Direct and indirect regulation of cytokine and cell cycle proteins by EBNA-2 during Epstein-Barr virus infection. J Virol 75, 3537-3546.
Spender, L.C., Cornish, G.H., Sullivan, A., Farrell, P.J., 2002. Expression of transcription factor AML-2 (RUNX3, CBF(alpha)-3) is induced by Epstein-Barr virus EBNA-2 and correlates with the B-cell activation phenotype. J Virol 76, 4919-4927.
Spender, L.C., Lucchesi, W., Bodelon, G., Bilancio, A., Karstegl, C.E., Asano, T., Dittrich-Breiholz, O., Kracht, M., Vanhaesebroeck, B., Farrell, P.J., 2006. Cell target genes of Epstein-Barr virus transcription factor EBNA-2: induction of the p55alpha regulatory subunit of PI3-kinase and its role in survival of EREB2.5 cells. J Gen Virol 87, 2859-2867.
Stevens, S.J., Verschuuren, E.A., Pronk, I., van Der Bij, W., Harmsen, M.C., The, T.H., Meijer, C.J., van Den Brule, A.J., Middeldorp, J.M., 2001. Frequent monitoring of Epstein-Barr virus DNA load in unfractionated whole blood is essential for early detection of posttransplant lymphoproliferative disease in high-risk patients. Blood 97, 1165-1171.
Stevens, S.J., Vervoort, M.B., van den Brule, A.J., Meenhorst, P.L., Meijer, C.J., Middeldorp, J.M., 1999. Monitoring of epstein-barr virus DNA load in peripheral blood by quantitative competitive PCR. J Clin Microbiol 37, 2852-2857.
Stowe, R.P., Kozlova, E.V., Sams, C.F., Pierson, D.L., Walling, D.M., 2011. Latent and lytic Epstein-Barr virus gene expression in the peripheral blood of astronauts. J Med Virol 83, 1071-1077.
Summers, W.C., Klein, G., 1976. Inhibition of Epstein-Barr virus DNA synthesis and late gene expression by phosphonoacetic acid. J Virol 18, 151-155.
Takada, K., 1984. Cross-linking of cell surface immunoglobulins induces Epstein-Barr virus in Burkitt lymphoma lines. Int J Cancer 33, 27-32.
Takada, K., Ono, Y., 1989. Synchronous and sequential activation of latently infected Epstein-Barr virus genomes. J Virol 63, 445-449.
Takada, K., Shimizu, N., Sakuma, S., Ono, Y., 1986. trans activation of the latent Epstein-Barr virus (EBV) genome after transfection of the EBV DNA fragment. J Virol 57, 1016-1022.
Tang, Q., Li, L., Ishov, A.M., Revol, V., Epstein, A.L., Maul, G.G., 2003. Determination of minimum herpes simplex virus type 1 components necessary to localize transcriptionally active DNA to ND10. J Virol 77, 5821-5828.
Teichmann, M., Meyer, B., Beck, A., Niedobitek, G., 2005. Expression of the interferon-inducible chemokine IP-10 (CXCL10), a chemokine with proposed anti-neoplastic functions, in Hodgkin lymphoma and nasopharyngeal carcinoma. J Pathol 206, 68-75.
Teruya-Feldstein, J., Jaffe, E.S., Burd, P.R., Kanegane, H., Kingma, D.W., Wilson, W.H., Longo, D.L., Tosato, G., 1997. The role of Mig, the monokine induced by interferon-gamma, and IP-10, the interferon-gamma-inducible protein-10, in tissue necrosis and vascular damage associated with Epstein-Barr virus-positive lymphoproliferative disease. Blood 90, 4099-4105.
Teruya-Feldstein, J., Jaffe, E.S., Burd, P.R., Kingma, D.W., Setsuda, J.E., Tosato, G., 1999. Differential chemokine expression in tissues involved by Hodgkin's disease: direct correlation of eotaxin expression and tissue eosinophilia. Blood 93, 2463-2470.
Teruya-Feldstein, J., Tosato, G., Jaffe, E.S., 2000. The role of chemokines in Hodgkin's disease. Leuk Lymphoma 38, 363-371.
Thapa, M., Welner, R.S., Pelayo, R., Carr, D.J., 2008. CXCL9 and CXCL10 expression are critical for control of genital herpes simplex virus type 2 infection through mobilization of HSV-specific CTL and NK cells to the nervous system. J Immunol 180, 1098-1106.
Thomas, J.A., Hotchin, N.A., Allday, M.J., Amlot, P., Rose, M., Yacoub, M., Crawford, D.H., 1990. Immunohistology of Epstein-Barr virus-associated antigens in B cell disorders from immunocompromised individuals. Transplantation 49, 944-953.
Thorley-Lawson, D.A., 2001. Epstein-Barr virus: exploiting the immune system. Nat Rev Immunol 1, 75-82.

Thorley-Lawson, D.A., Allday, M.J., 2008. The curious case of the tumour virus: 50 years of Burkitt's lymphoma. Nat Rev Microbiol 6, 913-924.
Thorley-Lawson, D.A., Babcock, G.J., 1999. A model for persistent infection with Epstein-Barr virus: the stealth virus of human B cells. Life Sci 65, 1433-1453.
Thorley-Lawson, D.A., Gross, A., 2004. Persistence of the Epstein-Barr virus and the origins of associated lymphomas. N Engl J Med 350, 1328-1337.
Tierney, R.J., Kirby, H.E., Nagra, J.K., Desmond, J., Bell, A.I., Rickinson, A.B., 2000. Methylation of transcription factor binding sites in the Epstein-Barr virus latent cycle promoter Wp coincides with promoter down-regulation during virus-induced B-cell transformation. J Virol 74, 10468-10479.
Tierney, R.J., Steven, N., Young, L.S., Rickinson, A.B., 1994. Epstein-Barr virus latency in blood mononuclear cells: analysis of viral gene transcription during primary infection and in the carrier state. J Virol 68, 7374-7385.
Timms, J.M., Bell, A., Flavell, J.R., Murray, P.G., Rickinson, A.B., Traverse-Glehen, A., Berger, F., Delecluse, H.J., 2003. Target cells of Epstein-Barr-virus (EBV)-positive post-transplant lymphoproliferative disease: similarities to EBV-positive Hodgkin's lymphoma. Lancet 361, 217-223.
Tomkinson, B., Robertson, E., Kieff, E., 1993. Epstein-Barr virus nuclear proteins EBNA-3A and EBNA-3C are essential for B-lymphocyte growth transformation. J Virol 67, 2014-2025.
Tosato, G., Jones, K., Breinig, M.K., McWilliams, H.P., McKnight, J.L., 1993. Interleukin-6 production in posttransplant lymphoproliferative disease. J Clin Invest 91, 2806-2814.
Tsai, S.C., Lin, S.J., Chen, P.W., Luo, W.Y., Yeh, T.H., Wang, H.W., Chen, C.J., Tsai, C.H., 2009. EBV Zta protein induces the expression of interleukin-13, promoting the proliferation of EBV-infected B cells and lymphoblastoid cell lines. Blood 114, 109-118.
Tsukamoto, Y., Uchida, T., Karnan, S., Noguchi, T., Nguyen, L.T., Tanigawa, M., Takeuchi, I., Matsuura, K., Hijiya, N., Nakada, C., Kishida, T., Kawahara, K., Ito, H., Murakami, K., Fujioka, T., Seto, M., Moriyama, M., 2008. Genome-wide analysis of DNA copy number alterations and gene expression in gastric cancer. J Pathol 216, 471-482.
Tsurumi, T., 1991. Primer terminus recognition and highly processive replication by Epstein-Barr virus DNA polymerase. Biochem J 280 ( Pt 3), 703-708.
Tsurumi, T., 2001. EBV replication enzymes. Curr Top Microbiol Immunol 258, 65-87.
Tsurumi, T., Daikoku, T., Kurachi, R., Nishiyama, Y., 1993. Functional interaction between Epstein-Barr virus DNA polymerase catalytic subunit and its accessory subunit in vitro. J Virol 67, 7648-7653.
Tsurumi, T., Daikoku, T., Nishiyama, Y., 1994. Further characterization of the interaction between the Epstein-Barr virus DNA polymerase catalytic subunit and its accessory subunit with regard to the 3'-to-5' exonucleolytic activity and stability of initiation complex at primer terminus. J Virol 68, 3354-3363.
Tsurumi, T., Fujita, M., Kudoh, A., 2005. Latent and lytic Epstein-Barr virus replication strategies. Rev Med Virol 15, 3-15.
Tsurumi, T., Kobayashi, A., Tamai, K., Yamada, H., Daikoku, T., Yamashita, Y., Nishiyama, Y., 1996. Epstein-Barr virus single-stranded DNA-binding protein: purification, characterization, and action on DNA synthesis by the viral DNA polymerase. Virology 222, 352-364.
Tsurumi, T., Kudoh, A., 2005. [Replication of Epstein-Barr virus and host cell response]. Seikagaku 77, 1180-1184.
Tugizov, S.M., Berline, J.W., Palefsky, J.M., 2003. Epstein-Barr virus infection of polarized tongue and nasopharyngeal epithelial cells. Nat Med 9, 307-314.
Uchihara, J.N., Krensky, A.M., Matsuda, T., Kawakami, H., Okudaira, T., Masuda, M., Ohta, T., Takasu, N., Mori, N., 2005. Transactivation of the CCL5/RANTES gene by Epstein-Barr virus latent membrane protein 1. Int J Cancer 114, 747-755.
Vajro, P., Lucariello, S., Migliaro, F., Sokal, E., Gridelli, B., Vegnente, A., Iorio, R., Smets, F., Quinto, I., Scala, G., 2000. Predictive value of Epstein-Barr virus genome copy number and BZLF1 expression in blood lymphocytes of transplant recipients at risk for lymphoproliferative disease. J Infect Dis 181, 2050-2054.

Vakiani, E., Basso, K., Klein, U., Mansukhani, M.M., Narayan, G., Smith, P.M., Murty, V.V., Dalla-Favera, R., Pasqualucci, L., Bhagat, G., 2008. Genetic and phenotypic analysis of B-cell post-transplant lymphoproliferative disorders provides insights into disease biology. Hematol Oncol 26, 199-211.
van Beek, J., Brink, A.A., Vervoort, M.B., van Zijp, M.J., Meijer, C.J., van den Brule, A.J., Middeldorp, J.M., 2003. In vivo transcription of the Epstein-Barr virus (EBV) BamHI-A region without associated in vivo BARF0 protein expression in multiple EBV-associated disorders. J Gen Virol 84, 2647-2659.
Vockerodt, M., Pinkert, D., Smola-Hess, S., Michels, A., Ransohoff, R.M., Tesch, H., Kube, D., 2005. The Epstein-Barr virus oncoprotein latent membrane protein 1 induces expression of the chemokine IP-10: importance of mRNA half-life regulation. Int J Cancer 114, 598-605.
Wagner, H.J., Fischer, L., Jabs, W.J., Holbe, M., Pethig, K., Bucsky, P., 2002. Longitudinal analysis of Epstein-Barr viral load in plasma and peripheral blood mononuclear cells of transplanted patients by real-time polymerase chain reaction. Transplantation 74, 656-664.
Wagner, H.J., Wessel, M., Jabs, W., Smets, F., Fischer, L., Offner, G., Bucsky, P., 2001. Patients at risk for development of posttransplant lymphoproliferative disorder: plasma versus peripheral blood mononuclear cells as material for quantification of Epstein-Barr viral load by using real-time quantitative polymerase chain reaction. Transplantation 72, 1012-1019.
Walker, R.C., 1995. Pretransplant assessment of the risk for posttransplant lymphoproliferative disorder. Transplant Proc 27, 41.
Walker, R.C., Paya, C.V., Marshall, W.F., Strickler, J.G., Wiesner, R.H., Velosa, J.A., Habermann, T.M., Daly, R.C., McGregor, C.G., 1995. Pretransplantation seronegative Epstein-Barr virus status is the primary risk factor for posttransplantation lymphoproliferative disorder in adult heart, lung, and other solid organ transplantations. J Heart Lung Transplant 14, 214-221.
Walling, D.M., Flaitz, C.M., Nichols, C.M., 2003. Epstein-Barr virus replication in oral hairy leukoplakia: response, persistence, and resistance to treatment with valacyclovir. J Infect Dis 188, 883-890.
Wang, D., Liebowitz, D., Kieff, E., 1985. An EBV membrane protein expressed in immortalized lymphocytes transforms established rodent cells. Cell 43, 831-840.
Wang, F., Gregory, C.D., Rowe, M., Rickinson, A.B., Wang, D., Birkenbach, M., Kikutani, H., Kishimoto, T., Kieff, E., 1987. Epstein-Barr virus nuclear antigen 2 specifically induces expression of the B-cell activation antigen CD23. Proc Natl Acad Sci U S A 84, 3452-3456.
Wang, F., Kikutani, H., Tsang, S.F., Kishimoto, T., Kieff, E., 1991. Epstein-Barr virus nuclear protein 2 transactivates a cis-acting CD23 DNA element. J Virol 65, 4101-4106.
Wang, P., Day, L., Dheekollu, J., Lieberman, P.M., 2005. A redox-sensitive cysteine in Zta is required for Epstein-Barr virus lytic cycle DNA replication. J Virol 79, 13298-13309.
Wei, M.X., Moulin, J.C., Decaussin, G., Berger, F., Ooka, T., 1994. Expression and tumorigenicity of the Epstein-Barr virus BARF1 gene in human Louckes B-lymphocyte cell line. Cancer Res 54, 1843-1848.
Wei, M.X., Ooka, T., 1989. A transforming function of the BARF1 gene encoded by Epstein-Barr virus. EMBO J 8, 2897-2903.
Weiss, L.M., Movahed, L.A., Warnke, R.A., Sklar, J., 1989. Detection of Epstein-Barr viral genomes in Reed-Sternberg cells of Hodgkin's disease. N Engl J Med 320, 502-506.
Williams, H., Macsween, K., McAulay, K., Higgins, C., Harrison, N., Swerdlow, A., Britton, K., Crawford, D., 2004. Analysis of immune activation and clinical events in acute infectious mononucleosis. J Infect Dis 190, 63-71.
Wingate, P.J., McAulay, K.A., Anthony, I.C., Crawford, D.H., 2009. Regulatory T cell activity in primary and persistent Epstein-Barr virus infection. J Med Virol 81, 870-877.
Woisetschlaeger, M., Jin, X.W., Yandava, C.N., Furmanski, L.A., Strominger, J.L., Speck, S.H., 1991. Role for the Epstein-Barr virus nuclear antigen 2 in viral promoter switching during initial stages of infection. Proc Natl Acad Sci U S A 88, 3942-3946.
Woisetschlaeger, M., Strominger, J.L., Speck, S.H., 1989. Mutually exclusive use of viral promoters in Epstein-Barr virus latently infected lymphocytes. Proc Natl Acad Sci U S A 86, 6498-6502.

Woisetschlaeger, M., Yandava, C.N., Furmanski, L.A., Strominger, J.L., Speck, S.H., 1990. Promoter switching in Epstein-Barr virus during the initial stages of infection of B lymphocytes. Proc Natl Acad Sci U S A 87, 1725-1729.
Wong, E., Wu, T.T., Reyes, N., Deng, H., Sun, R., 2007. Murine gammaherpesvirus 68 open reading frame 24 is required for late gene expression after DNA replication. J Virol 81, 6761-6764.
Wu, T.T., Park, T., Kim, H., Tran, T., Tong, L., Martinez-Guzman, D., Reyes, N., Deng, H., Sun, R., 2009. ORF30 and ORF34 are essential for expression of late genes in murine gammaherpesvirus 68. J Virol 83, 2265-2273.
Wyrwicz, L.S., Rychlewski, L., 2007a. Identification of Herpes TATT-binding protein. Antiviral Res 75, 167-172.
Wyrwicz, L.S., Rychlewski, L., 2007b. Identification of Herpes TATT-binding protein. Antiviral Res 75, 167-172.
Yang, J., Tao, Q., Flinn, I.W., Murray, P.G., Post, L.E., Ma, H., Piantadosi, S., Caligiuri, M.A., Ambinder, R.F., 2000. Characterization of Epstein-Barr virus-infected B cells in patients with posttransplantation lymphoproliferative disease: disappearance after rituximab therapy does not predict clinical response. Blood 96, 4055-4063.
Yao, Q.Y., Croom-Carter, D.S., Tierney, R.J., Habeshaw, G., Wilde, J.T., Hill, F.G., Conlon, C., Rickinson, A.B., 1998. Epidemiology of infection with Epstein-Barr virus types 1 and 2: lessons from the study of a T-cell-immunocompromised hemophilic cohort. J Virol 72, 4352-4363.
Yao, Q.Y., Rowe, M., Martin, B., Young, L.S., Rickinson, A.B., 1991. The Epstein-Barr virus carrier state: dominance of a single growth-transforming isolate in the blood and in the oropharynx of healthy virus carriers. J Gen Virol 72 ( Pt 7), 1579-1590.
Yates, J., Warren, N., Reisman, D., Sugden, B., 1984. A cis-acting element from the Epstein-Barr viral genome that permits stable replication of recombinant plasmids in latently infected cells. Proc Natl Acad Sci U S A 81, 3806-3810.
Yates, J.L., Warren, N., Sugden, B., 1985. Stable replication of plasmids derived from Epstein-Barr virus in various mammalian cells. Nature 313, 812-815.
Young, L., Alfieri, C., Hennessy, K., Evans, H., O'Hara, C., Anderson, K.C., Ritz, J., Shapiro, R.S., Rickinson, A., Kieff, E., et al., 1989. Expression of Epstein-Barr virus transformation-associated genes in tissues of patients with EBV lymphoproliferative disease. N Engl J Med 321, 1080-1085.
Young, L.S., Rickinson, A.B., 2004. Epstein-Barr virus: 40 years on. Nat Rev Cancer 4, 757-768.
Yuan, J., Cahir-McFarland, E., Zhao, B., Kieff, E., 2006. Virus and cell RNAs expressed during Epstein-Barr virus replication. J Virol 80, 2548-2565.
Yue, W., Gershburg, E., Pagano, J.S., 2005. Hyperphosphorylation of EBNA2 by Epstein-Barr virus protein kinase suppresses transactivation of the LMP1 promoter. J Virol 79, 5880-5885.
Yuling, H., Ruijing, X., Li, L., Xiang, J., Rui, Z., Yujuan, W., Lijun, Z., Chunxian, D., Xinti, T., Wei, X., Lang, C., Yanping, J., Tao, X., Mengjun, W., Jie, X., Youxin, J., Jinquan, T., 2009. EBV-induced human CD8+ NKT cells suppress tumorigenesis by EBV-associated malignancies. Cancer Res 69, 7935-7944.
Zalani, S., Holley-Guthrie, E., Kenney, S., 1996. Epstein-Barr viral latency is disrupted by the immediate-early BRLF1 protein through a cell-specific mechanism. Proc Natl Acad Sci U S A 93, 9194-9199.
Zawilinska, B., Kosinska, A., Lenart, M., Kopec, J., Piatkowska-Jakubas, B., Skotnicki, A., Kosz-Vnenchak, M., 2008. Detection of specific lytic and latent transcripts can help to predict the status of Epstein-Barr virus infection in transplant recipients with high virus load. Acta Biochim Pol 55, 693-699.
Zetterberg, H., Stenglein, M., Jansson, A., Ricksten, A., Rymo, L., 1999. Relative levels of EBNA1 gene transcripts from the C/W, F and Q promoters in Epstein-Barr virus-transformed lymphoid cells in latent and lytic stages of infection. J Gen Virol 80 ( Pt 2), 457-466.
Zhang, J., Chen, H., Weinmaster, G., Hayward, S.D., 2001. Epstein-Barr virus BamHi-a rightward transcript-encoded RPMS protein interacts with the CBF1-associated corepressor CIR to negatively regulate the activity of EBNA2 and NotchIC. J Virol 75, 2946-2956.
Zhang, Q., Gutsch, D., Kenney, S., 1994. Functional and physical interaction between p53 and BZLF1: implications for Epstein-Barr virus latency. Mol Cell Biol 14, 1929-1938.

Zhang, Q., Holley-Guthrie, E., Dorsky, D., Kenney, S., 1999. Identification of transactivator and nuclear localization domains in the Epstein-Barr virus DNA polymerase accessory protein, BMRF1. J Gen Virol 80 ( Pt 1), 69-74.
Zhang, Q., Holley-Guthrie, E., Ge, J.Q., Dorsky, D., Kenney, S., 1997. The Epstein-Barr virus (EBV) DNA polymerase accessory protein, BMRF1, activates the essential downstream component of the EBV oriLyt. Virology 230, 22-34.
Zhao, B., Maruo, S., Cooper, A., M, R.C., Johannsen, E., Kieff, E., Cahir-McFarland, E., 2006. RNAs induced by Epstein-Barr virus nuclear antigen 2 in lymphoblastoid cell lines. Proc Natl Acad Sci U S A 103, 1900-1905.
Zhao, X.F., Gartenhaus, R.B., 2009. Phospho-p70S6K and cdc2/cdk1 as therapeutic targets for diffuse large B-cell lymphoma. Expert Opin Ther Targets 13, 1085-1093.
Zhou, A., He, Z., Redding-Johanson, A.M., Mukhopadhyay, A., Hemme, C.L., Joachimiak, M.P., Luo, F., Deng, Y., Bender, K.S., He, Q., Keasling, J.D., Stahl, D.A., Fields, M.W., Hazen, T.C., Arkin, A.P., Wall, J.D., Zhou, J., 2010. Hydrogen peroxide-induced oxidative stress responses in Desulfovibrio vulgaris Hildenborough. Environ Microbiol 12, 2645-2657.
Zimmermann, J., Hammerschmidt, W., 1995. Structure and role of the terminal repeats of Epstein-Barr virus in processing and packaging of virion DNA. J Virol 69, 3147-3155.
Zipin-Roitman, A., Meshel, T., Sagi-Assif, O., Shalmon, B., Avivi, C., Pfeffer, R.M., Witz, I.P., Ben-Baruch, A., 2007. CXCL10 promotes invasion-related properties in human colorectal carcinoma cells. Cancer Res 67, 3396-3405.
Zutter, M.M., Martin, P.J., Sale, G.E., Shulman, H.M., Fisher, L., Thomas, E.D., Durnam, D.M., 1988. Epstein-Barr virus lymphoproliferation after bone marrow transplantation. Blood 72, 520-529.